

Miscellaneous Publication 182
(MCC Research Report 97-02)

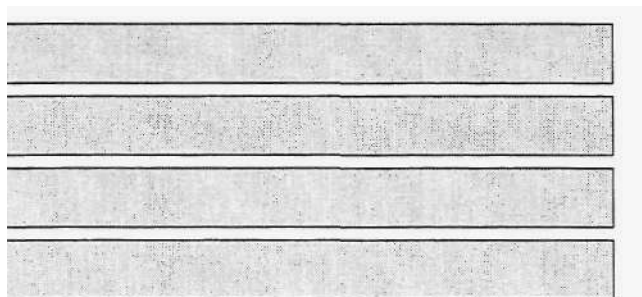


The Record Rainstorm on July 17-18, 1996 in Northern Illinois

Stanley A. Changnon, Scientific Editor

by
James R. Angel, Stanley A. Changnon, David Changnon, Floyd A. Huff,
Paul Merzlock, Steven R. Silberberg, and Nancy E. Westcott

May 1997



Illinois State Water Survey
Atmospheric Sciences Division
Champaign, Illinois

A Division of the Illinois Department of Natural Resources

The Record Rainstorm on July 17-18, 1996 in Northern Illinois

Stanley A. Changnon, Scientific Editor

James R. Angel, Stanley A. Changnon, David Changnon,
Floyd A. Huff, Paul Merzlock, Steven R. Silberberg,
and Nancy E. Westcott

Illinois State Water Survey

Champaign, Illinois

May 1997

This report was printed on recycled and recyclable papers.

Contents

	<i>Page</i>
Chapter 1. Introduction and Overview.	1
<i>Stanley A. Changnon, Illinois State Water Survey</i>	
Chapter 2. Meteorological Analysis.	5
<i>Steven R. Silberberg, Northern Illinois University</i>	
Chapter 3. Forecasting the Flood Event.	43
<i>Paul Merzlock, National Weather Service</i>	
Chapter 4. The Rainstorm Data and General Storm Dimensions.	63
<i>Stanley A. Changnon and Nancy E. Westcott, Illinois State Water Survey</i>	
Chapter 5. Hydrometeorological Characteristics.	74
<i>James R. Angel, Floyd A. Huff, Illinois State Water Survey;</i> <i>and David Changnon, Northern Illinois University</i>	
Chapter 6. Impacts and Responses to the Storm.	121
<i>Stanley A. Changnon, Illinois State Water Survey</i>	
Chapter 7. Comparison of the Storm Rainfall As Measured by Radar and by Raingages.	141
<i>Nancy E. Westcott, Illinois State Water Survey</i>	

Acknowledgments

Many persons and institutions contributed significantly to this study. Included among them are Jan Horton, Julie Kokolus, and Steve McMaster of the Disaster Recovery Office of the Illinois Emergency Management Agency, who provided data and information on impacts and response. We deeply appreciate Jan Horton's time and interest in reviewing Chapter 6.

Several people provided data: Robert Holmes and Jim Dancker, U.S. Geological Survey; Husain Hyder, Metropolitan Water Reclamation District of Chicago; Tony Charlton, DuPage County Department of Environmental Concerns-Stormwater Management Division; Alessandra Klimara, Argonne National Laboratory; Robert Brown, Extension Unit Leader in DeKalb County; Nan Armstrong, Extension Unit Leader in Kendall County; and Mark Synandin, Will County Farm Bureau Marketing Committee Rainfall Program. We thank each of them for their cooperation. Staff at the *Joliet Herald News* and *Aurora Beacon News* graciously provided copies of their newspapers covering many days during and after the storm.

Paul Dailey, Bill Nelson, and other staff of the National Weather Service were extremely helpful and cooperative. They provided a wide variety of data during and after the storm. Staff members at Northern Illinois University, in addition to the authors of this report, were helpful, including Ken Bowden, in providing rainfall and flood data.

We pay particular thanks to Jean Dennison and Joyce Fringer for their typing of this manuscript and to Eva Kingston for editing it. Many of the maps were drafted by Linda Hascall and Julie Horan.

Portions of the research were supported by the Midwestern Climate Center as part of Grant NA46WP0228 from the National Oceanic and Atmospheric Administration.

Chapter 1. Introduction and Overview

Stanley A. Changnon, Illinois State Water Survey

By the afternoon of July 18, 1996, Midwestern radio and television stations were issuing reports of extremely heavy rains and flash flooding in northeastern Illinois. The news reports indicated that a raingage in Aurora, Illinois, had received nearly 17 inches of rain during the rainstorm on July 17-18, 1996. In the storm center, hundreds of thousands of persons in the area were in shock because of the massive flooding and the sudden devastation with 35,000 homes experiencing flood damage in a matter of hours.

The maximum point rainfall value of 16.94 inches within a 24-hour period occurred at a raingage operated by a cooperative weather observer of the National Weather Service in Aurora. Inspection of historical precipitation records for all parts of the state indicated that this amount established a *new record* 24-hour rainfall for Illinois. The previous record rainfall was 16.5 inches in a storm in the East St. Louis area in 1957 (Huff et al., 1958). Clearly, the July 17-18, 1996, rainstorm was of record proportions. Information available by July 19 indicated that the resulting flood damages were extensive, particularly in south Chicago and across extensive suburban and rural areas located west, southwest, and south of the city. '

Figure 1-1 is an isohyetal map showing the total storm rainfall for the July 17-18 storm. Note that heavy rainfall was produced across a three-state area—Illinois, Indiana, and Wisconsin. This was an exceptionally large storm with rainfall amounts above 10 inches across wide areas of Illinois and a portion of southern Wisconsin. The axis of the storm was more than 600 miles long. The major axis of the storm rainfall was oriented from northwest to southeast, a somewhat unique position for a severe rainstorm. As part of the present study, the unusual weather conditions that created this storm and its odd placement were investigated (see Chapter 2).

Scientists of the Illinois State Water Survey and its Midwestern Climate Center answered a variety of questions about this severe rainstorm. These requests sought hydrometeorological and climatological interpretations of the significance of the heavy rains on July 17-18, along with detailed information on the rainstorm's dimensions and causes.

The Water Survey has a history of performing field-based studies of extreme rainstorms, an effort that began in 1951 with the study of two rainstorms (Larson et al., 1952; Illinois State Water Survey, 1952). These and subsequent studies of intense rainstorms, including the field collection of rainfall data in "bucket surveys," have provided unique data about the characteristics and dimensions of severe Midwestern convective rainstorms (Huff et al., 1955, 1958; Huff and Changnon, 1961; Changnon et al., 1977). The objectives of such storm studies were not only to collect data and make exhaustive scientific analyses to better define causes and dimensions, but also to provide a database on storm rainfall that could be used by others to serve a variety of purposes (Changnon and Vogel, 1980). Hence, an extensive meteorological-climatological analysis of the record-setting July 17-18 storm seemed a logical continuation of prior storm studies.

In considering the July 17-18 rainstorm as a event for an exhaustive case study, it was important that such a study fit the current goals of the Water Survey: to collect data and to monitor the weather and climate resources of Illinois. Thus, a study of the July 17-18 storm addressed the

mission of the Survey. Furthermore, the July 1996 storm had three special aspects that justified an intensive scientific investigation of the event. First, the maximum point rainfall amount of nearly 17 inches in 24 hours was a new record rainfall event in the 100-year history of quality weather records for Illinois. Second, the rainstorm occurred in a highly significant urban, suburban, and rural region of the state, and caused extensive and costly losses. Third, the operation of the new National Weather Service located near Joliet offered a first opportunity to assess how well this type of weather radar measured extreme rainfall events.

The goal of the study of the July 17-18 rainstorm was to define the physical features of the storm plus its major effects. The objectives of the study included the provision of: a) storm information to atmospheric scientists (storm modelers and forecasters), b) data and design information to water managers and hydrologists, and c) a variety of storm data and information to various local, state, and federal agencies involved in storm assessments, water and soil management, and regulatory activities related to water resources.

In planning the study and the contents of this report, certain topics were identified for analysis and presentation. The first topic involved a detailed meteorological analysis of the weather conditions that had caused this unique storm (Chapter 2). A second topic involved the actual forecasting of the extreme event (Chapter 3). The third topic concerned the sources of rainfall data and a general description of the total storm rainfall in space and time. The fourth area of study involved an extensive hydrometeorological and climatological assessment of the rainfall conditions (Chapter 5). The fifth area of investigation considered the primary impacts, both physical and socioeconomic, that the storm produced and responses to the storm damages (Chapter 6). The sixth topic was a special study assessing how well the new weather radar measured the heavy rainfall (Chapter 7).

A major activity done immediately after the storm was the collection of the storm data. Rainfall data collection had to be accomplished quickly to gather rainfall data from bucket surveys in the field, to obtain the raw radar data, and to collect detailed meteorological data, including existing satellite data, needed to analyze the causes of the event. Scientists at Northern Illinois University at DeKalb, which is close to the center of the storm, agreed to work with Survey scientists in the massive collection of the rainfall and synoptic weather data. Data collection was aided by dense raingage networks in four counties in the immediate storm area, and more than 600 point measurements of storm rainfall were ultimately collected.

Discussions with atmospheric scientists at Northern Illinois University and at the National Weather Service in Chicago also revealed their interest in analyzing various aspects of the storm. A plan was evolved to include them in a cooperative study organized by the Water Survey. These interactions resulted in a special new study including an analysis of the forecasting endeavors by the National Weather Service related to the rainstorm event (Chapter 3). Scientists at Northern Illinois University worked with Water Survey scientists to gather field data in an exhaustive analysis of the weather conditions that caused the storm and in the hydroclimatological assessment of the storm. Times of events are denoted in two ways. For localized analyses (Chapters 4-7), times are denoted as LST (local standard time) or CST (central standard time), which are interchangeable. For regional analyses (Chapters 2-3) where time zone boundaries are crossed, the standard meteorological practice is to denote time by UTC (universal time coordinate), and this is adopted here. The time reference for UTC is the Greenwich meridian, and UTC times are six hours ahead of CST. For example, 1200 UTC (or 12 UTC) is 0600 CST (or 06 CST).

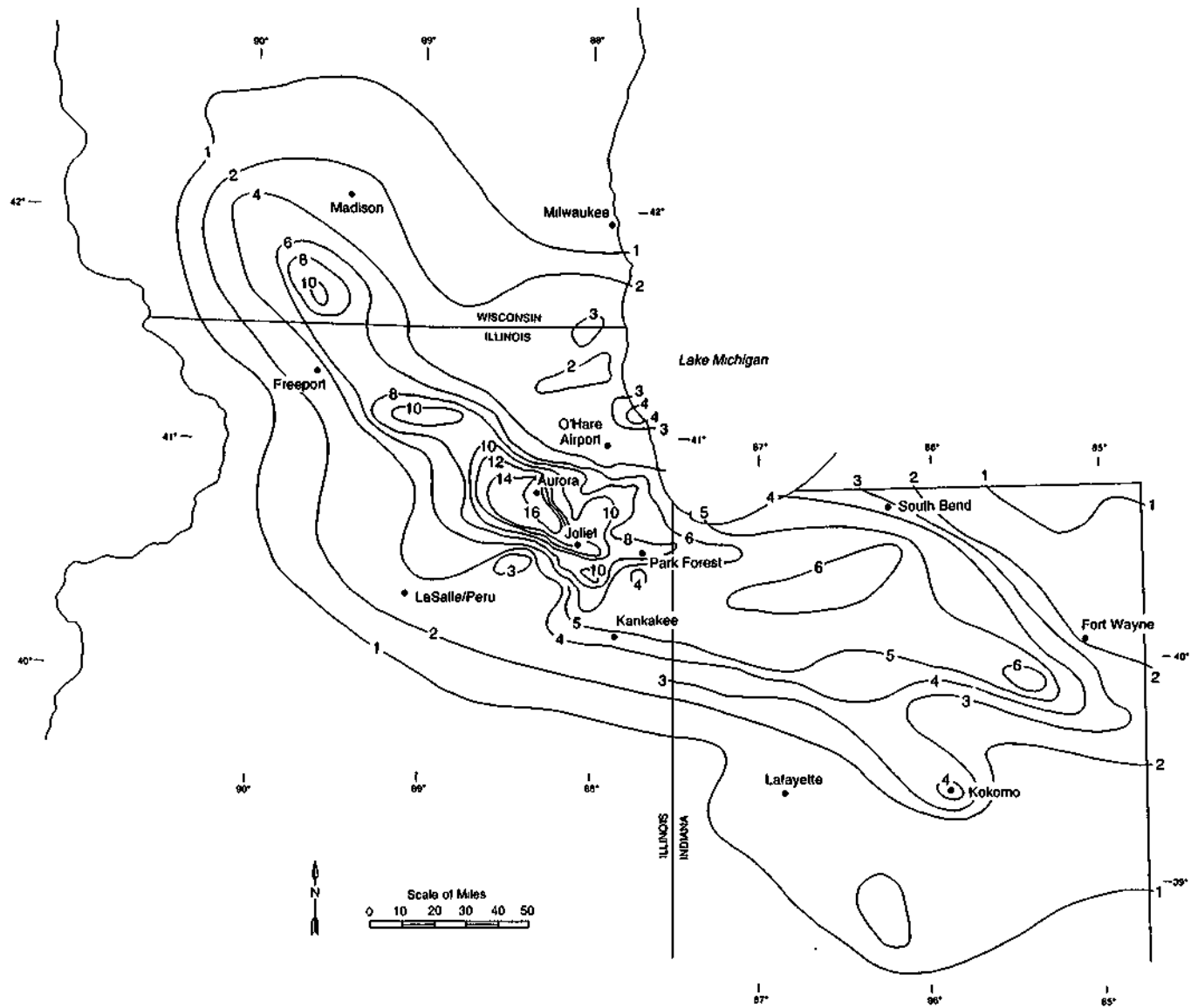


Figure 1-1. The pattern of total storm rainfall across the Midwest for July 17-18, 1996.

Thus, the study and this report are the joint efforts of scientists from three institutions working cooperatively to produce a comprehensive analysis of the single worst short-term rainstorm since rainfall records began in the late nineteenth century. The views expressed by authors from institutions other than the Illinois State Water Survey are not necessarily the views of the Illinois State Water Survey.

References

- Changnon, S.A., T.T. Fujita, and M. Hjelmfelt, 1977: Mesoscale study of record Chicago rainstorm using radar, satellite, and raingage data. *Preprints, Tenth Conference on Severe Local Storms*, American Meteorological Society, Boston, pp. 65-72.
- Changnon, S.A., and J.L. Vogel, 1980: The morphology of an isolated severe rainstorm and the hydroclimatological characteristics of such storms. *Preprints, Second Conference on Flash Floods*, American Meteorological Society, Boston, pp. 5-10.
- Huff, F.A., and S.A. Changnon, 1961: *Severe Rainstorms in Illinois, 1958-1959*. Report of Investigation 42, Illinois State Water Survey, Champaign, IL, 70 pp.
- Huff, F.A., H. Hiser, and G. Stout, 1955: *The October 1954 Storm in Northern Illinois*. Report of Investigation 27, Illinois State Water Survey, Champaign, IL, 23 pp.
- Huff, F.A., R.G. Semonin, S.A. Changnon, and D.M.A. Jones, 1958: *Hydrometeorological Analysis of Severe Rainstorms in Illinois, 1956-1957, with Summary of Previous Storms*. Report of Investigation 35, Illinois State Water Survey, Champaign, IL, 79 pp.
- Illinois State Water Survey, 1952: *The Storm of July 8, 1951, in North Central Illinois*. Report of Investigation 14, Champaign, IL, 45 pp.
- Larson, B.O., H. Hiser, and W. Daniels, 1952: *The Storm of July 18-19, 1952, Rockford, Illinois, and Vicinity*. Report of Investigation 24, Illinois State Water Survey, Champaign, IL, 14 pp.

Chapter 2. Meteorological Analysis

Steven R. Silberberg, Northern Illinois University

Introduction

Heavy summertime rainfall events over the Great Plains of the United States are associated with mesoscale convective systems (MCS), thunderstorm systems that exhibit a preference for nocturnal development. These systems remain stationary, move slowly, or persistently redevelop such that they "train" over a region (Maddox, 1980, 1983; Maddox et al., 1978, 1979; Chappell, 1986; Fritsch et al., 1986; Funk, 1991). An MCS forms in environments characterized by conditional instability and lifting mechanisms that are sustained in an atmosphere of relatively weak winds. In particular, an MCS requires an ample supply of low tropospheric water vapor typically supplied by a low-level jet stream (Bonner, 1968; Mitchell et al., 1995; Augustine and Caracena, 1994), and lifting mechanisms such as isentropic ascent along a boundary separating air masses of differing thermal and moisture characteristics, convergence at the nose of a low-level jet, and upper level dynamic forcing such as differential vorticity advection, ageostrophic circulations accompanying an upper level jet streak, or the coupling of upper and lower level jet streak circulations (e.g. Funk, 1991; Doswell et al., 1996). Analyses presented in this chapter will document the antecedent, development, and mature stages of the MCS that affected northern Illinois on July 17-18, 1996.

Antecedent Conditions

The MCS responsible for the flooding over northern Illinois was the second development of an MCS over the Great Plains in as many days. Figure 2-1 shows infrared satellite imagery of the first MCS, which produced flooding over Iowa the night prior to the northern Illinois flood. Two major convective storms, identified by the coldest temperatures in the infrared imagery (black within white) developed over east-central Nebraska and the Iowa, South Dakota, and Nebraska border at 0015 UTC on July 17, 1996 (1815 LST on July 16). These initial storms drifted eastward and weakened by 0215 UTC, whereupon a second convective system blossomed on the Nebraska-South Dakota border. This secondary convective storm developed into an MCS and flooded a large portion of Iowa as the storm slowly drifted eastward during the early morning hours on July 17.

Synoptic analyses from the National Centers for Environmental Prediction (NCEP) at 00 UTC on July 17, 1996 (Figure 2-2), illustrate conditions after the initial convective development over Nebraska and two hours prior to the development of the nocturnal MCS. At the surface (Figure 2-2D) an east-west oriented warm front extended from a weak low pressure center near North Platte, Nebraska, across the southern third of Nebraska. This boundary separated a southerly flow of maritime tropical air with high temperatures and water vapor content over southern Nebraska and Kansas from a southeasterly flow of cooler, slightly drier air over northern Nebraska, Iowa, and southern South Dakota. Large negative lifted indices and K-index values approaching 40°C were diagnosed over the Great Plains with precipitable water values reaching 1.78 inches and 157 percent of normal at Valley, Nebraska (Figures 2-2E, F), values that have been associated with heavy rain

events (e.g., Funk, 1991). Thunderstorm development occurred as boundary layer-rooted convection in the warm humid air south of the warm front in east-central Nebraska, and as elevated convection (e.g., Colman 1990a, b; Rochette and Moore, 1996) developed along the warm front in a region of large 3-hour pressure falls at the Nebraska, South Dakota, and Iowa borders ($-4.4 \text{ mb } 3\text{-h}^{-1}$ at Sioux City, Iowa).

Lower tropospheric analyses at 00 UTC showed an axis of low-level water vapor transport extending from Aberdeen, South Dakota, southward to Norman, Oklahoma, at 850 mb as southerly flow combined with dewpoints exceeding 17°C (Figure 2-2C). Enhanced with 1500 meter winds detected by the wind profiler demonstration network, the 850 mb analysis revealed an axis of winds exceeding 10 m s^{-1} extending northward across eastern Nebraska into eastern South Dakota and Minnesota with a maximum of 15 m s^{-1} at the Neligh wind profiler station in northeast Nebraska. MCS development typically occurs in regions of strong low-level warm advection and moisture transport associated with the low-level jet (e.g., Maddox, 1983; Funk, 1991; Augustine and Caracena, 1994; Rochette and Moore, 1996). Low to mid-tropospheric warm advection was situated over eastern Nebraska and Kansas as southerly 850 mb winds gave way to nearly westerly flow at 500 mb (Figure 2-2B). Along the South Dakota-Nebraska border where the MCS developed, relatively strong 850 mb moisture flux divergence was present at 00 UTC (not shown), a factor that impedes MCS development (Rochette and Moore, 1996). Analysis of the 305K isentropic level indicated that warm, moist surface air parcels in southeastern Nebraska ascended approximately 60 mb as they glided northward to the Nebraska-South Dakota border, an amount of ascent that was insufficient by itself to produce saturation and achieve the level of free convection.

At 200 mb (Figure 2-2A), a ridge axis was located upstream of eastern Nebraska as evidenced by northwesterly flow and height rises in excess of $30 \text{ m } 12\text{-h}^{-1}$, a typical diurnal 200 mb height rise over the United States at 00 UTC in summer. Large 200 mb height rises in excess of $100 \text{ m } 12\text{-h}^{-1}$ over eastern Kansas, Nebraska, South Dakota, Minnesota, Wisconsin, and Illinois indicated eastward progression of an upper tropospheric trough that persisted over the Great Lakes region for the first half of the summer. These height rises are consistent with hydrostatic warming in the relatively warm column produced by warm advection in the low- to mid-troposphere. A jet streak with a maximum wind of 42.5 m s^{-1} at Green Bay, Wisconsin, extended eastward from an entrance region over South Dakota and southern Minnesota to the Great Lakes with along-stream acceleration present along the jet axis from South Dakota to Wisconsin. Diffluent flow with downstream wind increases are evident over the South Dakota, Nebraska, Minnesota, and Iowa borders suggesting that upper level divergence was occurring there because the change of wind direction along the flow was not compensated by along stream windspeed decreases (e.g., Bluestein, 1993). Divergence calculations from radiosonde data and ageostrophic wind and divergence calculations from the 00 UTC initialization of the 48 kilometer (km) eta model (not shown) support this assertion. The calculations reveal southwesterly ageostrophic flow of $5\text{-}7.5 \text{ m s}^{-1}$ and a maximum of 200 mb wind divergence and ascent at 500 mb over this region, which was collocated with the largest surface pressure falls.

Between 00 and 02 UTC, prior to development of the nocturnal MCS, the Neligh 1500 m wind veered slightly south-southwest and increased to 20 m s^{-1} indicating strengthening of the low-level jet. Concomitant with low-level jet enhancement, moisture flux divergence weakened and was replaced by weak moisture flux convergence where the nocturnal MCS developed (Figure 2-3).

In summary, the first MCS formed north of a surface warm front in a region where warm moist conditionally unstable air was transported into the region by the low-level jet. Isentropic analysis revealed that insufficient ascent was present north of the warm front for air parcels to reach their level of free convection. Moisture flux divergence diagnosed at 00 UTC in that region was a factor that inhibited MCS development. The MCS developed underneath diffluent flow, upper-level divergence, and midtropospheric ascent associated with the right-rear entrance region of a 200 mb jet streak whose reflection on the surface was a strong three hour pressure fall at Sioux City, Iowa. In the two hours prior to MCS development, the low-level jet strengthened in northeast Nebraska, which generated low-level convergence where the MCS formed.

Daytime Pre-development, July 17

As the Iowa MCS neared the end of its lifecycle, a time sequence of infrared imagery during July 17 (Figure 2-4) shows that cloud-top temperatures warmed and elevated warm front thunderstorms spread eastward across Iowa and the northern half of Illinois. These storms produced heavy rain and severe weather in northern Illinois throughout the afternoon of July 17, although satellite cloud-top temperatures struggled to reach values colder than -50°C by 2115 UTC.

Synoptic conditions at 12 UTC on July 17 showed gradual eastward progression of surface features with the analyzed warm front draped southeastward from Nebraska to southern Illinois (Figure 2-5D). South of the warm front, clear skies with Fahrenheit temperatures in the upper 70s ($\sim 26^{\circ}\text{C}$) and dewpoints in the low 70s ($\sim 22^{\circ}\text{C}$) were observed, while north of the front, cloudy skies and light precipitation reflected the decaying stage of the MCS. Temperatures ranged from the upper 60s to low 70s ($\sim 21^{\circ}\text{C}$) and dewpoints were in the mid to upper 60's ($\sim 18^{\circ}\text{C}$). Surface mesoanalysis (Figure 2-5E) revealed that with the exception of a few convection contaminated northeast winds in south-central Iowa, the broad-scale surface wind flow was southerly throughout Missouri, Iowa, and Illinois. In particular, winds over northern Illinois ranged from southwesterly in the Chicago metropolitan area to light southeasterly in north-central Illinois. Dewpoint gradients were located across central Wisconsin and western Iowa with the 70°F isodrosotherm extending northward across the southern Iowa and Illinois borders.

Lifted index analyses at 12 UTC (Figure 2-5F) exhibited stability increases owing to the diurnal cycle. Positive values at Davenport reflected stabilization from the previous evening due to MCS passage, while negative values occurred at surrounding stations. Although the 12 UTC lifted indices indicated stabilization from the previous evening, K-index values increased $8\text{-}10^{\circ}\text{C}$ during the nighttime hours at Green Bay, Wisconsin, Davenport, Iowa, Topeka, Kansas, Chanhassen, Minnesota, and Springfield, Missouri, to values approaching 40°C signifying increased lower tropospheric water vapor, conditional instability, and the potential for flood-producing rainfall. Precipitable water exceeded 1.6 inches (40 millimeters or mm) over the region, and during the overnight period it doubled at Chanhassen and increased nearly 40 percent at Davenport, demonstrating the effects of strong water vapor transport in the lower troposphere.

In the low troposphere at 850 mb (Figure 2-5C), rawinsonde and 1500 m profiler winds showed a southwesterly low-level jet extending from northern Texas to Iowa with winds exceeding 15 m s^{-1} over northern Texas, eastern Nebraska, and northern Missouri. Strong water vapor transport and convection from the MCS during the preceding 12 hours increased 850 mb dewpoints at

Chanhassen, Davenport, and Lincoln to greater than 15°C, which is consistent with the precipitable water increases noted above. Weak 850 mb moisture flux convergence was diagnosed (not shown) with maxima over central Iowa, and southern and northern Wisconsin. In the mid-troposphere (Figure 2-5B), a short-wave trough with absolute vorticity of $16 \times 10^{-5} \text{ s}^{-1}$ was located over southern Minnesota. Dewpoints at 500 mb increased by 15°C at Davenport along with development of a 20 m s^{-1} wind, with nearly saturated conditions observed at Lincoln, Illinois.

The upper troposphere exhibited signs of convective influence (Figure 2-5A). Height rises in excess of 100 m 12-h^{-1} were observed in Wisconsin (Green Bay) and Michigan (Gaylord and Detroit), indicating continued ridging in that region. The jet streak over the Great Lakes continued to strengthen with maximum winds at Green Bay and Detroit increasing to 50 m s^{-1} and winds at Gaylord increasing to 45 m s^{-1} due to outflow from the previous evening's MCS. The entrance region of the jet streak extended across Minnesota and Iowa with diffluence and downstream wind increases suggesting divergence in the region. Diagnostic calculations (not shown) indicated southwesterly ageostrophic winds and maximum divergence over northeastern Iowa, which extended south-eastward across northern Illinois into northwestern Indiana.

Between 12 and 21 UTC on July 17, mesoscale surface analyses and difference fields (Figure 2-6) revealed dramatic changes in the water vapor, wind, and thermal fields that affected the strength and orientation of the surface warm front. Through 15 UTC (Figure 2-6A), dewpoint gradients were evident over Wisconsin and western Iowa, with a weak gradient extending southeastward across southern Iowa and central Illinois. Large dewpoint increases of 8°F (4.4°C) became apparent over Iowa by 18 UTC as a closed 74°F (23.3°C) isodrosotherm formed over Iowa, Illinois, Missouri, and adjacent South Dakota, Nebraska, and Kansas. No appreciable dewpoint gradient was noted across northern Illinois through 18 UTC (Figure 2-6B), although the dewpoint gradient noted across southern Iowa at 15 UTC shifted northeastward along the Iowa-Illinois border. Surface dewpoints continued to increase through 21 UTC to values in excess of 76°F (24.4°C) over most of Iowa, with peak values approaching 78°F (25.6°C) (Figure 2-6C). Between 12 and 21 UTC, surface dewpoints increased by 7 to 13°F (~4 to 7°C, Figure 2-6D) in a northwest-southeast swath from eastern South Dakota to central Illinois. During the same time period, dewpoints over central Wisconsin and Minnesota rose a mere 2 to 5°F (~1 to 3°C) to the mid 60s (~17°C) with the smallest increases noted on the western shore of Lake Michigan. This differential dewpoint change, with large increases across Iowa and central Illinois and small increases over Wisconsin and northeastern Illinois, strengthened dewpoint gradients associated with the warm front over northern Iowa and central Wisconsin and developed a dewpoint gradient over northern Illinois.

By combining the effects of solar heating and water vapor processes, mesoanalyses of surface θ_e and its changes during the day illustrate the evolution of the surface warm front (Figure 2-7). The front was oriented east/west with a northward protrusion in Nebraska and southward protrusion over Iowa at 15 UTC. A combination of surface dewpoint increases and daytime insolation south of the front in relatively cloud-free air (Figure 2-4) increased θ_e values in excess of 20K between 12 and 21 UTC over a northwest-southeast swath extending from eastern South Dakota to central Illinois. During this same time period, θ_e increased only 8K over southeastern Wisconsin and northeastern Illinois. The differential changes of surface θ_e strengthened the front across northern Illinois from about 5K/100 km at 15 UTC to 10K/100 km by 21 UTC. In addition, the differential θ_e changes modified the surface front orientation from east-west at 15 UTC to northwest-southeast by 21 UTC.

Analysis of the terms in the water vapor equation in isobaric coordinates (Bluestein, 1993),

$$\frac{\partial r}{\partial t} = -\mathbf{v} \cdot \nabla r - w \frac{\partial r}{\partial p} + E - C, \quad (2.1)$$

where r is mixing ratio, \mathbf{v} is horizontal velocity, ∇ is the horizontal del operator in isobaric coordinates, w is the pressure vertical velocity, E is evaporation, and C is condensation, suggests that the dewpoint increases over central Iowa resulted from strong evapotranspiration from agricultural fields. This suggestion is supported by the following observations and diagnostic calculations:

- First, closed dewpoint contours developed over Iowa in the presence of southerly flow (Figure 2-6C), suggesting that horizontal advection could not have contributed to the water vapor increases.
- Second, diagnostic calculations of horizontal advection at the surface (not shown) were near zero over Iowa, confirming the first observation.
- Third, water vapor values decreased upward from the surface (Figure 2-5C) indicating that vertical advection of higher values of water vapor due to the development of a mixed layer during the afternoon could not have increased water vapor values.
- Fourth, ω flux convergence analyses, shown in Figure 2-8, reveal moisture flux divergence over Iowa in the morning and moisture flux convergence only in northern and northeastern Iowa in the afternoon on the northern periphery of maximum surface dewpoint values.

The only remaining term that can account for water vapor increases over Iowa is evapotranspiration from the plentiful fields of corn and soybeans. Over Illinois, dewpoint increases were produced by evapotranspiration from agricultural fields and ω flux convergence, which was maximized over western and central portions of the state from the late morning through mid-afternoon.

Concomitant with modifications to the surface water vapor field, the surface wind field also underwent dramatic evolution during the day over northern Illinois (Figure 2-9). In the morning, winds strengthened on either side of the warm front with southerly flow in regions with dewpoints exceeding 72°F (~22°C) and general southeasterly flow elsewhere. By 21 UTC, southwesterly flow had increased across central Illinois, while southeast to east-northeast winds developed and strengthened across northern Illinois and southeastern Wisconsin. In particular, 5 to 7.5 m s⁻¹ winds from the southeast to northeast developed at eight stations along the western shore of Lake Michigan in the Chicago metropolitan region of northeastern Illinois. Vector wind and dewpoint differences for the nine-hour period from 12 to 21 UTC (Figure 2-9D) revealed southeast through northeast wind accelerations of 5-10 m s⁻¹ 9-h⁻¹ along the southeastern shore of Lake Michigan where dewpoints rose at most 2°F (~1 °C) during the day. These easterly winds advected relatively cooler air from Lake Michigan (lake temperature was 68°F, 20°C) across northern Illinois and southern Wisconsin, retarding the northward advance of the warm front. In addition, convective storms that periodically rumbled across northern Illinois during the afternoon through 21 UTC (Figure 2-4) spread rain-cooled air over the region and partially affected the observed winds and dewpoints. South of the front, vector wind differences showed southwesterly accelerations of 5-7.5 m s⁻¹ 9-h⁻¹ indicating that accelerations on either side of the front served to strengthen it during the day. The vector wind

accelerations are consistent with the couplet of surface 6_e flux divergence-convergence diagnosed over northeastern Illinois (Figure 2-8D).

Along with development of the surface water vapor, wind, and thermal fields, the surface pressure field, defined by altimeter settings, exhibited more subtle but discernible changes during the day over Illinois as the surface warm front strengthened. Shortly after daybreak at 12 UTC on July 17, a weak pressure trough was evident across central Illinois (Figure 2-5E). During the daytime (Figure 2-10), this pressure trough increased in amplitude and remained located on the warm, humid, southwesterly flow side of the front as depicted by analyses of 0_e (Figure 2-7), dewpoint, and wind (Figure 2-9). The surface pressure tendency field (Figure 2-10) revealed the gradual eastward progression of the largest pressure falls from north-central Iowa to eastern Iowa between 15 and 19 UTC. This region of maximum pressure falls remained nearly stationary over eastern Iowa through midafternoon and was associated with afternoon convective development (Figure 2-4) that drifted eastward across northern Illinois, producing heavy rains and occasional severe weather. When taken in aggregate, the largest pressure falls between 21 and 12 UTC occurred where the surface pressure trough amplified over Illinois and over eastern Iowa, where convection repeatedly developed (Figure 2-10D).

Evolution of the low-level jet and thermal advection pattern in the lowest layers above ground during July 17 is depicted by 1000 and 1500 m winds from the wind profiler network and by 925 mb and 850 mb winds from raob stations (Figure 2-11). Between 12 and 18 UTC, low-level winds increased and warm air advection developed over southwestern Wisconsin and Iowa, suggesting northeastward propagation of the low-level jet that extended from Texas to northern Missouri in the 12 UTC 850 mb analysis (Figure 2-5C). By 21 UTC, warm air advection was prevalent over Wisconsin, Illinois, Iowa, and Missouri, while wind speeds decreased over the region, consistent with daytime low-level jet behavior (Bonner, 1968; Mitchell et al., 1995). In particular, eastward movement of the low-level jet is suggested by wind increases at Winchester, Illinois, from 15 to 21 UTC, and this is confirmed by a comparison between the 12 UTC July 17 850 mb analysis with the 00 UTC July 18 wind profiler and raob wind plot (Figure 2-11D). This shows wind decreases on the western edge of the wind maximum and wind increases on the eastern edge. Strengthening of the low-level jet occurred between 21 UTC July 17 and 00 UTC July 18 as an area of winds in excess of 15 m s^{-1} developed across Wisconsin, Iowa, Illinois, and Missouri at 1500 m and 850 mb. Warm air advection was evident at nearly all stations by 00 UTC.

Early Development of the Major Rainstorm

Infrared satellite imagery suggests that a new phase of the rainstorm system began by 2215 UTC on July 17 (Figure 2-4). Prior to 2215 UTC, periodic convective development with relatively warm cloud tops occurred over eastern Iowa. These storms, some of which were severe, drifted eastward over northern Illinois. In particular, storm development southwest of Chicago at 2015 and 2115 UTC produced a tornado and severe weather along its eastward journey. The 2215 UTC image indicates the *first* development of an east-west oriented line of convection with cold tops over northern Illinois. Impressive anvil expansion and cloud-top cooling occurred between 2215 UTC July 17 and 0115 UTC July 18 as the system drifted eastward. Of interest is the less notable development of convection in eastern Iowa and western Illinois at 0015 and 0115 UTC July 18. This

apparently innocuous convective development hinted of future system evolution during the evening hours.

Synoptic analyses at 00 UTC July 18 (Figure 2-12) reveal the meteorological conditions in place prior to nocturnal development of the MCS, and after the eruption of convection across northern Illinois and the daytime changes described above. The large-scale surface analysis (Figure 2-12D) showed that in the 12-hour period ending at 00 UTC, the surface warm front advanced 250 km northeastward and draped southeastward from eastern South Dakota across southern Minnesota and northeastern Iowa into north-central Illinois. On the warm side of the front, clear skies and southerly winds were associated with temperatures near 90°F (~32°C) and dewpoints in the upper 70s (~26°C). Just north of the front, temperatures remained in the mid-70s (~24°C), dewpoints were in the low 70s (~22°C), and cloudy skies with embedded precipitation occurred with southeasterly winds. Surface mesoanalysis (Figure 2-12E) revealed that northern Illinois and portions of eastern Iowa remained north of the surface warm front with easterly flow extending from Lake Michigan westward to the Mississippi River, and a minimum of surface dewpoint along the western shore of Lake Michigan in the Chicago metropolitan area.

Lifted index analysis (Figure 2-12F, left) showed an axis of instability stretching east-west across Iowa and central Illinois, with maximum instability located over the Iowa-Nebraska border. K-index values of 40°C were diagnosed at Valley and Davenport, while precipitable water increased further to values in excess of 2 inches (50 mm) over Iowa. Davenport reported a precipitable water of 2.17 inches (55 mm), a value that was 192 percent of normal. Thus, by 00 UTC July 18, a deep layer of conditionally unstable air with high water vapor content had developed south of the surface warm front over Iowa and southern and western Illinois.

The 00 UTC 850 mb analysis (enhanced with 1500 m profiler winds, Figure 2-12C) reveals a southwesterly low-level jet with winds in excess of 15 m s⁻¹ over Iowa and western Illinois extending southwestward to eastern Kansas. This southwesterly flow was associated with warm air advection from Kansas to Wisconsin. High values of water vapor and nearly saturated conditions were evident at Aberdeen, South Dakota, Chanhassen, Minnesota, and Davenport, Iowa, on the northern edge of the warm, moist air mass as defined by the 00 UTC surface analyses. Although high water vapor values were associated with the low-level jet, maximum moisture flux divergence was diagnosed over eastern Iowa and western Illinois and Wisconsin, suggesting that large-scale conditions were not conducive for MCS development in that region at 00 UTC at 850 mb. Moisture flux convergence at 850 mb was diagnosed over the eastern South Dakota-North Dakota border and over extreme eastern Illinois and western Indiana, regions where convection was occurring at 00 UTC (for example, Figures 2-4G, H, I).

In the mid-troposphere at 500 mb (Figure 2-12B), a short-wave trough was east of Illinois and a short-wave ridge was located upstream over Iowa and Minnesota. Over Wisconsin, Iowa, and Illinois, mid-tropospheric winds remained lighter than 17.5 m s⁻¹, a necessary condition for slow moving nocturnal convective systems. At 200 mb (Figure 2-12A) the 50 m s⁻¹ jet streak located over Wisconsin and Michigan at 12 UTC July 17 moved eastward to New York, and in response, winds at Green Bay, Gaylord, and Detroit decreased nearly 50 percent to values between 25 and 30 m s⁻¹. Nearly zero 200 mb mass divergence was diagnosed over Wisconsin, Iowa, and Illinois, which is consistent with weak alongstream acceleration and negligible diffluence over this region, suggesting that upper level forcing was not an important process at 00 UTC.

Low-level forcing of ascent, moisture transport, and the role of the low-level jet are more clearly revealed through analyses of the 305K and 310K isentropic surfaces at 12 UTC July 17 and 00 UTC July 18, which have been enhanced with wind profiler observations (Figure 2-13). Between 12 UTC July 17 and 00 UTC July 18, the analyses show that a gradient of isentropic pressure topography of nearly $50 \text{ mb } 100 \text{ km}^{-1}$ developed over Wisconsin, Iowa, and Illinois at both 305K and 310K. In addition, mixing ratios increased 30-60 percent over this same region with the highest mixing ratio values of 19 g/kg^{-1} occurring where the sloped isentropic surfaces were closest to the ground. With winds from the low-level jet stream originating in regions of mixing ratio maxima, and with the winds oriented nearly perpendicular to the isobars on the two isentropic surfaces, these analyses reveal a sloping, ascending low-level jet supplying maximal amounts of water vapor over southwestern Wisconsin, northeastern Iowa, and northern Illinois at 00 UTC July 18, 1996.

The amount of instability present over southwestern Wisconsin, northeastern Iowa, and northern Illinois at 00 UTC July 18, 1996, is shown by thermodynamic sounding diagrams for Davenport and Lincoln (Figure 2-14). Lincoln, which was south of the surface warm front, measured warm surface temperatures and high dewpoints at the base of a relatively shallow mixed layer 1 km deep, which was capped by a shallow isothermal layer. This sounding structure yielded a convective available potential energy (CAPE) of $1885 \text{ m}^2 \text{ s}^{-2}$ and a convective inhibition (CIN) of $79 \text{ m}^2 \text{ s}^{-2}$ based on a parcel analysis from the lowest 100 mb. A nearly saturated layer was evident from 600 to 700 mb, and above this layer the sounding showed drier conditions with two weak subsidence inversions at 470 mb and 370 mb. Lincoln also exhibited a veering wind profile and windspeeds at or below 20 m s^{-1} throughout its depth, which supplied a storm-relative helicity of $172 \text{ m}^2 \text{ s}^{-2}$. With a level of free convection (LFC) of 779 mb, a mid-level cloud deck between 600 and 700 mb, and weak synoptic and mesoscale ascent available (Figures 2-12 and 2-13), air parcels would not be able to reach the level of free convection to initiate thunderstorm development.

The Davenport sounding for 00 UTC July 18 (Figure 2-14A), released approximately 50 km north of the surface warm front position as analyzed in Figure 2-12, reveals a more favorable environment for convective development. While beginning with nearly the same amount of surface water vapor as at Lincoln, by virtue of being located north of the surface warm front, the sounding shows a frontal inversion from just above the surface to 950 mb and a strongly veering wind profile. Winds veered from east at 5 m s^{-1} at the surface to westerly at 20 m s^{-1} at 730 mb, supplying a storm-relative helicity of $525 \text{ m}^2 \text{ s}^{-2}$. Above the frontal inversion, a moist, saturated layer was evident from 950 to 820 mb, and this layer was capped by a weak subsidence inversion that was accentuated by diabatic cooling of a wet rawinsonde as it emerged from the moist, saturated layer. Similar to the Lincoln sounding, a nearly saturated layer was observed between 600 and 700 mb at Davenport, and above this layer the sounding showed drier conditions with a weak subsidence inversion at 520 mb. Parcel analysis of the Davenport sounding yielded a CAPE of $3080 \text{ m}^2 \text{ s}^{-2}$, a CIN of $13 \text{ m}^2 \text{ s}^{-2}$, and an LFC of 895 mb ($\sim 1 \text{ km}$). In contrast with the Lincoln sounding, the Davenport sounding contained nearly twice the CAPE and helicity, values which can support severe thunderstorms containing large hail and tornadoes. Moreover, the Davenport sounding possessed an LFC located close to the surface, where isentropic analysis revealed a large supply of high water vapor content air that could easily reach the LFC in a plume associated with the low-level jet. This combination of large instability, large helicity, low LFC, and ready access to high values of water vapor and

ascent by the low-level jet indicated the potential for nocturnal MCS development and the production of heavy rainfall near and downstream of Davenport.

Nocturnal Storm Development

Nocturnal evolution of the MCS exhibited a variety of convective development scenarios that are described by infrared satellite imagery and the 3-hour accumulated precipitation and base reflectivity products from the National Weather Service WSR 88-D Doppler Radar at Chicago, Illinois. Infrared satellite imagery (Figure 2-15) begins at 0115 UTC on July 18, with the latter stages of the early storm over eastern Illinois and Indiana and a new secondary development over northwestern Illinois. Similar to the behavior of the prior night's MCS secondary system over the North and South Dakota borders, the new secondary development over northwestern Illinois underwent explosive intensification between 0115 and 0215 UTC with the anvil extending northeastward. By 0315 UTC, the highest and coldest anvil clouds assumed a triangular shape that contained anvil vertices in southwestern Wisconsin and northwestern Illinois and a sharp gradient in cloud-top temperature along the anvil's western edge. The anvil showed signs of being blown southeastward from the northwest vertex, and extended northeastward from the southwestern vertex. Note that new convection was developing upstream of the triangular anvil in extreme eastern Iowa.

Multiple vertices were evident along the western flank of the anvil at 0415 UTC, suggesting that multiple convective developments were occurring in northwestern Illinois and southwestern Wisconsin. Small areas of relatively warm cloud tops continued to develop in northeastern Iowa during this time. Three main vertices could be distinguished along the western flank of the anvil at 0515 UTC, and these vertices occurred further west than their counterparts at 0415 UTC. New convection still continued to develop upstream of the main cold anvil in eastern Iowa. Westward development of the cold anvil continued such that by 0615 UTC, a vertex on the western flank was located in eastern Iowa, while the southernmost vertex appeared less distinct. A dual vertex anvil structure is apparent at 0715 UTC and the anvil east of the vertices begins to become oriented from northwest to southeast. The vertices become less distinct by 0815 UTC and the western edge of the anvil began to progress slowly eastward. Multiple vertex structure was still evident at 1015 UTC and the cold anvil shifted eastward to northeastern Illinois. Throughout the life cycle of the nocturnal MCS, multiple anvil vertices developed, shifted westward and strengthened, and then weakened and progressed eastward.

The time-averaged radar reflectivity of the WSR 88-D 3-hour precipitation (3HP) product from the Romeoville office of the National Weather Service (Figure 2-16) discloses further structure concerning the multiple vertex nature of the MCS as viewed from geostationary satellite. During the early development stage between 20 and 23 UTC on July 17, east-west oriented radar echoes were located across northern Illinois with 3HP precipitation amounts approaching 1.5 inches (38 mm). These echoes were consistent with the satellite view of the initial convective anvil cloud (Figure 2-4). In the subsequent three-hour period, the early development echoes progressed southeastward across Illinois to the Indiana border, while new echoes developed in eastern Iowa, western Illinois, and southwestern Wisconsin. A particularly large, nearly circular 3HP maximum in extreme northwest Illinois was associated with the secondary developing storm system in the infrared imagery. This system developed in the large CAPE/helicity environment sampled by the Davenport

00 UTC July 18 sounding and became a supercell thunderstorm (denoted by S in Figure 2-16), which produced a tornado, large hail, and rainfall totals in excess of 2.5 inches (~64 mm) in the 23 to 02 UTC period. The 3HP field for the 02 to 05 UTC period shows a complicated time-averaged radar reflectivity evolution and structure. Axes of multiple maximum 3HP extend eastward from eastern Iowa into northern Illinois. In southwestern Wisconsin a circled area denoted by an H indicates development of a heavy precipitation axis with 3-hour totals in excess of 3 inches (76 mm). These axes were nearly collocated with the anvil vertices observed in infrared satellite imagery. During the 02 to 05 UTC period, the supercell thunderstorm tracked southeastward, then eastward across northern Illinois and gradually dissipated. Between 05 and 08 UTC, the 3HP field exhibited compact east-west axes of precipitation totals in excess of 3 inches (76 cm) embedded within a more general northwest-southeast-oriented precipitation maximum. These local precipitation maxima were coincident with storm total rainfall shown in Figure 1-1. Eastern Iowa remained a locus of radar reflectivity that extended eastward into northern Illinois and intersected the main northwest-southeast precipitation axis.

Base reflectivity (BREF) snapshots from the WSR 88-D at a 0.5° elevation (Figure 2-17) help place the time-averaged 3HP and infrared satellite images in perspective. An east-west axis of reflectivity is depicted in the BREF image for 2315 UTC on July 17, which agrees with satellite and 3HP analyses. Three hours later, at 0240 UTC on July 18, the original east-west line of echoes drifted eastward into Indiana. It is also apparent that multiple convective development occurred over eastern Iowa, southern Wisconsin, and northern Illinois. A supercell was located east of Sterling, Illinois (SQI), and newly developing storms were tracking eastward from eastern Iowa into Illinois.

Although not evident from a single static radar image, individual reflectivity maxima were developing on the western edge of the northwest-southeast Wisconsin reflectivity axis and moving eastward across the main axis and then dissipating (Corfidi et al., 1966). The 05 UTC BREF image shows three distinct axes of reflectivity over the region. One axis was located in southwestern Wisconsin and oriented northwest-southeast. Along this axis individual reflectivity maxima were still forming on the western edge and merging with this axis as they progressed eastward. A second axis extended eastward from eastern Iowa across northern Illinois. Storms were continually forming in eastern Iowa and intensifying as they drifted eastward across northern Illinois and eventually merged into the northwest-southeast line south of Rockford. The third axis extended northeastward from southeast of SQI into the northwest-southeast axis. Radar echoes along this axis moved northeastward and merged into the northwest-southeast line. These axes were still apparent an hour later at 0605 UTC.

A transition of radar echo structure becomes evident between 0605 UTC and 0750 UTC on July 18 (Figure 2-18A and B). The various radar reflectivity axes coalesced into a more linear structure along a northwest-southeast axis across southern Wisconsin and northern Illinois by 0657 UTC. During this process, however, individual reflectivity maxima still moved from west to east, forming on the western edge of the main high reflectivity axis. In the next hour, the maximum reflectivity axis bends with the northern segment oriented more north-south and the southern segment oriented more east-west. Between 0657 and 0750 UTC, the northern axis began to progress eastward across southern Wisconsin, while the southern segment sank southward across northern Illinois. By 1058 UTC, the two segments weakened in intensity, and areal coverage of high

reflectivity echoes decreased. The northern segment continued to progress eastward while the southern segment progressed southward. The storm was ending.

The complicated radar echo behavior may be partially explained by an examination of the nocturnal evolution of the thermal, moisture, and wind fields. Figure 2-19 indicates that the surface warm front weakened during the night but remained oriented northwest-southeast with low θ_e values along the western shore of Lake Michigan. Although the axis of maximum θ_e progressed eastward across Minnesota during the night, the southeastern end of the gradient remained anchored to the west of the Chicago metropolitan area, suggesting the importance of Lake Michigan to the maintenance of the orientation of the surface warm front.

Low-level jet structure during the night played an important role for MCS and radar echo evolution. Figure 2-20 shows the evolution of the 1000 and 1500 m winds at wind profiler sites during the night and was augmented with rawinsonde winds from 925 and 850 mb at 12 UTC on July 18. The analysis indicates sustained warm air advection upstream of the convective line by virtue of a veering wind profile between the 1000 and 1500 m winds. During the night, the low-level jet strengthened to 25 m s^{-1} over Iowa and Wisconsin and veered to become more westerly. The veering of the low-level jet to a more westerly direction was evident throughout a deep layer in the low troposphere and was particularly pronounced in a time-height cross section at Blue River, Wisconsin, between 06 and 08 UTC (Figure 2-21A). Similar westward veering was evident at Winchester, Illinois, and Slater, Iowa, between 06 and 10 UTC.

Detailed structure of the low-level jet and its evolution during the event are available from 6-minute observations of the velocity azimuth wind profile (VWP) product from the WSR 88-D in Romeoville and displayed as multiple time-height cross sections (Figure 2-22). The cross sections show development of a 20 m s^{-1} low-level jet between 02 and 07 UTC with the maximum low-level jet occurring between 0430 and 0630 UTC. Rapid transition to a westerly low-level jet occurred between 06 and 08 UTC, and the low-level jet weakened rapidly between 07 and 08 UTC. Concomitant with the transition to the westerly low-level jet at Blue River, Wisconsin, the radar reflectivity assumed a more linear shape and bent into two portions. The northern portion progressed eastward and the southern portion progressed southward. The nearly simultaneous transition of radar reflectivity and low-level jet structure is suggestive of the important role the low-level jet played in determining radar echo development, movement, and the distribution of precipitation during this event.

Summary

Meteorological conditions during the heavy rainfall and severe flooding over northern Illinois on July 17-18, 1996, were conducive to the generation and maintenance of mesoscale convective systems. Their development over Iowa the previous night had saturated most of Iowa and provided sorely needed rains over northern Illinois. This water, in turn, evaporated during the morning and afternoon of July 17 to produce excessively high water vapor contents in the atmosphere. This served to strengthen the warm front that slowly advanced northeastward to a position just south of northern Illinois.

The development of easterly flow over northern Illinois transported cool, damp air from Lake Michigan into northern Illinois that anchored the surface warm front at its southern margin. The resulting atmospheric stability in the vicinity of the surface warm front was strongly unstable when

air parcels reached a thunderstorm initiation point that was located only one kilometer above the surface.

Development of the low-level jet at sunset led to an accelerating plume of slantwise ascending air along the warm front with high water vapor content. This slantwise ascending plume of moist air readily reached the thunderstorm initiation point at sunset and an initial supercell thunderstorm containing a tornado and large hail developed over northwest Illinois. The slantwise ascending moist plume strengthened further and led to development of an MCS.

The MCS exhibited multiple axes of thunderstorm development and movement over eastern Iowa, southwestern Wisconsin, and northern Illinois. Heavy rain-producing thunderstorms formed in eastern Iowa and strengthened as they moved eastward into northern Illinois. There they merged into the main northwest-southeast heavy precipitation axis that was oriented parallel to the surface warm front. Other heavy precipitation-producing thunderstorms formed in southwestern Wisconsin and traveled eastward to create the northwestern portion of the heavy precipitation axis. A separate line of storms formed in northern Illinois and progressed northeastward and merged with the heavy precipitation axis over the western suburbs of Chicago. As development of the MCS progressed during the night of July 17-18, the main northwest-southeast-oriented precipitation axis bent, forming a north-south segment and an east-west segment. The north-south segment remained in southern Wisconsin and progressed eastward, while the east-west segment sank southward across northern Illinois and the western suburbs of Chicago. The behavior of the MCS heavy precipitation line was the direct result of the westward veering of the low-level jet during the night. A few hours before sunrise on July 18, the two lines weakened and began to progress eastward, heralding the end of the rainstorm.

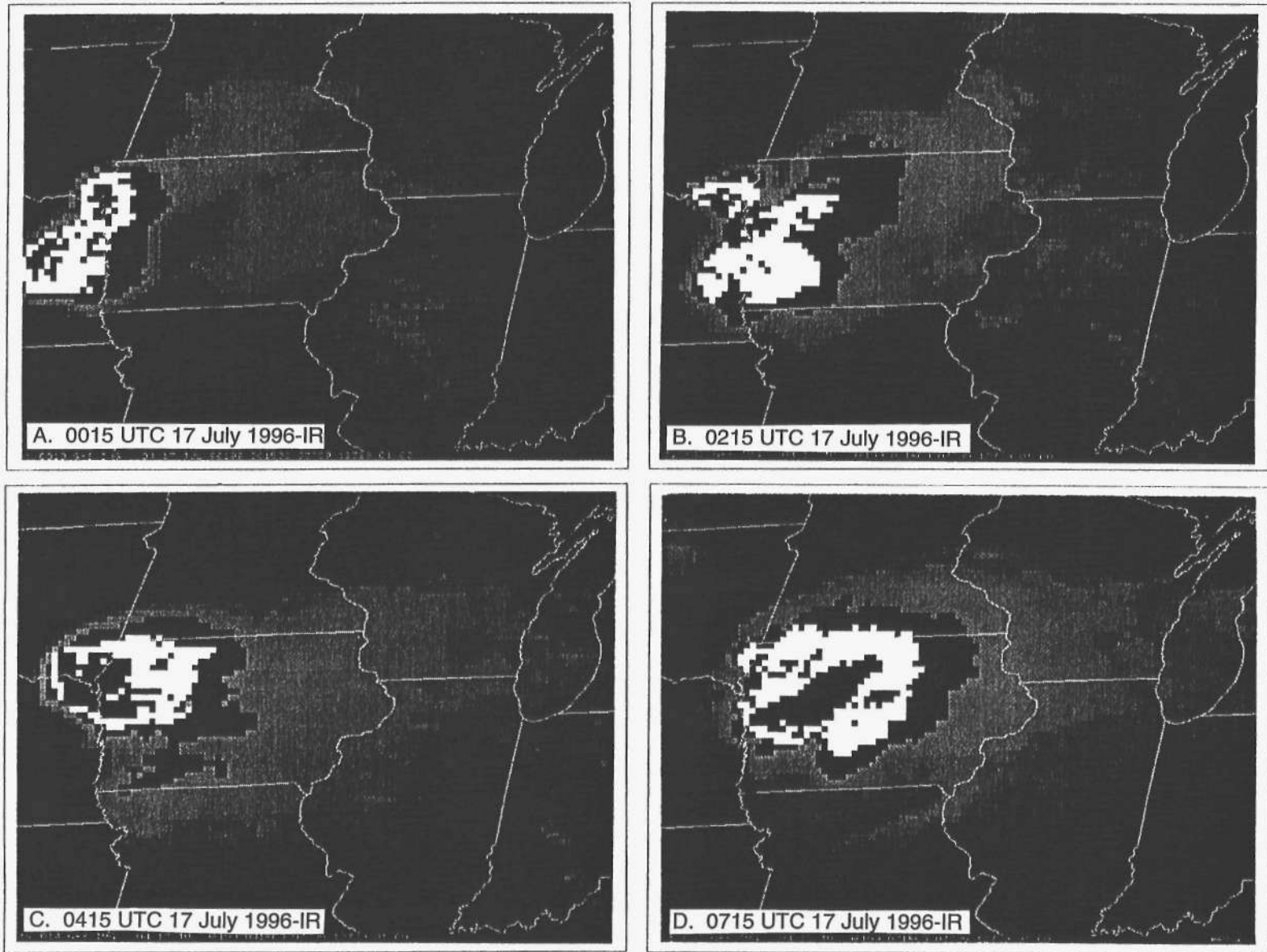
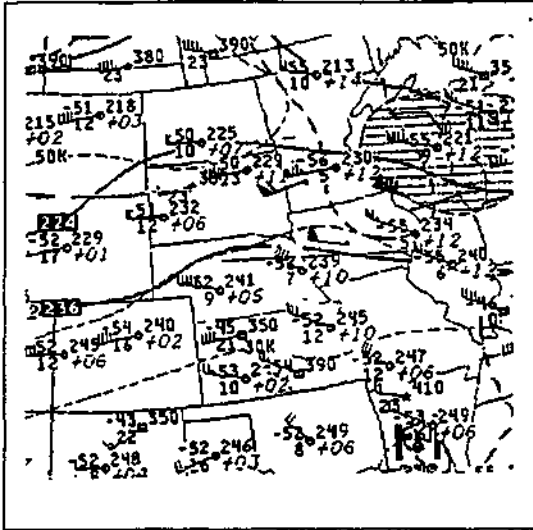
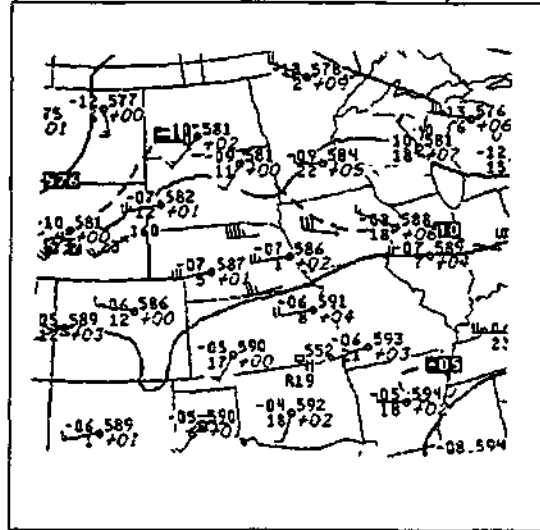


Figure 2-1. Infrared satellite images from GOES-8 taken on July 17,1996 at A) 0015 UTC, B) 0215 UTC , C) 0415 UTC, and D) 0715 UTC. Images were enhanced such that dark gray is -40 to -50°C, white is -50 to -60°C, and black is colder than -60°C.

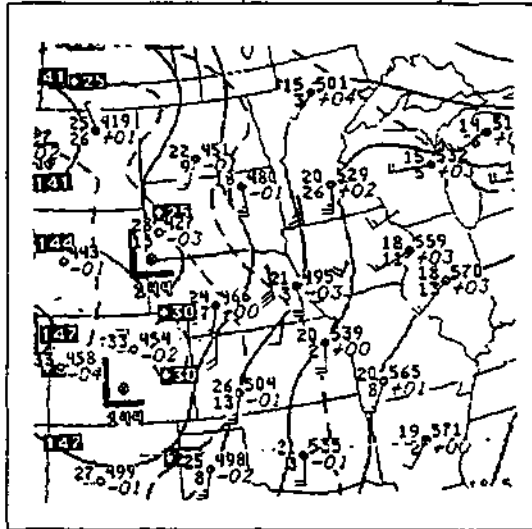
A. 200 mb Ht/Isotach 00 UTC 17 July 1996



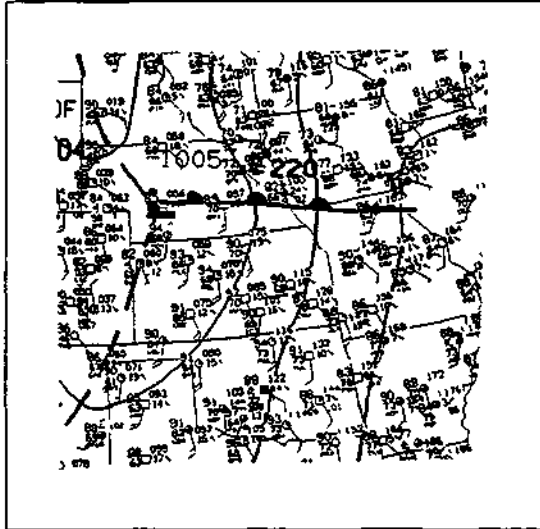
B. 500 mb Ht/Temp 00 UTC 17 July 1996



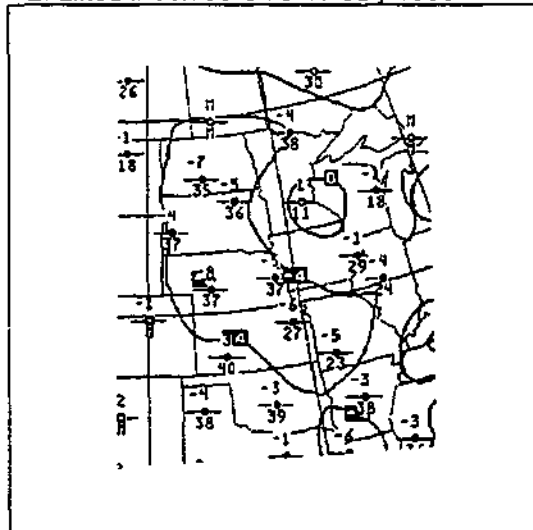
C. 850 mb Ht/Temp 00 UTC 17 July 1996



D. Sfc Anal 00 UTC 17 July 1996



E. Lifted Index 00 UTC 17 July 1996



F. PrecipWtr/%Norm 00 UTC 17 July 1996

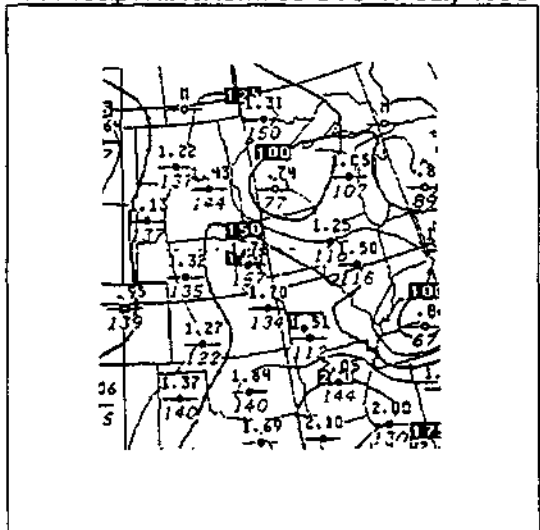


Figure 2-2. U.S. National Centers for Environmental Prediction Analyses for 00 UTC July 17, 1996 at A) 200 mb plot, heights (120 m interval), isotherms (5°C interval, dashed), and isotachs (20 knot interval shading greater than 70 knots), B) 500 mb plot, heights (60 m interval), isotherms (5°C interval, dashed), C) 850 mb plot, heights (30 m interval), isotherms (5°C interval, dashed), wind profiler wind barbs added, D) surface analysis of mean-sea-level-pressure (4 mb) and fronts with temperature and dewpoints in °F, E) lifted and K indexes (°C, lifted is contoured such that lifted is plotted as the numerator and K index is the denominator, and F) precipitable water (inches plotted as numerator, contoured every 0.25 inches) and precipitable water percent of normal (percent, plotted as denominator). A wind barb pennant is 50 knots (25 m s^{-1}), a full barb is 10 knots (5 m s^{-1}), and a half barb is 5 knots (2.5 m s^{-1}).

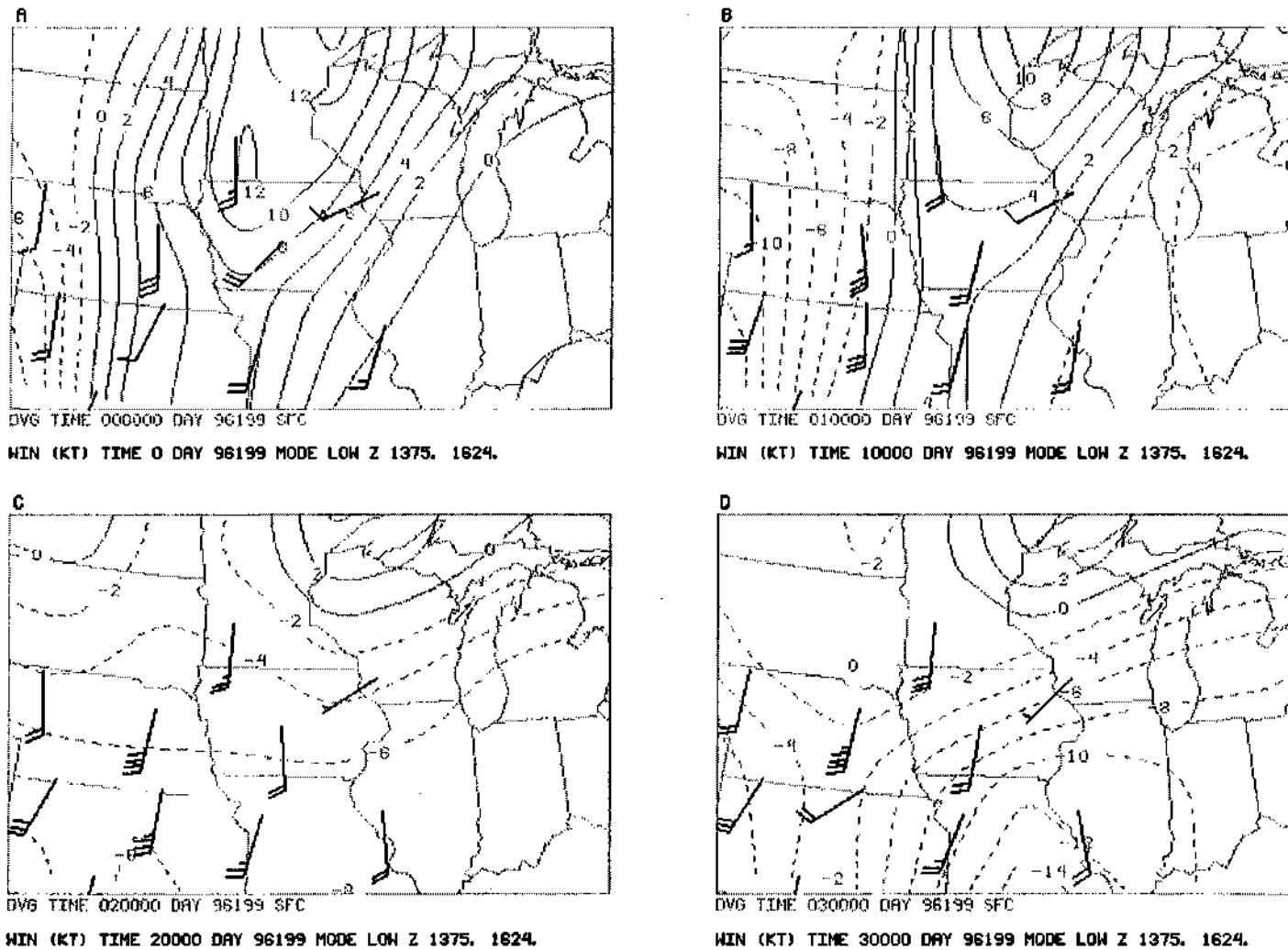


Figure 2-3. Wind profiler plots and contours of divergence diagnosed from profiler winds (contoured every 10^{-6} s^{-1}) for July 17, 1996 at A) 00 UTC, B) 01 UTC, C) 02 UTC, and D) 03 UTC. Wind barbs are plotted such that a pennant is 50 knots (25 m s^{-1}), a full barb is 10 knots (5 m s^{-1}), and a half barb is 5 knots (2.5 m s^{-1}).

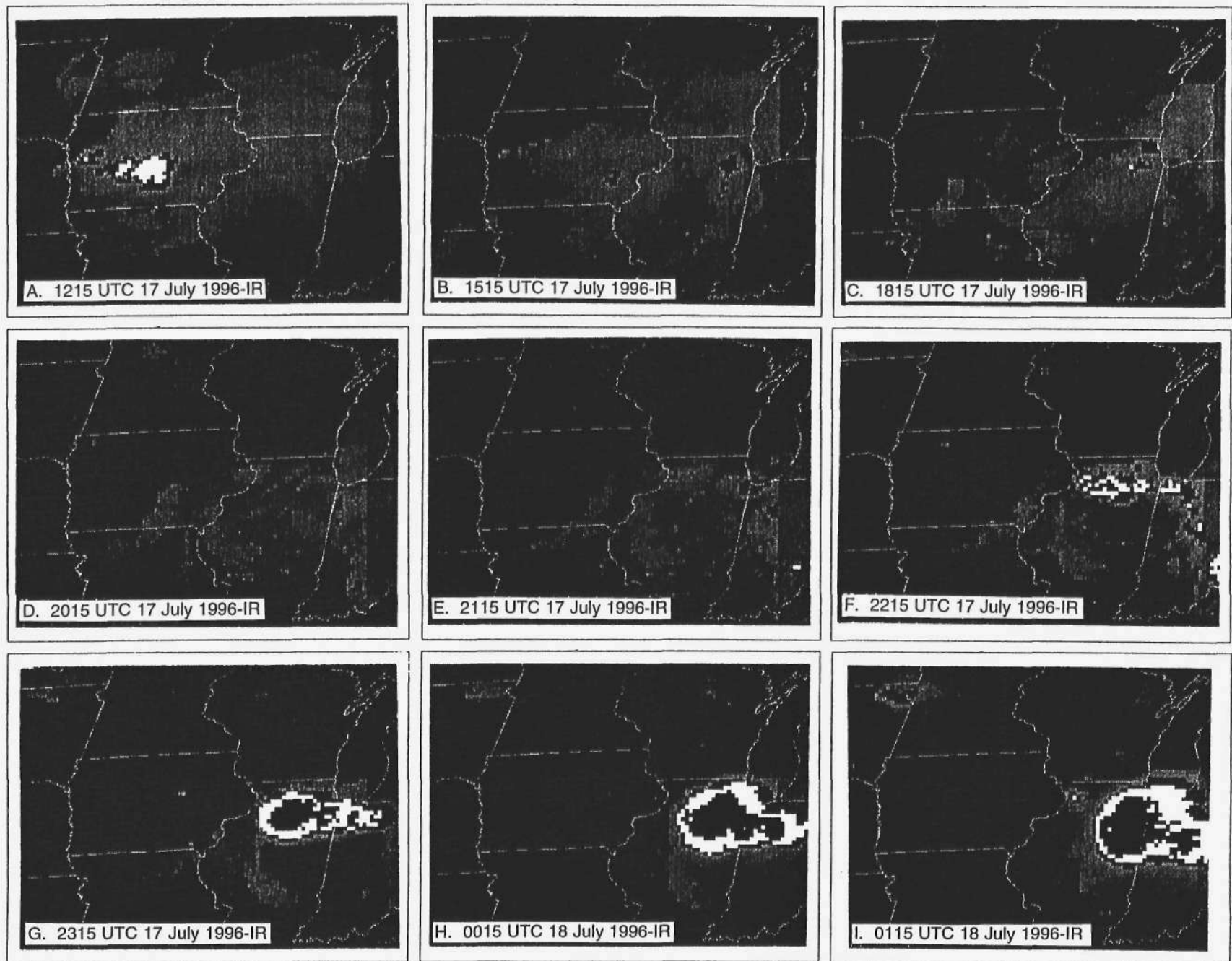


Figure 2-4. Infrared satellite images from GOES-8 on July 17-18,1996 at A) 1215 UTC, B) 1515 UTC , C) 1815 UTC, D) 2015 UTC, E) 2115 UTC, F) 2215 UTC, G) 2315 UTC, H) 0015 UTC on July 18, and I) 0115 UTC on July 18. Images are enhanced such that dark gray is -40 to -50°C, white is -50 to -60°C, and black is colder than -60°C.

Figure 2-5. U.S. National Centers for Environmental Prediction Analyses for 12 UTC July 17, 1996 at A) 200 mb plot, heights (120 m interval), isotherms (5°C interval, dashed), and isotachs (20 knot interval shading greater than 70 knots), B) 500 mb plot, heights (60 m interval), isotherms (5°C interval, dashed), C) 850 mb plot, heights (30 m interval), isotherms (5°C interval, dashed), wind profiler wind barbs added, D) Surface analysis of mean-sea-level-pressure (4 mb) and fronts with temperature and dewpoints in °F, and E) mesoscale surface analysis at 12 UTC July 17, 1996. Winds and temperature (°F) are plotted, isodrosotherms contoured dashed every 2°F and altimeter setting converted to millibars contoured light solid every 1 mb, and F) Left: Lifted and K indexes (°C, lifted is contoured) such that lifted is plotted as the numerator and K index the denominator. Right: precipitable water (inches, plotted as numerator, contoured every 0.25 inches) and precipitable water percent of normal (percent, plotted as denominator). Wind barbs are plotted such that a pennant is 50 knots (25 m s^{-1}), a full barb is 10 knots (5 m s^{-1}), and a half barb is 5 knots (2.5 m s^{-1}).

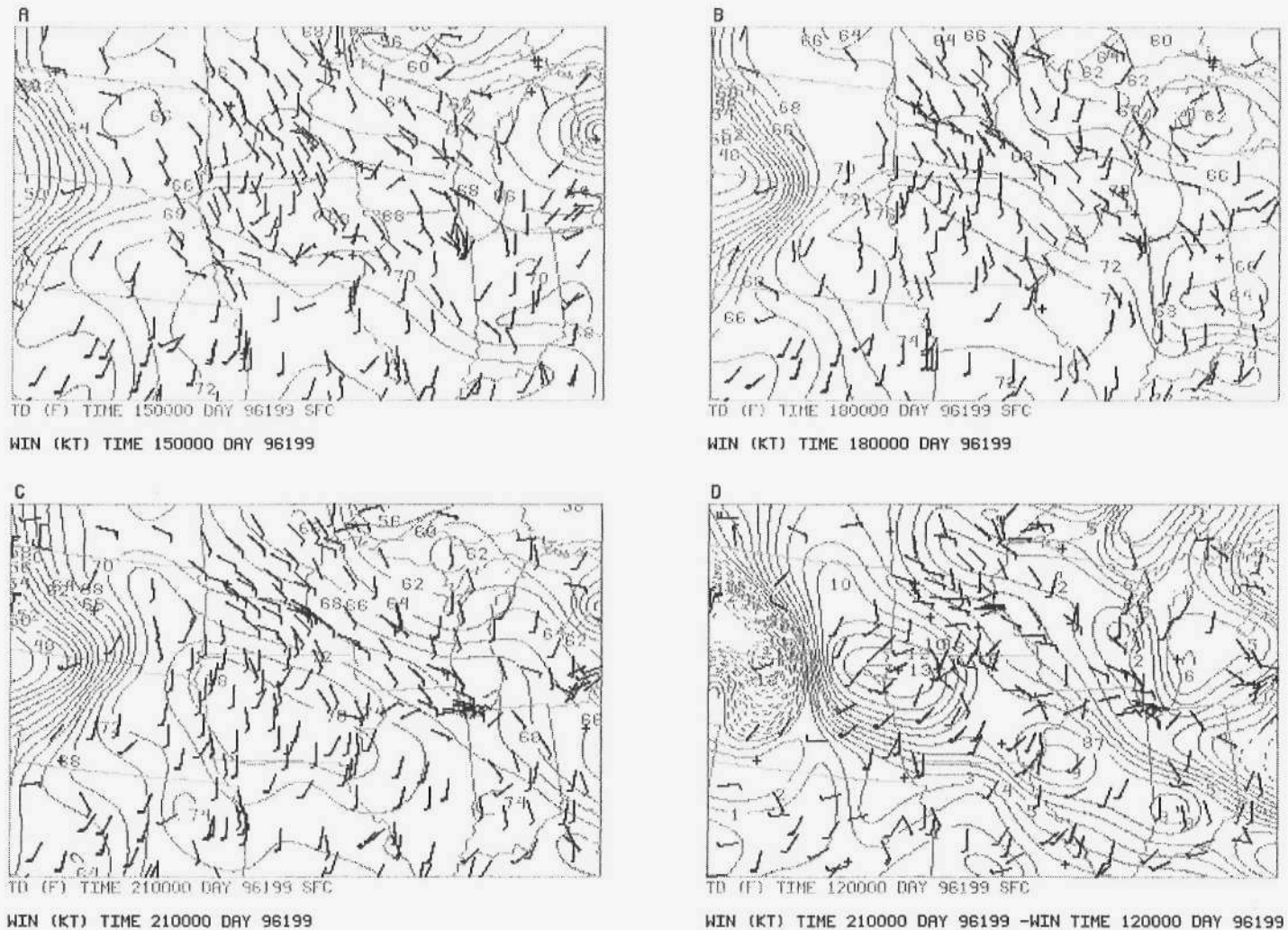
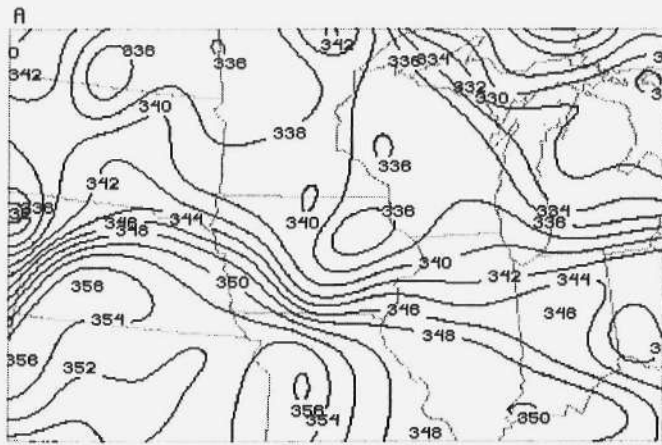
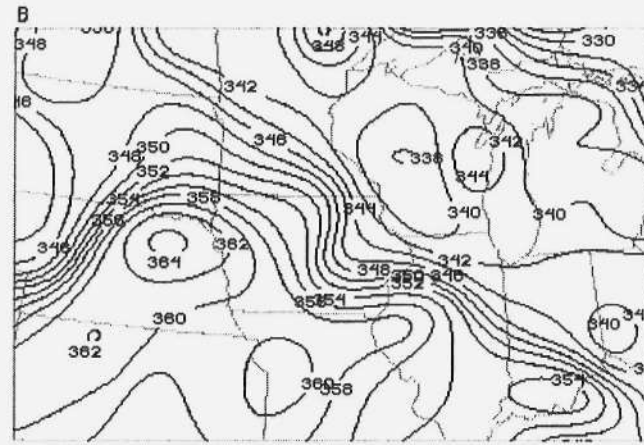


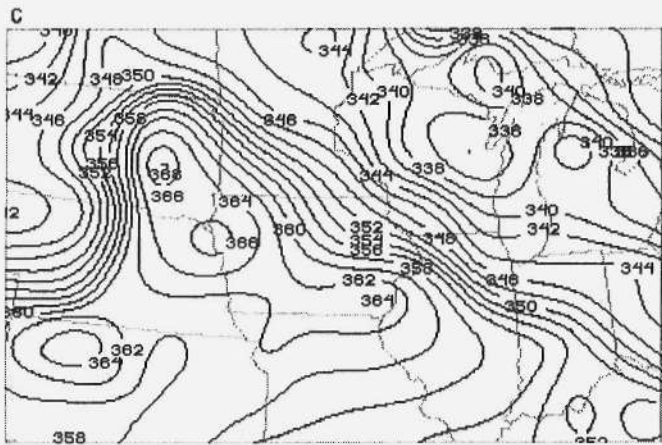
Figure 2-6. Surface mesoanalyses of wind [barbs are plotted such that a pennant is 50 knots (25 m s^{-1}), a full barb is 10 knots (5 m s^{-1}), and a half barb is 5 knots (2.5 m s^{-1})] and dewpoint temperature (solid contours every 2°F) for July 17, 1996 at A) 15 UTC, B) 18 UTC, C) 21 UTC, and D) vector wind difference (plotted as barbs with same convention as above) and dewpoint difference (contoured every 1°F , negative values are dashed) for 21-12 UTC.



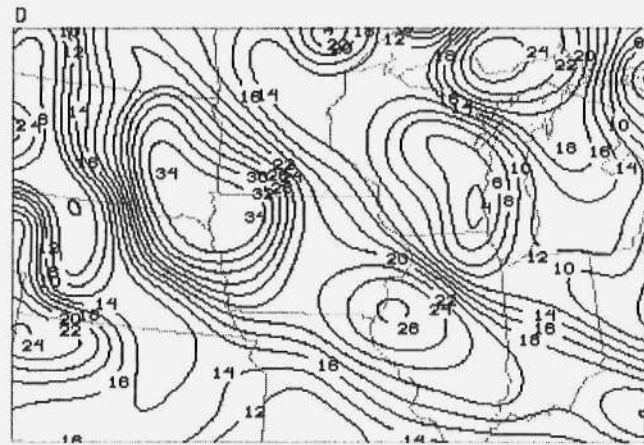
THRE (K) TIME 150000 DAY 96199 SFC



THRE (K) TIME 180000 DAY 96199 SFC

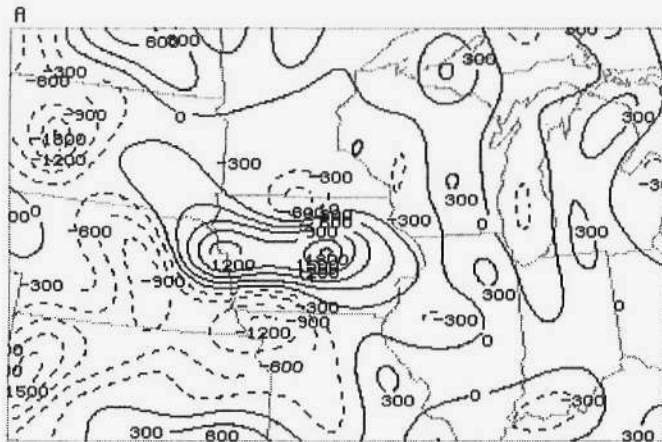


THRE (K) TIME 210000 DAY 96199 SFC

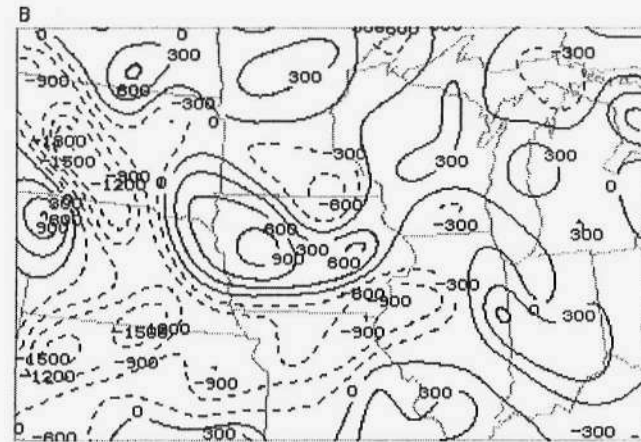


THRE (K) TIME 120000 DAY 96199 SFC

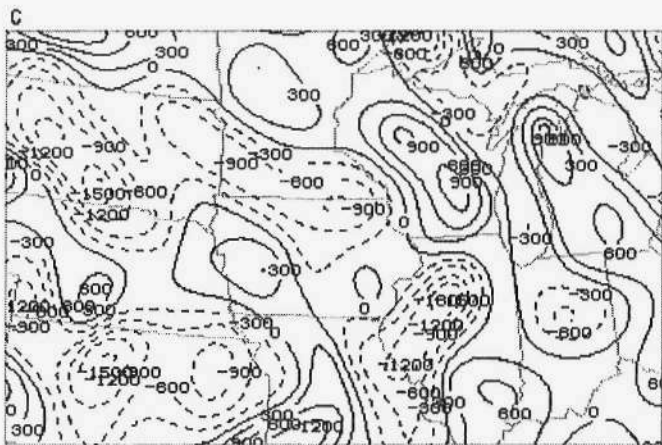
Figure 2-7. Surface mesoanalyses of equivalent potential temperature (contoured every 2K) on July 17, 1996 at A) 15 UTC, B) 18 UTC, C) 21 UTC, and D) equivalent potential temperature difference for 21-12 UTC.



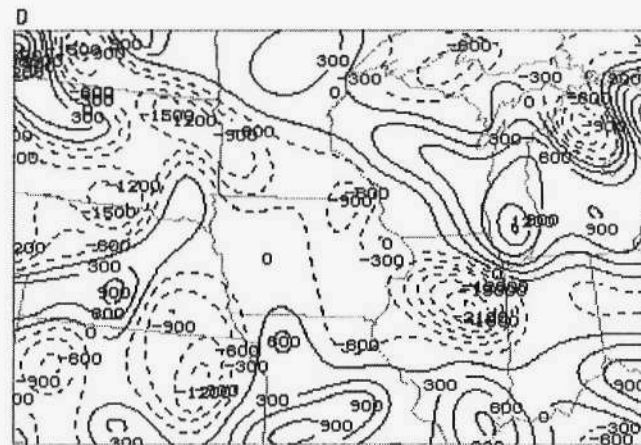
TDVG TIME 120000 DAY 96199 SFC



TDVG TIME 150000 DAY 96199 SFC



TDVG TIME 180000 DAY 96199 SFC



TDVG TIME 210000 DAY 96199 SFC

Figure 2-8. Equivalent potential temperature flux divergence (contoured every 300 K day⁻¹, dashed is convergence) on July 17, 1996 at A) 12 UTC, B) 15 UTC, C) 18 UTC, and D) 21 UTC.

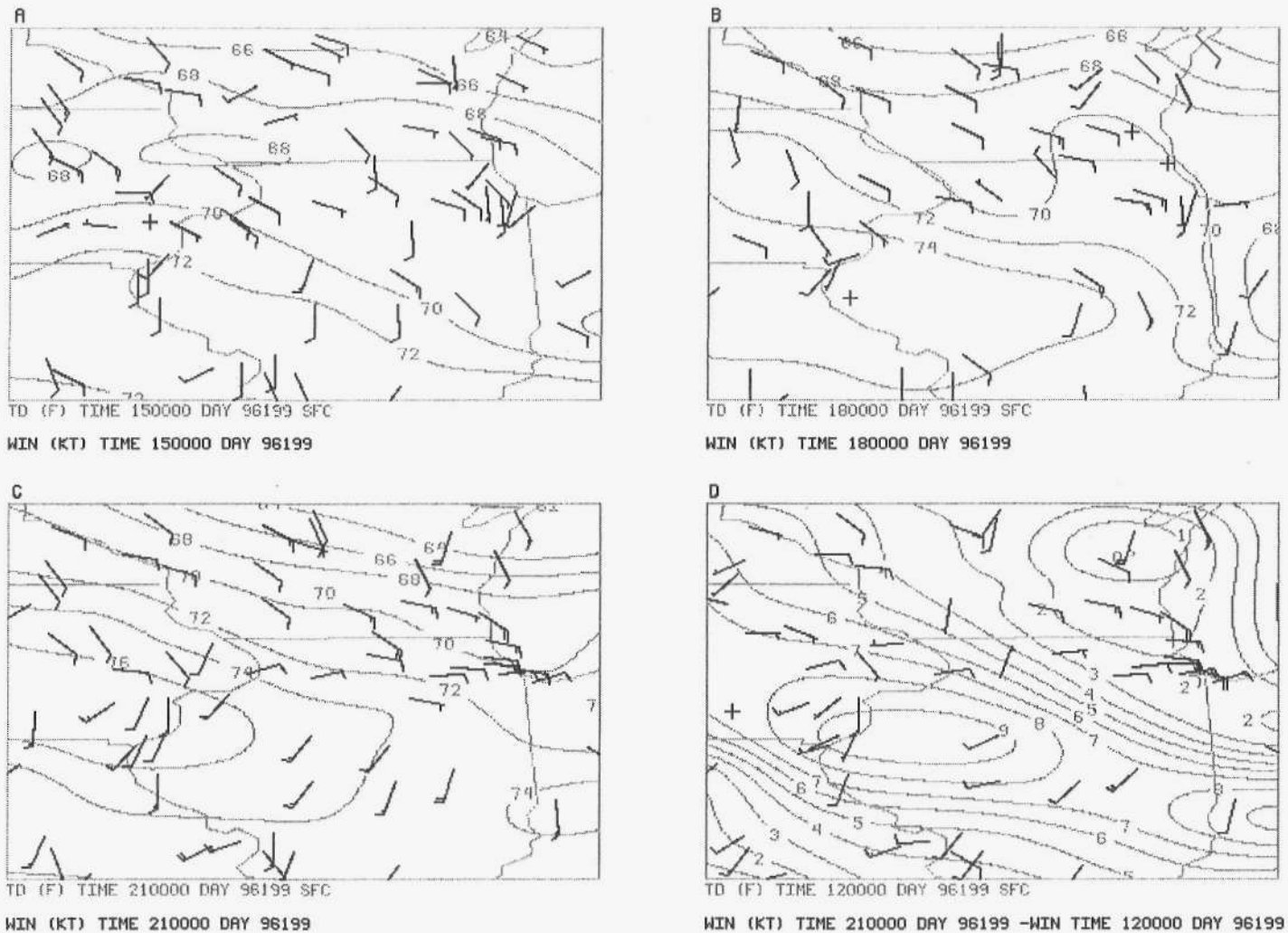
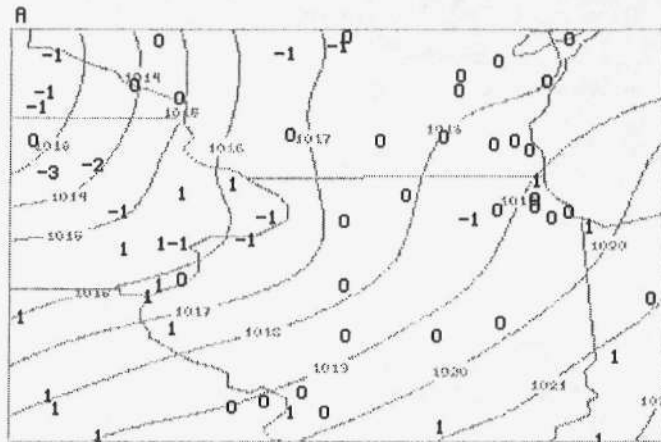
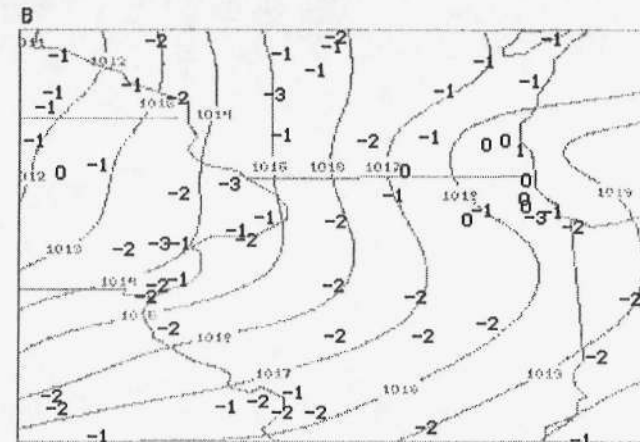


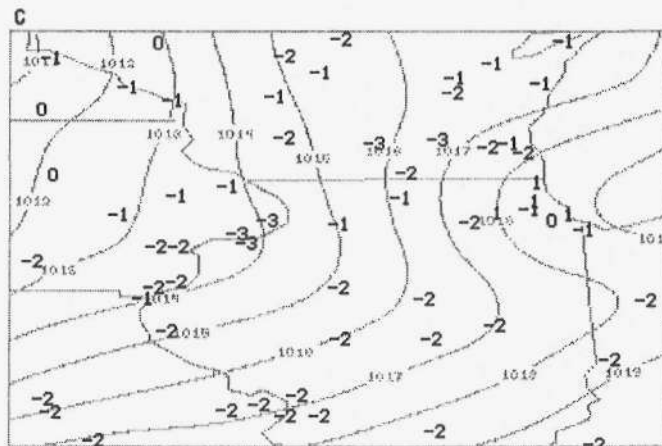
Figure 2-9. Detailed surface mesoanalyses of wind and dewpoint over northern Illinois and adjacent states for July 17, 1996 at A) 15 UTC, B) 18 UTC, C) 21 UTC, and D) vector wind difference (plotted as barbs with same convention as above) and dewpoint difference (contoured every 1 °F, negative values are dashed) for 21-12 UTC. Wind barbs are plotted such that a pennant is 50 knots (25 m s^{-1}), a full barb is 10 knots (5 m s^{-1}), and a half barb is 5 knots (2.5 m s^{-1}). Dewpoint temperature is contoured solid every 2°F.



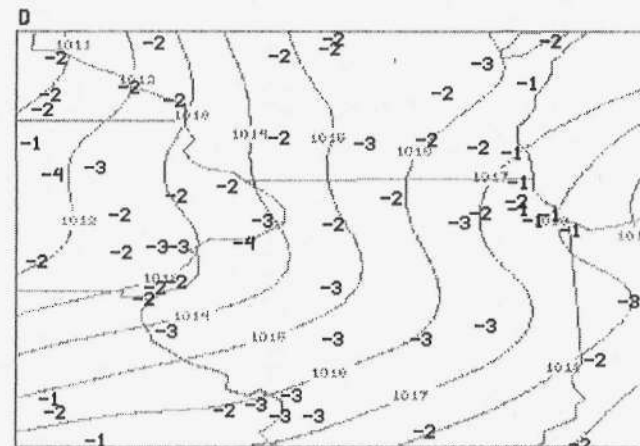
PSL (MB) TIME 150000 DAY 96199 @PSL TIME 120000 DAY 96199



PSL (MB) TIME 190000 DAY 96199 @PSL TIME 150000 DAY 96199



PSL (MB) TIME 200000 DAY 96199 @PSL TIME 170000 DAY 96199



PSL (MB) TIME 210000 DAY 96199 @PSL TIME 120000 DAY 96199

Figure 2-10. Plots of altimeter setting tendencies ($\text{mb } 3\text{h}^{-1}$) and contours of altimeter setting (every 1 mb) for July 17-18, 1996 at A) 15-12 UTC, B) 19-15 UTC (tendency units: $\text{mb } 4\text{h}^{-1}$), C) 20-17 UTC, and D) 21-12 UTC (tendency units: $\text{mb } 9\text{h}^{-1}$).

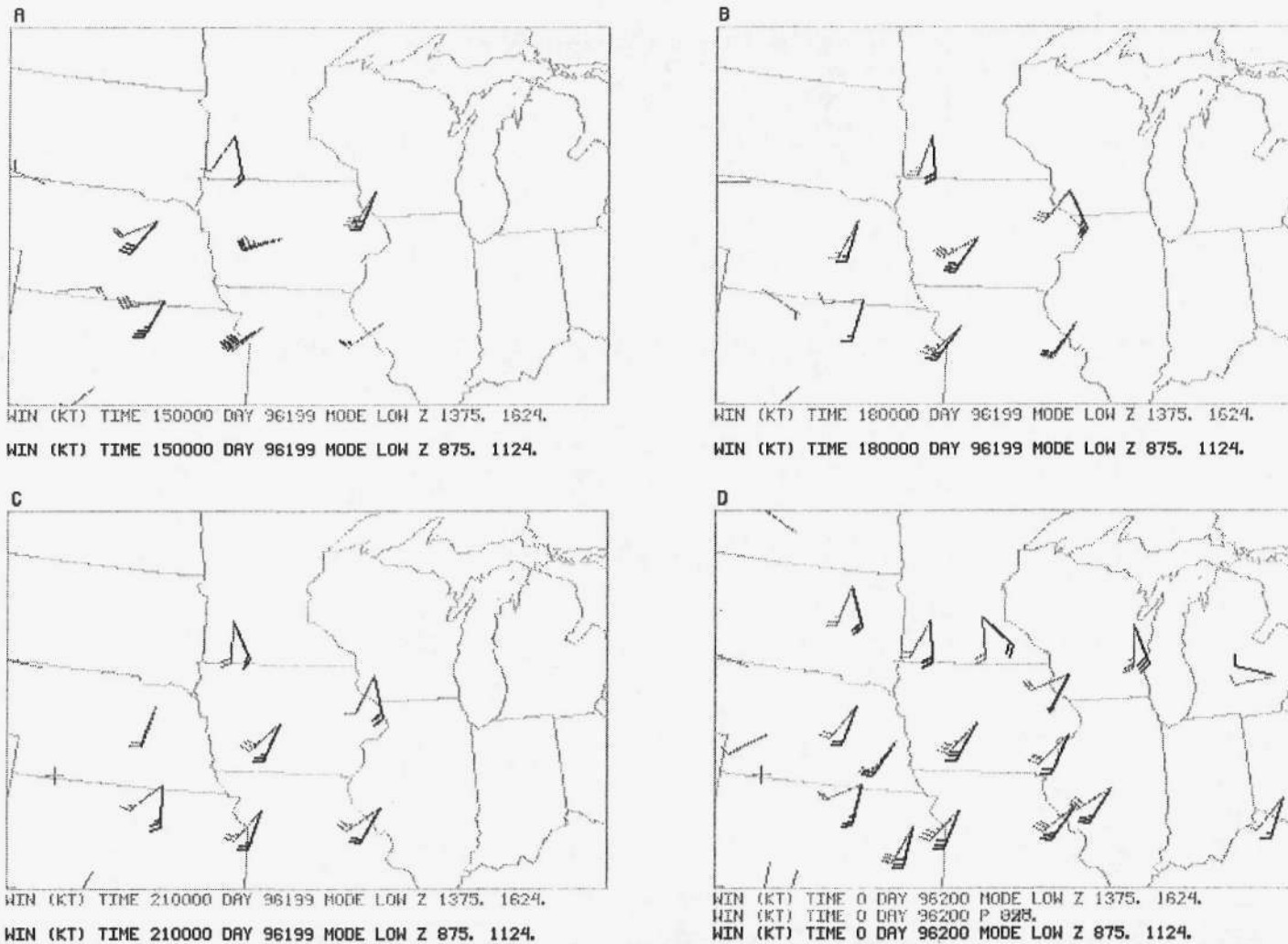
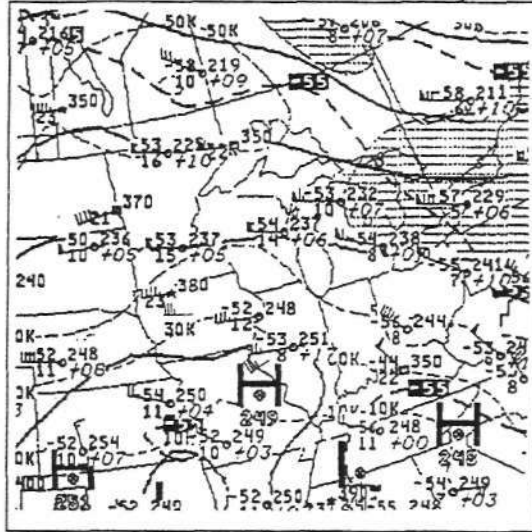
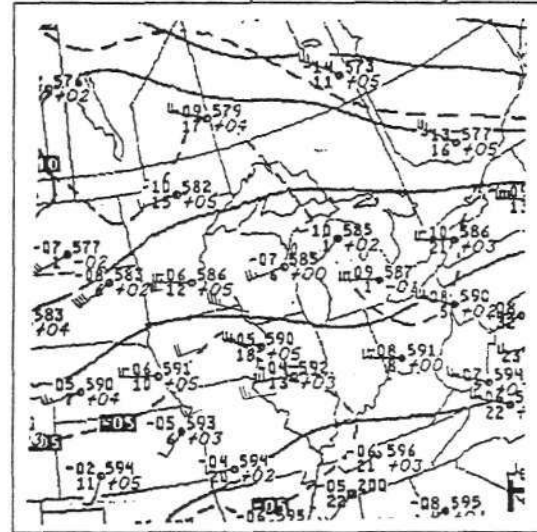


Figure 2-11. Plots of wind profiler observations and rawinsonde winds for July 17-18,1996 at A) 15 UTC, B) 18 UTC, C) 21 UTC, and D) 00 UTC on July 18, which includes rawinsonde winds at 850 mb. Wind barbs are plotted such that a pennant is 50 knots (25 m s^{-1}), a full barb is 10 knots (5 m s^{-1}), and a half barb is 5 knots (2.5 m s^{-1}). At profiler stations 1000 m winds are black and 1500 m winds are gray. At raob stations, 925 mb winds are black and 850 mb winds are gray.

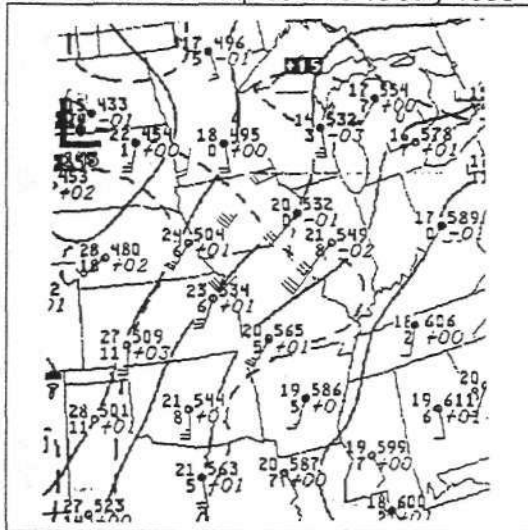
A. 200 mb Ht/Isotach 00 UTC 18 July 1996



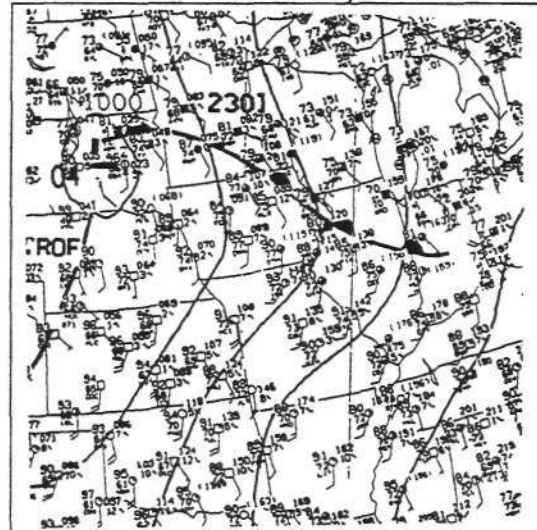
B. 500 mb Ht/Temp 00 UTC 18 July 1996



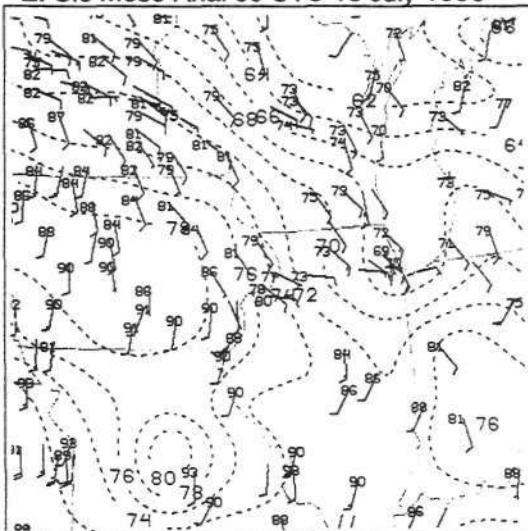
C. 850 mb Ht/Temp 00 UTC 18 July 1996



D. Sfc Anal 00 UTC 18 July 1996



E. Sfc Meso Anal 00 UTC 18 July 1996



F. LI, PW, %Norm 00 UTC 18 July 1996

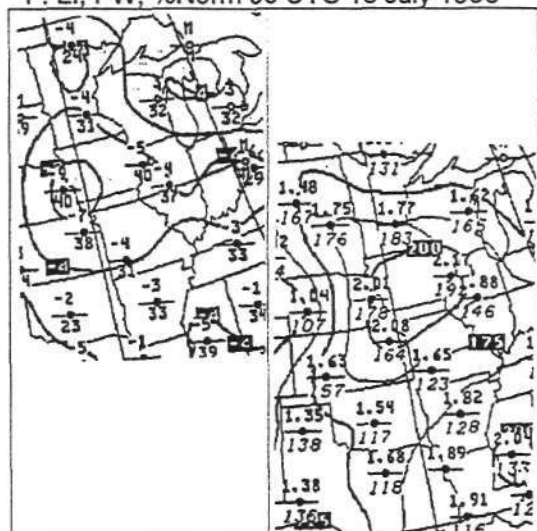


Figure 2-12. U.S. National Centers for Environmental Prediction Analyses for 00 UTC July 18, 1996 at A) 200 mb plot, heights (120 m interval), isotherms (5°C interval, dashed), and isotachs (20 knot interval shading greater than 70 knots), B) 500 mb plot, heights (60 m interval), isotherms (5°C interval, dashed), C) 850 mb plot, heights (30 m interval), isotherms (5°C interval, dashed), wind profiler wind barbs added, D) surface analysis of mean-sea-level-pressure (4 mb) and fronts with temperature and dewpoints in °F, and E) Mesoscale surface analysis at 12 UTC July 17, 1996. Winds and temperature (°F) are plotted and isodrosotherms contoured dashed every 2°F, F) Left: Lifted and K indexes (°C, lifted is contoured) such that lifted is plotted as the numerator and K index the denominator. Right: precipitable water (inches, plotted as numerator, contoured every 0.25 inches) and precipitable water percent of normal (percent, plotted as denominator). Wind barbs are plotted such that a pennant is 50 knots (25 m s^{-1}), a full barb is 10 knots (5 m s^{-1}), and a half barb is 5 knots (2.5 m s^{-1}).

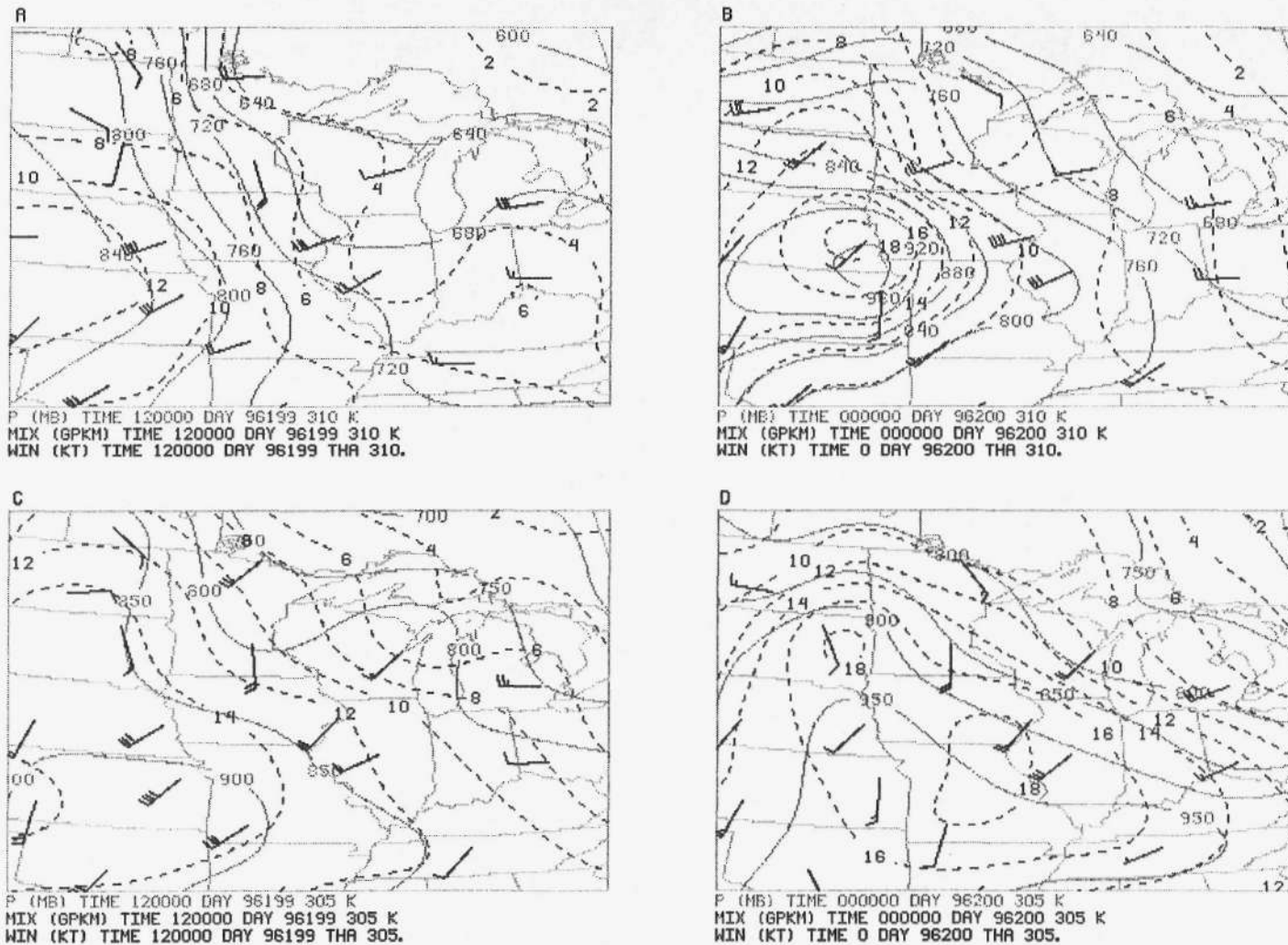
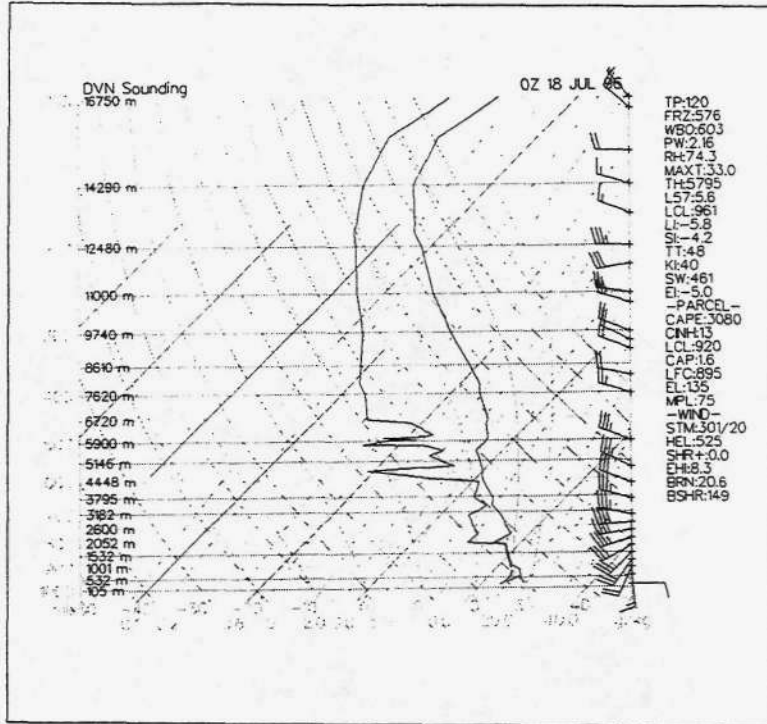


Figure 2-13. Isentropic analyses of pressure (solid, every 40 mb), mixing ratio (dashed, every 2 g kg^{-1}) for A) 310K at 12 UTC July 17, B) 310K at 00 UTC July 18, C) 305K at 12 UTC July 17, and D) 305K at 00 UTC July 18. Wind barbs are plotted such that a pennant is 50 knots (25 m s^{-1}), a full barb is 10 knots (5 m s^{-1}), and a half barb is 5 knots (2.5 m s^{-1}). Wind profiler observations were interpolated using isentropic pressure, raob soundings to determine height, and time-height cross sections of wind profiler observations.

A. Davenport, IA 74455 00 UTC 18 July 1996



B. Lincoln, IL 74560 00 UTC 18 July 1996

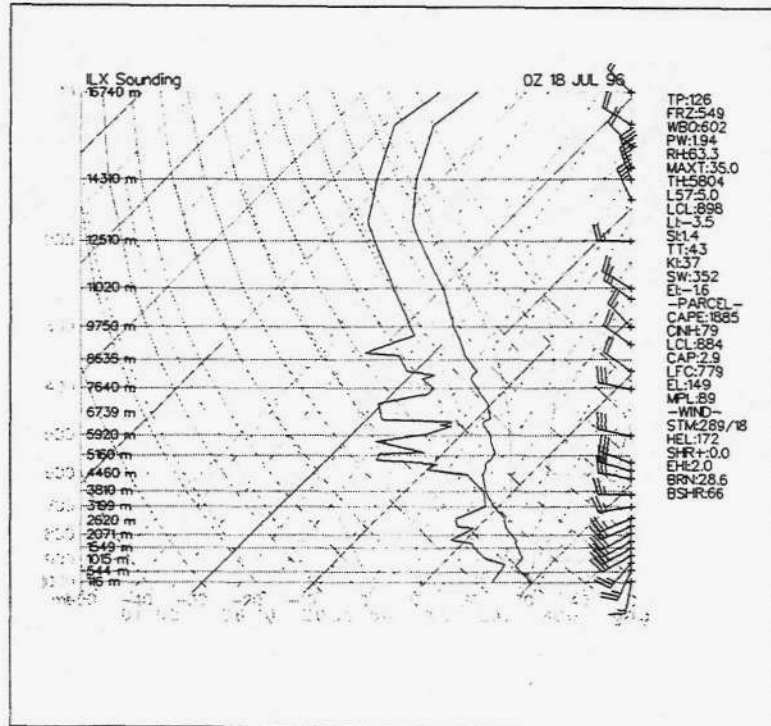


Figure 2-14. SkewT-LogP sounding analysis for 00 UTC July 18, 1996 for A) Davenport, Iowa (DVN, 74455) and B) Lincoln, Illinois (ILX, 74560). Parcel analysis is based on thermodynamic profiles in the lowest 100 mb. Wind barbs are plotted such that a pennant is 50 knots (25 m s^{-1}), a full barb is 10 knots (5 m s^{-1}), and a half barb is 5 knots (2.5 m s^{-1}).

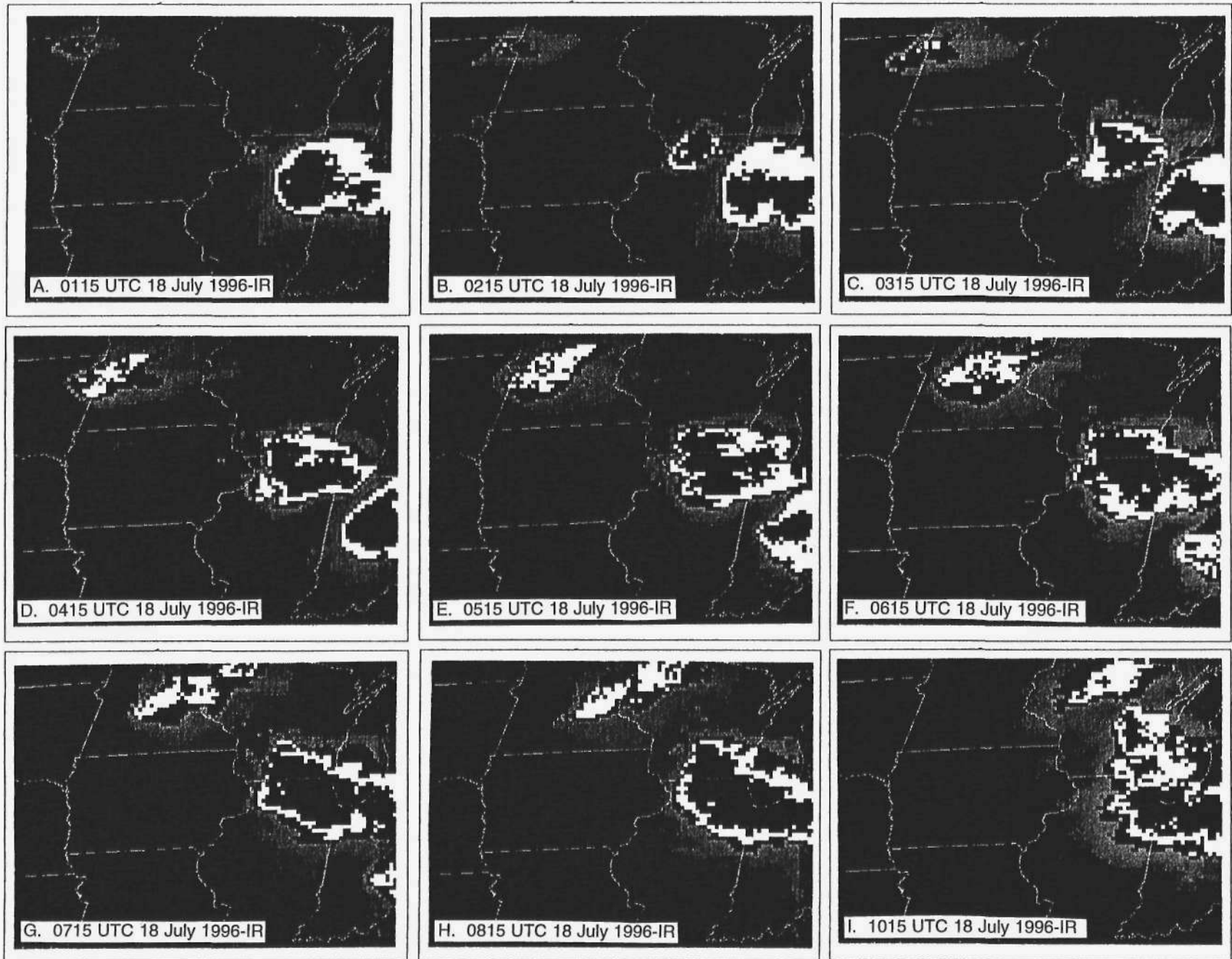
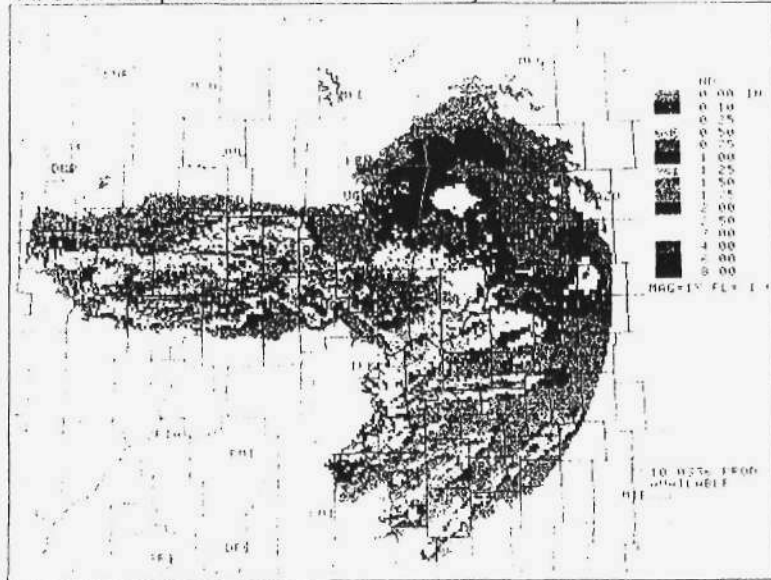
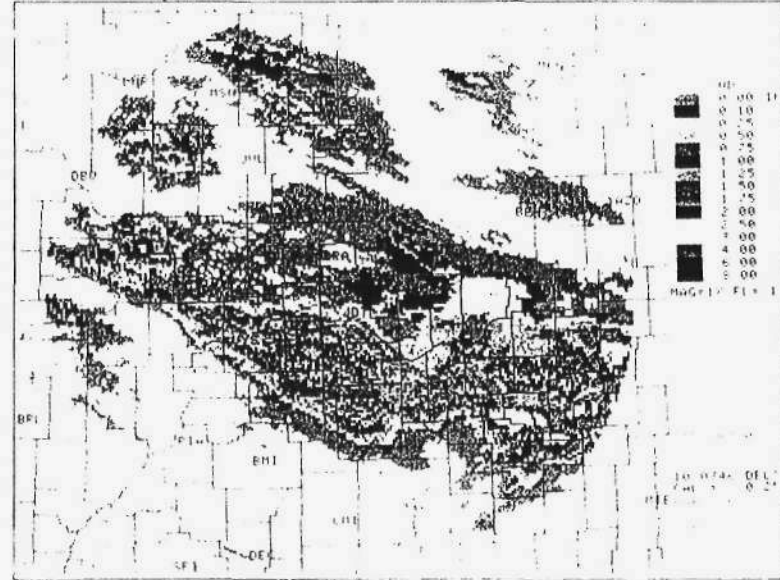


Figure 2-15. Infrared satellite images from GOES-8 on July 18, 1996 at A) 0115 UTC, B) 0215 UTC, C) 0315 UTC, D) 0415 UTC, E) 0515 UTC, F) 0615 UTC, G) 0715 UTC, H) 0815 UTC, and I) 1015 UTC. Images are enhanced such that dark gray is -40 to -50°C , white is -50 to -60°C and black is colder than -60°C .

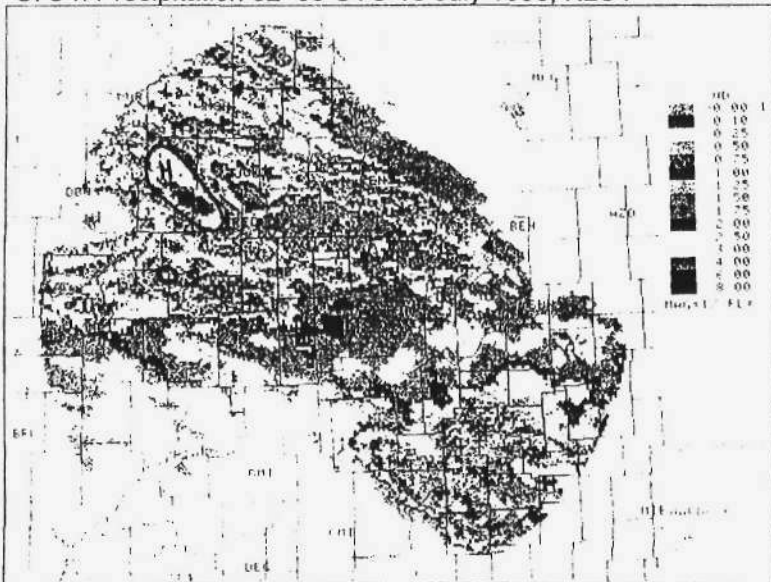
A. 3-h Precipitation 20–23 UTC 17 July 1996; KLOT



B. 3-h Precipitation 23–02 UTC 17-18 July 1996; KLOT



C. 3-h Precipitation 02–05 UTC 18 July 1996; KLOT



D. 3-h Precipitation 05–08 UTC 18 July 1996; KLOT

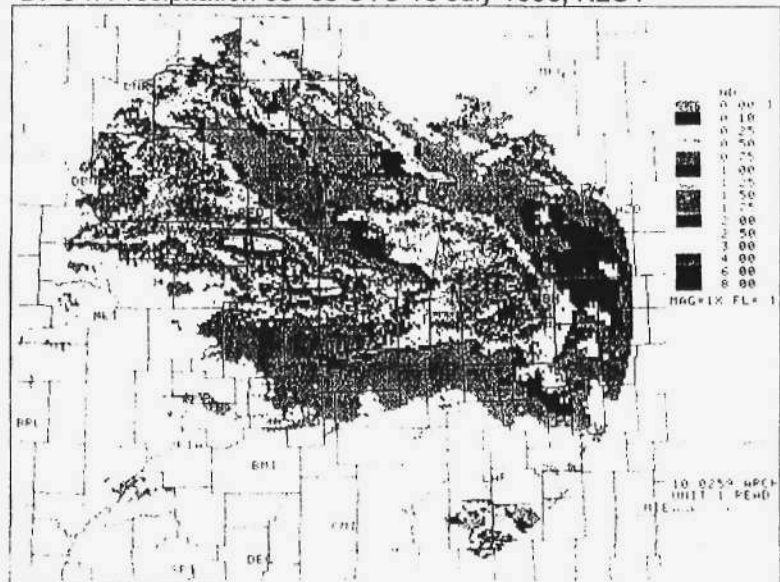
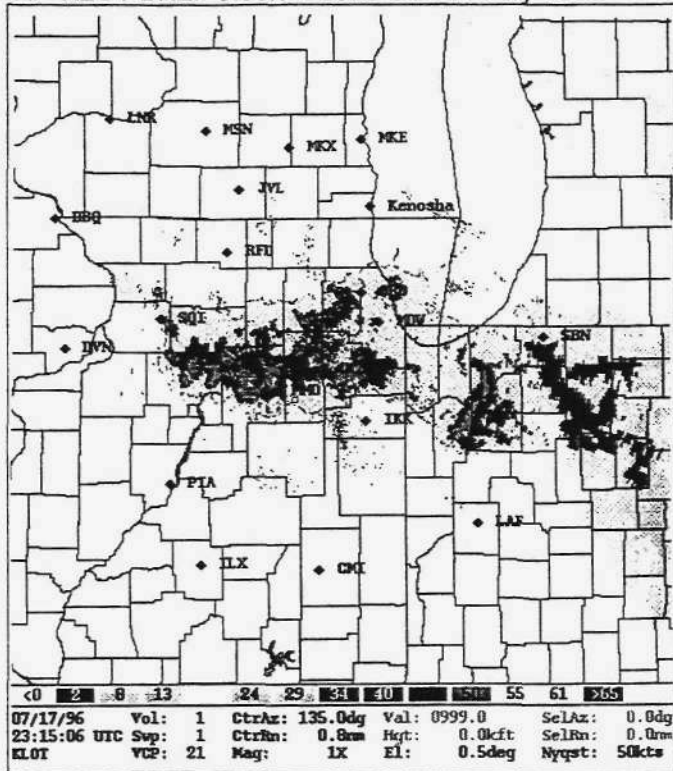
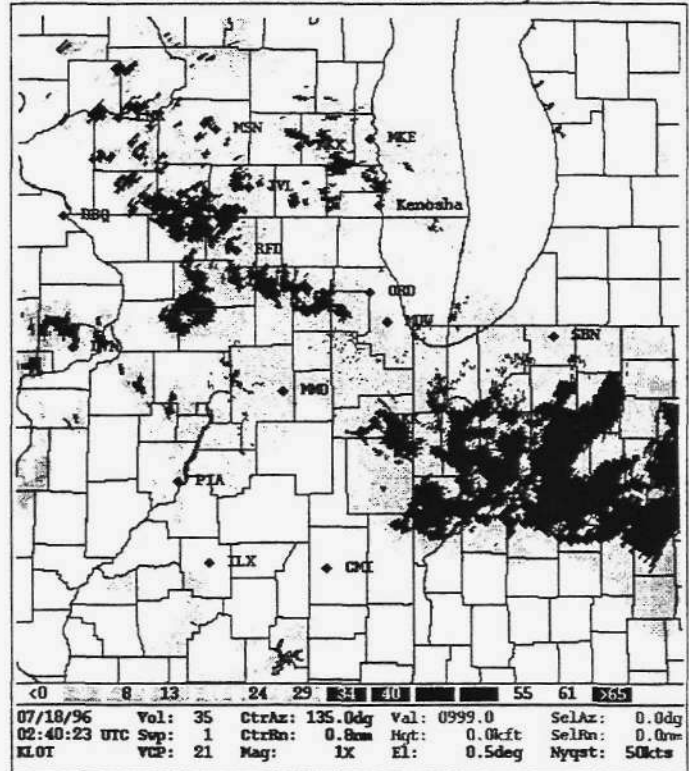


Figure 2-16. 3-hour accumulated precipitation (inches) from the Chicago, Illinois WSR-88-D at Romeoville, IL (KLOT) on July 17-18, 1996: A) 20-23 UTC July 17, B) 23-02 UTC July 17-18, C) 02-05 UTC July 18, and D) 05-08 UTC July 18.

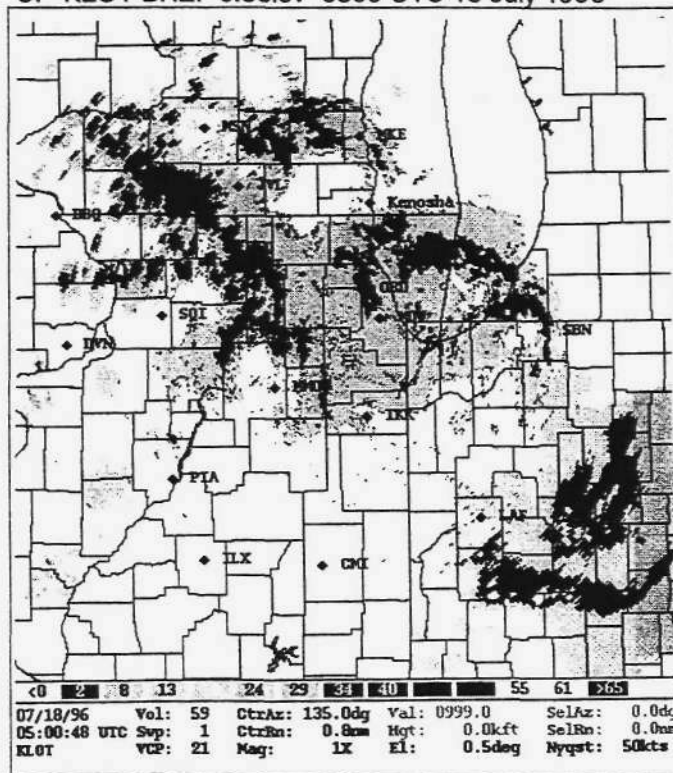
A. KLOT BREF 0.5elev 2315 UTC 17 July 1996



B. KLOT BREF 0.5elev 0240 UTC 18 July 1996



C. KLOT BREF 0.5elev 0500 UTC 18 July 1996



D. KLOT BREF 0.5elev 0605 UTC 18 July 1996

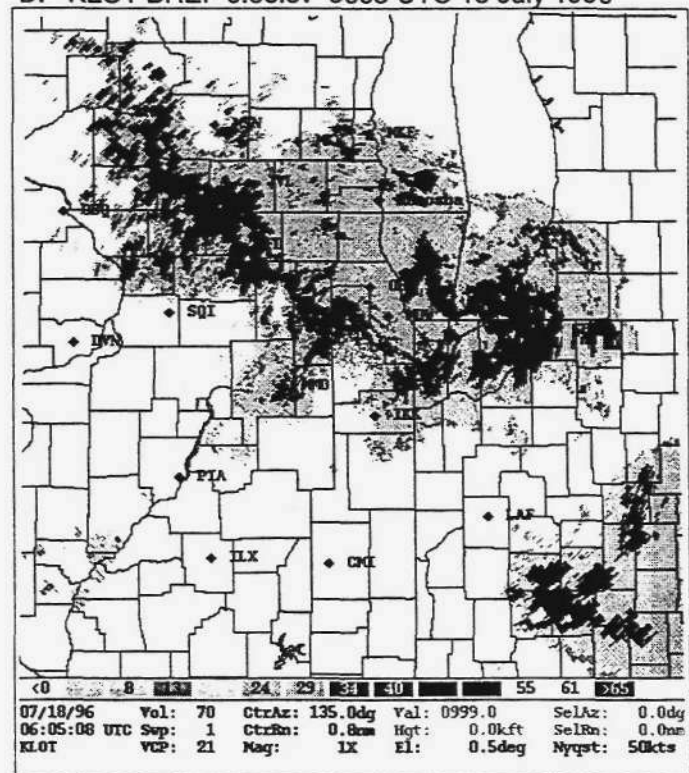
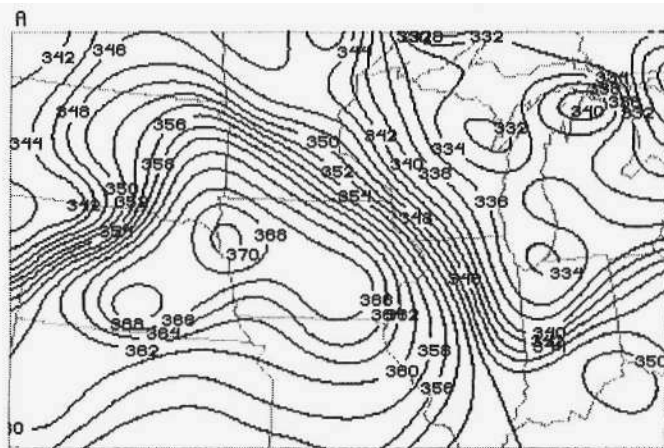
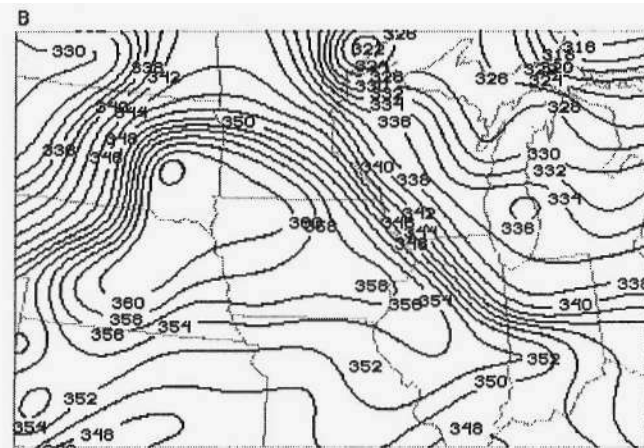


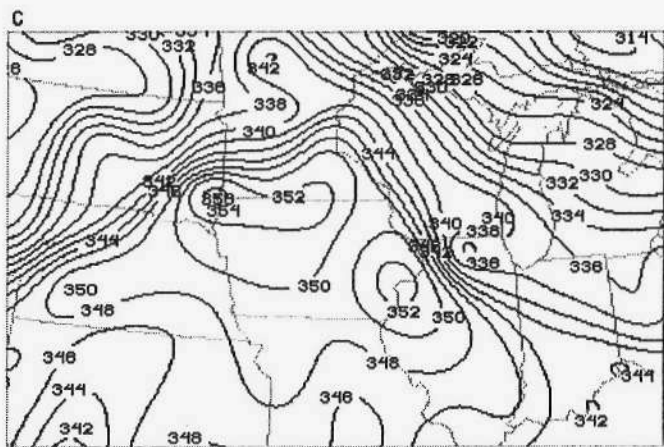
Figure 2-17. Base reflectivity at 0.5 elevation angle (dbZ) from the Chicago, Illinois WSR-88-D at Romeoville, Illinois (KLOT) on July 17-18, 1996. A) 2315 UTC July 17, B) 0240 UTC July 18, C) 0500 UTC July 18, and D) 0605 UTC July 18.



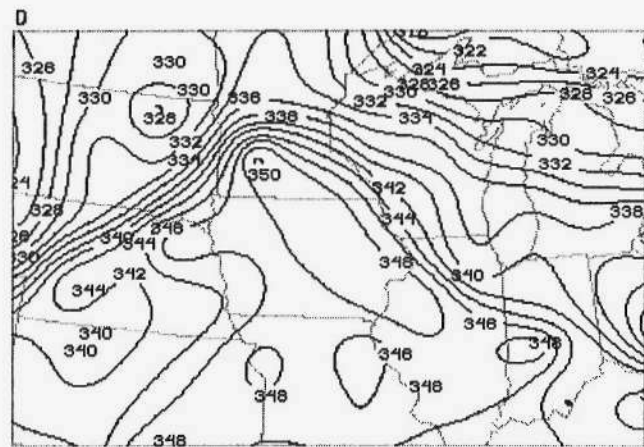
THRE (K) TIME 000000 DAY 96200 SFC



THRE (K) TIME 040000 DAY 96200 SFC



THRE (K) TIME 080000 DAY 96200 SFC



THRE (K) TIME 120000 DAY 96200 SFC

Figure 2-19. Surface mesoanalyses of equivalent potential temperature (contoured every 2K) on July 18, 1996 at A) 00 UTC, B) 04 UTC, C) 08 UTC, and D) 12 UTC.

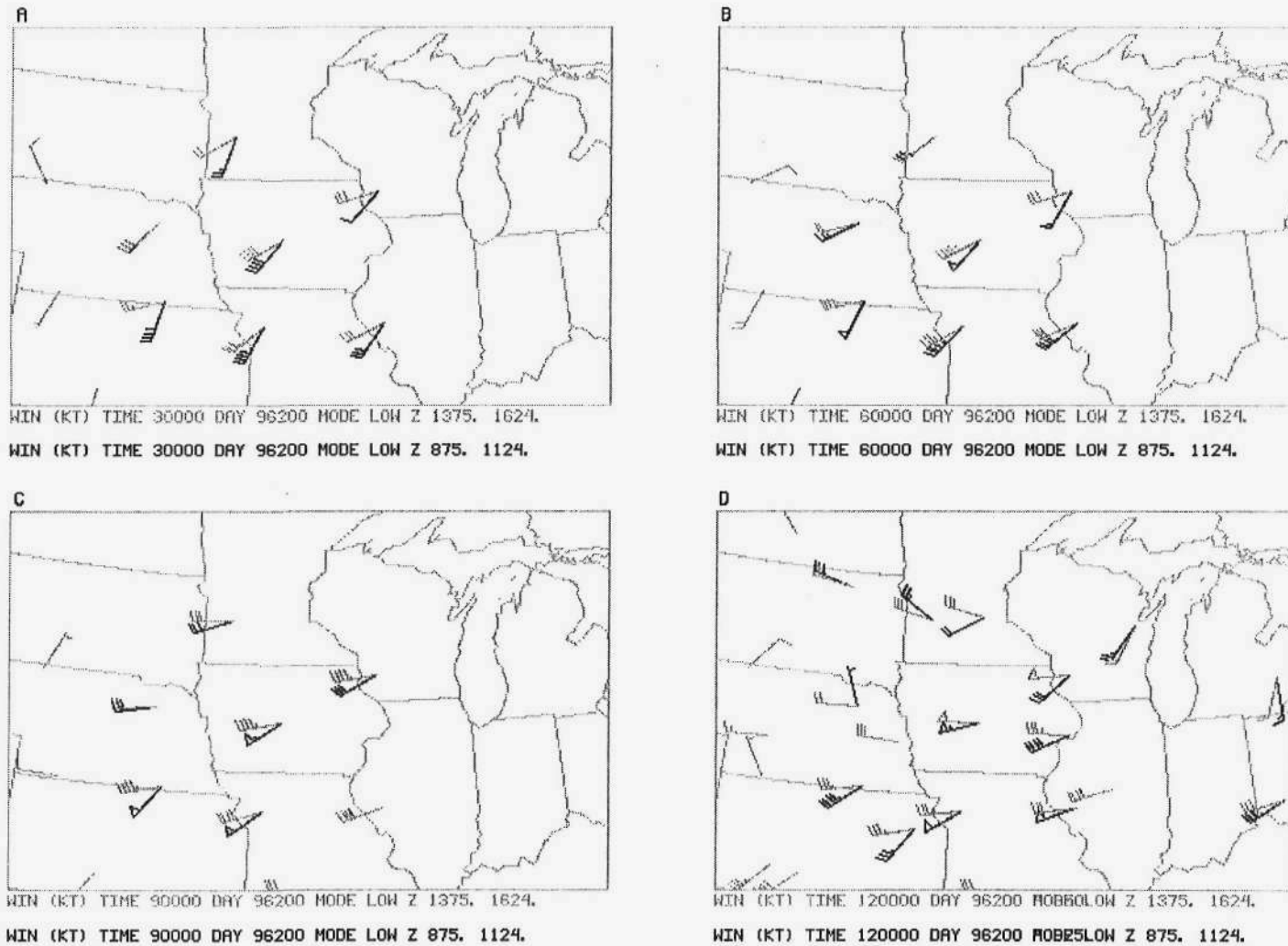


Figure 2-20. Plots of wind profiler observations and rawinsonde winds for July 18, 1996 at A) 03 UTC, B) 06 UTC, C) 09 UTC, and D) 12 UTC, which includes rawinsonde winds at 850 mb. Wind barbs are plotted such that a pennant is 50 knots (25 m s^{-1}), a full barb is 10 knots (5 m s^{-1}), and a half barb is 5 knots (2.5 m s^{-1}). At profiler stations, 1000 m winds are black and 1500 m winds are gray. At raob stations, 925 mb winds are black and 850 mb winds are gray.

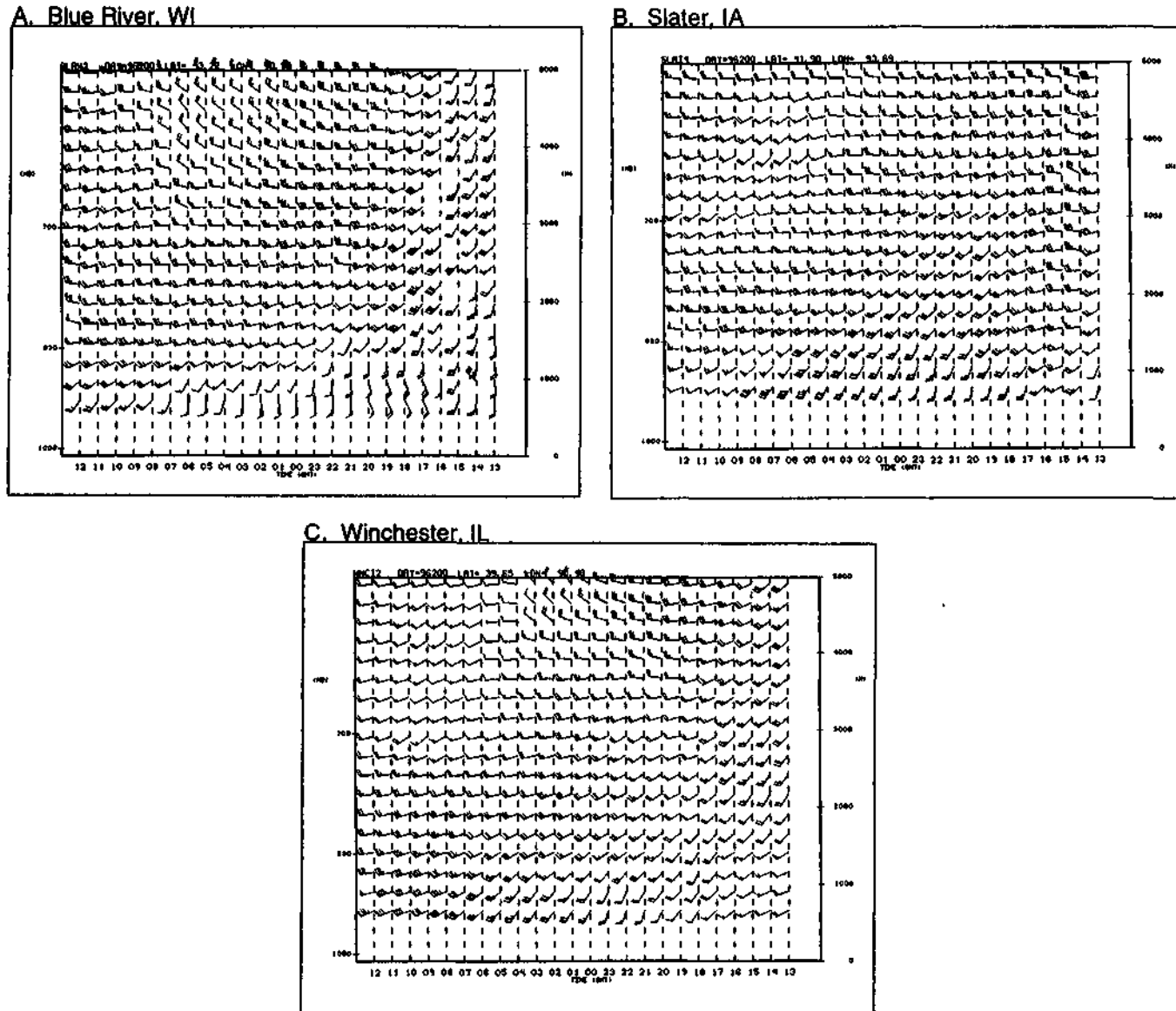


Figure 2-21. Time-height cross-section plots of wind profiler observations for July 17-18, 1996 for A) Blue River, Wisconsin, B) Slater, Iowa, and C) Winchester, Illinois. Time runs from right to left beginning at 13 UTC July 17, and ending at 12 UTC July 18. Wind barbs are plotted such that a pennant is 50 knots (25 m s^{-1}), a full barb is 10 knots (5 m s^{-1}), and a half barb is 5 knots (2.5 m s^{-1}).

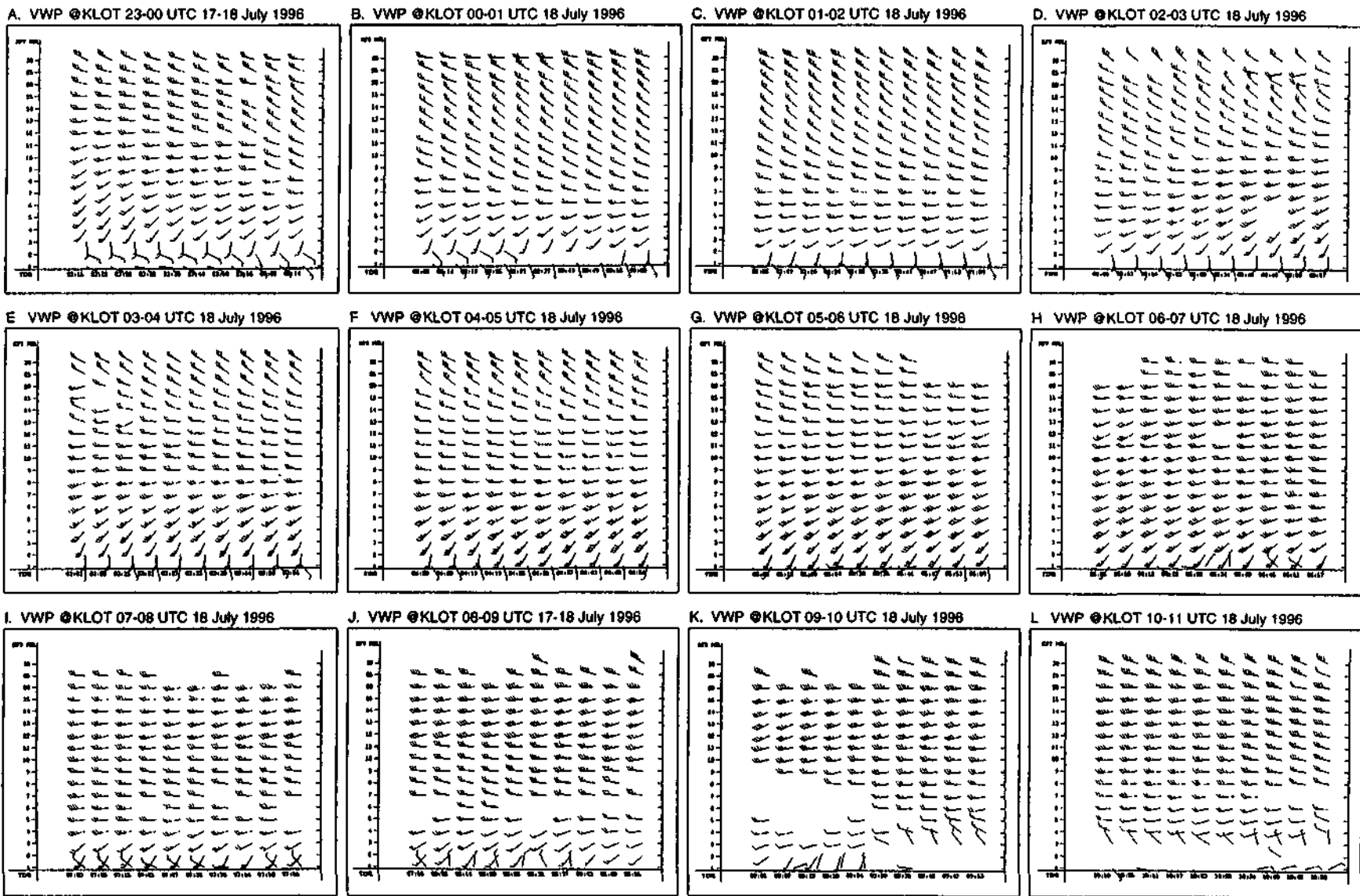


Figure 2-22. Time-height cross-sections of the velocity azimuth display from the Chicago, Illinois WSR-88-D at Romeoville, Illinois (KLOT) on July 17-18, 1996: A) 23-00 UTC July 17-18, B) 00-01 UTC July 18, C) 01-02 UTC July 18, D) 02-03 UTC July 18, E) 03-04 UTC July 18, F) 04-05 UTC July 18, G) 05-06 UTC July 18, H) 06-07 UTC July 18, I) 07-08 UTC July 18, J) 08-09 UTC July 18, K) 09-10 UTC July 18, and L) 10-11 UTC July 18. Wind bars are plotted such that a pennant is 50 knots (25 m s^{-1}), a full bar is 10 knots (5 m s^{-1}), and a half bar is 5 knots (2.5 m s^{-1}). Time increases from left to right in each panel.

References

- Augustine, J. A., and F. Caracena, 1994: Lower tropospheric precursors to nocturnal MCS development over the central United States. *Wea. Forecasting.*, **9**, 116-135.
- Bluestein, H. B., 1993: *Synoptic-Dynamic Meteorology in Midlatitudes*. Volume I. Oxford University Press, Cambridge, 431 pp.
- Bonner, W. D., 1968: Climatology of the low-level jet. *Mon. Wea. Rev.*, **96**, 833-850.
- Chappell, C. F., 1986: Quasi-stationary convective events. *Mesoscale Meteorology and Forecasting*, P. S. Ray (ed.), Amer. Meteor. Soc, 280-310.
- Colman, B. R., 1990a: Thunderstorms above frontal surfaces without positive CAPE. Part I: A climatology. *Mon. Wea. Rev.*, **118**, 1103-1121.
- Colman, B. R., 1990b: Thunderstorms above frontal surfaces without positive CAPE. Part II: Organization and instability mechanisms. *Mon. Wea. Rev.*, **118**, 1121-1144.
- Corfidi, S. F., J. H. Merritt, and J. M. Fritsch, 1996: Predicting the movement of mesoscale convective complexes. *Wea. Forecasting*, **11**, 41-46.
- Doswell, C. A. III H. E. Brooks, and R. A. Maddox, 1996: Hash flood forecasting: An ingredients-based methodology. *Wea. Forecasting*, **11**, 560-581.
- Fritsch, J. M., R. J. Kane, and C. R. Chelius, 1986: The contribution of mesoscale convective weather systems to the warm-season precipitation in the United States. *J. Climate Appl. Meteor.*, **25**, 1333-1345.
- Funk, T. W., 1991: Forecasting techniques utilized by the forecast branch of the National Meteorological Center during a major convective rainfall event. *Wea. Forecasting*, **6**, 548-564.
- Maddox, R. A, 1980: Mesoscale convective complexes. *Bull. Amer. Meteor. Soc*, **61**, 1374-1387.
- Maddox, R. A., 1983: Large-scale meteorological conditions associated with midlatitude, mesoscale convective complexes. *Mon. Wea. Rev.*, **111**, 1475-1493.
- Maddox, R.A., C. F. Chappel, and L. R. Hoxit, 1979: Synoptic and meso- scale aspects of flash flood events. *Bull. Amer. Meteor. Soc*, **60**, 115-123.
- Maddox, R. A., L. R. Hoxit, C. F. Chappel, and F. Caracena, 1978: Comparison of meteorological aspects of the Big Thompson and Rapid City flash floods. *Mon. Wea. Rev.*, **106**, 375-389.
- Mitchell, M. J., R. W. Arritt, and K. Labas, 1995: A climatology of the warm-season Great Plains low-level jet using wind profiler observations. *Wea. Forecasting*, **10**, 576-591.
- Rochette, S. M., and J. T. Moore, 1996: A case study of a heavy rainfall event with elevated convection. *Wea. Forecasting*, **11**, 417-437.

Chapter 3. Forecasting the Flood Event

Paul Merzlock, National Weather Service, Chicago, Illinois

Based on the extensive meteorologic analyses depicting the morphology of the "Flood of 1996" as presented in Chapter 2, it is obvious in retrospect why the record rainfall occurred on July 17-18, 1996. To understand the forecasting of the rainstorm requires a description of the events as they actually occurred.

The weather forecaster is initially faced with biases that may not necessarily be meteorological. Among these is an inherent responsibility not to panic the public and civil agencies by forecasting an extreme event unless a high degree of confidence exists that it will indeed occur. Unfortunately, seldom does enough evidence present itself to justify the forecasting of a record event. This is especially true in convective regimes. More subjectively, for verification purposes it is best not to deviate wildly from climatology or numerical guidance. This conservative approach becomes less applicable as the event nears, which is the reason for graduated forecasts of severe or extreme weather in terms of outlooks, watches and finally, warnings. Nonetheless, even when the occurrence of adverse weather is expected within 12 hours, rarely is the true magnitude of the event forecast. This is especially true with precipitation forecasts.

A chronological approach is best suited to discussing meteorological considerations in forecasting extreme events. Moreover, it is in this vein that the forecasting rationale is realistically presented. In addition, it permits incorporation of "intangibles" into the decision mix, such as forecast coordination, incoming storm reports, and the issuance of nonroutine forecast products.

Early Indications of Heavy Rain Potential

Concern about a possibly severe convective event involving heavy rainfall initially became apparent based on the 1200 UTC (0600 LST) ETA model run of July 16, 1996. Of particular interest was the forecast evolution of theta surfaces and associated areas of adiabatic lift. This particular form of guidance is used in forecasting areas of heavy precipitation, and its operational use is well documented (Truett, 1987). Furthermore, the method can graphically depict changes in a three-dimensional atmosphere, making it an extremely valuable tool. Figure 3-1 represents 12-hour forecasts of the 306 K surface through 48 hours of the abovementioned model run. Through 0000 UTC July 17, an area of rather weak adiabatic lift was indicated over northwestern Iowa and southern Minnesota. More importantly though, was the forecast strengthening of this region of lift as flow along the isentropic surface was to increase and become more normal to the slope. The area was also forecast to be a transitory feature that would bring the threat of deep convection into Wisconsin and perhaps far northern Illinois by the afternoon of July 17, 1996.

In addition to the 306 K theta surface, the forecast of other parameters such as lifted index (LI), precipitable water (PW), and the energy helicity index (EHI) also suggested the evolution of a potentially severe convective event within 36 hours (Maddox, 1983; Maddox and Doswell, 1982).

Pre-Storm Analyses

Awareness of the possibility of a major convective event was heightened early on July 17, 1996. After observing satellite imagery covering the previous 12 hours, (Figure 2-1), and considering the model output of the previous day, it became apparent that the ensuing weather situation warranted close monitoring. Rainfall across northwestern Iowa was extreme (see Figure 3-2 below) during the 12 hours ending at 1200 UTC on July 17. Furthermore, the synoptic conditions that produced this event had been forecast to intensify and shift eastward during the upcoming 12-hour period.

Surface and mandatory level upper air analyses from 1200 UTC on July 17 (Figure 2-5) indicated that a frontal boundary from eastern Nebraska through southern Iowa to far southern Indiana separated a modified air mass to the north from deep maritime tropical air to the south. The air over much of Iowa had been modified convectively and convective debris had been blown eastward across northern Illinois, setting the stage for accentuated mesoscale forcing (Cotton et al., 1989) as very moist and unstable air continued flowing over the increasingly strong low-level boundary. Figure 3-3 shows a plot of the 1200 UTC 1 kilometer (km) winds on July 17. Low-level flow of 40 knots (20 meters per second or m/s) or higher was present and continued to produce abundant low-level moisture convergence north of the frontal boundary.

Sounding data from Davenport, Iowa, observed at 1200 UTC already indicated moderate amounts of instability (Figure 2-5f). This is in spite of the fact that many of the stability indices are surface- or boundary-layer based, and that the data indicate an obvious case of elevated instability. Of particular note is the helicity which at 1200 UTC was analyzed at 110 m/s in the lowest 3 km of the atmosphere. Although this value is not outrageously high, it is the trend with time that would have the greatest implications concerning the upcoming forecast.

Model consistency also played an important role in determining the threat of heavy rainfall. The 1200 UTC ETA model run indicated that the 24-hour forecast of the 306 K surface and associated adiabatic lift from the previous day's run (Figure 3-1b) was accurate in terms of locating a lift area over northwestern Iowa, but had underforecast its magnitude (Figure 3-4). This also indicated that a strong core of isentropic lift was indeed located over the area that had just received heavy rainfall. The 1200 UTC run on July 17 remained consistent with movement of this area eastward across northern Illinois and southern Wisconsin by that evening (Figure 3-4). One subtle difference with the previous runs, however, is that the zone of strongest lift was a little further south than forecast earlier.

Consistency was noted in precipitable water and lifted index fields as well. Precipitable water values of 2 inches (51 millimeters or mm) or greater were observed over portions of eastern Iowa at 1200 UTC, and this degree of available moisture was also forecast to shift eastward in phase with the isentropic lift core mentioned above. In addition, lifted index prognosis suggested that very unstable air would continue to be advected into an area having a steep isentropic slope, a condition prone to repeated thunderstorm development (Maddox and Doswell, 1982) [refer to Figure 3-5].

At 1700 UTC on July 17, the routine issuance of the Illinois zone forecast package was completed. This included the unqualified mention of thunderstorms across northern Illinois. Soon after issuance of the forecast, thunderstorms began to intensify across portions of northern Illinois, helping to prompt the issuance of severe thunderstorm watch number 792, which would be valid until 2100 UTC.

Onset of the Event

Thunderstorms continued to increase in coverage and intensity through the early afternoon on July 17. However, the storms did not meet severe storm criteria for winds, hail, or heavy rains.

Even though ongoing thunderstorms were producing localized rainfall amounts of 2.5 inches (64 mm) per hour in areas just southwest of Chicago, there was little immediate threat of flooding as the area had been dry for several weeks preceding this event. Flash flood guidance was on the order of 3.5 inches (89 mm) in 3 hours, which is considered rather high. This means that these rainfall rates would be required over a sufficiently large area in order to produce flash flooding. Therefore, the thunderstorms that developed early on the afternoon of July 17 were not of great concern. A turning point in the decision to forecast a flash flood event arose largely from analysis of various data observed from 1600 to 2000 UTC, which pointed to an increasing likelihood that repeated thunderstorm development was imminent.

Among the most useful sources of data was the 1800 UTC surface analysis. Of primary concern was the pooling of high dewpoint air immediately upstream of a strengthening warm frontal boundary (Figure 2-7b). This was combined with a core of pressure falls observed in the isallobaric field over eastern Iowa and extreme northwestern Illinois in the cool air to the north of the boundary, suggesting an increase in low-level moisture convergence. Nephanalyses incorporated from visible satellite imagery also confirmed that the threat of repeated thunderstorm development was increasing (Maddox et al., 1980). This imagery (Figure 3-6) indicated that dense convective debris was enhancing the low-level frontal discontinuity from central Iowa southeastward into east-central Illinois. By 1945 UTC, deep convection was already developing again in the region of pressure falls over eastern Iowa.

Graphics and profiler information also proved valuable from the standpoint of accentuating the degree of available instability and low-level moisture convergence. Figure 3-7 uses the ADAP-produced surface streamline and surface based lifted index to illustrate the destabilization of the air mass being lifted into the zone of convective development with values lowering to less than -10 over a widespread area. Combining these data with 1000 m profiler wind plots suggests that strong low-level moisture convergence was focusing in the region from northern Illinois westward into eastern Iowa. Note the 40 knot (20 m/s) southwest winds at Slater, Iowa, and Conway, Missouri, by 2000 UTC (refer to Figure 3-8).

Concern not only for excessive rainfall, but also for supercell development, was on the increase during the early afternoon hours. Severe thunderstorm watch 792 remained in effect. Coordination with the Storm Prediction Center (SPC) also reinforced the growing potential for severe weather based on "incredible moisture convergence into northern Illinois." The KLOT WSR 88-D VAD wind profiles also drew attention by suggesting that helicity values were increasing as surface and boundary layer winds backed into the southeast and east (Zhong et al., 1996), meaning the profile of wind shear in the atmosphere was becoming more favorable for rotating updrafts; a feature of major storms. Hodographs from the profiler at Blue River, Wisconsin, indicated increasing helicity as well (Figure 3-9). Due to its relatively similar position with respect to the northwest-to-southeast-oriented frontal boundary Blue River was actually more representative of what was occurring in northern Illinois than the data from Winchester, Illinois.

As mentioned above, the increase in helicity values seemed even more extreme when considering the VAD wind profiles from the KLOT WSR 88-D radar (Figure 3-10). Note the backing of the 1 km winds between 1800 and 2200 UTC, and the increase in speed as well. This occurred while mid-level winds veered slightly to a west-southwesterly direction. Hodographs produced from these profiles graphically illustrate the increase in the potential for rotating thunderstorm updrafts. Although a quantitative value of helicity is not available from the VAD winds, a modified sounding from Davenport, Iowa, revealed storm relative helicity values of 435 (m/s)^2 , and the observed sounding at 0000 UTC on July 18 produced a value of 525 (m/s)^2 .

While the threat of severe thunderstorms was increasing during the afternoon of July 17, heavy rainfall potential was also materializing. The initial band of thunderstorms that produced locally heavy rainfall across the southern and southwestern suburbs of Chicago during the early afternoon hours had moved into northwestern Indiana by 2300 UTC (Figure 3-11). More importantly, note the new thunderstorm development westward along the frontal boundary into northwestern Illinois.

As mentioned earlier, the potential for flash flooding had increased to the extent that forecasters had enough confidence to proceed with issuance of a flash flood watch for northern Illinois. This alert was disseminated with the routine issuance of the Illinois zone forecasts. However, these forecasts, normally issued at 2030 UTC, were delayed as the anticipated severe thunderstorms materialized (see Figure 3-12). The following excerpts highlight some of the products formulated from all the above mentioned analyses. The state forecast discussion, an explanation of forecast rationale, was issued at 1920 UTC (1420 CDT), with an update at 2028 UTC (1528 CDT) due to the evolution of a potentially tornadic thunderstorm just northwest of the forecast office. This warranted the issuance of a tornado warning at 2035 UTC (1535 CDT). The actual flash flood watch issuance was delayed until 2111 UTC (1611 CDT) due to ongoing severe weather and the issuance of tornado watch.

By 2300 UTC on July 17, concerns about increasing helicity continued to be realized. At 2242 UTC, storm relative motion data from the KLOT WSR 88-D indicated a strong mesocyclone associated with a thunderstorm just southwest of Joliet, Illinois (Figure 3-13). A tornado warning had just been issued for this storm, and by 2303 UTC, the circulation strengthened into a tornado vortex signature or TVS (Figure 3-14).

Continuation of the Storm Event

By 2130 UTC on July 17, routine forecast duties had been completed and the remainder of the evening and nighttime hours were spent performing radar surveillance and issuing warnings. Both radar and satellite data continued to verify that the forecast scenario of repeated thunderstorm development was accurate (Figure 2-9). Also, as data from 0000 UTC on July 18 became available, it became apparent from isentropic analyses that the ETA model used early in the forecasting process was verifying as a perfect prognosis with strong adiabatic lift occurring across eastern Iowa and northwestern Illinois.

Conclusions

A myriad of data is available for use in forecasting extreme events. As beneficial as these detailed data sets are, they are only useful in the field if readily available to the forecaster. During the July 17-18 event, gridded data, particularly isentropic forecasts, played a key role in highlighting the potential for a heavy rainfall as much as 36 hours before the actual event. Radar and satellite interpretation became increasingly important as the storms developed. Forecasting this event involved consistent and increasingly accurate numerical guidance. However, it must be stressed that selecting model guidance as the basis for a forecast should be substantiated with subsequent analyses for the benefit of forecast continuity. Hard copy capability of graphic analyses must be available for these purposes.

Referring again to the introductory comments of this chapter, most forecasters have some nonmeteorological biases and conservatism that to some degree may ensure that routine forecasts are issued responsibly. Conversely, for the few times that extreme events present themselves, this view needs to change, as illustrated by the July rainstorm case. Although flash flood guidance is a good gauge of how susceptible an area is to flash flooding, preceding dryness is not always a key factor. Remember, excessive rainfall events are how many dry periods and droughts are ended. The point is that analysis of this event should serve as an example that in the handling of extreme precipitation situations, a somewhat conservative approach taken towards flash flood forecasts in relatively flat areas with humid climates may need to be abandoned in favor of a more "southwestern U.S." (dry climate) approach to flash flooding.

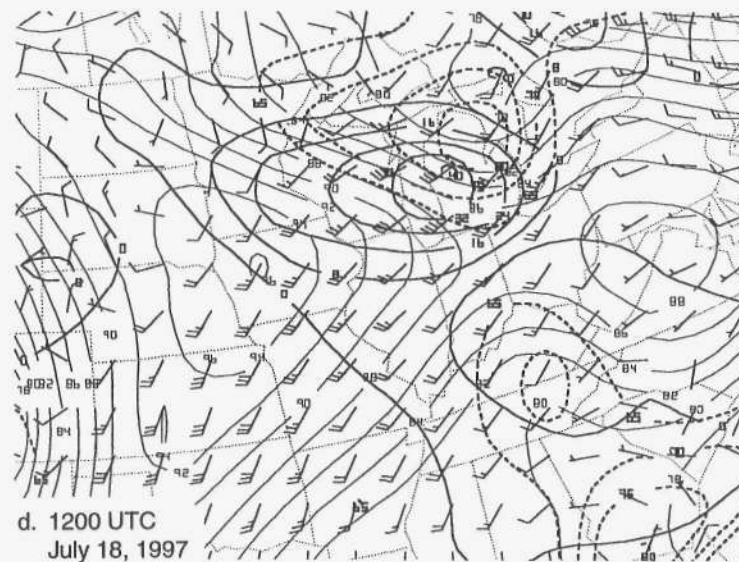
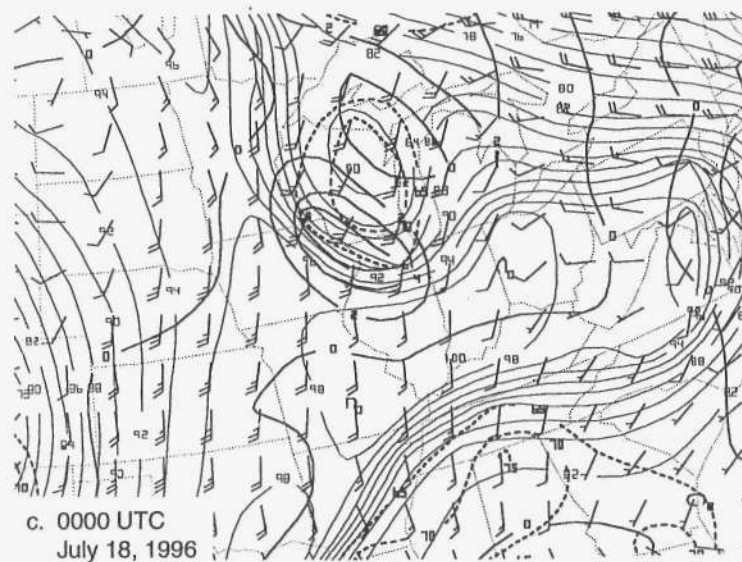
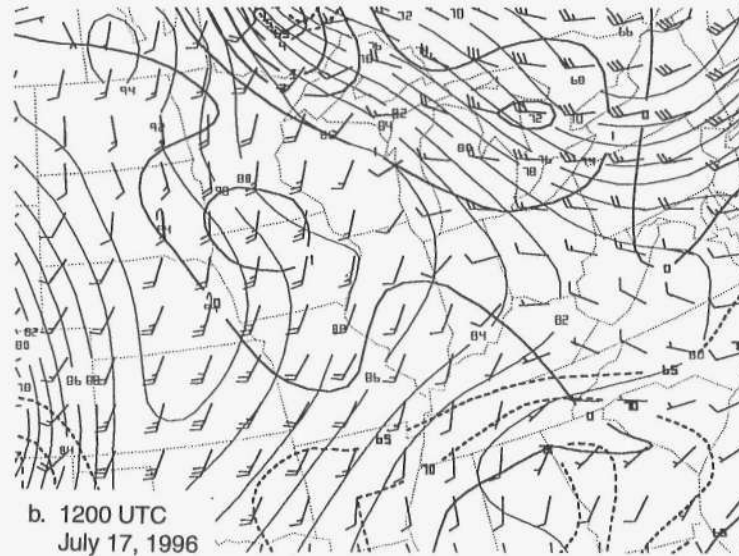
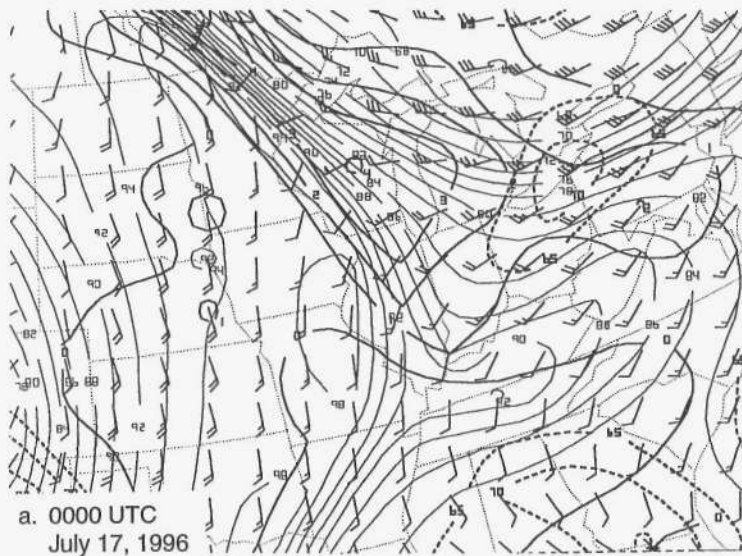


Figure 3-1. Forecast pressure, adiabatic lift, wind and relative humidity along the 306 K surface on July 17, 1996 at a) 0000 UTC and b) 1200 UTC, and on July 18, 1996 at c) 0000 UTC and d) 1200 UTC.

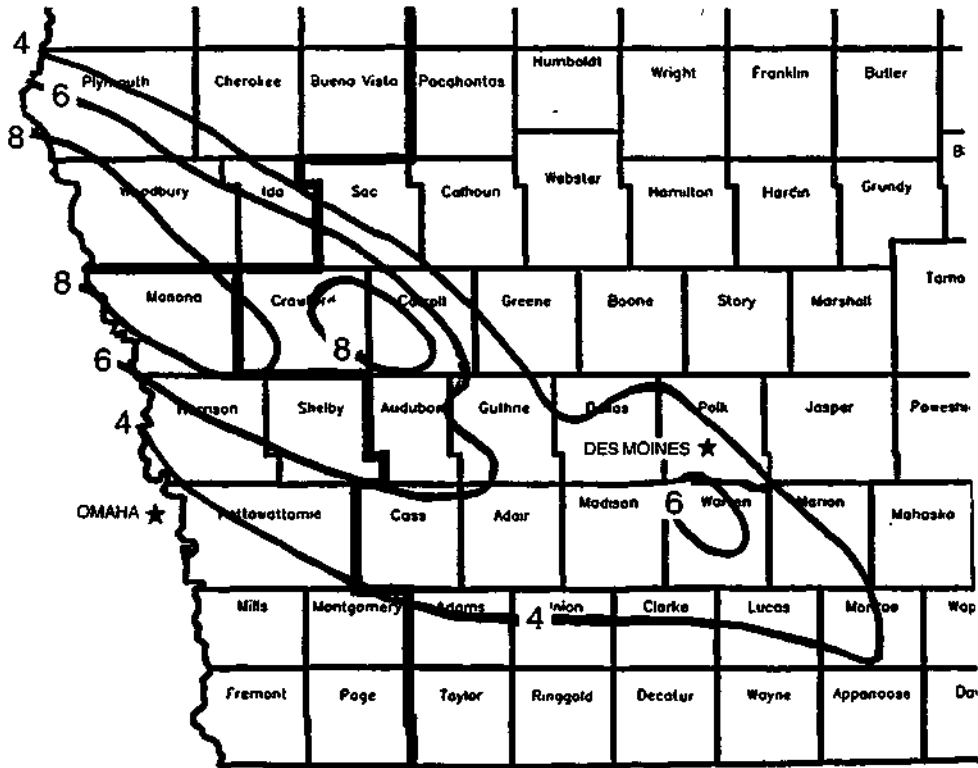


Figure 3-2. Rainfall distribution map of northwestern Iowa for the 12 hours ending at 1200 UTC on July 17, 1996.

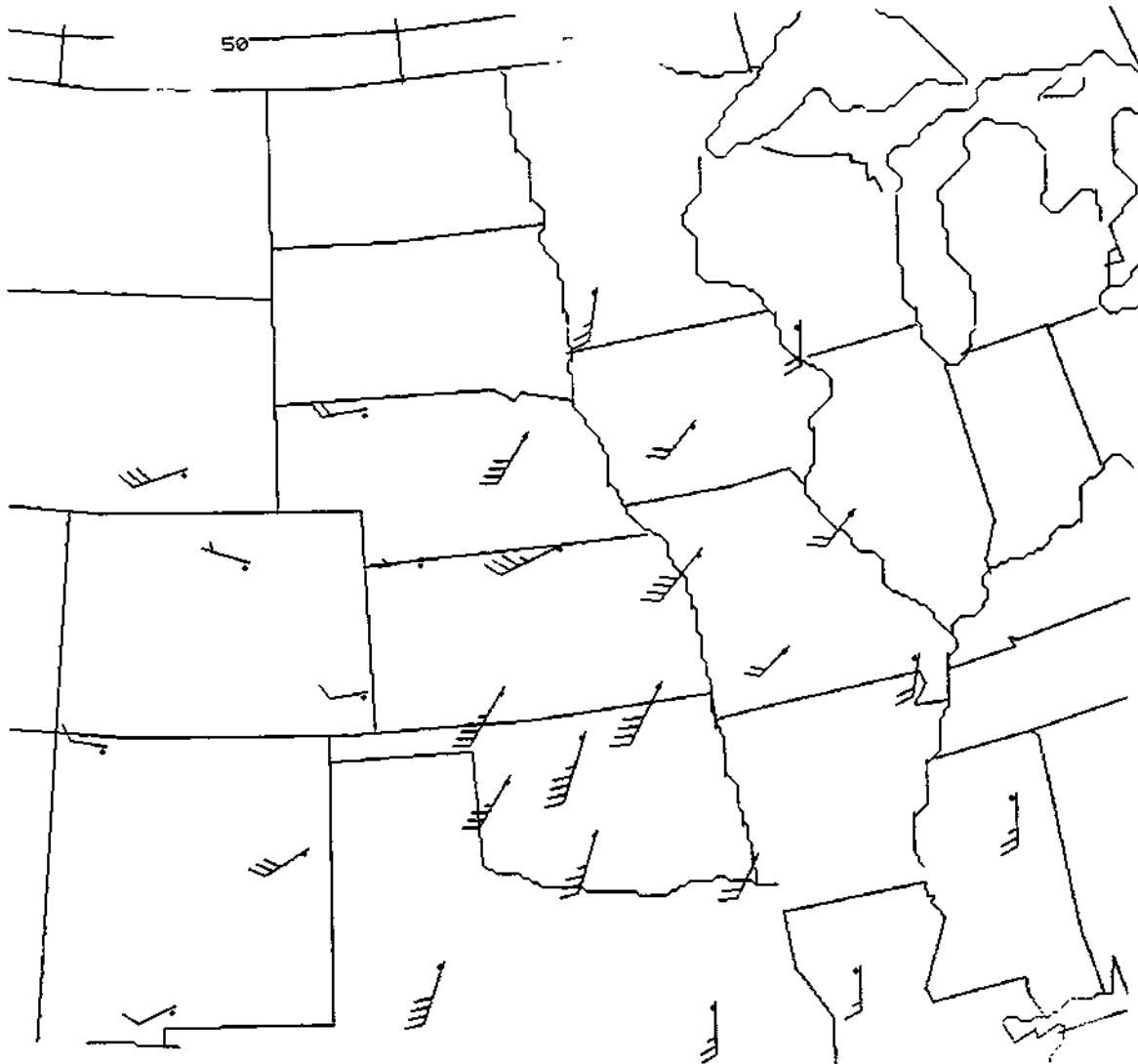


Figure 3-3. A map of 1000 m profiler winds at 1200 UTC on July 17, 1996.

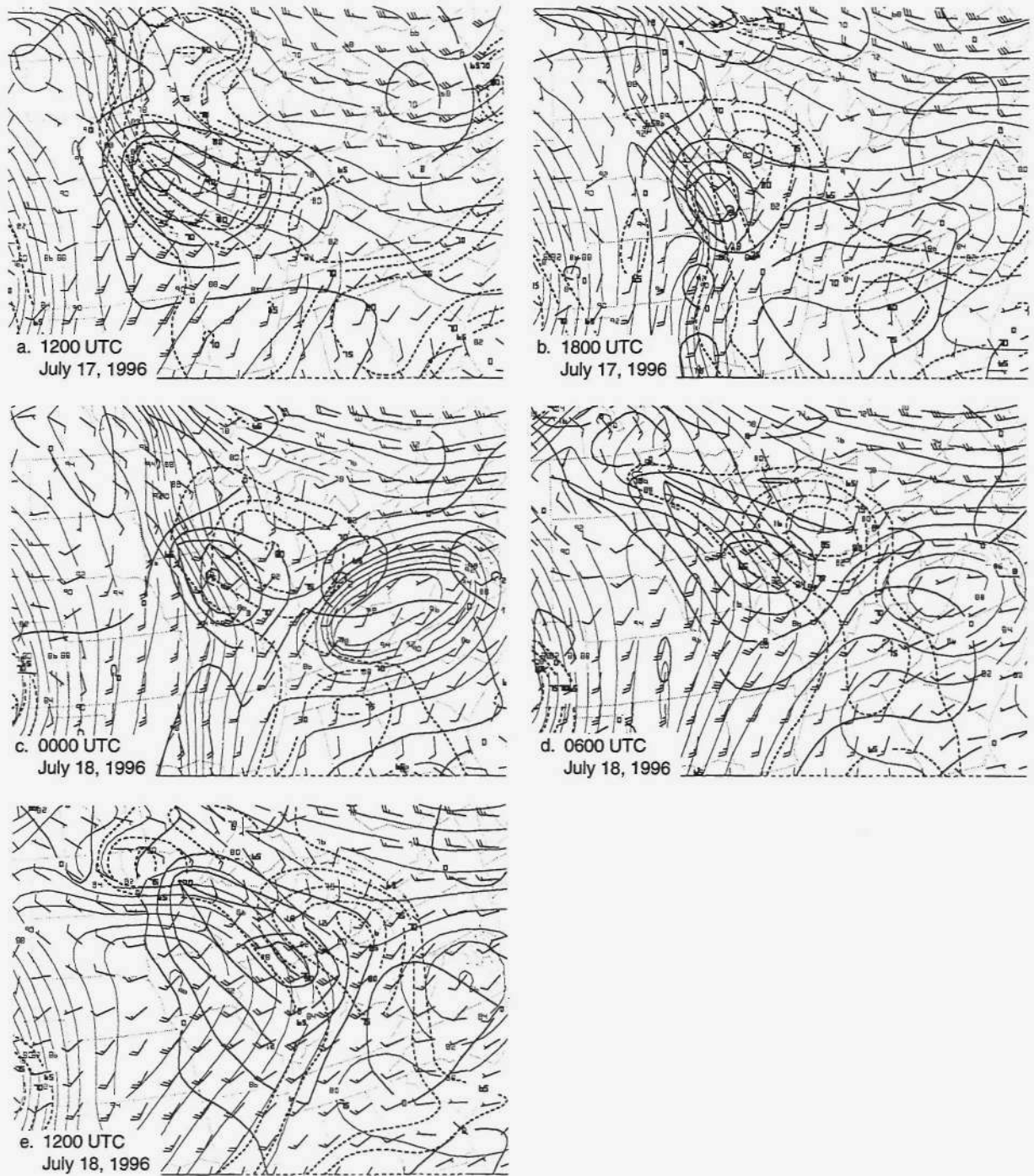


Figure 3-4. Initial and forecast pressure, adiabatic lift, wind and relative humidity along the 306 K surface on July 17, 1996 at a) 1200 UTC and b) 1800 UTC, and on July 18, 1996 at c) 0000 UTC, d) 0600 UTC, and e) 1200 UTC.

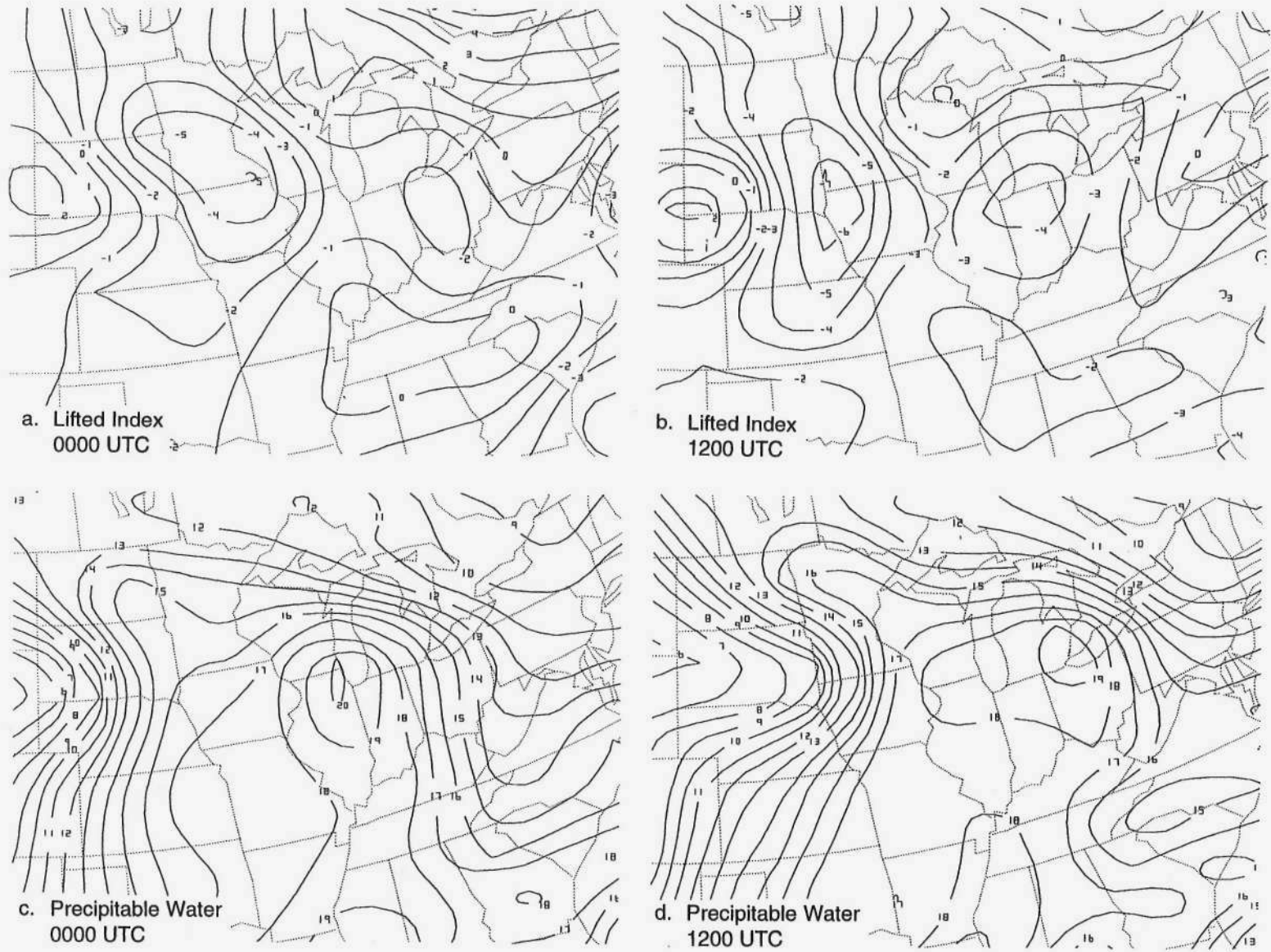


Figure 3-5. Forecast values of lifted index and precipitable water on July 18, 1996.

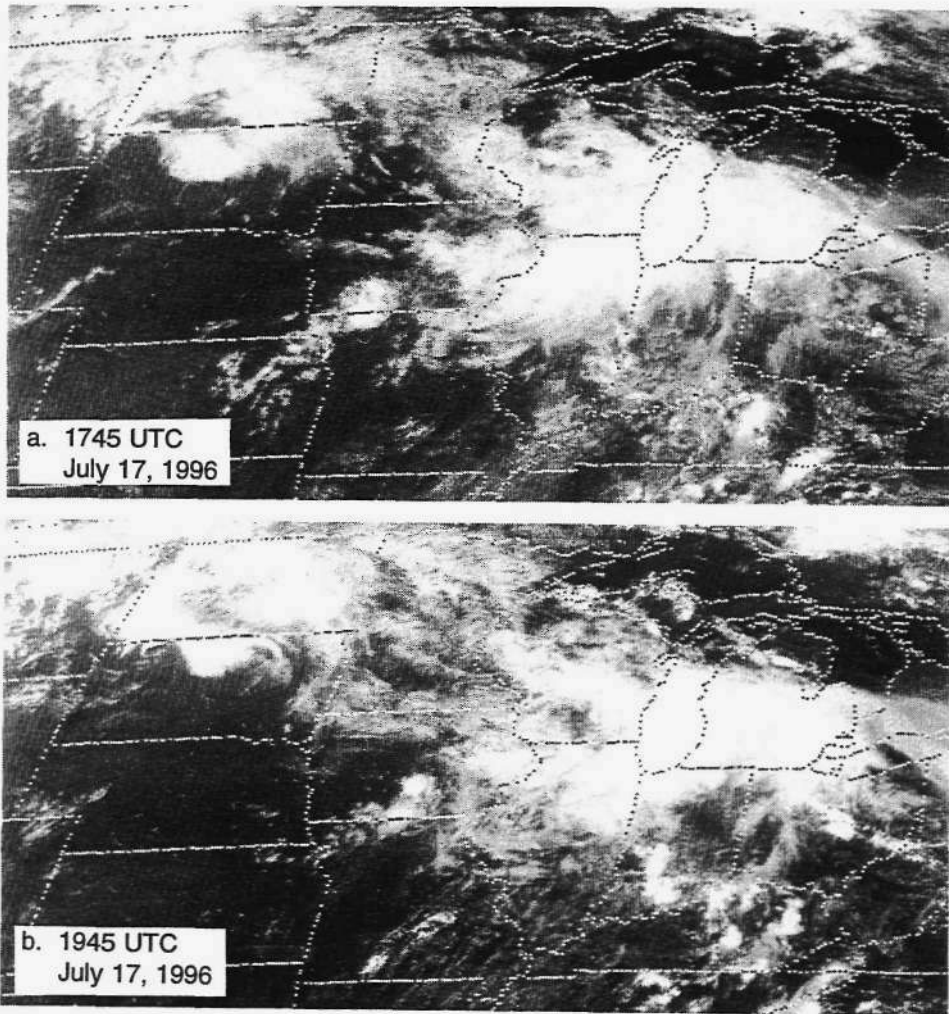


Figure 3-6. GOES 8 visible imagery observed on July 17, 1996 at a) 1745 UTC, and b) 1945 UTC.

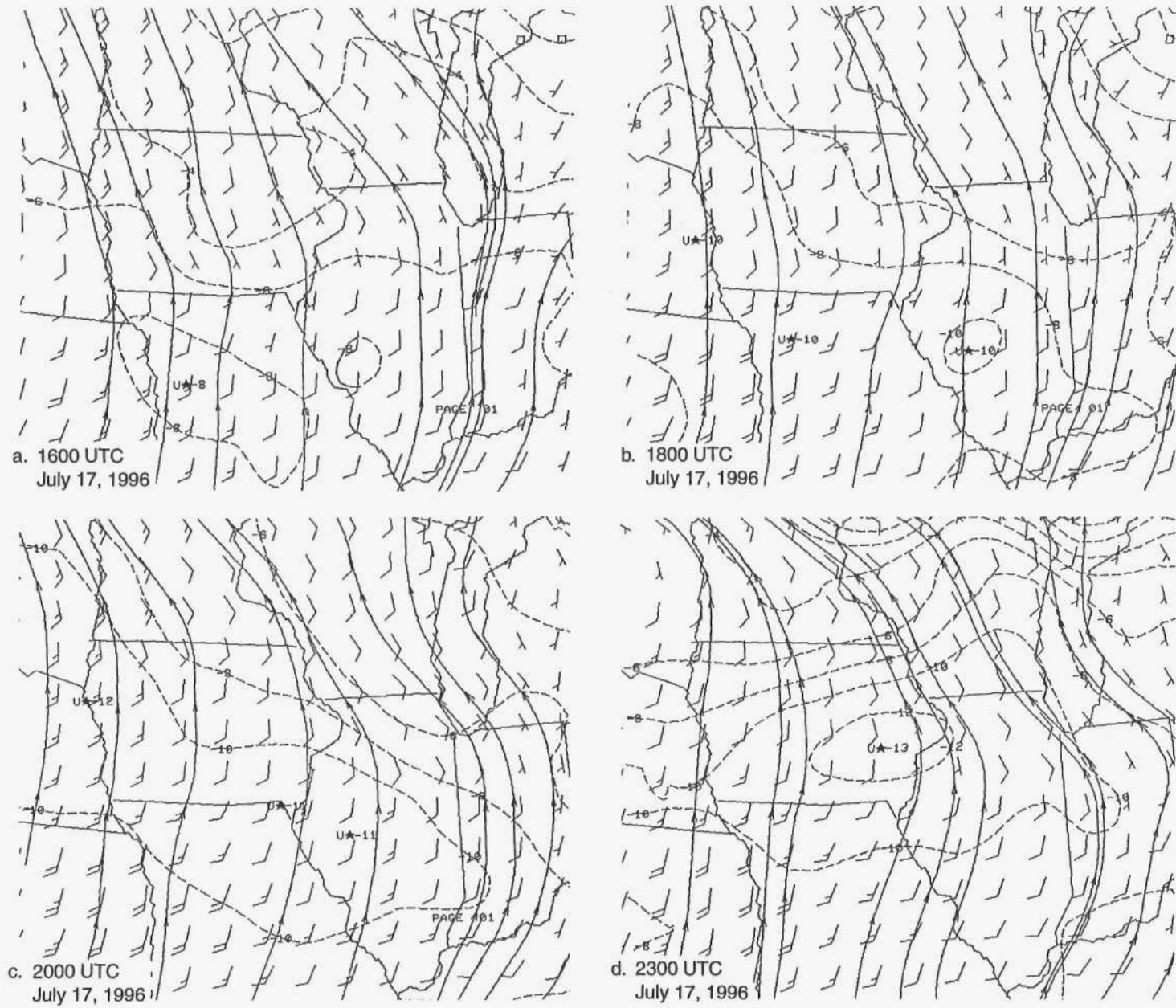


Figure 3-7. ADAP surface-based streamlines and lifted index on July 17, 1996 at a) 1600 UTC, b) 1800 UTC, c) 2000 UTC, and d) 2300 UTC.

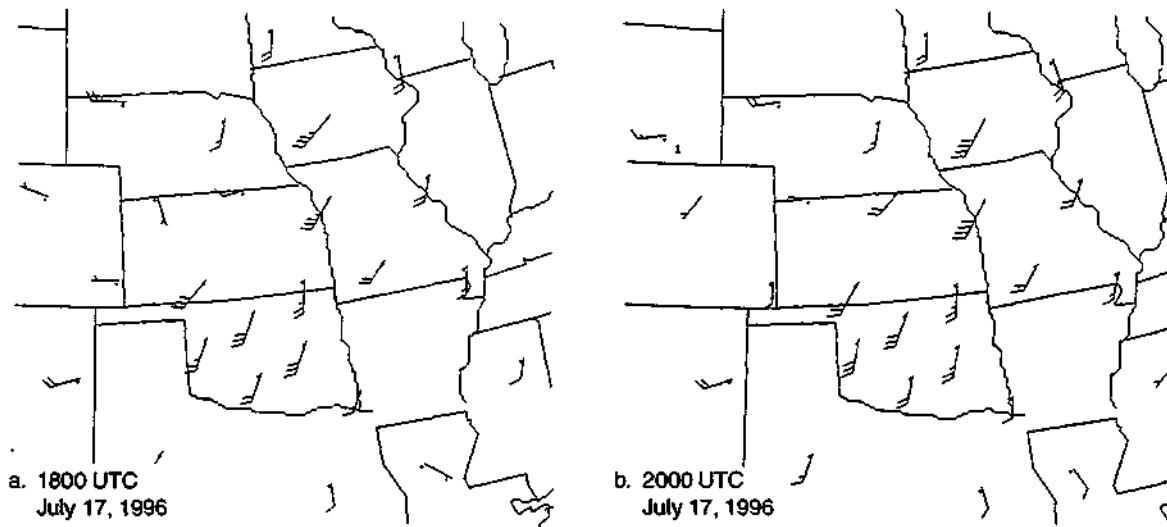


Figure 3-8. Profiler plan views of 1000 m winds on July 17, 1996 at a) 1800 UTC and b) 2000 UTC.

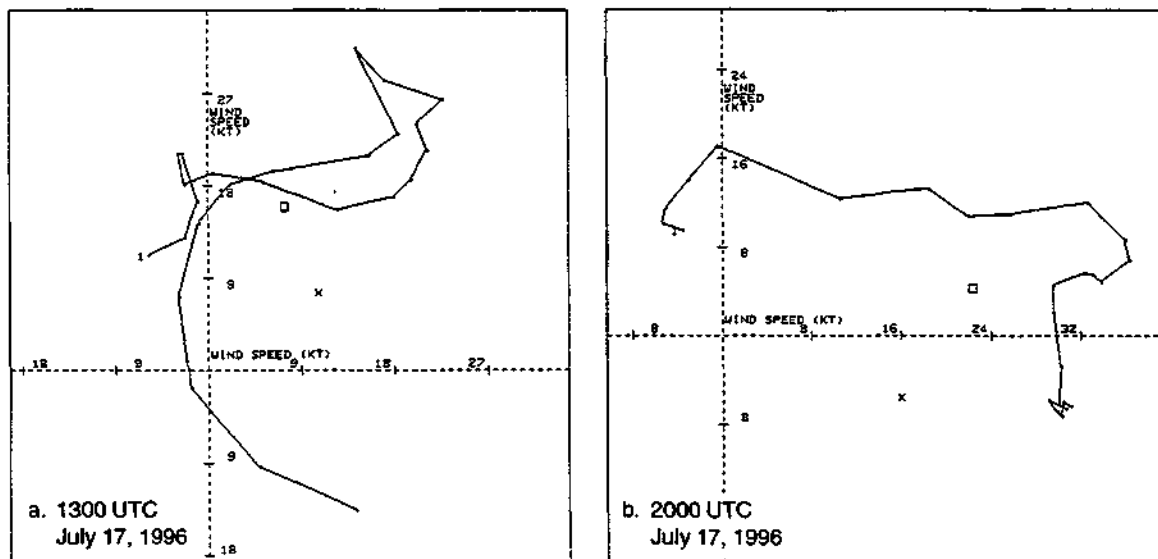
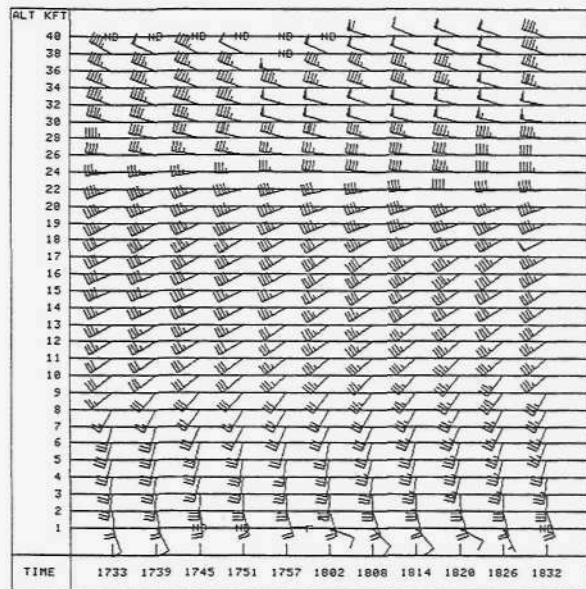


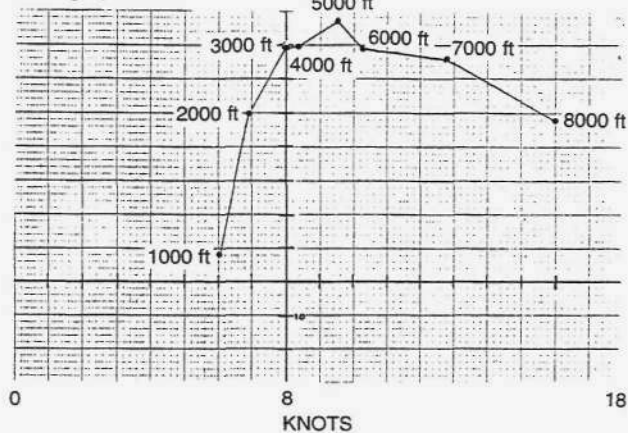
Figure 3-9. Hodographs from the profiler at Blue River, Wisconsin, on July 17, 1996 at a) 1300 UTC and b) 2000 UTC.

Wind Profile

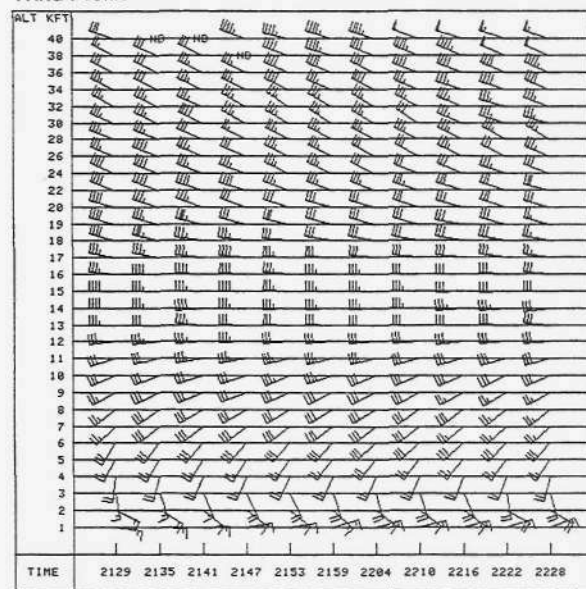


a. 1830 UTC

Hodograph



Wind Profile



b. 2230 UTC

Hodograph

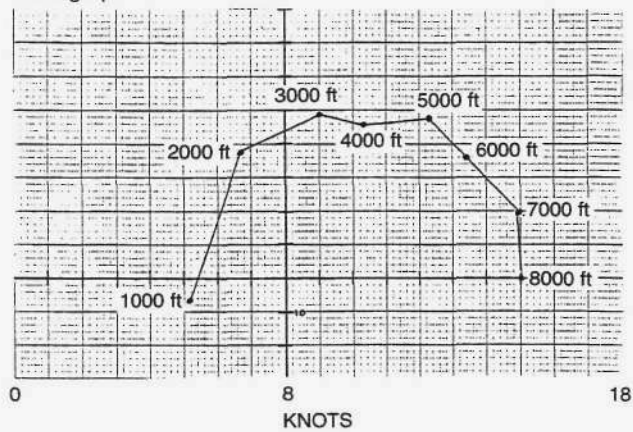


Figure 3-10. VAD wind profiles and associated hodographs from the KLOT WSR 88-D radar on July 17, 1996 at a) 1830 UTC and b) 2230 UTC.

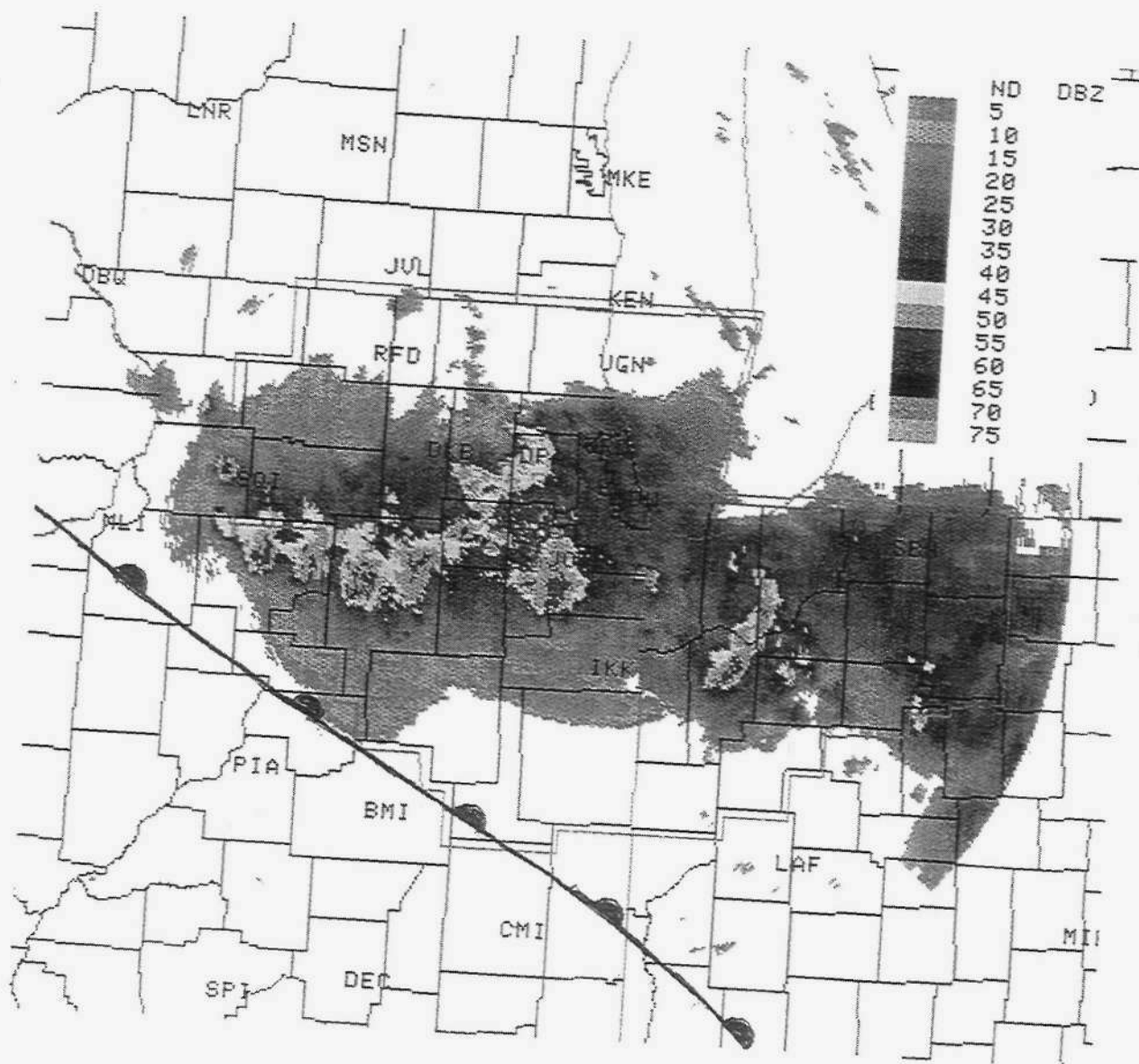


Figure 3-11. Composite reflectivity data from the KLOT WSR 88-D radar on July 17, 1996 at 2303 UTC.

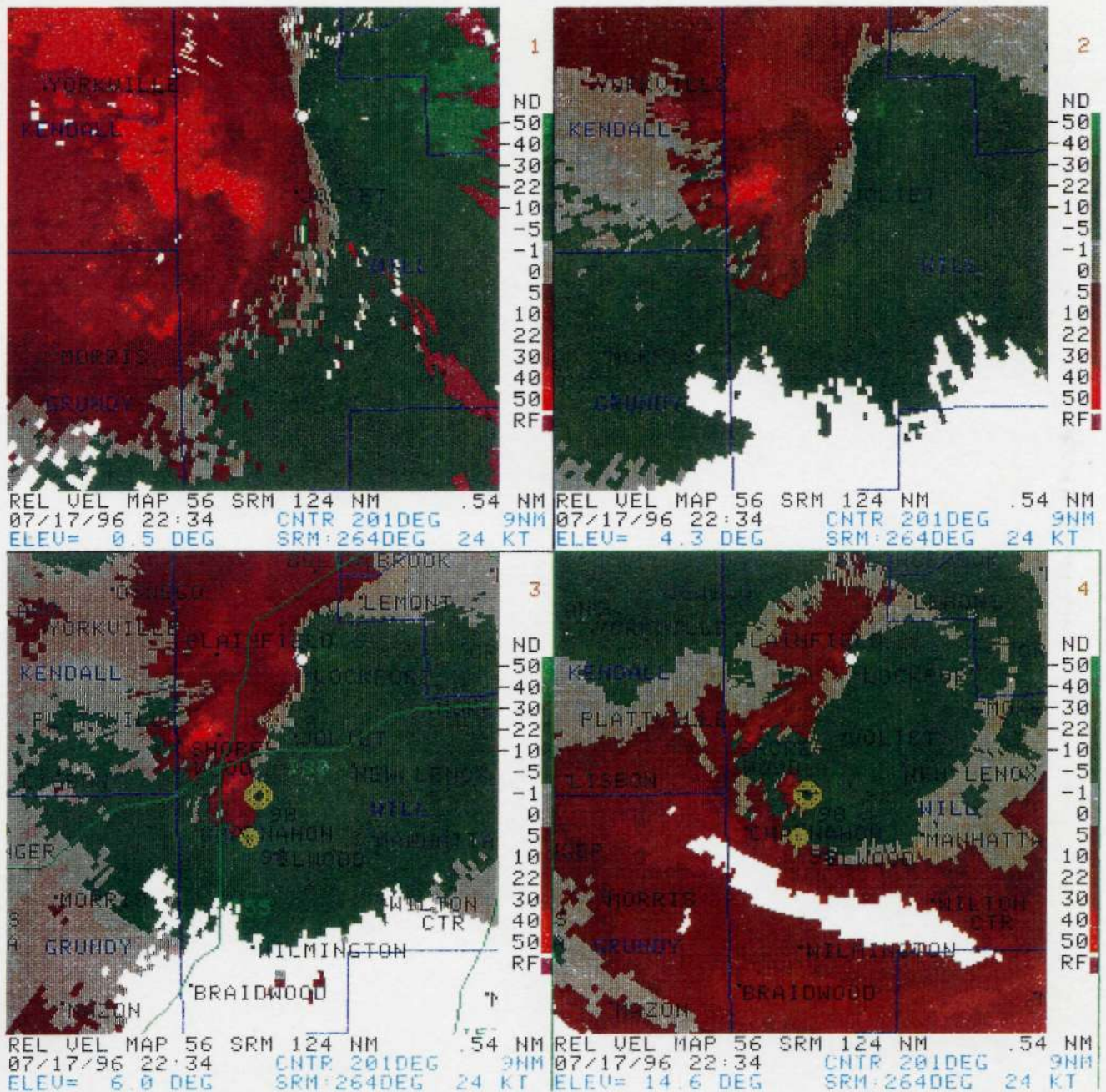


Figure 3-13. Storm relative motion observed by the KLOT WSR 88-D radar on July 17, 1996 at 2242 UTC.

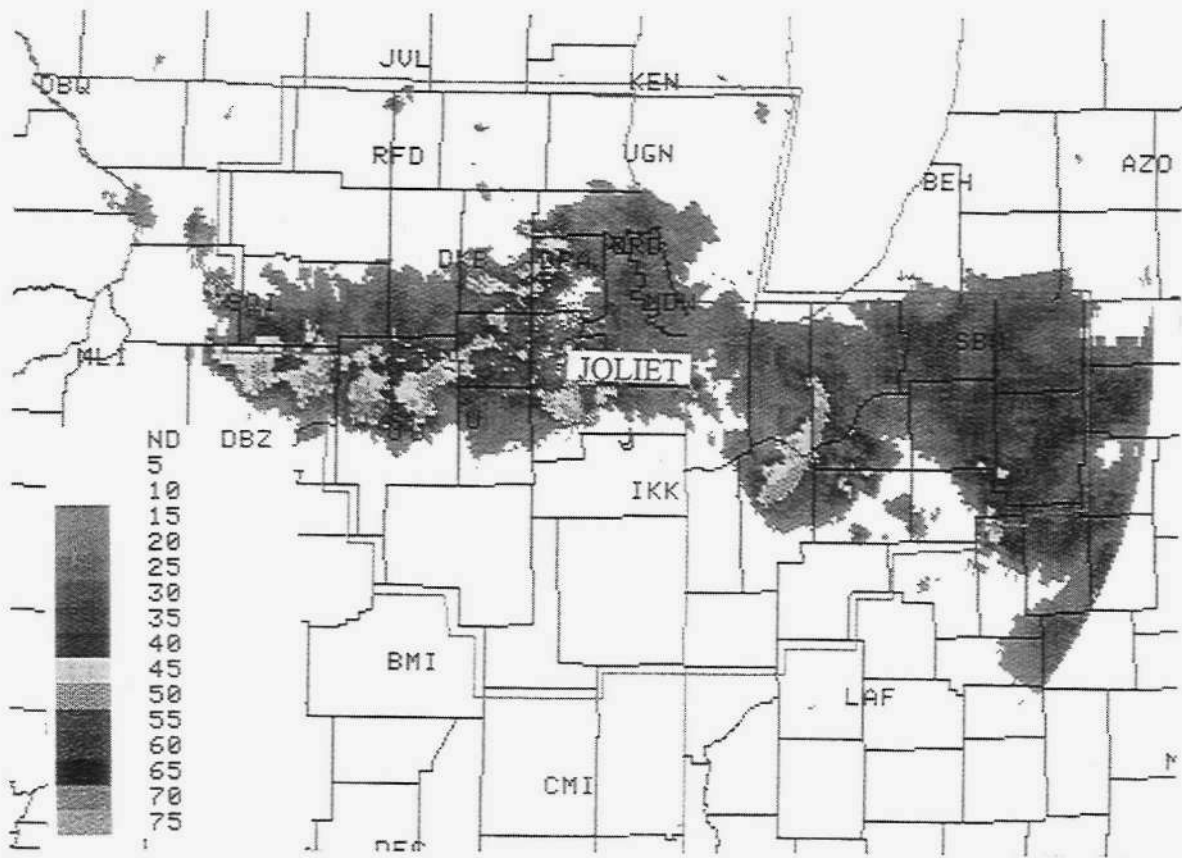


Figure 3-14. Base reflectivity data from the KLOT WSR 88-D radar on July 17, 1996 at 2303 UTC.

References

- Cotton, W. R., M-S. Lin, R.L. McAnelly, and C. J. Trembock, 1989: A Composite Model of Mesoscale Convective Complexes. *Monthly Weather Review*, **117**, 765-783.
- Maddox, R.A., 1983: Large-scale Meteorological Conditions Associated with Mid-latitude Mesoscale Convective Complexes. *Monthly Weather Review*, **111**, 1475-1493.
- Maddox, R.A., and C. A. Doswell III 1982: An Examination of Jet Stream Configurations, 500 mb Vorticity Advection and Low-Level Thermal Advection Patterns During Extended Periods of Intense Convection. *Monthly Weather Review*, **110**, 184-19
- Maddox, R. A., L.R. Hoxit, and C. F. Chappell, 1980: A Study of Tornadic Thunderstorm Interactions with Thermal Boundaries. *Monthly Weather Review*, **108**, 322-336.
- Truett, S. C, 1987: *Isentropic Analysis*. National Weather Service Technical Attachment 87-4, Washington, DC.
- Zhong, S., J. D. Fast, and X. Bian, 1996: A Case Study of the Great Plains Low-Level Jet Using Wind Profiler Network Data and a High-Resolution Mesoscale Model. *Monthly Weather Review*, **124**,785-806.

Chapter 4. The Rainstorm Data and General Storm Dimensions

Stanley A. Changnon and Nancy E. Westcott, Illinois State Water Survey

The initial reports of heavy rainfall from the Aurora and Joliet areas on July 18, 1996, indicated point rainfall amounts ranging from 14 to 17 inches, 1-day rainfall values well in excess of those expected to occur once in 100 years. Once the decision to make a study of the July 17-18 storm was made, the initial project effort entailed collection of rainfall data in and around the heavy rainfall zone

The rainstorm across northern Illinois covered a 29-hour period, with the earliest rain beginning at 0800 LST (CST) on July 17, and the last rain ending at 1300 LST on July 18. The maximum hourly rainfall amount somewhere in the storm area during the entire storm exceeded 0.50 inch. During three periods, (1100-1700, 2100-2300, and 0100-0600 LST), an inch or more of rain per hour was reported by at least one of the 90 recording raingages in northeastern Illinois. During the 1400-2100 LST period, there were also reports of hail, damaging lightning, and tornadoes in parts of northern Illinois. Strong mesoscale circulations were located on the WSR-88D Doppler radar. A tornado and 0.75-inch-diameter hail were observed around 2000 LST in northwestern Illinois. Hail also was reported in Bureau County around 1700 LST, with 0.5-inch-diameter hailstones at Princeton and 1.5-inch stones at Walnut.

The radar indicated strong convective activity across northern Illinois, with reflectivities of 50-60-dBZ. The maximum height of echo tops during most of the storm ranged from 14 to 18 kilometers or km. Tops were highest in the 2000-2300 LST period, 17-18 km. Echoes of these heights typically indicate a high potential for severe weather in Illinois (Grosh, 1978).

Rainfall Data

Rainfall data for the July 17-18 storm came from three basic sources: bucket surveys by surveyors traveling in the storm area, raingages operated by various government agencies, and special raingage networks operated by various entities. Bucket surveys conducted by county farm agents, scientists at Northern Illinois University, and Water Survey staff collected 107 point rainfall measurements in Illinois. Most of these data were collected within a week after the end of the storm in and near the heavier rainfall areas as defined by 3 or more inches for the total storm rainfall.

Another major source of rainfall data for this unique storm was five existing dense networks of 121 raingages. Two of these networks are operated by the Illinois State Water Survey: Cook County Network, a network of 25 recording raingages in Cook County, and the Illinois Climate Network, which had four recording raingages within the storm area. Three counties in the area were also operating raingage networks. Will County has 42 cooperative observers, and Kendall County has 36 cooperative observers in networks that collect daily and weekly rainfall data from farmers and other citizens using personal raingages. DuPage County has a network of 14 recording raingages installed by the U.S. Geological Survey.

A third source of rainfall data was raingages operated by various local, state, and federal agencies, with the major contributor being the National Weather Service (NWS). Within the storm area, which comprised three states (Illinois, Indiana, and Wisconsin), the National Weather Service had 373 nonrecording raingages that provided daily amounts of rain from the storm in the three-state area. Raingage values were obtained from 201 NWS stations located in Illinois. The NWS also had 20 recording raingage stations scattered around the storm area, including 14 stations in Illinois. The U.S. Army Corps of Engineers had six recording raingages located in northeastern Illinois. The Metropolitan Water Reclamation District of Greater Chicago had 15 recording raingages scattered throughout the Chicago urban area. The U.S. Geological Survey had 11 recording raingages in various parts of the heavy rain area in northeastern Illinois. Three cities in the region maintained their own raingages, of which one was a recording gage, and the Argonne National Laboratory maintained its own recording gage. Thus, point rainfall data were obtained from 479 raingages scattered throughout the Illinois storm area and operated by these various government entities. Furthermore, 90 of these were recording raingages.

The two Water Survey raingage networks provided data from 29 recording raingage sites, and DuPage County had 14 more, producing a total of 43 recording raingages. These 43 recording gages plus the 47 gages from other agencies resulted in 90 recording raingages for the storm, an abnormally large number for a heavy localized rainstorm. This extensive recorded rainfall data facilitated the detailed hydrometeorological analysis of this storm event. The storm rainfall pattern and related analyses were based on data from 657 raingages in the three-state area, and 479 were located in Illinois.

Figure 4-1 displays the storm area in northeastern Illinois with dots representing sites where storm rainfall totals were obtained from nonrecording raingages and circled dots representing the 90 recording raingages from which storm totals were obtained. The pattern shows an amazingly dense set of measurements throughout much of the heavy rain area of this storm in Illinois, which has been defined by a better series of observations than obtained in most previous studies of heavy rains in Illinois.

Total Storm Rainfall

Figure 4-2 shows the total storm rainfall pattern for Illinois. An area of greater than 8 inches of rainfall extends from just south of Rockford through southern Cook County (to Park Forest). The area receiving 8 inches or more rainfall in this storm, which largely fell over 20 hours or less, covered 1,692 square miles, or 3 percent of Illinois. The area of 6 inches or more rainfall (2,873 square miles in Illinois) extended from southern Wisconsin into Stephenson County, Illinois, and then eastward into northern Indiana.

The storm rainfall pattern is considered reasonably uniform, in relation to past storms, and concentrated around the path of heavy rainfall. A minor rainfall low occurred northeast of O'Hare Airport.

Moreover, the same weather system that produced the July 17-18 rainstorm in Illinois had produced a rainstorm in Iowa and Nebraska on July 16 that resulted in several 8- to 10-inch amounts. Then the same weather system moved east from the Midwest into Canada and produced 10- to 12-

inch amounts in the Quebec Province on July 19-20. Storms and flooding in Canada resulted in ten deaths compared to five deaths in Illinois, and three in the Iowa floods.

Figure 4-3 presents the total storm rainfall map based on the measurements of the NWS weather radars. There is a good correlation between this pattern and that of Figure 4-2, which is based on 657 raingage measurements. Both maps show the heavy rain core of the storm enters northern Illinois in the same location, extends southeastward, and then assumes a more easterly orientation from Chicago into Indiana.

Time-distribution curves for five Illinois raingages in and near the center of the storm (Figure 4-4) illustrate the temporal distribution of the July 17-18 rainfall. The recording gage near DeKalb is in the western end of the high rainfall zone (Figure 4-2), and the easternmost gage (# 25) is close to Park Forest at the storm's eastern end (Figure 4-2). These time distribution curves show that most rain fell during two periods of heavy rainfall.

The first heavy rainfall period began in mid- to late morning on July 17 at all raingages. Varying amounts of rain fell from a series of showers and thunderstorms during the afternoon with most heavy rain ending by 2000 LST on July 17. However, a few raingages continued to experience showers producing about 0.25 inch per hour between 2000 and 0000 LST on July 18.

The second major rain period began between midnight and 0100 LST on July 18. Heavy rains occurred at all raingages from that time until between 0400 and 0700 LST. Rain showers continued until 1000 LST.

The shapes of the rainfall distribution curves (Figure 4-4) reveal that both the afternoon storm system and the ensuing morning storm system were composed of a series of convective showers. Interestingly, gage 15 near Lemont had slightly over 5.2 inches in the July 17 afternoon storm and then 5.5 inches in the July 18 morning storms, nearly equal amounts. At the other four gages, the nocturnal rain period was the heavier period. Studies of many other severe convective rainstorms in Illinois have shown that the heaviest rains typically occur nocturnally, as was found in the July 17-18 storm period (Huff et al., 1958).

Storm Morphology

The morphology of the rainstorms on July 17-18 was analyzed using NWS radar data from the radar located at Romeoville. Figure 4-5 shows radar echo maps at selected times during the storm.

From 1100 to 1300 LST on July 17, the radar depicted the growth of new cells occurring between two lines: 1) a northwest-southeast line of echoes in western Illinois, and 2) a north-south broken line in eastern Illinois near Lake Michigan. This new echo development resulted in the merger of many of these storms that moved through DeKalb, Kane, DuPage, Cook, Kendall, and Will Counties.

By 1400 LST, there were four areas of thunderstorms across northern Illinois (labeled a-d in Figure 4-5). They were roughly organized into a west-east area of echoes extending from the Iowa-Illinois border on the west to Lake Michigan. This area of many echoes drifted to the east and east-southeast, and became more pronounced with time as more cells developed. Sporadic tornadic activity occurred between 1435 and 1755 LST in the area (see 1600 LST, Figure 4-5). The tornadoes

were associated with one of the easternmost echoes in this large echo area, and hail fell around 1700 LST from one of the western cells in the line.

By 1800 LST, this huge area of storms had merged into a cohesive unit (Figure 4-5), and the individual storms within it were moving towards the southeast. Progression of this area of strong storms across northeastern Illinois during the afternoon produced large amounts of rain.

New thunderstorm cells were beginning to develop at 1800 LST (Figure 4-5), and by 1830 LST they began to form a new large echo area across northern Illinois. Again, storms extended from the Iowa border to Lake Michigan, and some were further north in southern Wisconsin. There were three identifiable areas of convection: 1) a broken northwest-southeast line in eastern Wisconsin (e in Figure 4-5), 2) a small echo area in southwestern Wisconsin (f in Figure 4-5), and 3) the strongest complex along the Iowa-Illinois border (g in Figure 4-5). By 1900 LST, all three areas were increasing in both size and intensity, and the original (afternoon) system (a-c in Figure 4-5) was weakening and moving southward. These three new storm areas continued to become more organized and enlarge with time, and by 1930 LST, new isolated cells began developing in northern Illinois. These new cells were east of the Iowa-Illinois echo complex (g in Figure 4-5), and located between Rockford and Aurora. By 2000 LST, these new cells had merged to form a small line (h in Figure 4-5).

The three westernmost areas of convection in Illinois (f-h in Figure 4-5) became dominant in rain areas by 2030 LST. They were slowly moving to the east, and the southern line (a-c in Figure 4-5), which had developed at 1400 LST, had moved into Indiana. Tornadoes (at 1917 LST at Savanna; and 2009 LST at Coleta) and 0.75-inch-diameter hail (Coleta) were produced by the storm system that had originated at 1830 LST (g in Figure 4-5) along the Iowa-Illinois border. The three late afternoon storm areas persisted and continued their eastward movement during 2100-2200 LST.

By 2300 LST, new cell growth occurred between the Iowa-Illinois storm (g in Figure 4-5) and the northwest-southeast oriented echo complex located in south-central Wisconsin. This resulted in a fairly continuous line of cells (see 2200 LST, f-g in Figure 4-5). The line was oriented northwest-southeast from south-central Wisconsin through Aurora to the southern tip of Lake Michigan and into northern Indiana by 0000 LST on July 18. Two new areas of ceEs also developed along the Illinois-Iowa border (i in Figure 4-5), and these moved eastward across the region and merged into this huge northwest-southeast line of rain by 0200 LST. Thereafter, this echo area slowly moved east through the Chicago area producing heavy precipitation and then dissipated during the morning of July 18.

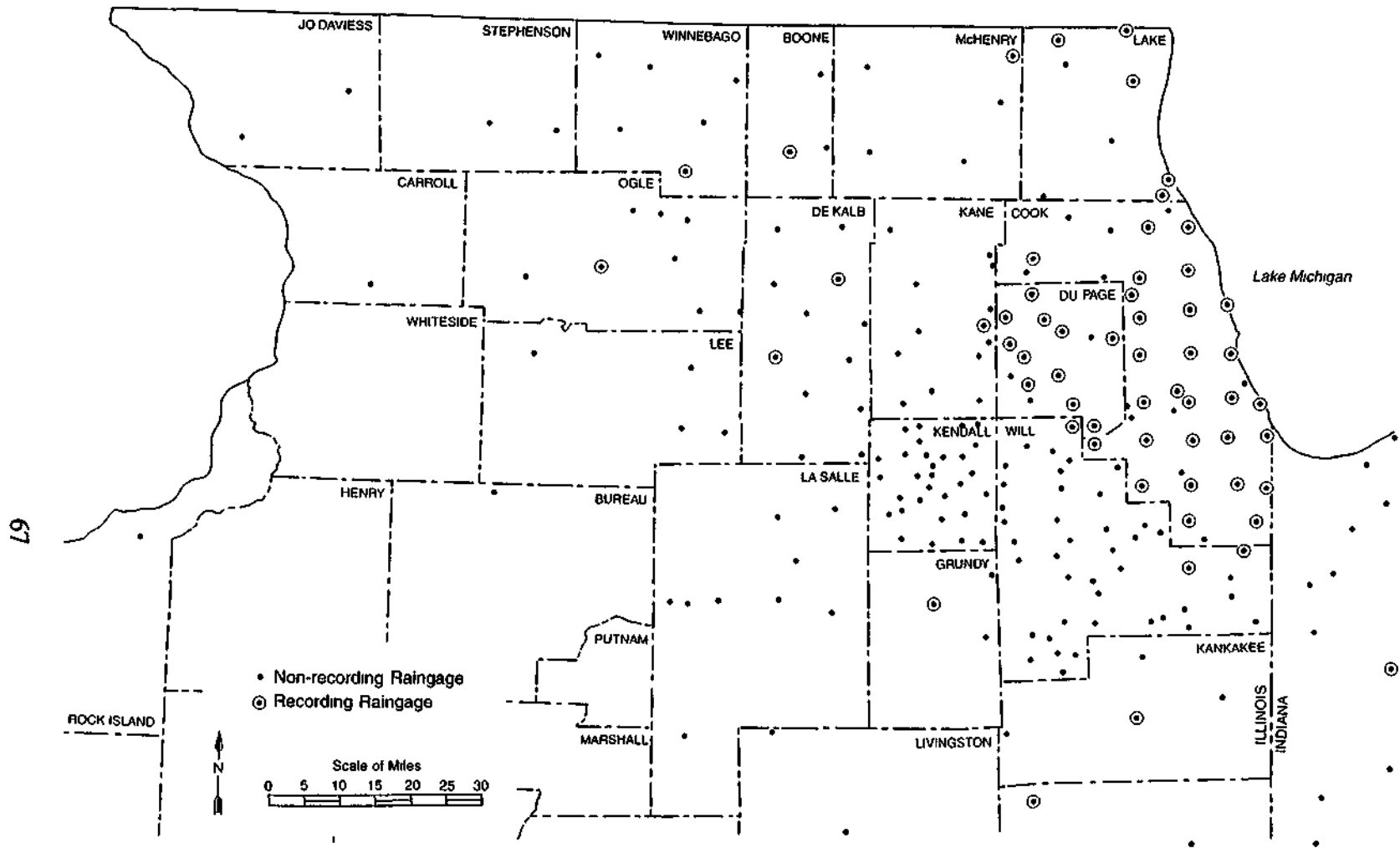


Figure 4-1. Locations where storm rainfall data were collected.

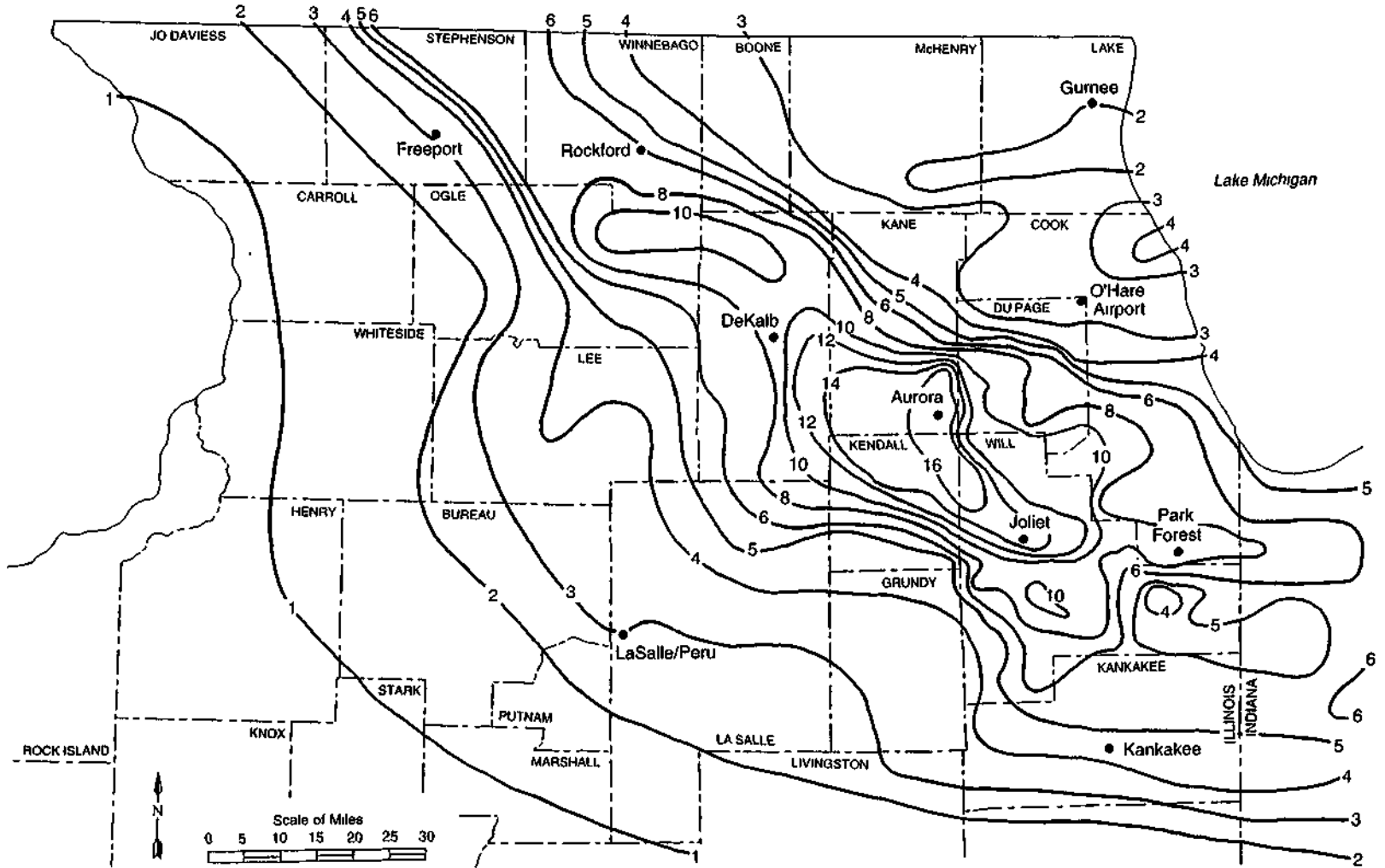


Figure 4-2. Total rainfall for the storm on July 17-18, 1996.

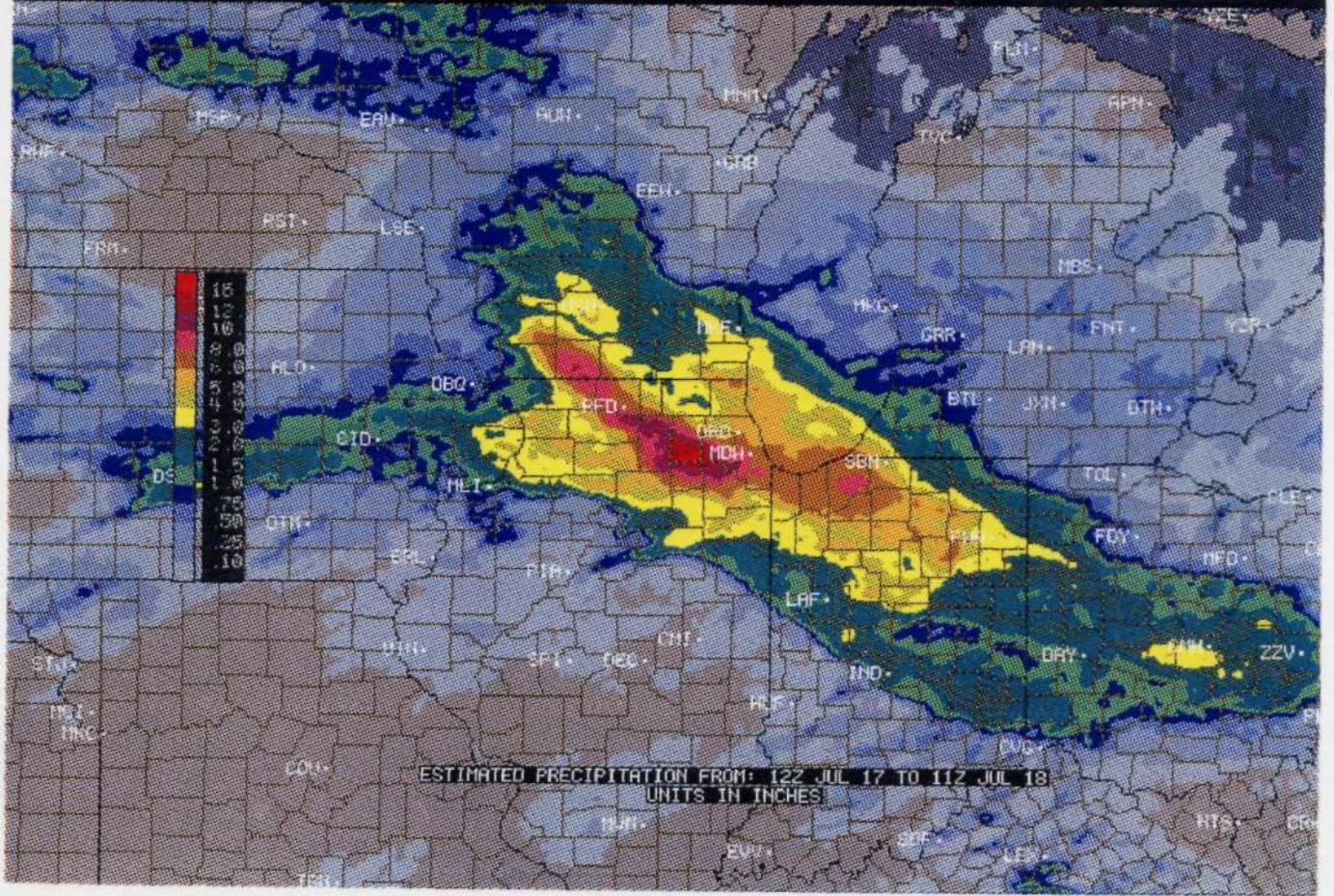


Figure 4-3. Total storm rainfall as defined by National Weather Service weather radar systems.

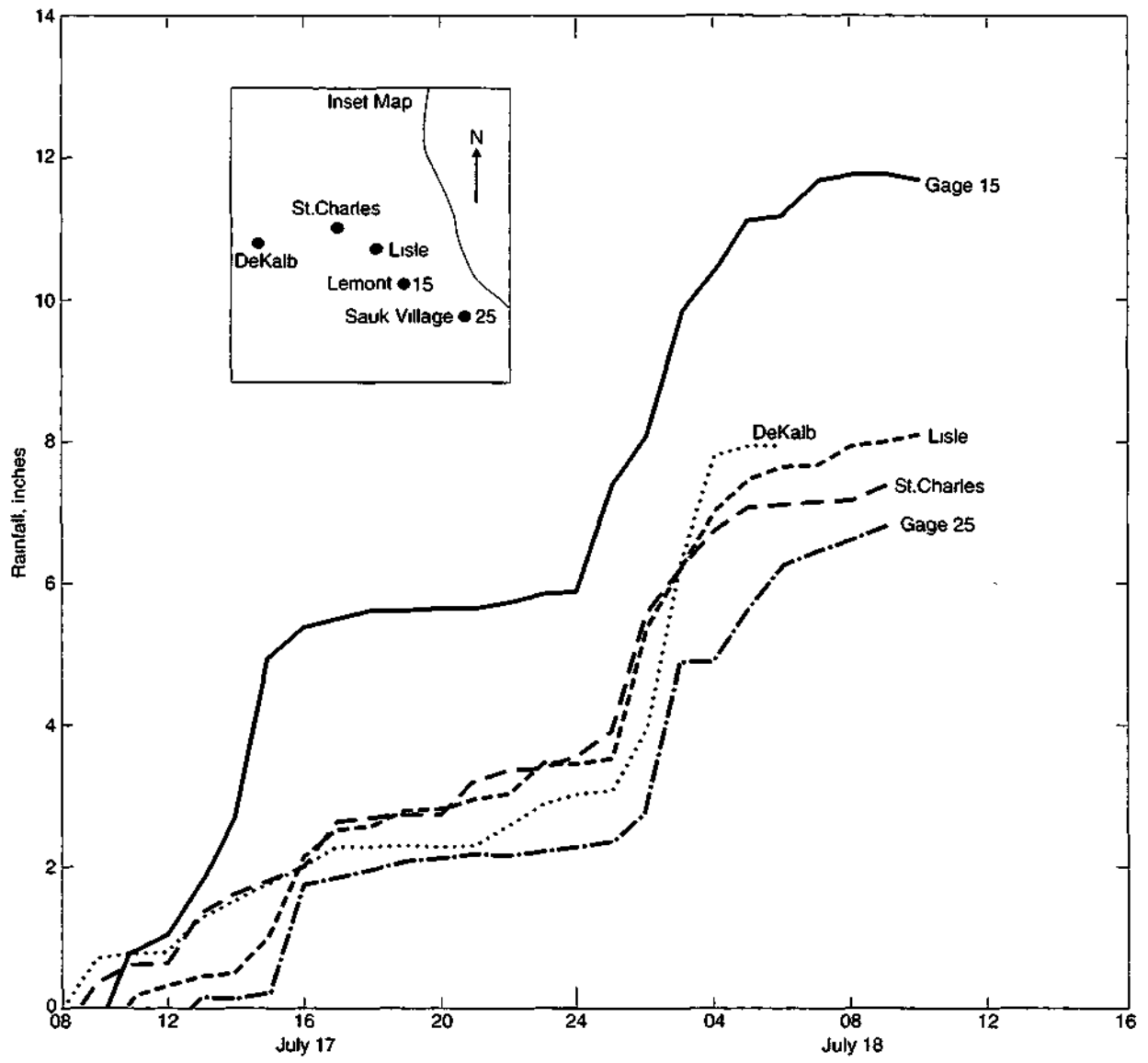


Figure 4-4. Temporal distribution of the storm rainfall at five raingages.

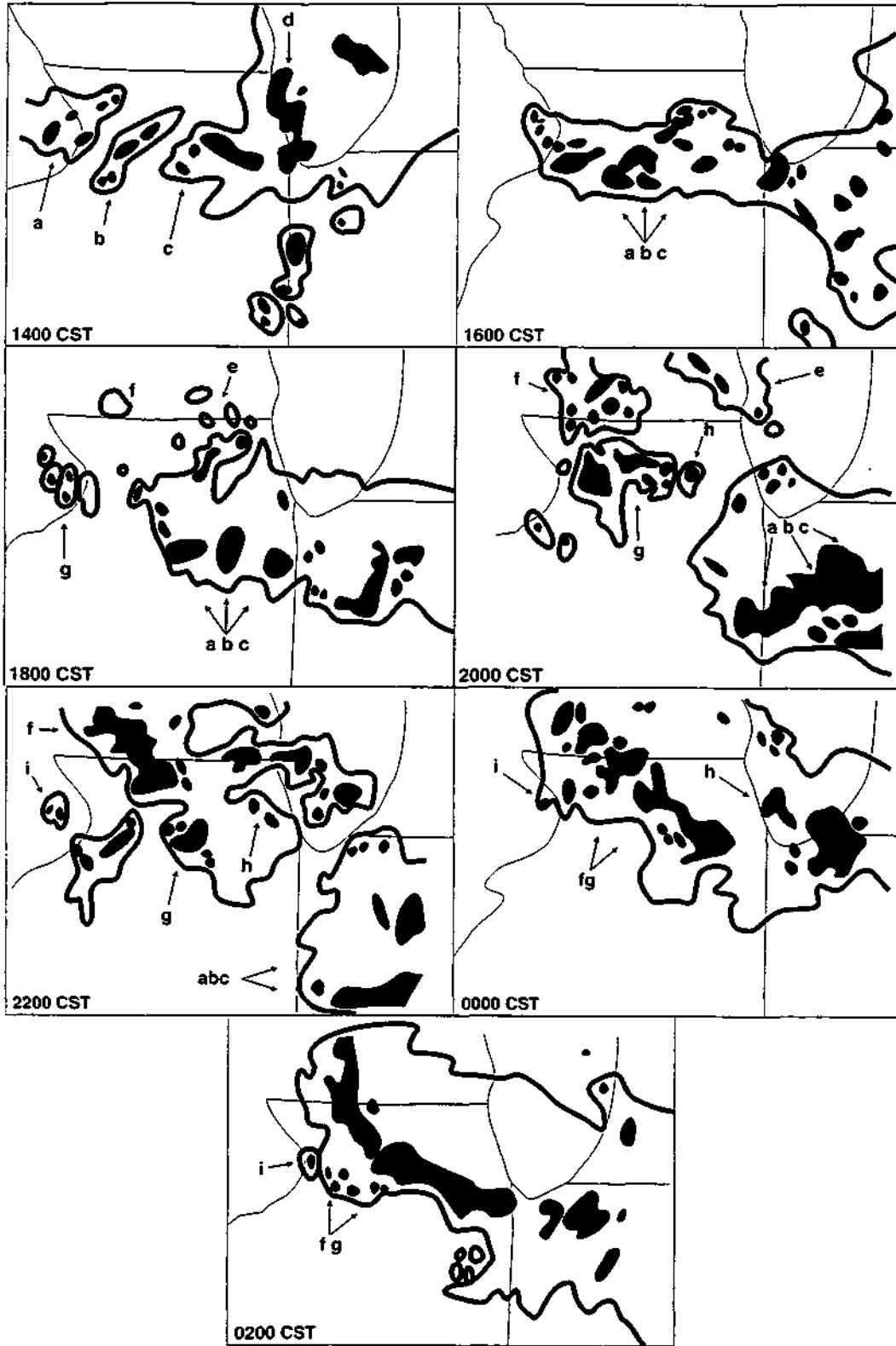


Figure 4-5. Major echo areas at different times during the storm.

References

- Grosh, R.C., 1978: *Operational Prediction of Severe Weather*. Technical Letter 27, Illinois State Water Survey, Champaign, IL, 4 pp.
- Huff, F.A., R. Semonin, S.A. Changnon, and D. Jones, 1958: *Hydrometeorological Analysis of Severe Rainstorms in Illinois, 1956-1957*. Report of Investigation 35, Illinois State Water Survey, Champaign, IL, 80 pp.

Chapter 5. Hydrometeorological Characteristics

*James R. Angel and Floyd A. Huff, Illinois State Water Survey,
and David Changnon, Northern Illinois University*

Part 1. Total Storm Rainfall Analyses

Characteristics of the total rainfall distribution were derived from a combination of spatial and temporal analyses. These included definition of the spatial characteristics through the derivation of standard area-depth curves and envelope curves, and hydrologic reduction ratios. Temporal characteristics were determined by analyses of rainfall amounts obtained from recording raingages available within the confines of the storm. These data were used to calculate the time distribution of hourly amounts and the percentage time distribution of total storm rainfall.

Standard Area-Depth Curves

Figure 5-1 shows a standard area-depth curve for an area of 10,000 square miles surrounding the primary storm center near Aurora, Illinois. The area-depth curve provides a measure of average rainfall over the entire storm area, the maximum point rainfall, and the average rainfall at any selected subarea about the storm center. The regression curve was closely approximated by an expression in which rainfall depth was related to the cube root of the area. This transformation has most frequently provided the best fit for such large-area, severe rainfall events in Illinois. Area-depth curves can be used to assess heavy rainstorms that produce floods.

Reference to the area-depth curve in Figure 5-1 shows an estimated maximum rainfall of approximately 17.4 inches at the storm center. The maximum rainfall measured at a raingage was 16.94 inches at Aurora. The mean rainfall about the storm center gradually decreases to 16.9 inches at 50 square miles, and to 16.3, 15.4, 14.0, 12.6, 11.0, 8.2, and 5.2 inches at 100, 200, 500, 1000, 2000, 5000, and 10,000 square miles, respectively.

An immediate question that will occur to many readers is, how does the spatial distribution in this storm compare with that in other severe storm events in Illinois? Figure 5-2 provides a partial answer to this question with maximum 24-hour area-depth curves for the July 1996 storm and for four other storms that are among the most severe rain events ever observed in Illinois and which have been subjected to detailed analyses as part of the Water Survey's program in hydrometeorology. Rainfall data over the 2000-square-mile area immediately surrounding the storm centers were used to construct the curves.

Storms providing the two heaviest 24-hour amounts ever recorded in Illinois were those on July 17-18, 1996, and on June 14, 1957. They had the steepest rainfall gradients around the storm centers as illustrated by the curve slopes. Although the storms are among the most severe rain events in history, the rainfall gradients are much smaller in the other three storms illustrated, and they are more typical of other large-area severe events studied by the Water Survey. Figure 5-2 shows that the five storms were similar with respect to curve fitting (cube root transformations), but there were

major differences in rainfall gradients and in maximum point rainfall exist between these severe rainstorms.

Additional information on the magnitude of the July 1996 storm, with respect to other extreme rain events in Illinois, was obtained from a review of the Water Survey's data bank of area-depth relations. As part of the hydroclimatic research program at the Water Survey, area-depth relations have been determined for more than 400 storms in which the 100-year frequency of point rainfall was equaled or exceeded for storms of various durations (Huff, 1993). All storms that met the above criteria for storms of 24-hour or less duration were selected and their area-depth curves were compared with that for the July 1996 storm.

Because of a major interest in small basin hydrology, a previous study involved spatial distributions (area-depth relations) over areas up to 2000 square miles in and surrounding the centers of the 100-year event storm, and Table 5-1 compares the ten storms with the heaviest 24-hour rainfall over areas of 2000 square miles.

The July 1996 storm had the greatest mean rainfall among the 10 storms, followed closely by storms in 1910 and 1946. All three storms were storms of large areal extent and produced tremendous flooding problems. Six of the top 10 storms have occurred since 1950 when such extreme events became the subject of field surveys to improve the data samples and for detailed analyses of the rainfall distribution, which may provide a partial explanation for the apparent temporal bias. Examination of mean rainfall for the 5000 square miles surrounding the storm centers showed that the three storms also ranked first, second, and third.

Table 5-2 provides additional information about the magnitude of the July 1996 storm using the estimated 10-square-mile rainfall obtained from area-depth curves for the ten top storms. This curve-derived maximum almost always exceeds the maximum recorded point rainfall because the measured point rainfall rarely occurs at the exact center of the storm. Therefore, the curve-derived maximum is considered a better estimate of the actual point maximum.

Table 5-1. Comparison of the Mean Rainfalls for 2000 Square Miles among the Top-Ranked Extreme Rainfall Events in 1901-1996

<i>Rank</i>	<i>Date</i>	<i>Mean rainfall (inches)</i>	<i>Recorded maximum (inches)</i>	<i>Storm location</i>
1	July 17, 1996	11.3	16.94-Aurora	Northeast
2	October 4, 1910	11.1	10.71 - Harrisburg	South, Southeast
3	August 14, 1946	10.7	13.41 - Belleville	Southwest
4	June 14, 1957	9.3	16.54-E. St. Louis	Southwest
5	October 9, 1954	9.2	12.13-Waterman	Northeast
6	October 10, 1919	8.5	8.96 - Nashville	South
7	June 27, 1957	8.4	13.20 - Paris	East
8	July 12, 1957	7.7	11.10-Kankakee	Northeast
9	August 16, 1959	7.5	10.58 - W. Frankfort	South
10	August 20, 1915	7.5	8.03 - Waterloo	South

**Table 5-2. Estimated 10-Square-Mile Mean Rainfall
in Storms Shown in Table 5-1**

<i>Rank</i>	<i>Date</i>	<i>Rainfall (inches)</i>	<i>Rank</i>	<i>Date</i>	<i>Rainfall (inches)</i>
1	July 17, 1996	17.3	6	October 9, 1954	12.8
2	June 14, 1957	16.7	7	July 8, 1951	12.5
3	August 14, 1946	16.5	8	July 12, 1957	11.5
4	October 4, 1910	14.4	9	August 16, 1959	10.5
5	June 27, 1957	12.9	10	October 26, 1919	10.1

Thus, Table 5-2 provides a measure of the rain intensity at or near the storm center. Nine of the ten storms are the same as those in Table 5-1, but the order is different. The July 1996 storm ranked first again in Table 5-2. The top four ranks are the same in both tables, but their order is different.

The foregoing statistics show that the three 24-hour superstorms of 1996, 1946, and 1910 were the most severe storms encountered in Illinois since the start of this century with respect to intensity and areal extent. Of the three storms, the July 1996 storm ranked first in intensity over the 5000 square miles immediately surrounding the storm center. It was truly an extreme event.

Area-Depth Envelope Curves

Computations of area-depth envelope curves were made to provide information on the distribution of point rainfall amounts about the storm center. These curves, in conjunction with the standard area-depth curves, provide pertinent information needed by users of storm rainfall spatial relationships (hydrologists, climatologists, hydrometeorologists, and others).

Figure 5-3 shows an area-depth envelope curve. In this data presentation, the point rainfall equaled or exceeded is related to the area enveloped about the storm center. This type of curve is very useful in evaluating the storm impacts with respect to the frequency distribution of point rainfall within the storm area.

Figure 5-3 also shows pertinent recurrence-interval information with respect to the storm. Based on the latest frequency information for northeastern Illinois (Huff and Angel, 1989), the curve indicates that an area of 4650 square miles experienced 24-hour point rainfall amounts that exceeded those expected to occur, on the average, of once in 10 years at a given location. Similarly, the 25-year, 50-year, and 100-year frequency values were exceeded over areas of 2600, 1900, and 1350 square miles, respectively. The 24-hour rainfall amounts values for the above recurrence intervals are:

<u><i>Frequency (years)</i></u>	<u><i>Rainfall (inches)</i></u>
10	4.47
25	5.51
50	6.46
100	7.58

The average county size in Illinois is approximately 1000 square miles. The above analysis shows that the area encompassed by 100-year rainfall amounts was larger than the average-sized county. This increases to an area approaching that of two counties for 50-year events, and five counties for 10-year events. As indicated elsewhere in this report, both the size and intensity of the July 1996 storm were exceptional for Illinois and the Midwest.

Reduction Ratios

For many hydrologic applications, users prefer to relate the spatial distribution characteristics to maximum point rainfall at the storm center. Therefore, the original area-depth curve (Figure 5-1) was converted to this form. Table 5-3 summarizes results following the format used by Huff (1993). The ratios of subarea mean rainfall to maximum point rainfall at the storm center for selected subareas along the area-depth curve are calculated. These values are commonly called *reduction ratios or coefficients*. The area-depth computed value of maximum point rainfall has been used in deriving Table 5-3. The observed maximum point rainfall (16.94 inches in the July 1996 storm) will almost always be exceeded by the actual maximum. The curve-computed maximum is considered a more realistic estimate of the actual maximum.

The last column in Table 5-3 shows median reduction ratios derived from a study of all 24-hour storms in Illinois in this century, in which point rainfall at the storm center equaled or exceeded the 100-year frequency of point rainfall (Huff, 1993). It is apparent from comparison of columns 2 and 3 in Table 5-3 that the July storm reduction ratios were typical of those found in storms that exceed the 100-year frequency values at their centers.

Table 5-4 shows reduction coefficients in seven previous outstanding storms. These storms have been selected from a large number on file to illustrate the variability that exists between such

Table 5-3. Total Storm Reduction Ratios for July 17-18, 1996

<i>Area enveloped (mi)</i>	<i>Storm ratios*</i>	<i>Medians</i>
25	0.98	0.98
50	0.96	0.95
100	0.93	0.92
200	0.88	0.88
350	0.84	0.85
500	0.80	0.81
750	0.76	0.77
1000	0.72	0.74
1500	0.67	0.69
2000	0.63	0.65

Note:

*Ratios based on area-depth curve value for maximum point rainfall (17.6 vs. a maximum of 16.94 inches).

**Median values based on all severe 24-hour rainstorms since 1901 (Huff 1993).

Table 5-4. Examples of Ratio Relation in Other 24-Hour Storm Periods with Point Maxima 100-Year Frequency

<i>Date</i>	<i>Ratio for given area (sq. mi.)</i>							
	<i>25</i>	<i>50</i>	<i>100</i>	<i>200</i>	<i>500</i>	<i>1000</i>	<i>1500</i>	<i>2000</i>
August 16, 1959	0.98	0.96	0.93	0.90	0.84	0.76	0.73	0.70
June 14, 1957	0.98	0.95	0.90	0.85	0.74	0.65	0.60	0.55
June 27, 1957	0.97	0.94	0.90	0.87	0.80	0.73	0.70	0.66
July 12, 1957	0.97	0.95	0.92	0.89	0.82	0.75	0.71	0.66
May 21, 1957	0.96	0.95	0.93	0.89	0.83	0.77	0.73	0.70
October 9, 1954	0.99	0.98	0.96	0.92	0.87	0.84	0.80	0.76
August 14, 1946	0.98	0.96	0.93	0.90	0.82	0.77	0.70	0.65
7-storm median	0.98	0.95	0.93	0.89	0.82	0.76	0.71	0.66
July 17-18, 1996	0.98	0.96	0.93	0.88	0.80	0.72	0.62	0.63

storms. Most of the storms listed in Table 5-4 were subjected to extensive field surveys to establish storm characteristics, and several were partially contained in one of the various dense raingage networks operated by the Water Survey during the past 45 years. Thus, the storm of August 16, 1959 (Table 5-4) was centered on the Water Survey's Little Egypt dense raingage network in southern Illinois. The June 14, 1957, storm was centered in southwestern Illinois and was subjected to a comprehensive field survey by Water Survey meteorologists. Similar field surveys were conducted in the east-central Illinois storm of June 27, 1957, and the northeastern Illinois storms of July 12, 1957, and October 9, 1954.

Table 5-4 also shows the median values for the seven storms, which agree closely with those in Table 5-3 for the entire storm sample, and with the July 1996 storm values. The reduction coefficients provide a measure of the rainfall gradients in a storm. The foregoing analyses indicate that gradients in the July 1996 storm were typical of those in which 100-year rainfall frequencies are exceeded in the storm center.

Temporal Distribution Characteristics

Temporal characteristics of the July 1996 storm were determined from hourly rainfall amounts obtained from recording raingages available within the confines of the storm. Graphical plots of the hourly data provide information on the rainfall intensity, its variability over time, and identifies the period(s) of peak intensity within the storm. A second analysis that provides valuable information for the users of time distribution characteristics has been obtained from derivation of percentage time distribution curves. These show the hourly percentage of total storm rainfall at each sampling point. Frequently, a major percentage of the total storm rainfall occurs within a relatively small portion of the storm's duration, as was typical of the July 1996 storm near the storm center.

Figure 5-4a illustrates the temporal distribution characteristics for the raingage at the Sycamore sewage plant, located about 28 miles northwest of the storm center at Aurora. A total of seven rain bursts occurred with the storm system: one major nocturnal burst (a convective entity), three moderate bursts, and three minor bursts.

The heaviest convective burst reached a maximum intensity of 2 inches per hour from 0200-0300 LST on July 18. The total storm rainfall at Sycamore was 9.53 inches. The hourly maximum of 2.0 inches represents 21 percent of the storm total. During the 3-hour period, 0000-0300 LST, 53 percent of the 24-hour total rainfall was recorded. Figure 5-4b shows that 78 percent of the total storm rainfall occurred in the major nocturnal rain period. It is obvious from Figure 5-4 that the nocturnal storm period dominated the total rainfall distribution in the July 1996 storm, and that a major portion of the storm rainfall occurred in a relatively small portion of the total rain duration.

Figure 5-5a shows the time distribution at the DeKalb raingage of the Illinois Climate Network (ICN), located approximately 33 miles west-northwest of Aurora and 15 miles southwest of Sycamore. The distribution was similar to that at Sycamore and consisted of six bursts that produced a rainfall total of 7.52 inches. The heaviest rainfall reached 2.23 inches per hour at 0100-0200 LST, and the nocturnal storm period contributed 72 percent of the total storm rainfall.

There were six recording raingages along an approximate northwest-southeast line, extending from Sycamore through Kane County into southwestern DuPage County, and the southwestern and southeastern parts of Cook County. This line was only a short distance north of the main axis of the total rainfall pattern (Figure 4-2). The raingage at St. Charles in Kane County showed time distributions similar to those at Sycamore. The maximum hourly amount of 1.56 inches occurred from 0100-0200 LST, the storm consisted of six bursts, and the nocturnal storm period produced 62 percent of the total rainfall of 6.86 inches (Figure 5-6).

In the DuPage County Network, the rain at gage 31 showed a distinctly different distribution than the Sycamore and St. Charles gages. At gage 31, the time distribution curves (Figure 5-7) indicate two major storm periods nearly equivalent to each other in maximum intensity during the daytime and nocturnal storm periods. However, the nocturnal period continued to dominate in the production of rainfall, and accounted for 64 percent of the total storm rainfall. This was the closest recording gage to the maximum point rainfall of 16.94 inches. Gage 31 is located about 8 miles east of Aurora, and would normally be expected to correspond most closely to the characteristics of the time distribution of rainfall at Aurora among the available recording gages. If so, the Aurora extreme value may have been caused largely by the greater relative strength of the daytime storm period, compared with amounts in the immediate surrounding storm area.

At gage 31, 54 percent of the 24-hour total storm rainfall occurred in the 3-hour period from 0100 to 0400 LST on July 18. Adding the 1.51 inches from 1500-1600 LST in the earlier daytime storm, the four hours (17 percent of total rain period) accounted for 73 percent of the total storm rainfall.

The nearly equivalent daytime and nocturnal storm intensities were also found at gage 15 in southwestern Cook County, where a rainfall total of 11.0 inches was recorded (Figure 5-8). The daytime maximum intensity of 2.18 inches per hour exceeded the nocturnal maximum, but the total output of the nocturnal storm period was 52 percent of the total storm rainfall, compared with 48 percent for the daytime storm.

Gage 21, located southeast of gage 15, had a distribution that was very similar to Gage 15 (Figures 5-9). However, gage 25 in extreme southeastern Cook County reverted to the Sycamore and DeKalb type of distribution (Figure 5-10). The nocturnal maximum intensity exceeded the daytime maximum, and the nocturnal period produced 68 percent of the storm total.

Overall, the nocturnal storm period was the greatest producer of rainfall in the heaviest part of the total storm rainfall pattern (Figure 4-2). For the most part, the nocturnal storms were also the producers of the heaviest hourly rainfall intensities in the storm system. Typical of extreme convective rainfall events, a major portion of the rainfall occurred during a relatively small portion of the total storm duration.

Maximum 3-Hour and 6-Hour Rainfall Distributions

Combining information provided by the available recording raingages and the many total rainfall measurements throughout the storm area, isohyetal patterns (maps) and area depth relations were derived for the maximum 3-hour and 6-hour rainfall amounts. This information is valuable in analyzing and evaluating the hydrologic characteristics of this unusually severe flood-producing event.

For these computations, the total 24-hour rainstorm event was divided into two distinct rain periods. The first period was concentrated in the middle to late afternoon of July 17, and the second period peaked in the early morning hours of July 18. For each map, the maximum 3- and 6-hour amounts for the two rain periods were based on the maximum 3- and 6-hour amounts *at each station*. Therefore, the particular 3- and 6-hour time periods when the maximum rainfall occurred may change between stations. Differences in the timing of the maximum 3- and 6-hour rainfall was most noticeable during the first period on the afternoon of July 17, with starting times ranging from 1100 to 1600 LST. However, for a majority of the stations, the time of the 3-hour maximum for the first rain period was 1300-1600 LST and the time of the 6-hour maximum was 1200-1800 LST. For the second rain period on the morning of July 18, the starting times only varied by one or two hours between stations. For most stations, the time of the 3-hour maximum was 0100-0400 LST and the time of the 6-hour maximum was 0000-0600 LST.

Figures 5-11 to 5-14 display the isohyetal patterns within the heavier portions of the storm. Each map uses an isohyetal spacing of one inch. The greater intensity of the nocturnal storm period is evident from the maps. Maps for the nocturnal period maintained the general northwest-southeast orientation of the rainfall pattern, observed in the total storm period (Figure 4-2), while maps for the earlier daytime storm period show a general west-east orientation. The orientation of the surface rainfall patterns is generally closely related to the movement of the rain-producing synoptic weather system (Huff, 1979).

Figures 5-15 and 5-16 show area-depth curves corresponding to the four isohyetal presentations in Figures 5-11 to 5-14. These provide an additional measure of the spatial distribution characteristics of the rainfall displayed on the isohyetal maps. The greater intensity and rain output in the nocturnal storm period is obvious.

For the maximum 3-hour and 6-hour rainfall in the nocturnal storm period, analyses were performed to determine the area enveloped by recurrence intervals of 10 to 100 years. The nocturnal maxima also qualified as the maximum 3-hour and 6-hour rainfalls for the entire storm period. Figures 5-17 and 5-18 show the distribution patterns and Table 5-5 summarizes the statistical analysis.

Within the approximately 6300 square miles incorporated in the sampling area in Figures 5-17 and 5-18, the 3-hour maximum showed an area of 630 square miles in which the rainfall exceeded the 100-year average recurrence interval. This area increased to 1000, 1395, and 1830 square miles,

Table 5-5. Area Enveloped by Recurrence Intervals of Various Magnitude in the 3-hour and 6-hour Maximum Rainfalls

<i>Recurrence interval (years)</i>	<i>Area enveloped (square miles)</i>	
	<i>3-hour</i>	<i>6-hour</i>
10	1830	2150
25	1395	1610
50	1000	1195
100	630	755

respectively, for recurrence intervals of 50, 25, and 10 years. Thus, an area the size of an average Illinois county had rainfall that exceeded the 3-hour amount to be expected, on the average, of once in 50 years. The area of the 10-year recurrence interval approached the size of two typically sized counties.

Similarly, the 6-hour maximum rainfall exceeded the amount expected to occur, on the average, over areas ranging from 755 square miles for a 100-year event, to 2150 square miles for a 10-year event. Table 5-5 provides another measure of the severity of the July 1996 storm.

Comparison of July 1996 Storm With Expected Extreme Events

Engineers use expected rainfall amounts at select return periods to determine the design of water-handling structures such as storm drains and retention ponds. Most of the design considerations are based on return periods of 100 years or less. One concern resulting from a major rainfall event, such as the July 1996 storm, is the potential impact on these expected rainfall amounts.

As shown in Figure 5-19, the 16.94 inch amount, the maximum rainfall measured at a raingage during the July 1996 storm, is well above any previously recorded amount in the 97-year precipitation record at Aurora. If the rainfall frequencies in Bulletin 70 (Huff and Angel, 1989) are extended to 200 years and beyond for both Aurora and northeastern Illinois, and the 16.94 inch storm is fit to the line, it appears to exceed even the 1000-year, 24-hour storm event. This approach assumes that the statistical distribution fit to the frequencies out to 100 years would also be appropriate out to 1,000 years. This assumption cannot be validated because of our limited historical records; however, the result shows that the storm is far beyond what is normally expected in any 100-year period. Therefore, the 16.94 inch amount would be considered a true statistical outlier.

Usually, for a station such as Aurora with 97 years of record, an outlier such as this will not have a large influence on the resulting distribution of expected extreme rainfall because of the way that the rainfall frequency values are calculated. The typical procedure is to find the highest rainfall for each year of the record. This annual maximum time series is then fit to a statistical distribution using various fitting techniques (e.g., graphical, maximum likelihood, or L-moments methods). This statistical distribution is used to calculate the expected rainfall amounts at the return periods of interest, to smooth out the year-to-year variations, and to reduce the influence of outliers. A more

detailed explanation of the factors involved in determining the rainfall frequency values can be found in Huff and Angel (1989).

According to Huff and Angel (1989), the expected 100-year, 24-hour storm for Aurora is 8.40 inches. Using the Generalized Extreme Value (GEV) distribution and both the maximum likelihood and L-moments methods of fitting the distribution (Huff and Angel, 1992), inclusion of the 16.94 inches increased the amount of the 100-year, 24-hour storm value to 9.91 inches (maximum likelihood method) and to 11.17 inches (L-moments method) as shown in Figure 5-19. This sizeable increase would have a significant impact on the design of water-handling structures. However, Huff and Angel (1989) recommended the use of *regional averages* to reduce the variability associated with values at any particular station. The average 100-year, 24-hour storm for northeastern Illinois is 7.58 inches (Huff and Angel, 1989). The eight stations in northeastern Illinois used for the regional average were Aurora, Chicago, DeKalb, Joliet, Kankakee, Marengo, Ottawa, and Waukegan. Except for Aurora, the expected rainfall for the 100-year, 24-hour storm has not changed appreciably with the addition of data through 1996 for these stations. Inclusion of the July 1996 storm for Aurora would increase the regional average of the 100-year, 24-hour storm to approximately 7.77 inches (maximum likelihood method) and 7.93 inches (L-moments method).

Based on this analysis, the use of the statistical distribution and the regional average diminishes the influence of this large storm. Therefore, the rainfall value of 16.94 inches for Aurora would not materially change the expected regional average rainfall amounts found in Huff and Angel (1989).

Climatology of Heavy 24-Hour Precipitation Amounts in Northern Illinois

Historical daily precipitation amounts from 24 northern Illinois stations of the National Weather Service or NWS (Figure 5-20) were assessed to determine how the July 1996 rainfall values ranked when compared with other regional rainstorms. Eight stations were considered "long term" with daily precipitation records available back to 1900. Fourteen additional stations were considered "short term" with daily precipitation records dating back to 1950 (Figure 5-20). Two other stations examined, Chicago Midway and Waukegan, had records beginning in the 1920s.

All daily precipitation amounts were ranked for each station, and the top ten daily amounts were determined and exceeded three inches at all stations. The most frequent dates when these top ten values occurred were determined for stations in the long-term and short-term groups. Dates when two or more long-term stations and four or more short-term stations experienced a top ten daily precipitation amount were identified. The dates shown in Table 5-6 appear to be the important heavy rain events in northern Illinois. Values in Table 5-6 indicate that since 1950 the storm of October 10, 1954, produced 13 ten events, followed by the storm of July 17-18, 1996, with 9 of these events.

The greatest daily precipitation total for each station was assessed to discern the most common date of greatest precipitation among both groups of stations (Table 5-7). When considering all 24 stations (and the 1950-1996 period), six stations reported their greatest daily precipitation amount on July 18, 1996. The July 18, 1996, amounts for Aurora (16.92 inches) and Joliet Brandon Dam (13.60 inches) are 4 to 7 inches greater than the next highest amount among the 24 stations, 9.56 inches at Peotone. The July 1996 values in each group are marked in Table 5-7, revealing that two of eight long-term stations (Aurora and DeKalb), three of 14 short-term stations (Joliet Brandon

Dam, Park Forest, and Wheaton), and Chicago Midway all experienced their greatest daily amount during the July 1996 rainstorm. Among the two groups this was the most frequent date, revealing that the magnitude of this event makes it climatically unique.

Table 5-6. Dates of Large Daily Precipitation Amounts and Number of Stations (in Parentheses) Experiencing One of Their Top Ten Daily Totals on That Date

<i>1901-1996 Record*</i>	<i>1950-1996 Record**</i>
October 11, 1931 (2)	October 10, 1954 (9)
July 8, 1951 (3)	July 13, 1957 (6)
October 10, 1954 (4)	September 14, 1961 (6)
May 17, 1974 (3)	August 16, 1968 (4)
September 13, 1978 (2)	June 16, 1978 (4)
August 15, 1981 (2)	December 3, 1982 (4)
July 22, 1982 (2)	July 18, 1996 (7)
June 24, 1994 (2)	
July 18, 1996 (2)	

Notes:

*Based on 8 long-term stations.

**Based on 14 short-term station.

Table 5-7. Greatest Daily Precipitation Amount (in inches) at Stations

Long-term stations	Short-term stations	Other stations
Aurora (16.92)*	Antioch (4.96)	Midway (7.69)*
DeKalb (8.09)*	Channahan (7.46)	Waukegan (4.00)
Dixon (5.08)	Chicago University (5.13)	
Marengo (4.07)	Elgin (4.56)	
Morrison (6.10)	Freeport (5.25)	
Mt. Carroll (5.01)	Galena (4.80)	
Ottawa (8.77)	Geneseo (4.88)	
Walnut (6.38)	Joliet (13.60)*	
	Park Forest (6.55)*	
	Paw Paw (6.92)	
	Peotone (9.56)	
	Rockford (7.42)	
	Stockton (4.55)	
	Wheaton (7.24)*	

Note:

*These values occurred during the July 1996 rainstorm.

Table 5-8. Distribution of Top Ten Daily Precipitation Amounts by Decade

<i>Decade</i>	<i>Long-term stations</i>		<i>Short-term stations</i>
1900s	3		
1910s	3		
1920s	9		
1930s	5		
1940s	7	Sub-total: <u>27</u>	
<hr/>			
1950s	17		33
1960s	3		24
1970s	12		32
1980s	15		22
1990s*	6	Subtotal: <u>53</u>	23

Note:
* 1900-1996 only.

The number of top ten daily precipitation amounts by decade were identified for long-term and short-term stations (Table 5-8). There were 80 top ten daily precipitation values for the eight long-term stations: 27 in the first 50 years (1900-1949) and 53 since 1950. Large daily rainfall amounts occurred nearly twice as often in the last half of the century, agreeing with the finding that it has been a wetter climate regime since 1950 (Changnon, 1985). Among the short-term stations, the number of top ten daily values ranged from 33 in the 1950s, 22 in the 1980s, and 23 in the 1990s through July 1996.

The climatological assessment of daily rainfall events revealed the heavy rainstorm on October 10, 1954, provided the greatest number of heavy rainfall amounts over the most stations (i.e., more area). However, the actual rainfall amounts associated with that event were less than those of the July 18, 1996 rainstorm. More stations reported their greatest ever daily precipitation amount with the July 1996 storm than on any other storm date since 1900, suggesting this event was unique for this region of Illinois. Finally, the greater frequency of large rainstorms since 1950, including the large number since 1983 (Huff and Angel, 1989), reflects the recent wetter climatic regime.

Part 2. Chicago Metropolitan Area Storm Rainfall

A detailed analysis of the July storm characteristics in the Chicago metropolitan area was made possible by the presence of a dense recording raingage network of 25 gages spaced at approximately equal distances (5 miles apart) throughout Cook County. This network is operated in a joint project of the U.S. Army Corps of Engineers and the Illinois State Water Survey (Westcott, 1996). Additional storm information was obtained from a partially installed recording raingage network in DuPage County west of the metropolitan area.

Total Storm Rainfall

Figure 5-21 shows an isohyetal map of total storm rainfall in the metropolitan area. The heaviest rainfall occurred at gage 15 in the southwestern part of the network. Total rainfall of 10.99 inches and 7.95 inches, respectfully, at gages 15 and 16 exceeded the 100-year frequency of storm rainfall for 24 hours (Huff and Angel, 1989). The 10.99 inches at gage 15 is the maximum 24-hour rainfall ever recorded in the urban area. Totals at gages 11, 12, and 17 exceeded the 50-year recurrence value. As indicated by Figure 5-21, the heaviest rainfall occurred over the southern half of the metropolitan area. The exceptionally heavy rainfall in the southwestern part of the network was part of the storm core that extended west-northwest to the primary storm center near Aurora (Figure 4-2), where a storm total of 16.94 inches was recorded (discussed in Chapter 4).

Storm Periods

Analyses showed that the storm rainfall in the network occurred in two separate periods. The first storm period reached a maximum in the middle to late afternoon on July 17. The second storm began in late evening, reached a maximum from 0200-0400 LST, and ended at most locations by 1300 on July 18. Figure 5-22 depicts isohyetal maps for the two distinct storm periods (daytime and nocturnal). Both storm periods were most intense in the southwestern part of the metropolitan network.

Figure 5-23 depicts the isohyetal patterns for the 3-hour period of heaviest rainfall in the two storm periods. Again, the intensity centers for both periods were located in the southwestern part of the network, in agreement with the total storm period isohyetal patterns. The 3-hour values for both storm periods at gage 15 correspond to approximately 25 recurrence interval amounts (Huff and Angel, 1989).

Figure 5-24 depicts the isohyetal patterns for the 6-hour period of maximum rainfall in each of the two storm periods. The daytime period occurred from 1100 to 1700 LST. The nocturnal maximum occurred from 0000 to 0600 LST on July 18. In both 6-hour periods, gage 15 experienced rainfall amounts that exceeded the 50-year frequency of point rainfall in the storm region (Huff and Angel, 1989). Overall, the isohyetal patterns in the 6-hour periods closely resembled those for total storm rainfall.

Time Distribution Characteristics in Metropolitan Area

The heavy rainfall in the July 1996 storm was concentrated in the southern part of the metropolitan area, as indicated in Figure 5-21, which incorporated gages 11-25. The time distribution characteristics for gages 15, 21, and 25 have been discussed previously in conjunction with the analyses of the entire storm system. These network gages were located along the major axis of the storm system that extended from northeastern Illinois into northwestern Indiana.

Time distribution curves at four other gages were included in the metropolitan analyses (Figures 5-25 to 5-28) to provide additional information on the storm's characteristics. At gage 12, near the northern boundary of heaviest rainfall, the time distribution curves show the most intense rainfall occurred in the daytime storm period (Figure 5-25). Of the 6.51-inch rainfall total, about 70

percent of the rainfall was recorded in this part of the storm system. Rainfall was heavier in the nocturnal storm period about 6 miles south of gage 12 at gage 17. At this gage (Figure 5-26), the nocturnal storm period accounted for about 44 percent of the storm total of 5.65 inches (compared with 30 percent at gage 12).

Proceeding southward to network gage 22, which was located near the major axis of the storm system, a reversal in the time distribution characteristics occurred (Figure 5-22). At this point, the nocturnal storm became the major rainfall producer, 54 percent of the 5.14-inch total storm rainfall. Daytime and nocturnal distribution were similar to that at gage 15 (Figure 5-8), which was also near the main storm axis.

Figure 5-28 shows time distribution curves for gage 24 near the southwest boundary of the network. The nocturnal storm was more pronounced at this location, which is also near the major axis of the July 1996 storm. Of the 6.40-inch total rainfall, 74 percent was associated with the nocturnal storm period.

As indicated earlier in this chapter, gage 31 in the DuPage County network recorded the amount to the total storm's 16.94-inch maximum at Aurora. Gage 15 in the metropolitan network was also relatively close to the Aurora center. Both gage 31 (7.96 inches) and gage 15 (10.99 inches) showed similar time distributions with extremely heavy rainfall amounts in both the daytime and nocturnal storm periods. At gage 31, 63 percent of the storm total was associated with the nocturnal storm period, compared with 52 percent at gage 15. Most other gages near the main axis of the storm system showed either the daytime or the nocturnal storm period dominating rain production.

Spatial Distribution of Network Rainfall

Figure 5-29 shows the area-depth curve for total storm rainfall on the Cook County Network. The spatial distribution was closely approximated by a cube root relationship, similar to the curve developed for the entire storm area (Figure 5-1). The observed maximum was 10.99 inches at gage 15, the curve estimated maximum was 11.25 inches, and the network average was 5.03 inches. Average rainfall over the 50-square-mile area of heaviest rainfall was 8.70 inches. This decreased gradually to 8.05 inches for 100 square miles, 6.65 inches for 300 square miles, and 5.85 inches for 500 square miles. As indicated previously, the heaviest rainfall was concentrated over the southern part of the network.

Area-depth curves for the daytime and nocturnal portions of the storm are presented in Figures 5-30 and 5-31. The two curves are very similar in appearance, and the subarea mean rainfalls along the curves have only small differences. For example, the curves vary by only 0.10 inches at 100 square miles and by 0.05 inches at 500 square miles. Thus, the two curves are nearly replicas with respect to their spatial distribution characteristics.

Comparison with Other Storms in Metropolitan Chicago

Recording rain gage networks have been maintained in the Chicago urban area since 1949. Until 1989, the urban network included 16 gages operated by various government agencies (Metropolitan Sanitary District, Chicago Engineering Office, and the National Weather Service). During 1976-1980, the original network was augmented by a much larger network of recording gages

in conjunction with a major hydrometeorological research project conducted by the Illinois State Water Survey. In 1989, the original 16-gage network was replaced and expanded to 25 gages.

These network data show that the July 1996 storm was the fourth in the 45 years since 1949 to produce 24-hour point rainfall amounts in excess of the 100-year frequency for point rainfall. The first storm occurred on October 9-10, 1954. This storm was centered in the Aurora area, similar to the July 1996 storm, and produced 24-hour amounts in excess of 11 inches at its center (Huff et al., 1955). Amounts exceeding the 100-year frequency value extended eastward across the southern part of the metropolitan area, also similar to the July 1996 storm. Figure 5-32 shows the isohyetal pattern across the metropolitan area.

The next 24-hour event with values exceeding the 100-year amount occurred on July 12, 1957. At the Midway station in the north-central part of the metropolitan area, a total of 7.69 inches was recorded, and 50-year values were exceeded at the other urban stations. This storm was centered in the Chicago region in the afternoon, after which it drifted southward on the night of July 12-13, 1957, producing amounts greater than 11 inches in the Kankakee region (compared with a maximum of 7.7 inches recorded at one of the urban gages). Figure 5-33 shows the urban area pattern.

The next 100-year event occurred during the night of August 14-15, 1987, when a total of 9.18 inches over a period of less than 12 hours was recorded at the Chicago O'Hare weather station. This amount became the official all-time record storm rainfall value in Chicago. Figure 5-34 shows the isohyetal pattern of this storm over the urban area (constructed from the dense urban raingage network data). The storm maximized over the northern part of the metropolitan area. Figure 5-35 shows the pattern of point recurrence intervals for the total rainfall.

Another storm that produced massive flooding in some urban areas occurred on June 7, 1993. This storm was well-defined by the Water Survey network. Amounts equal to a 75-year frequency were observed at the storm center. This severe rainstorm event was concentrated over the southern part of the metropolitan area, similar to the 1954 and 1996 storms (Figure 5-36).

Summary

The rainstorm on July 17-18, 1996, in northern Illinois produced three rainfall records. The 16.94-inch total storm rainfall at Aurora was the maximum point rainfall recorded for storm durations of 24 hours or less in the present century in Illinois. The 10.99-inch storm rainfall recorded in the southwestern part of the Chicago metropolitan area was the heaviest 24-hour amount ever recorded in that city. Recording raingage networks in Chicago date back to the late 1940s. The July 1996 storm also produced the heaviest 24-hour mean rainfall recorded in Illinois over areas of 2000 and 5000 square miles immediately surrounding a storm center since the start of the century.

Analyses show that the July 1996 storm resulted primarily from the occurrence of two distinct mesoscale precipitation systems centered over approximately the same region. The first system occurred on July 17 in mid- to late afternoon, and the second system occurred in the early morning hours of July 18, a time when many previous rainstorms have been most intense. Chapter 2 explains the atmospheric conditions causing these two systems on July 17-18.

Analyses indicated that the 100-year recurrence interval of 12-hour point rainfall was exceeded over an area of 1900 square miles within the storm system. The 50-year recurrence interval

was exceeded over 2600 square miles, and the 25-year value was exceeded over 3450 square miles. These statistics further illustrate the magnitude of this storm.

Time distribution analyses of hourly rainfall were made at available recording raingages. These showed that the nocturnal storm was the major rain producer over most of the storm area. Although the afternoon storm was heavier in the vicinity of the Aurora center than over the rest of the storm area, the nocturnal storm was still the heavier rain producer regionally. Heavy rainfall in the afternoon storm was an important contributor to the occurrence of the storm center in the Aurora region.

As in most of the heavy storm events, a large portion of the July 1996 storm occurred during a very small percentage of the total storm duration. Thus at gage 31, the closest recording gage to the storm center at Aurora, 73 percent of the total storm rainfall occurred in 17 percent of the total storm duration.

Maximum 3-hour and 6-hour rainfall amounts in the storm were derived. From these, it was determined that the 100-year recurrence interval of point rainfall was exceeded over areas of 630 and 755 square miles, respectively, in the 3-hour and 6-hour spatial distributions. For 50-year recurrences, the corresponding areas were 1000 and 1195 square miles, respectively. These are further illustrations of the intensity and areal extent of the July 1996 storm.

Analyses similar to those used in evaluating the distribution characteristics of the entire storm system were applied in evaluating the storm over the Chicago metropolitan area. Area-depth and time distribution characteristics were very similar to those obtained for the entire storm system. The southern part of the metropolitan area was along or very close to the major axis of the storm system. The presence of the Water Survey's recording raingage network provided quite detailed definition of space and time distribution.

This was the fourth storm, since the Water Survey initiated their hydrometeorological program in 1948, in which 100-year return period, point rainfall amounts were equaled or exceeded for storm durations of 24 hours or less in the Chicago metropolitan area. All of these storms have been subjected to detailed analyses to provide much needed information on the space and time distribution characteristics of such storms in large urban areas.

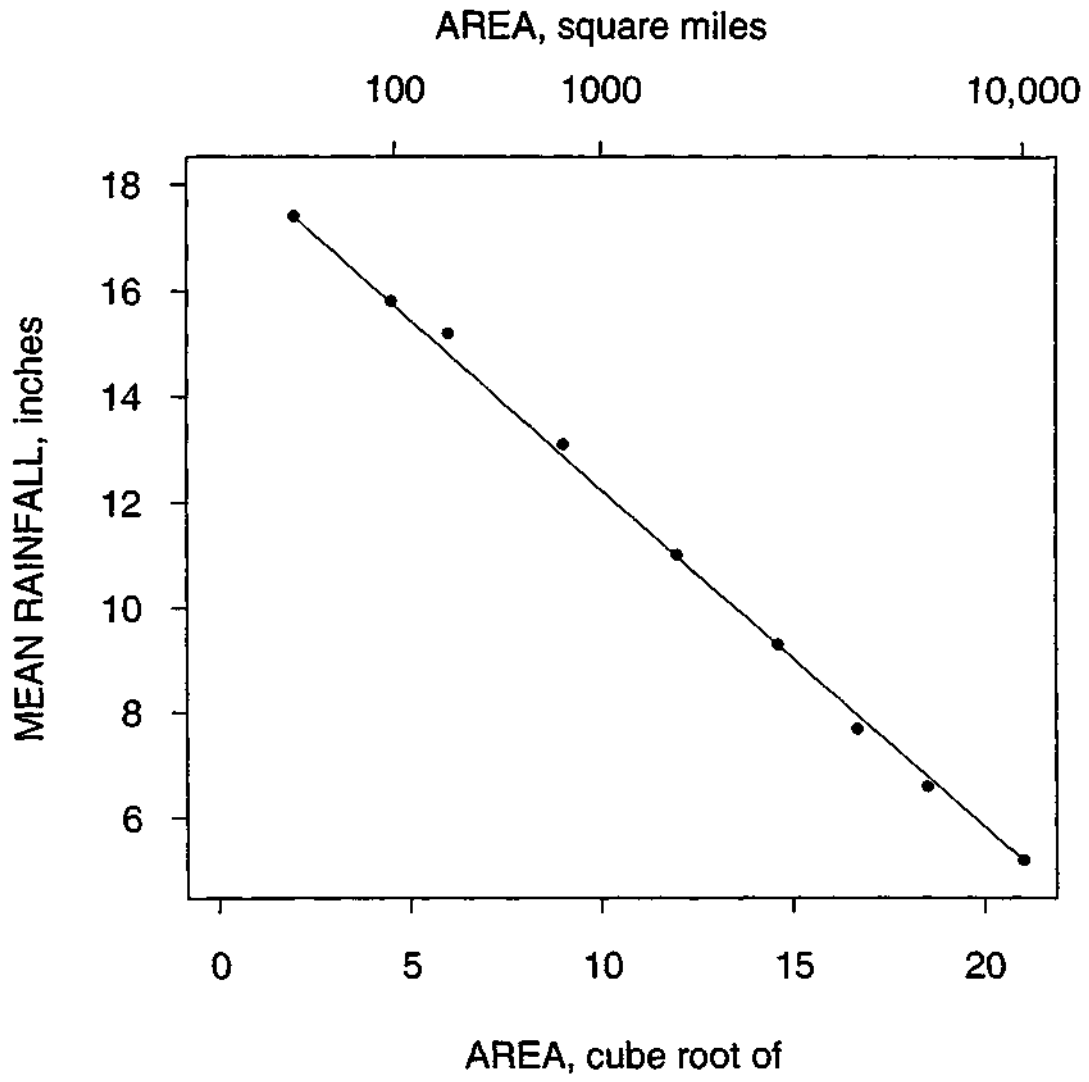


Figure 5-1. Area-depth relationship for the total rainfall for the storm on July 17-18, 1996.

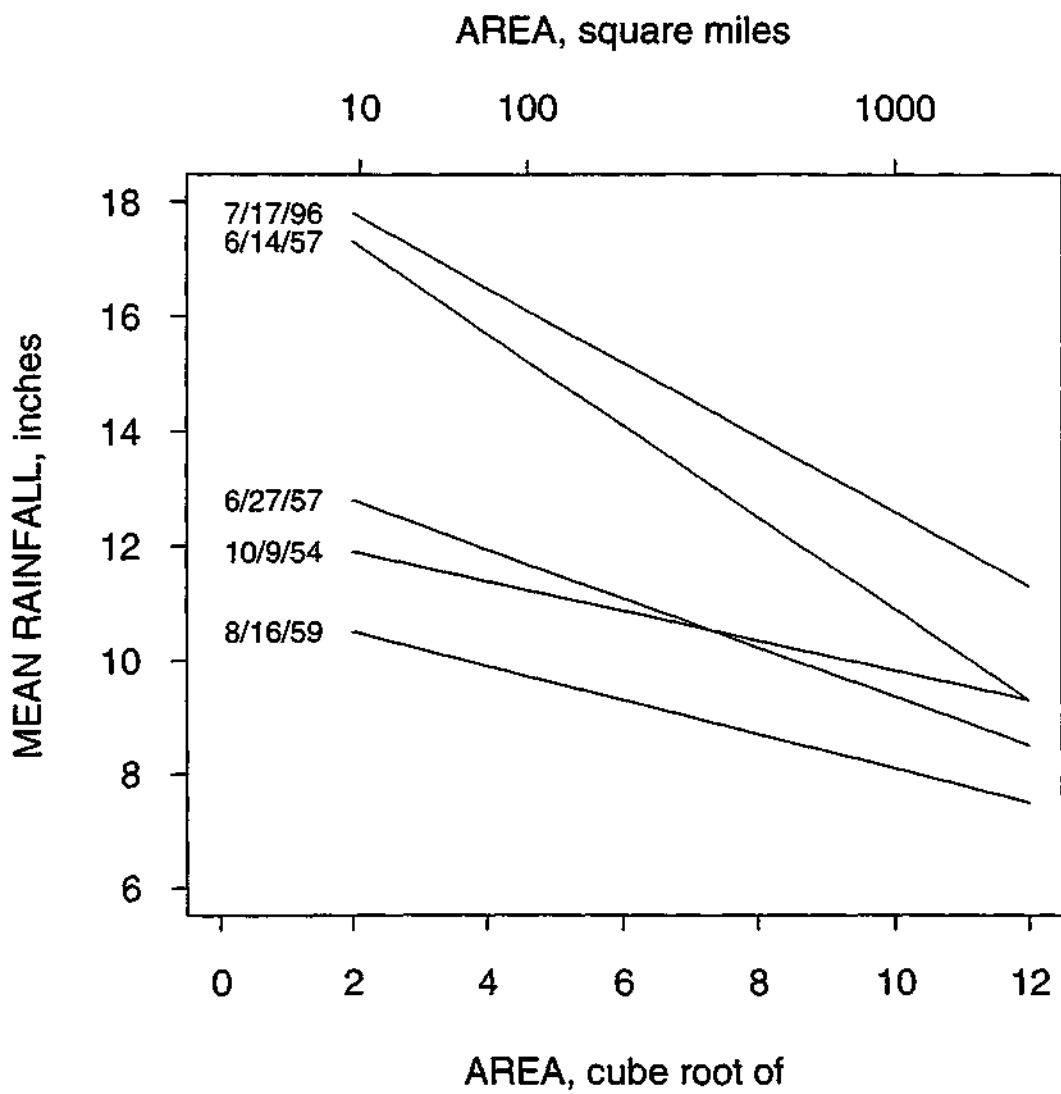


Figure 5-2. Comparative area-depth relationships for selected 100-year events.

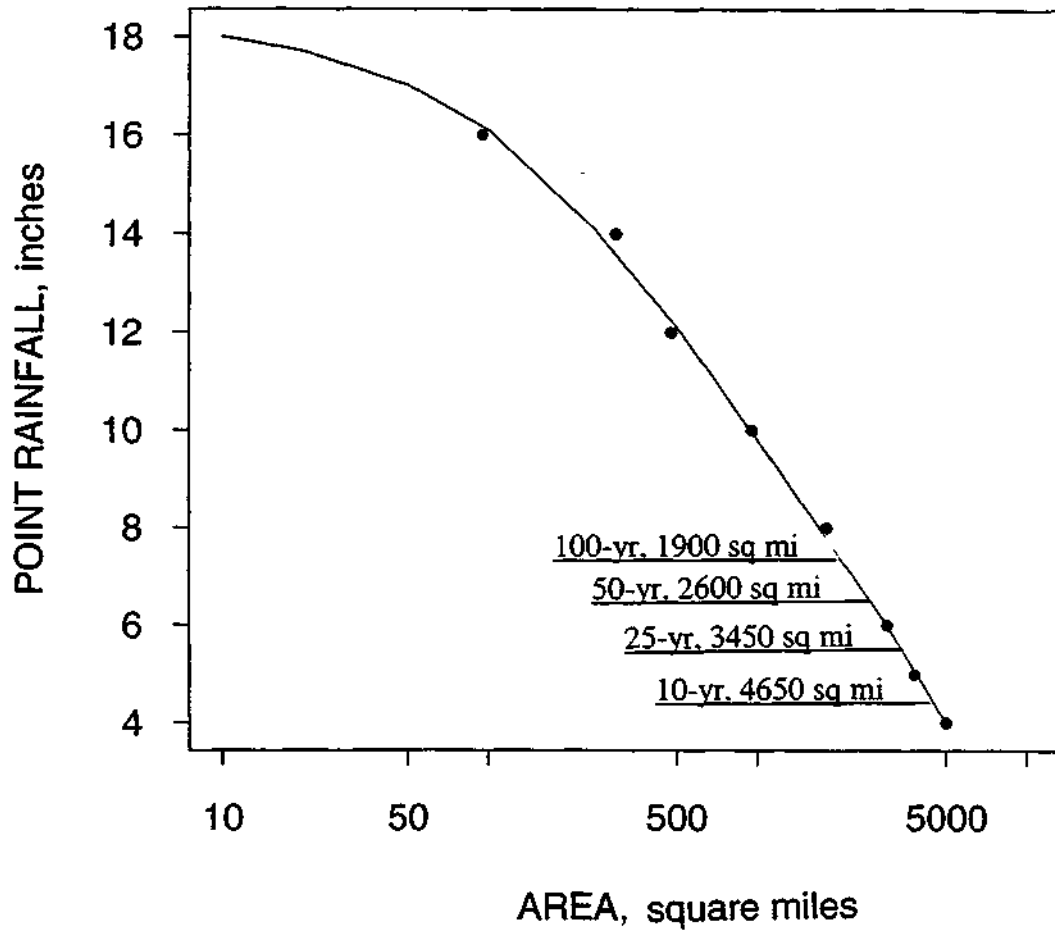


Figure 5-3. Point rainfall envelope curve of the total rainfall for the storm on July 17-18, 1996.

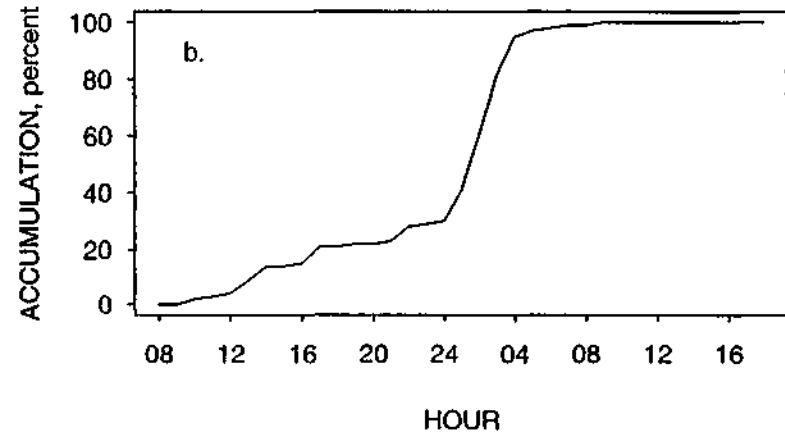
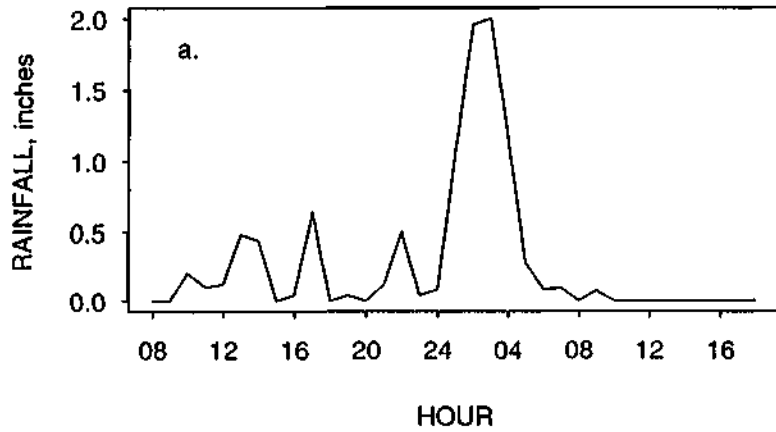


Figure 5-4. Time distribution of (a) rainfall and (b) accumulated rainfall at Sycamore.

76

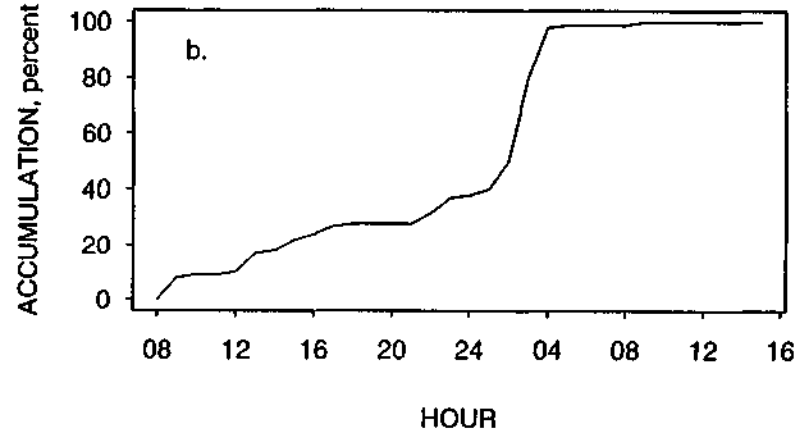
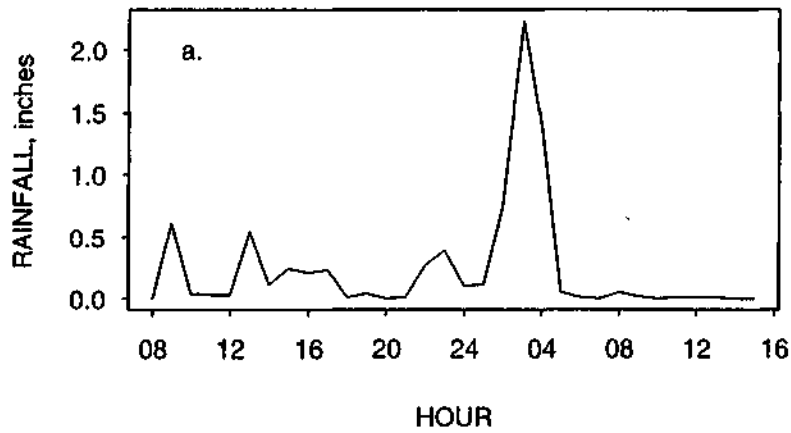


Figure 5-5. Time distribution of (a) rainfall and (b) accumulated rainfall at DeKalb.

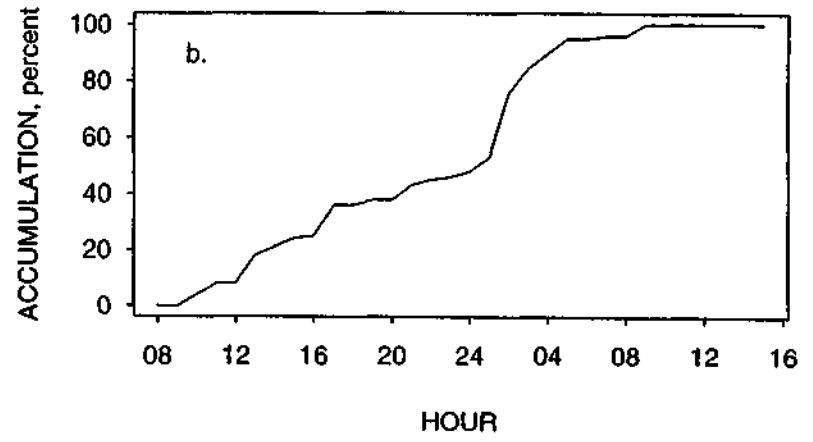
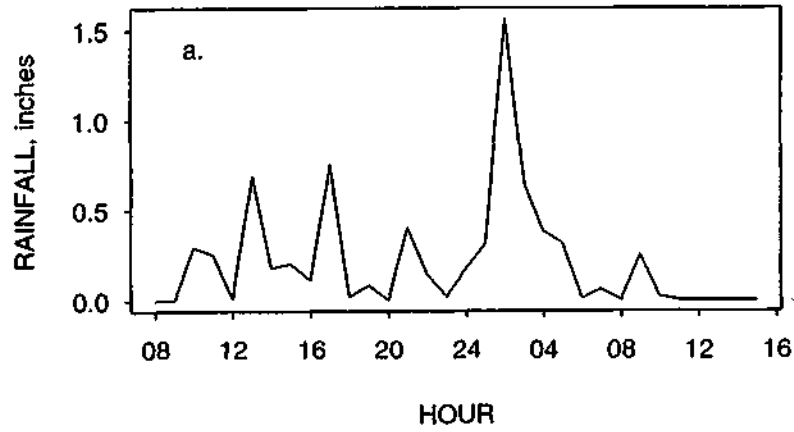


Figure 5-6. Time distribution of (a) rainfall and (b) accumulated rainfall at St. Charles.

56

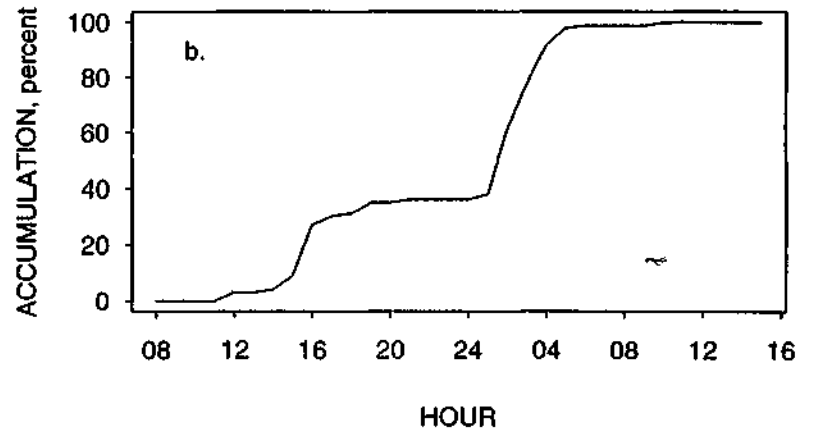
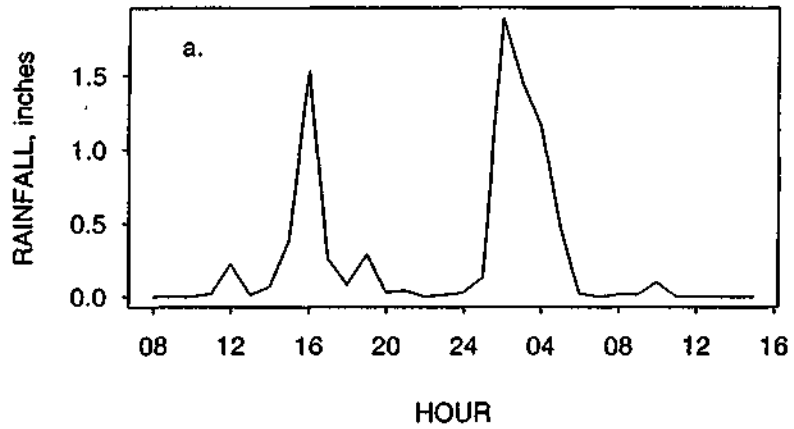


Figure 5-7. Time distribution of (a) rainfall and (b) accumulated rainfall at DuPage County gage 31.

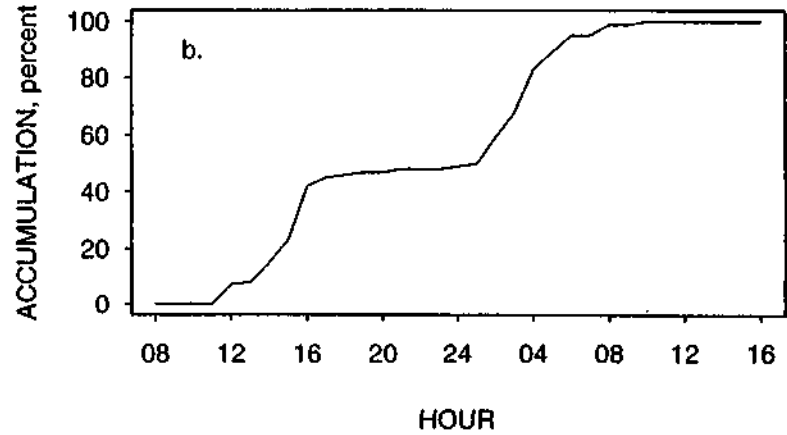
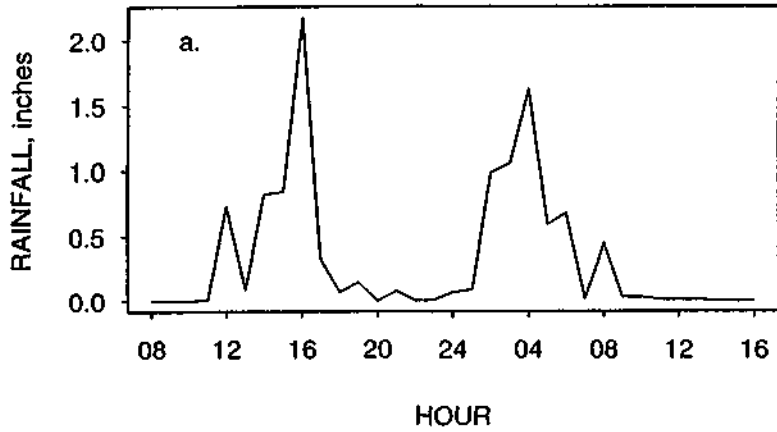


Figure 5-8. Time distribution of (a) rainfall and (b) accumulated rainfall at Chicago urban gage 15.

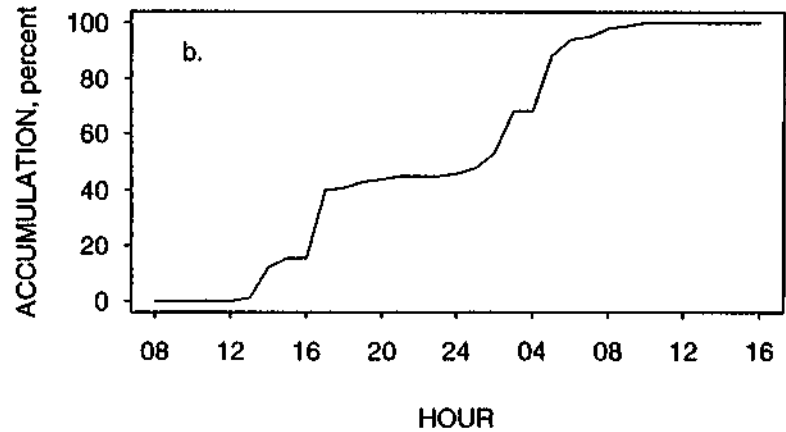
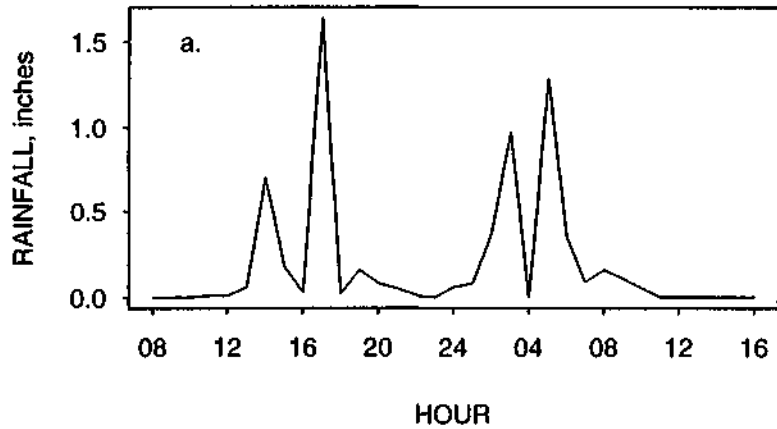


Figure 5-9. Time distribution of (a) rainfall and (b) accumulated rainfall at Chicago urban gage 21.

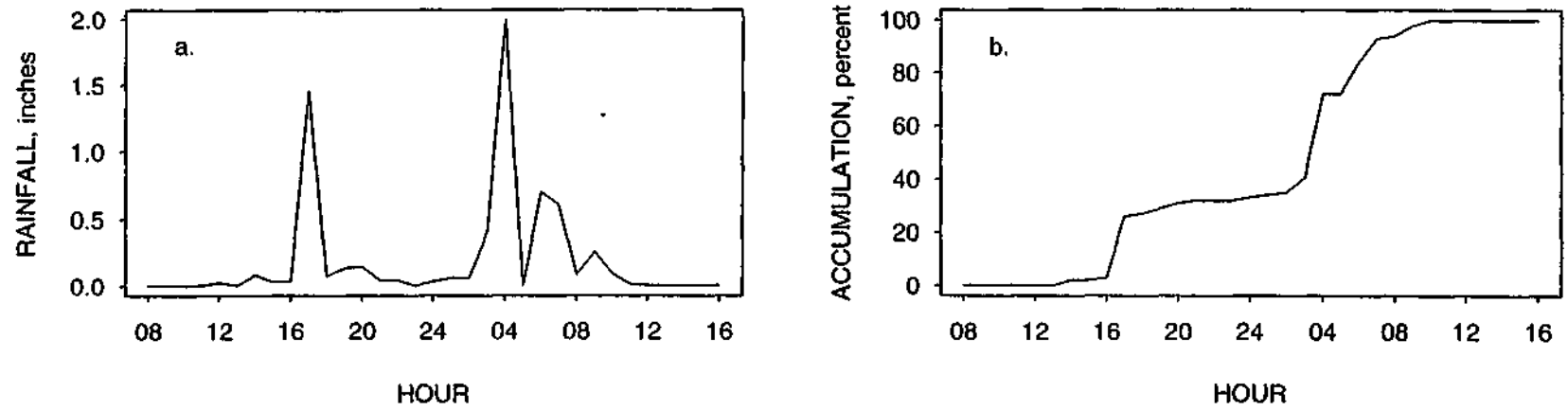


Figure 5-10. Time distribution of (a) rainfall and (b) accumulated rainfall at Chicago urban gage 25.

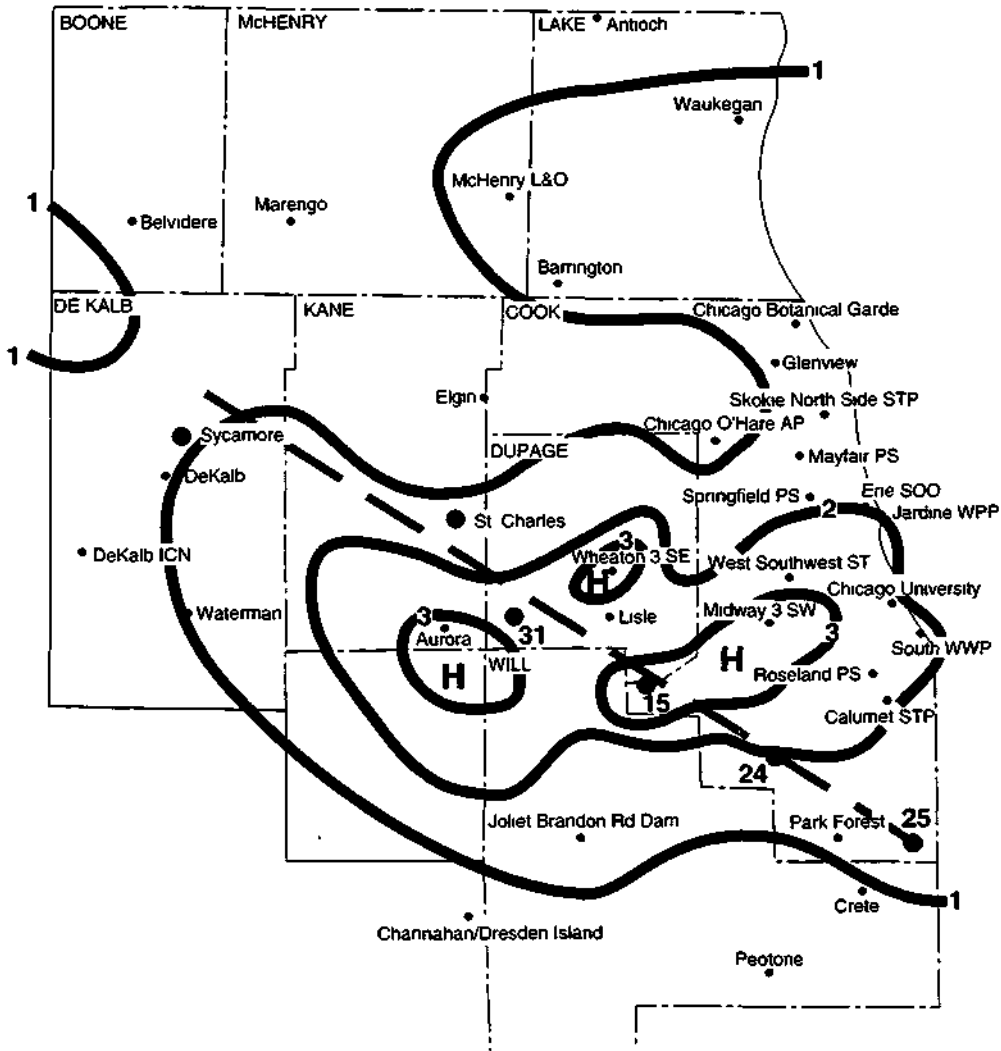


Figure 5-11. Maximum 3-hour rainfall (inches) in the daytime storm of July 17, 1996.

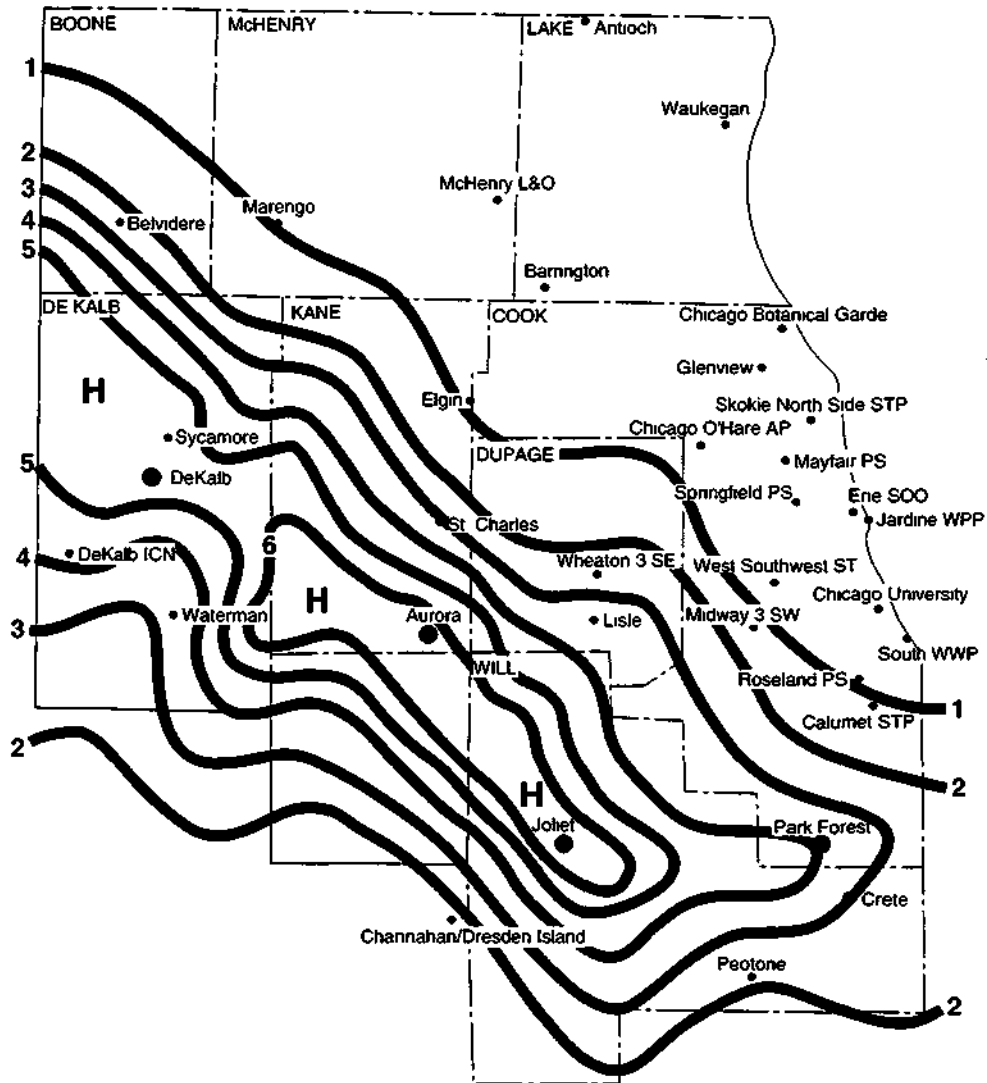


Figure 5-13. Maximum 3-hour rainfall (inches) in the daytime storm of July 18, 1996.

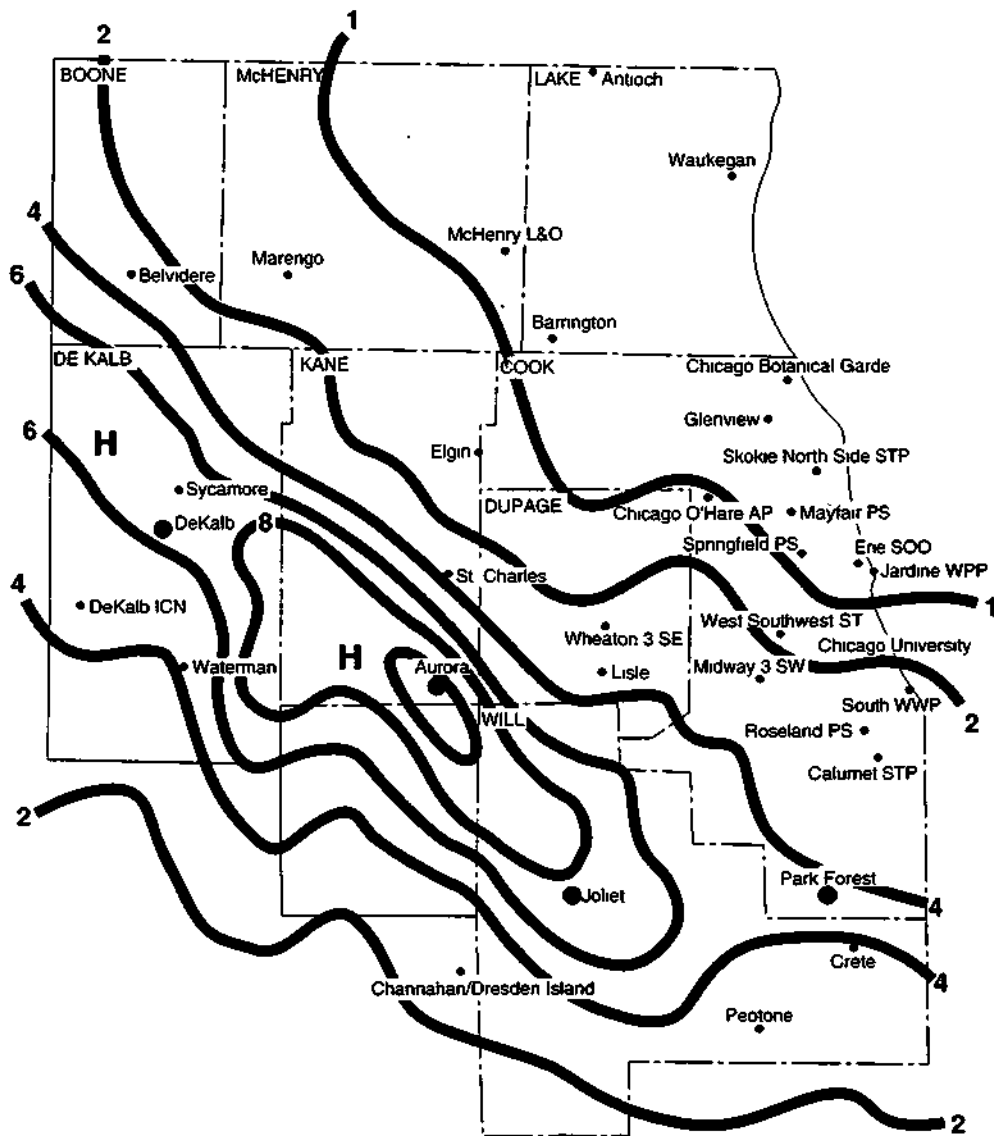


Figure 5-14. Maximum 6-hour rainfall (inches) in the daytime storm of July 18, 1996.

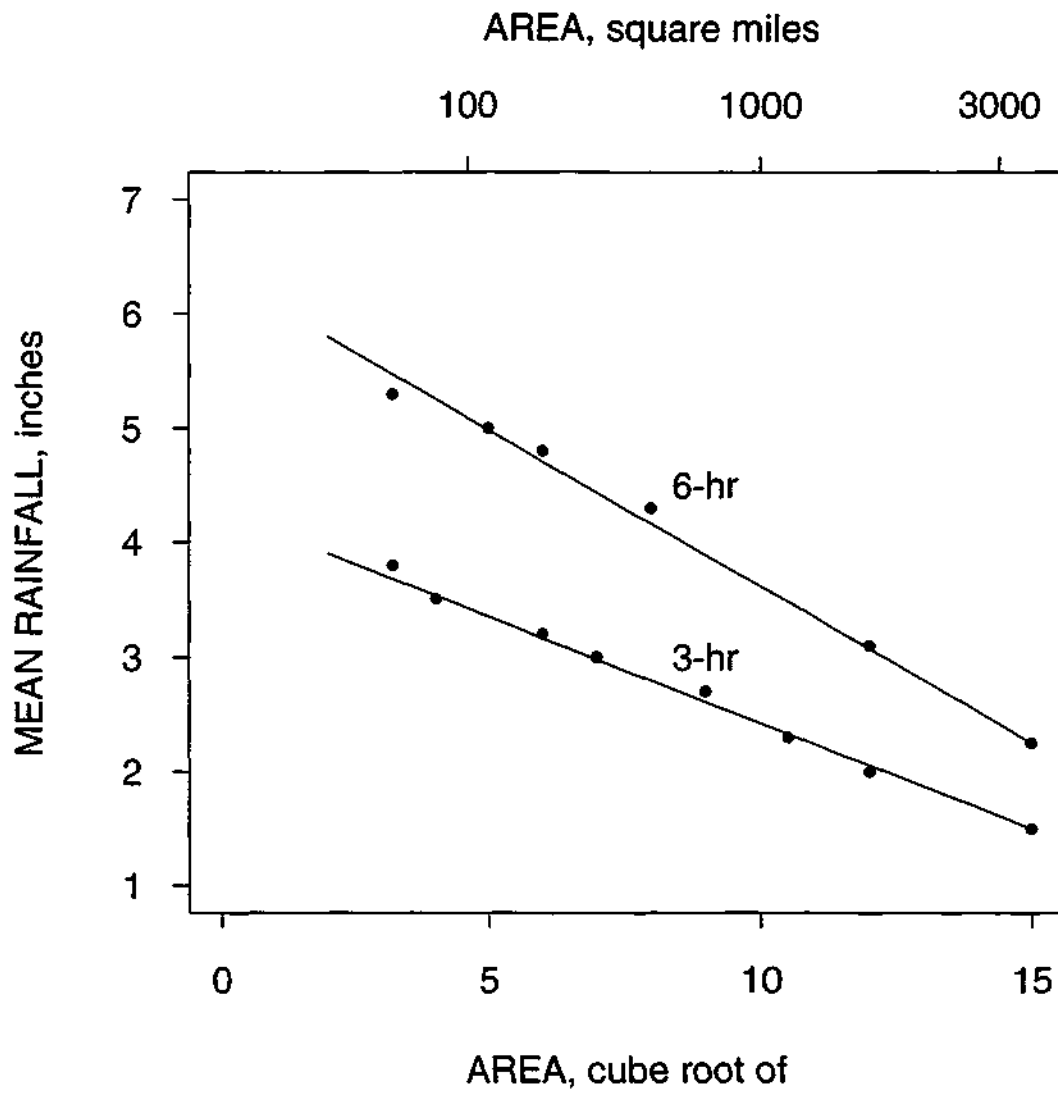


Figure 5-15. Area-depth relationship for maximum 3-hour and 6-hour rainfall in the daytime storm of July 17, 1996.

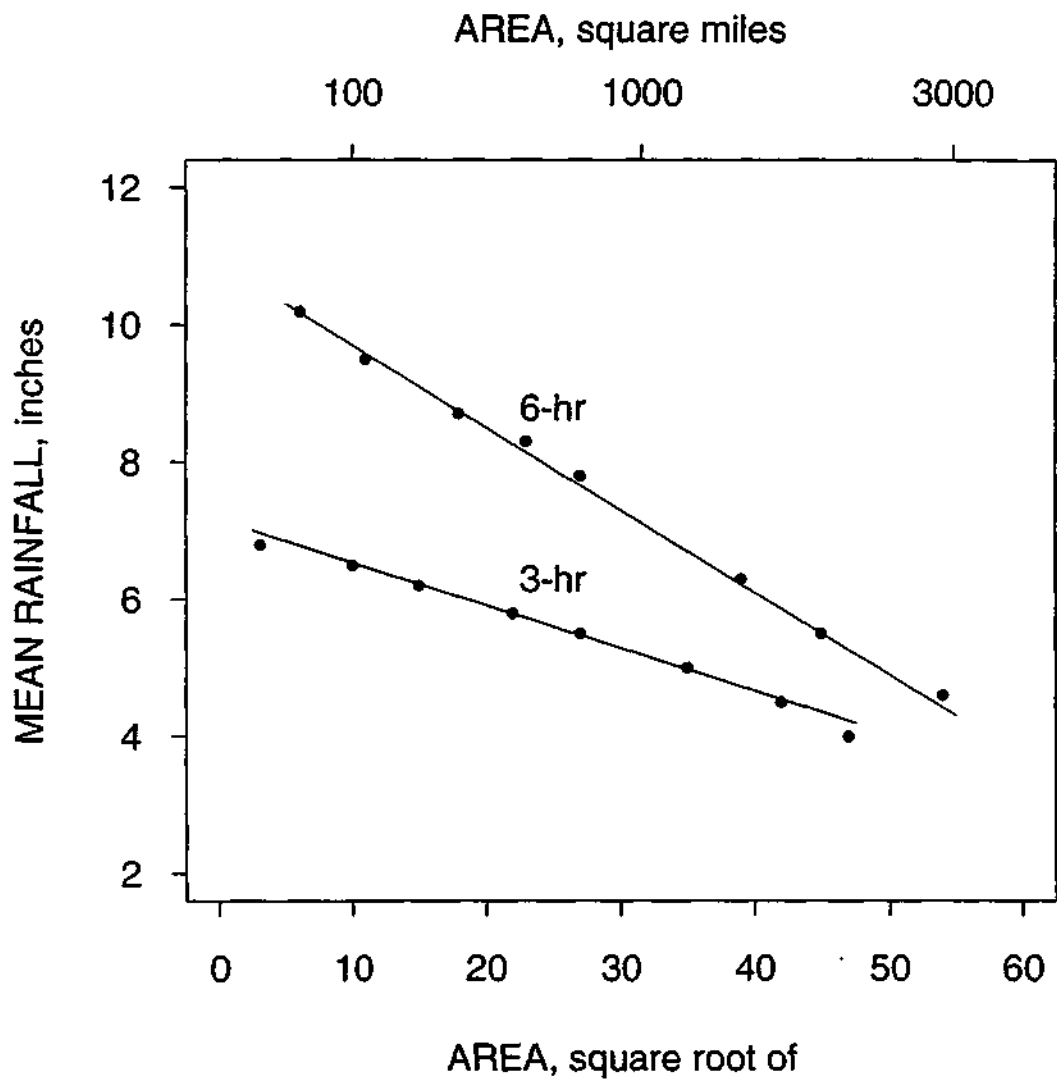


Figure 5-16. Area-depth relationship for maximum 3-hour and 6-hour rainfall in the nocturnal storm of July 18, 1996.

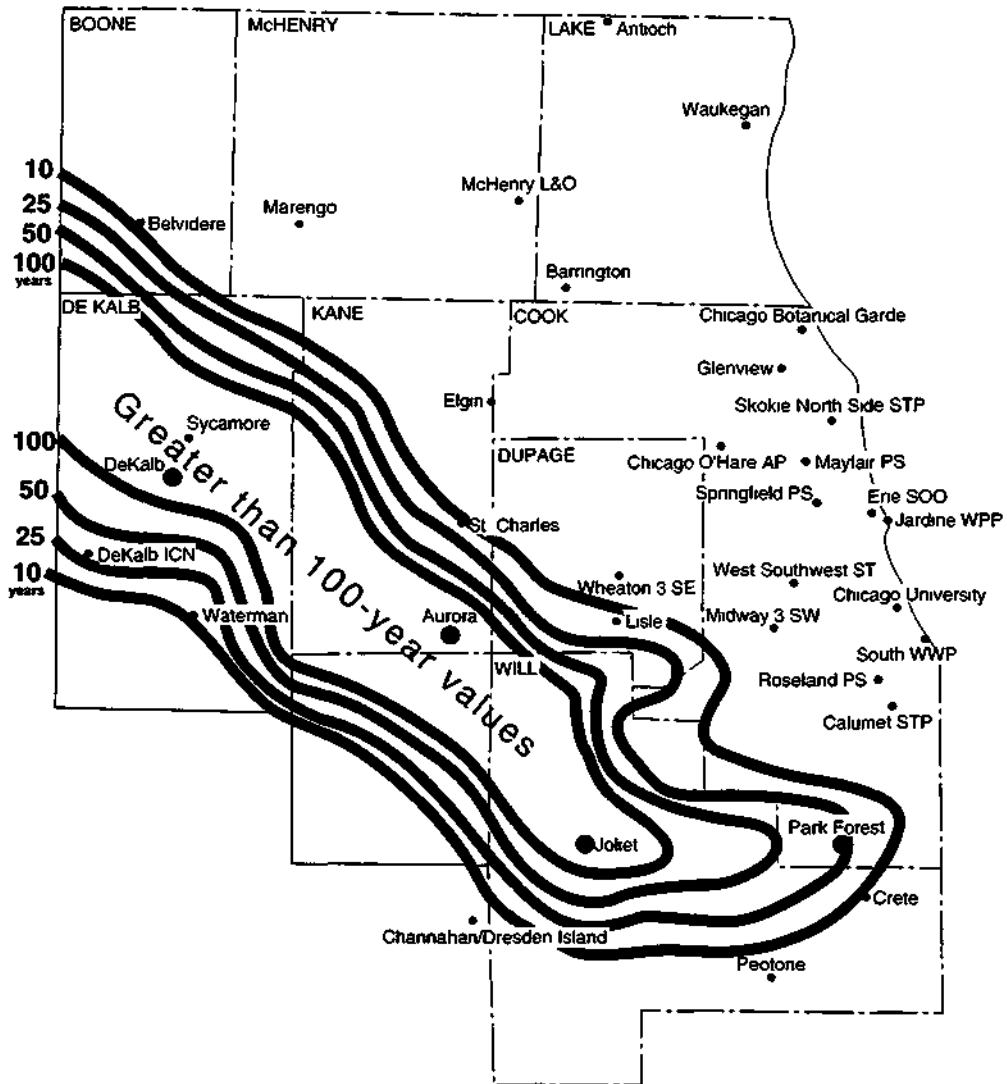


Figure 5-17. Recurrence intervals of maximum 3-hour rainfall in the nocturnal storm of July 18, 1996.

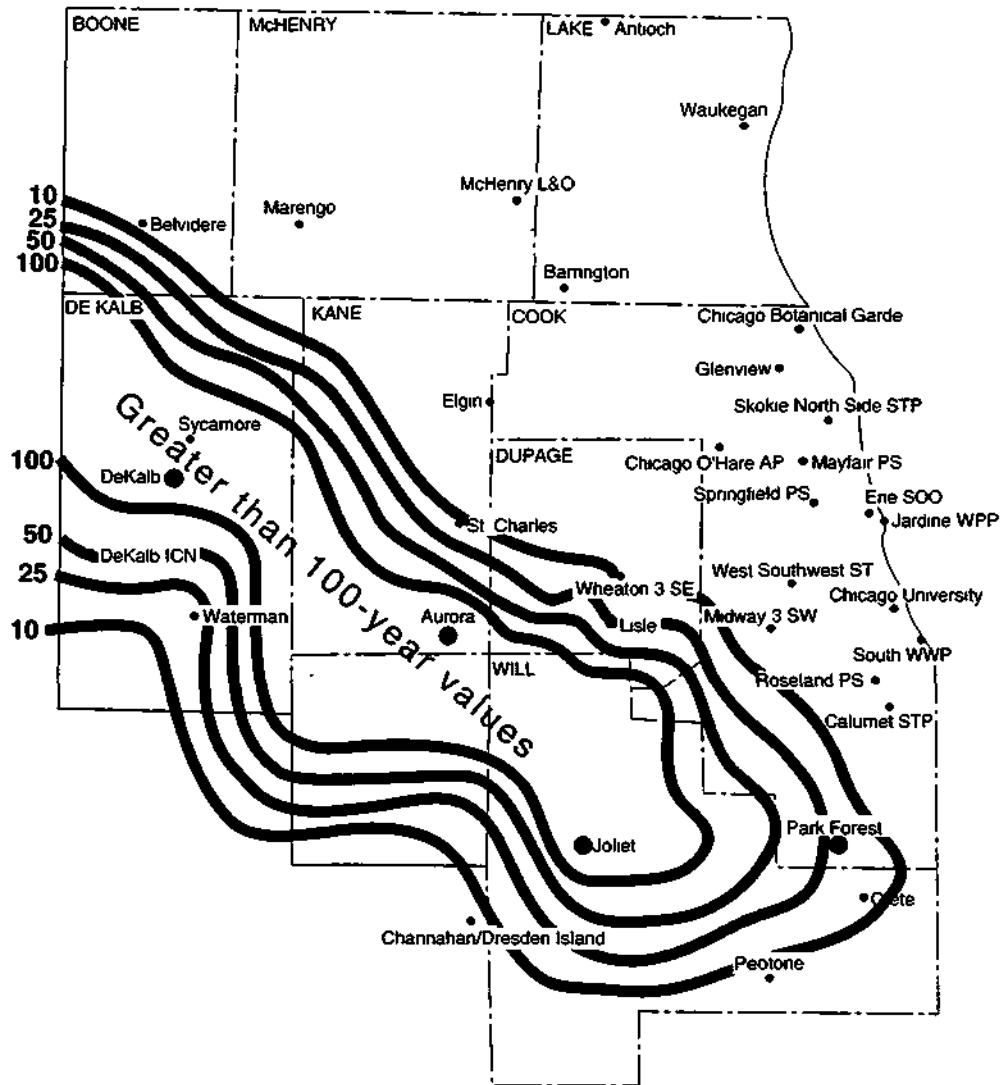


Figure 5-18. Recurrence intervals of maximum 6-hour rainfall in the nocturnal storm of July 18, 1996.

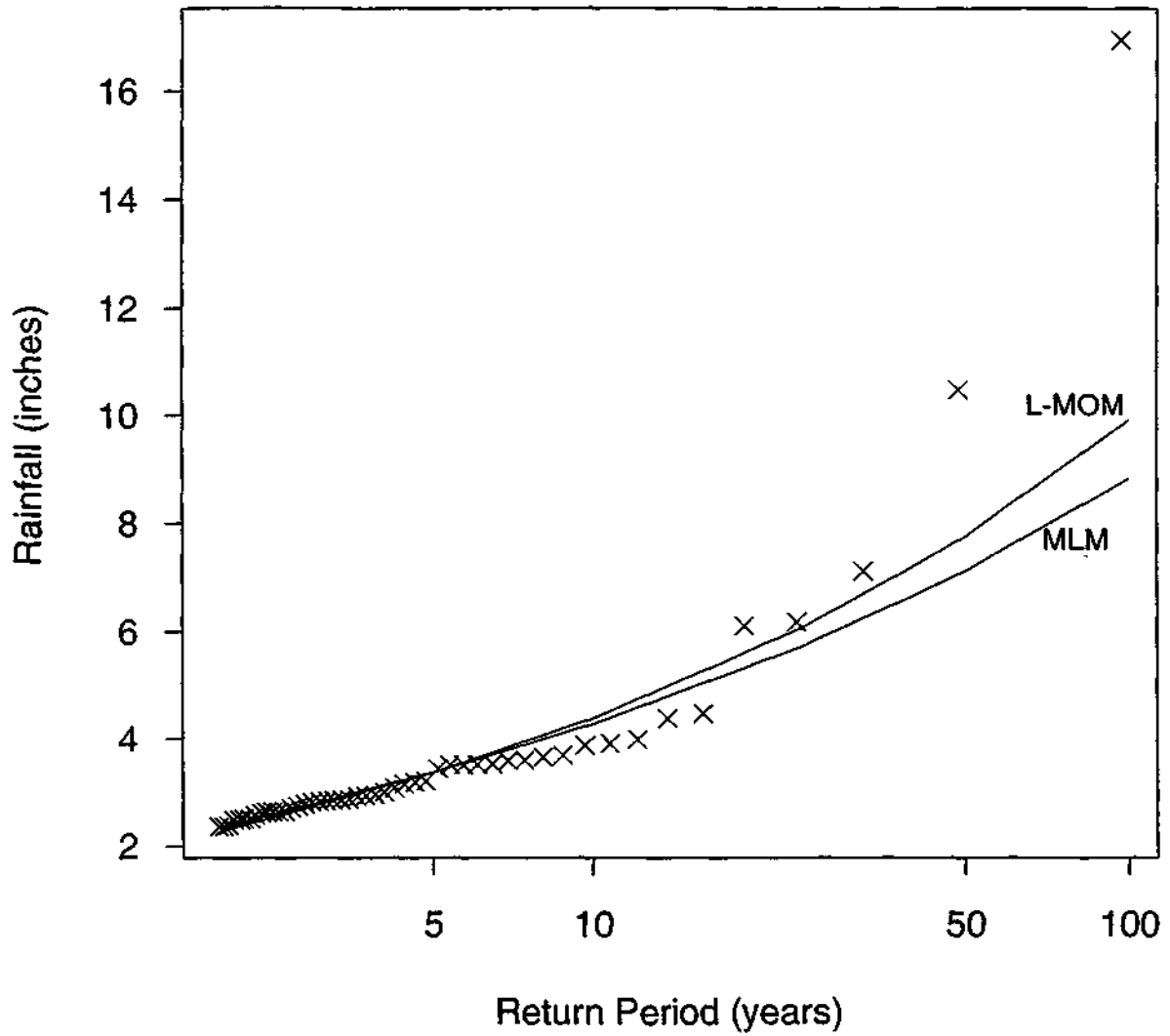


Figure 5-19. Annual maximum rainfall for Aurora 1900 to 1996 showing the statistical fit of the Generalized Extreme Value (GEV) distribution with both the L-moments (L-MOM) and maximum likelihood (MLM) fitting periods.

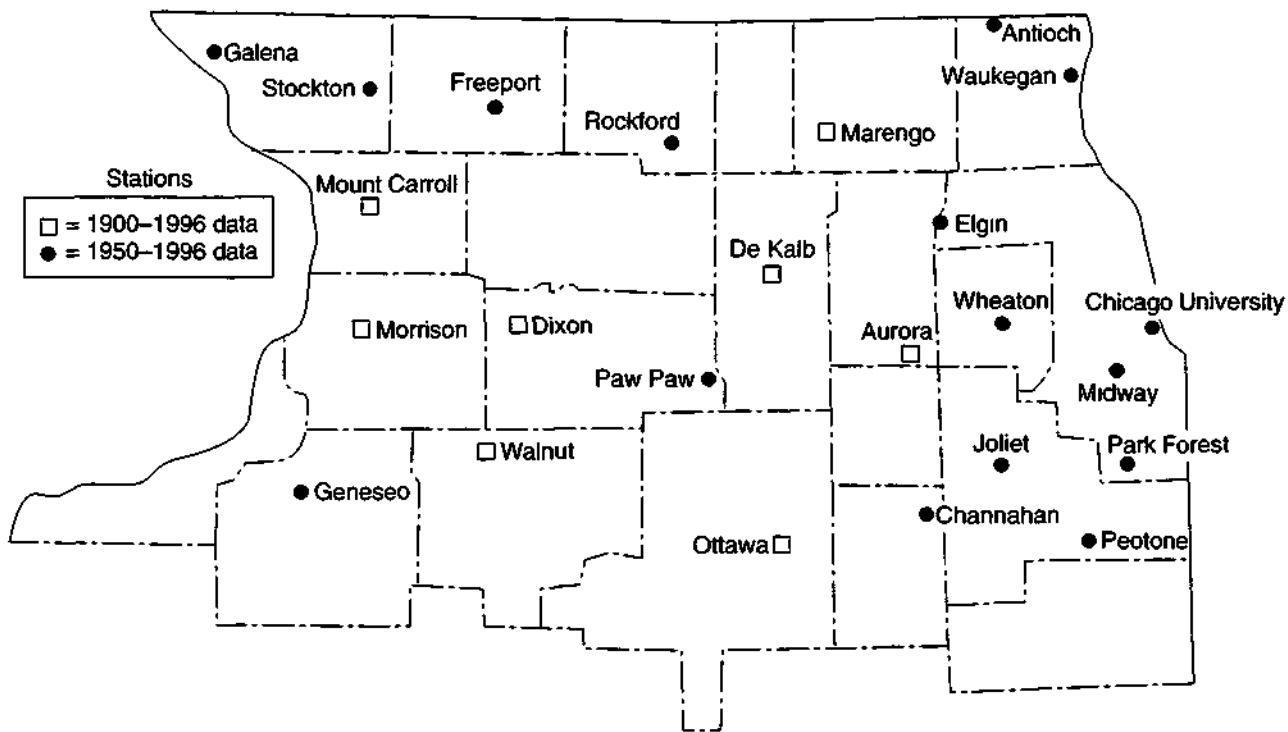


Figure 5-20. Climate stations used to compare historical heavy precipitation events in northern Illinois.

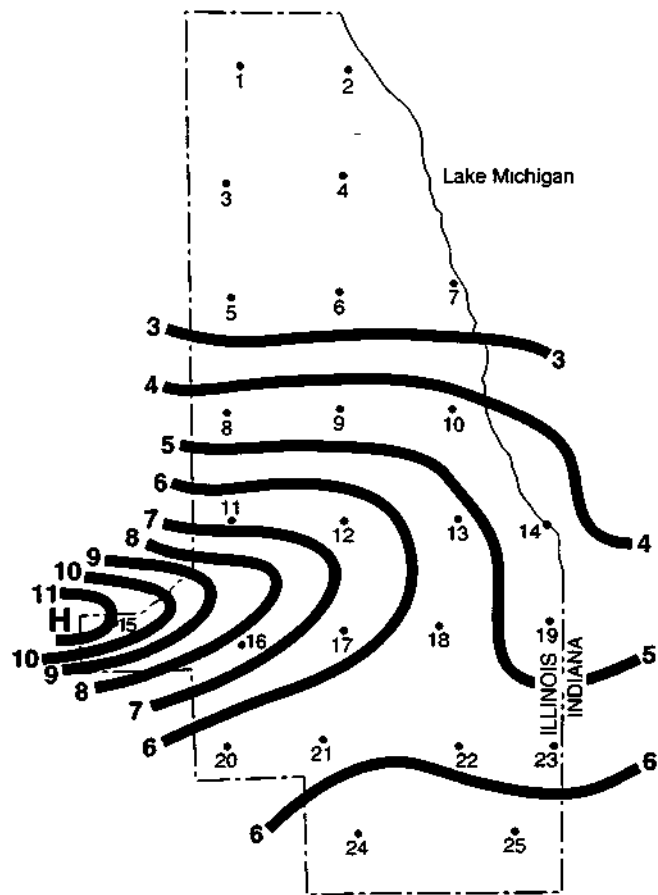


Figure 5-21. Total storm rainfall (inches) in the Chicago metropolitan area for July 17-18, 1996.

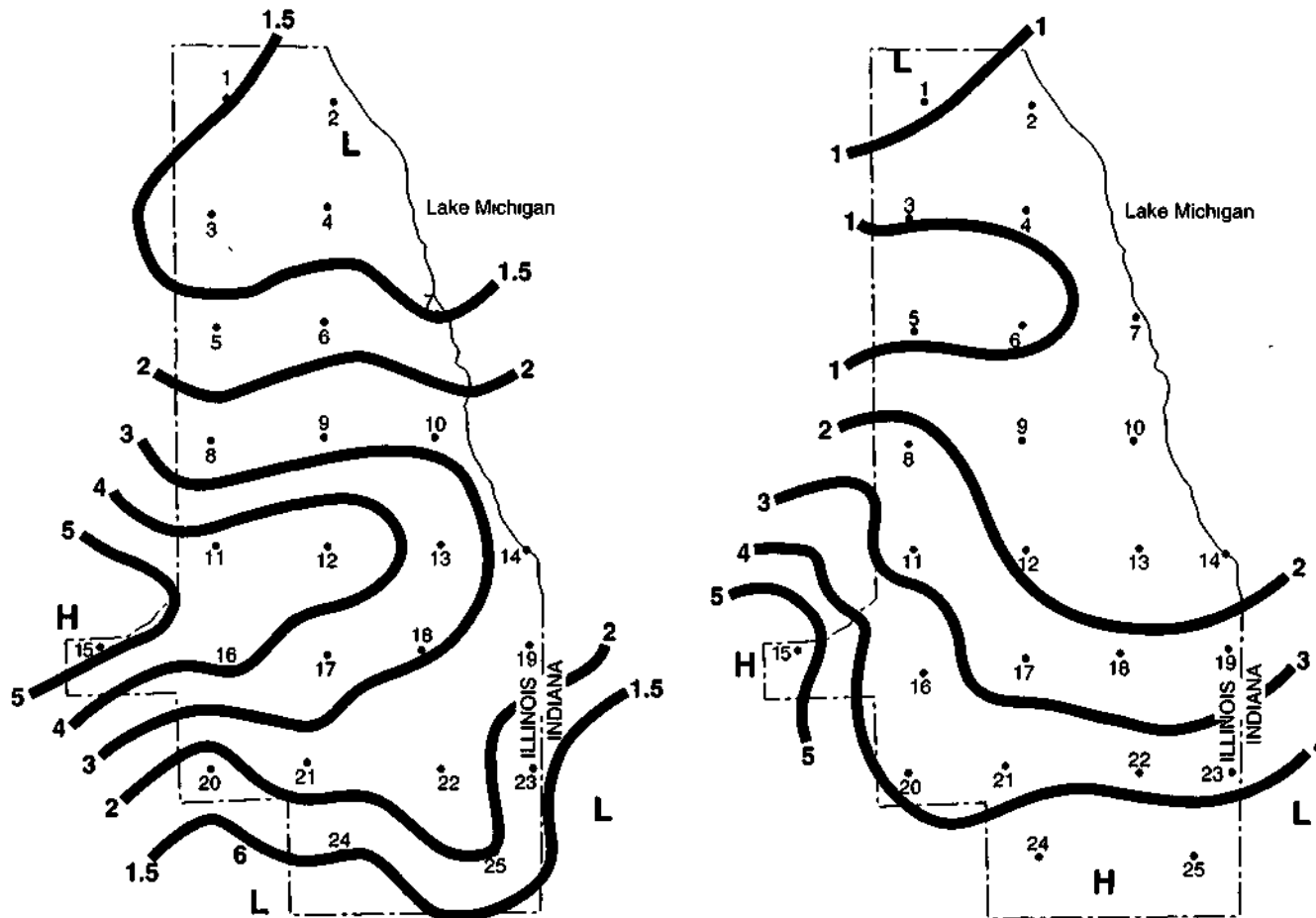


Figure 5-22. Storm rainfall (inches) in the Chicago metropolitan area for a) the daytime storm period of July 17, 1996, and b) the nocturnal storm period of July 18, 1996.

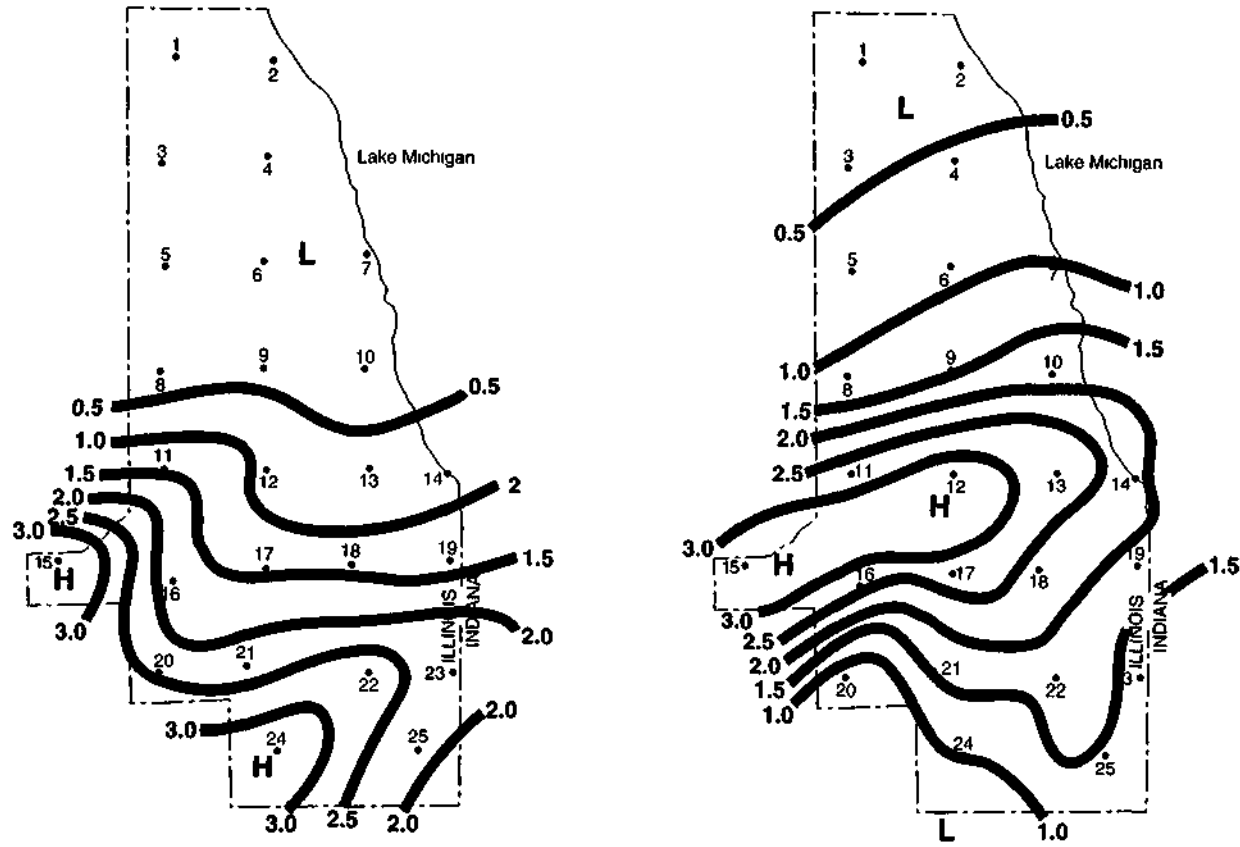


Figure 5-23. Storm rainfall (inches) for the 3-hour period of heaviest rainfall for a) the daytime storm period of July 17, 1996, and b) the nocturnal storm period of July 18, 1996.

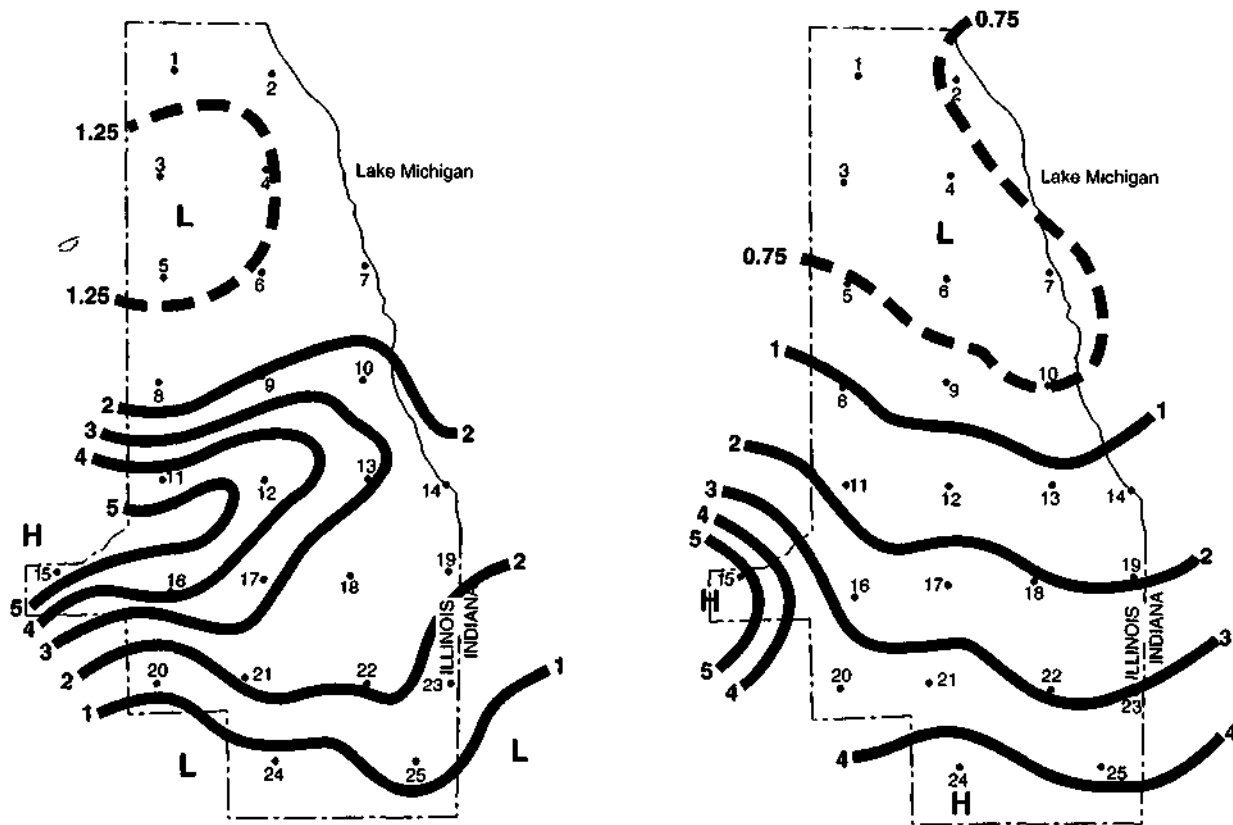


Figure 5-24. Storm rainfall (inches) for the 6-hour period (1100-1700 LST) of heaviest rainfall for a) the daytime storm period of July 17, 1996, and b) the nocturnal storm period of July 18, 1996.

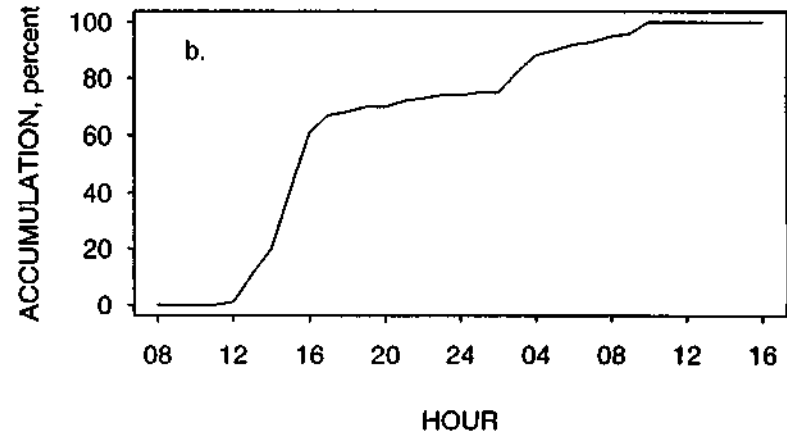
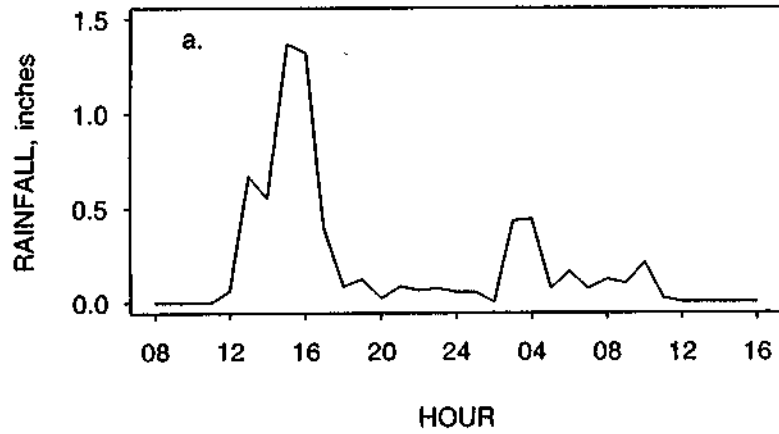


Figure 5-25. Time distribution of (a) rainfall and (b) accumulated rainfall at Chicago urban gage 12.

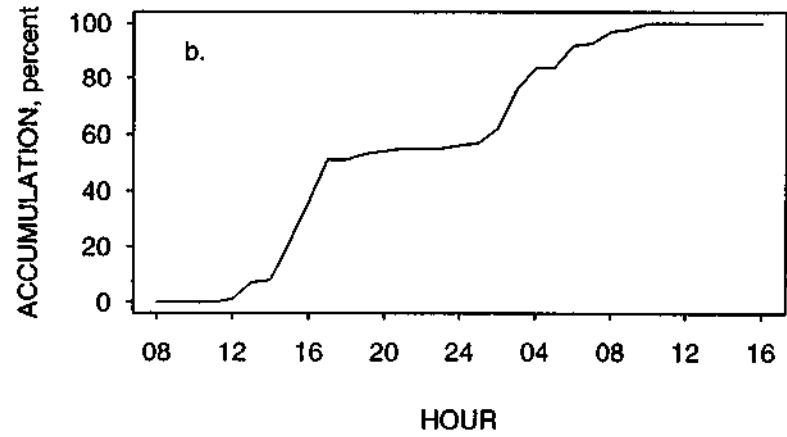
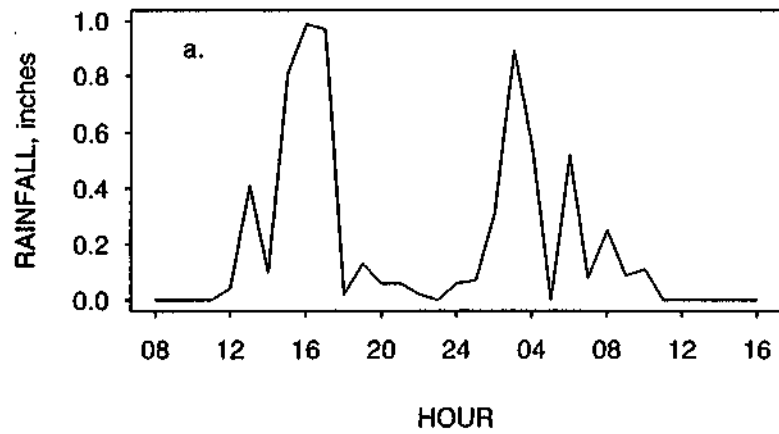


Figure 5-26. Time distribution of (a) rainfall and (b) accumulated rainfall at Chicago urban gage 17.

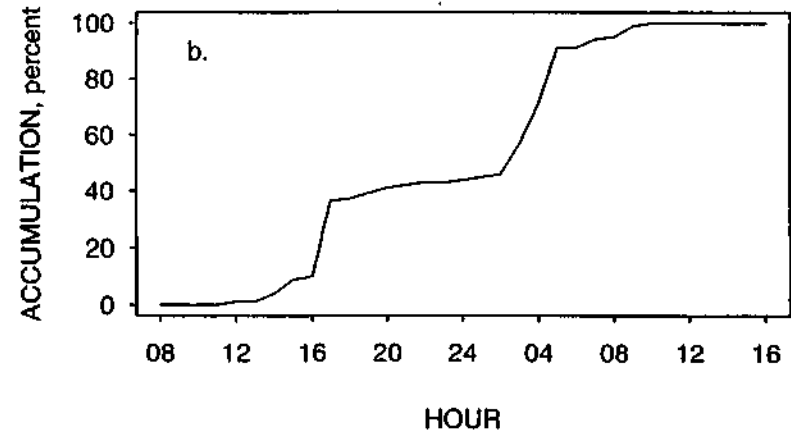
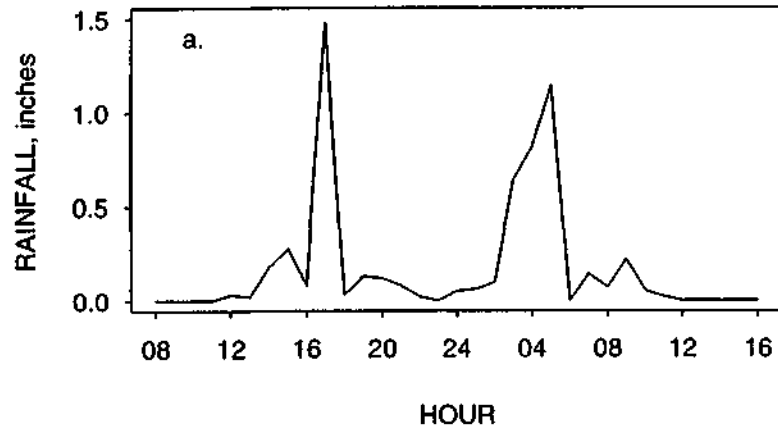


Figure 5-27. Time distribution of (a) rainfall and (b) accumulated rainfall at Chicago urban gage 22.

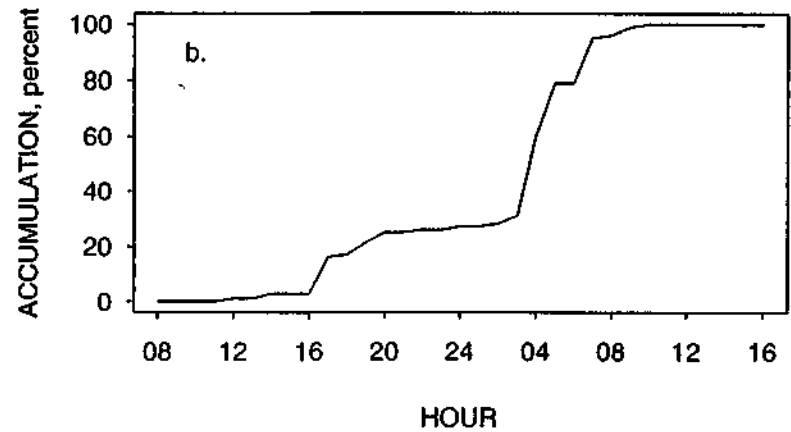
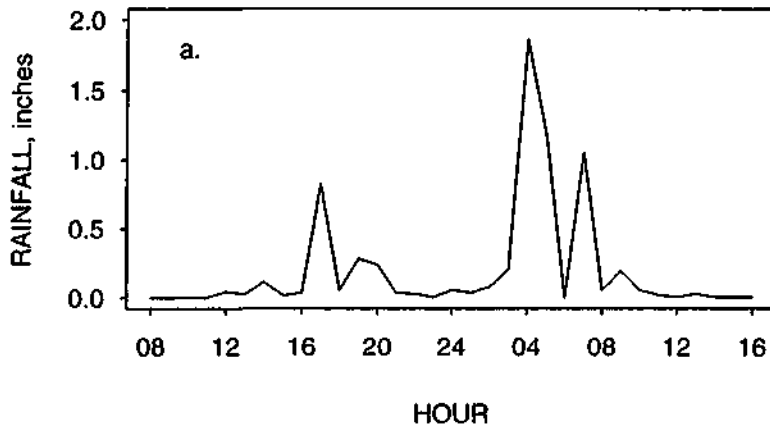


Figure 5-28. Time distribution of (a) rainfall and (b) accumulated rainfall at Chicago urban gage 24.

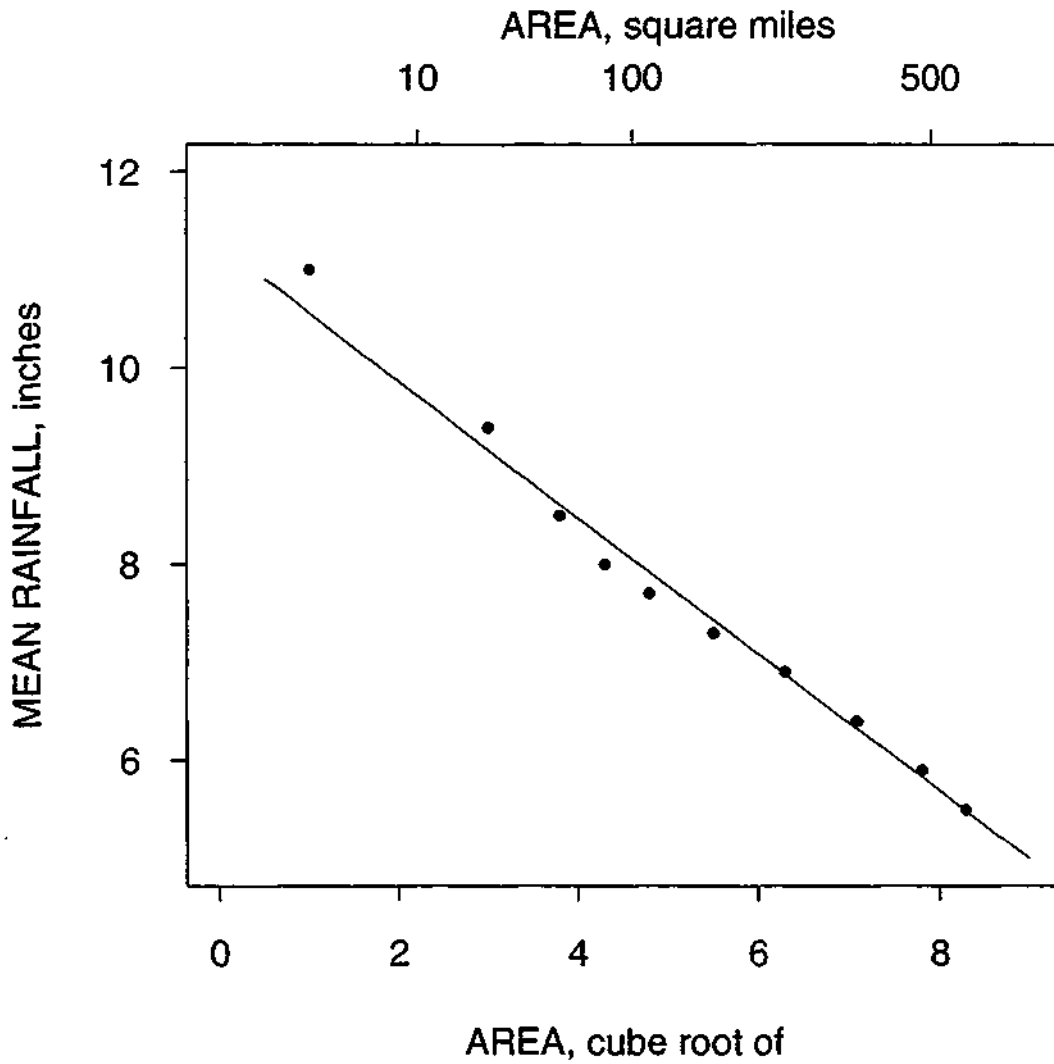


Figure 5-29. Area-depth relationship for the total rainfall for the storm in the Chicago metropolitan area, July 17-18, 1996.

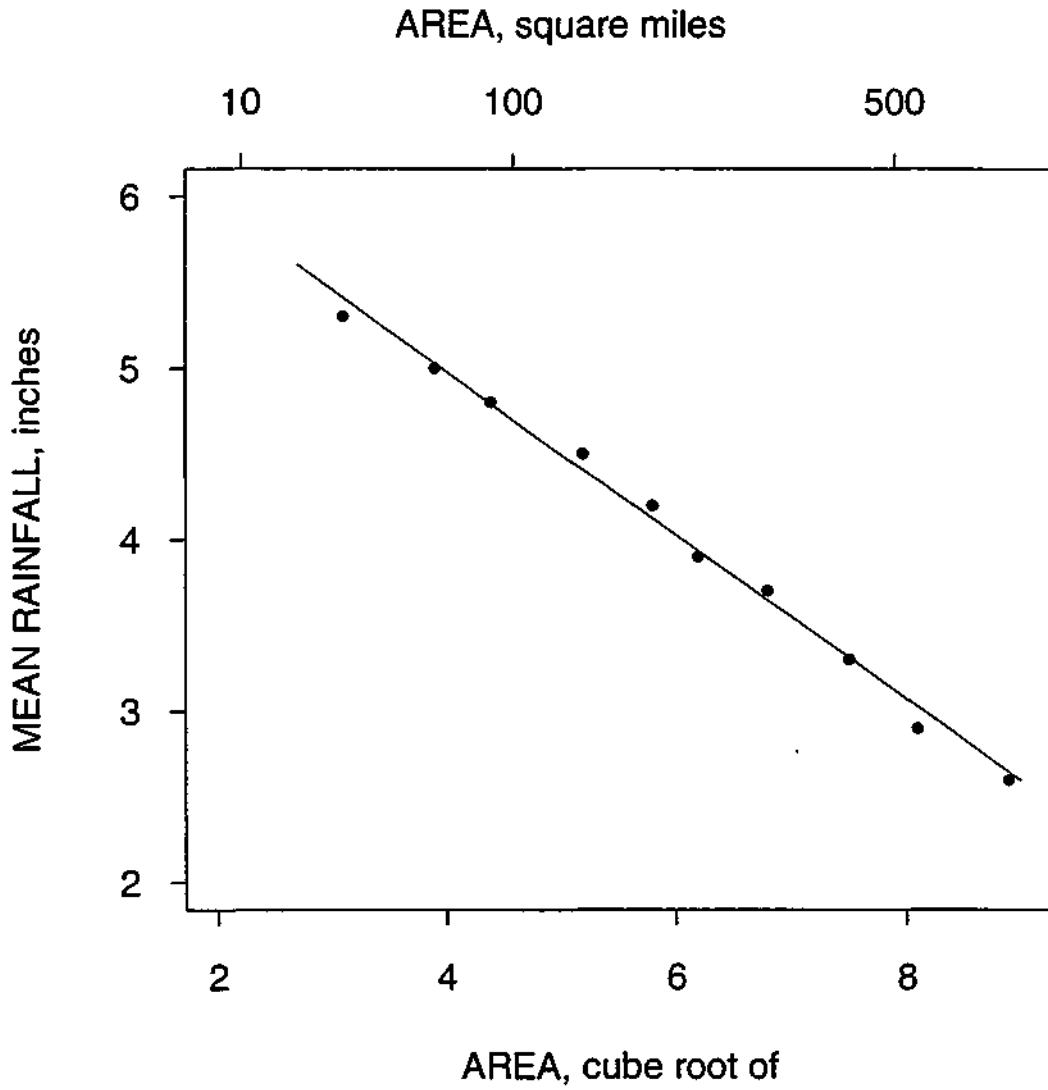


Figure 5-30. Area-depth relationship for the daytime storm period in the Chicago metropolitan area, July 17, 1996.

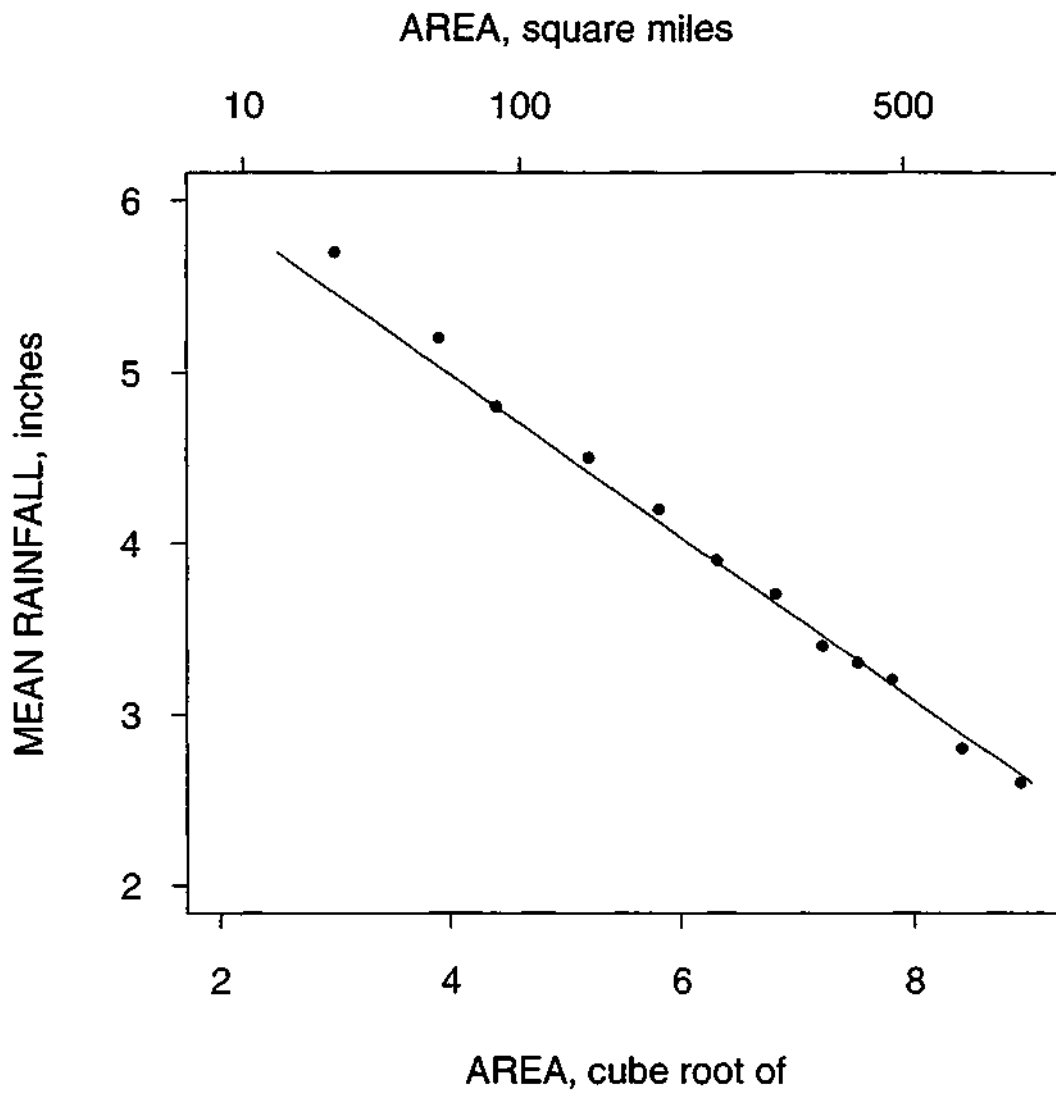


Figure 5-31. Area-depth relationship for the nocturnal storm period in the Chicago metropolitan area, July 18, 1996.

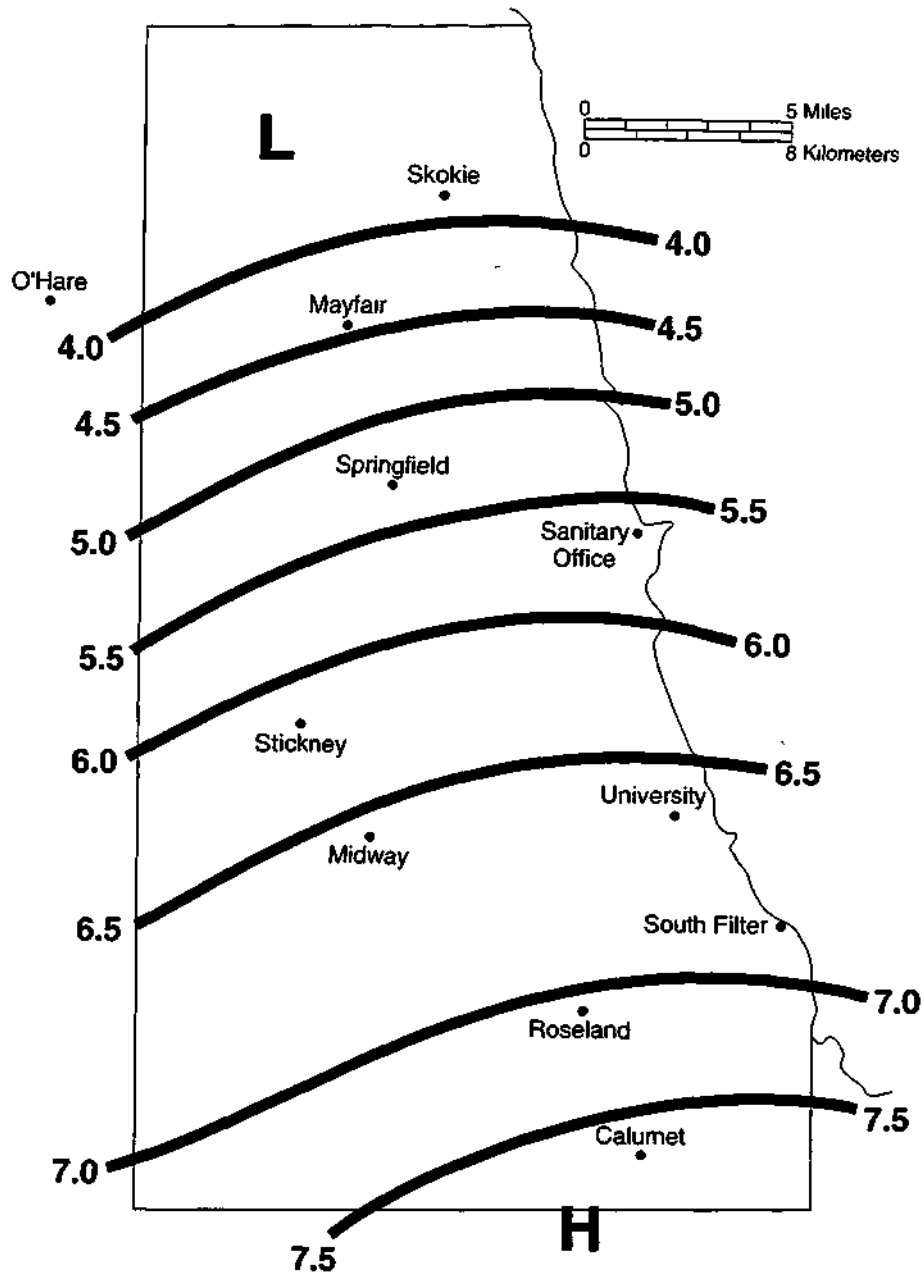


Figure 5-32. Maximum 24-hour rainfall (inches) in the storm in the Chicago metropolitan area, October 9-10, 1954.

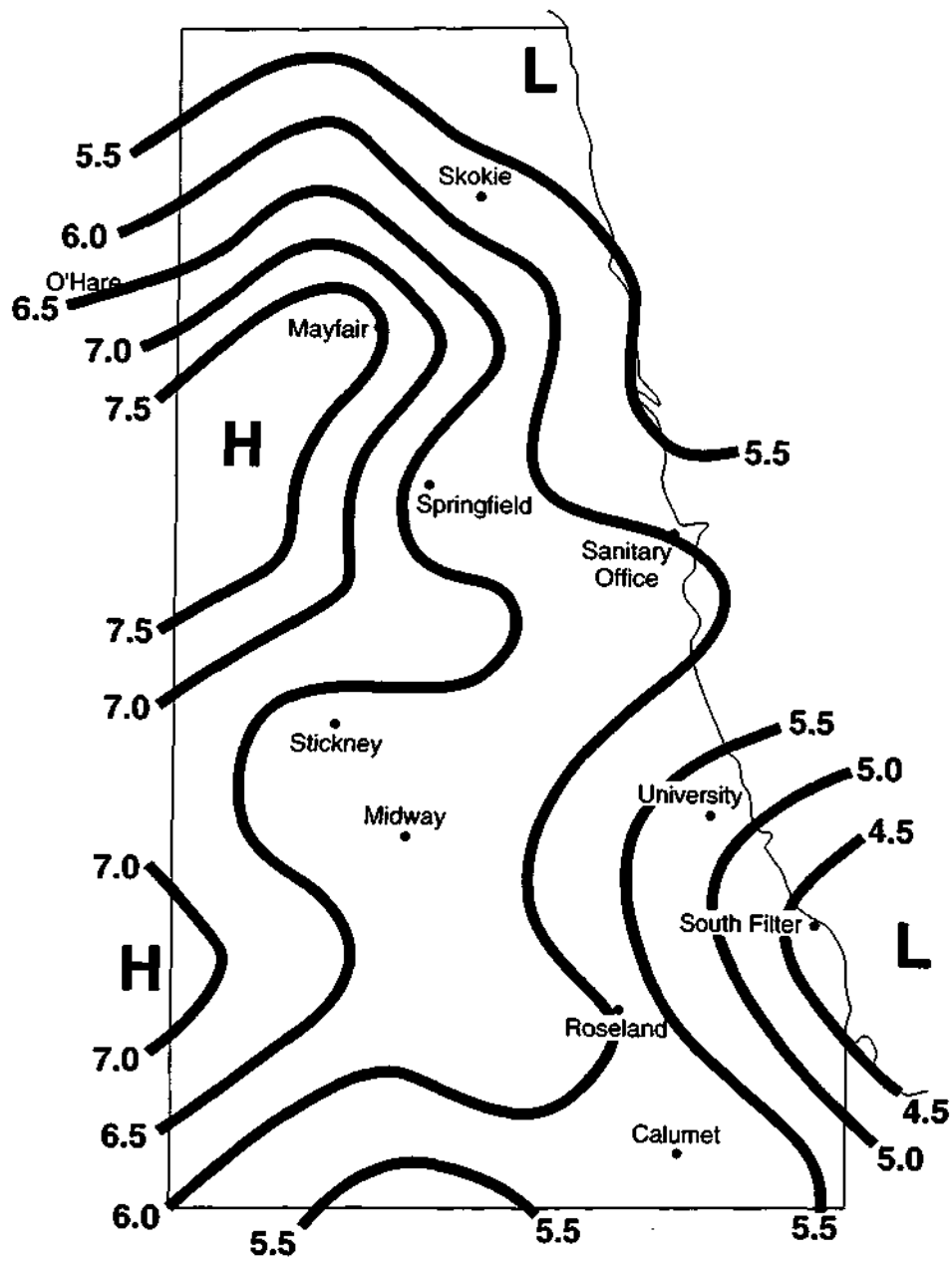


Figure 5-33. Maximum 24-hour rainfall (inches) in the storm in the Chicago metropolitan area, July 12-13, 1957.

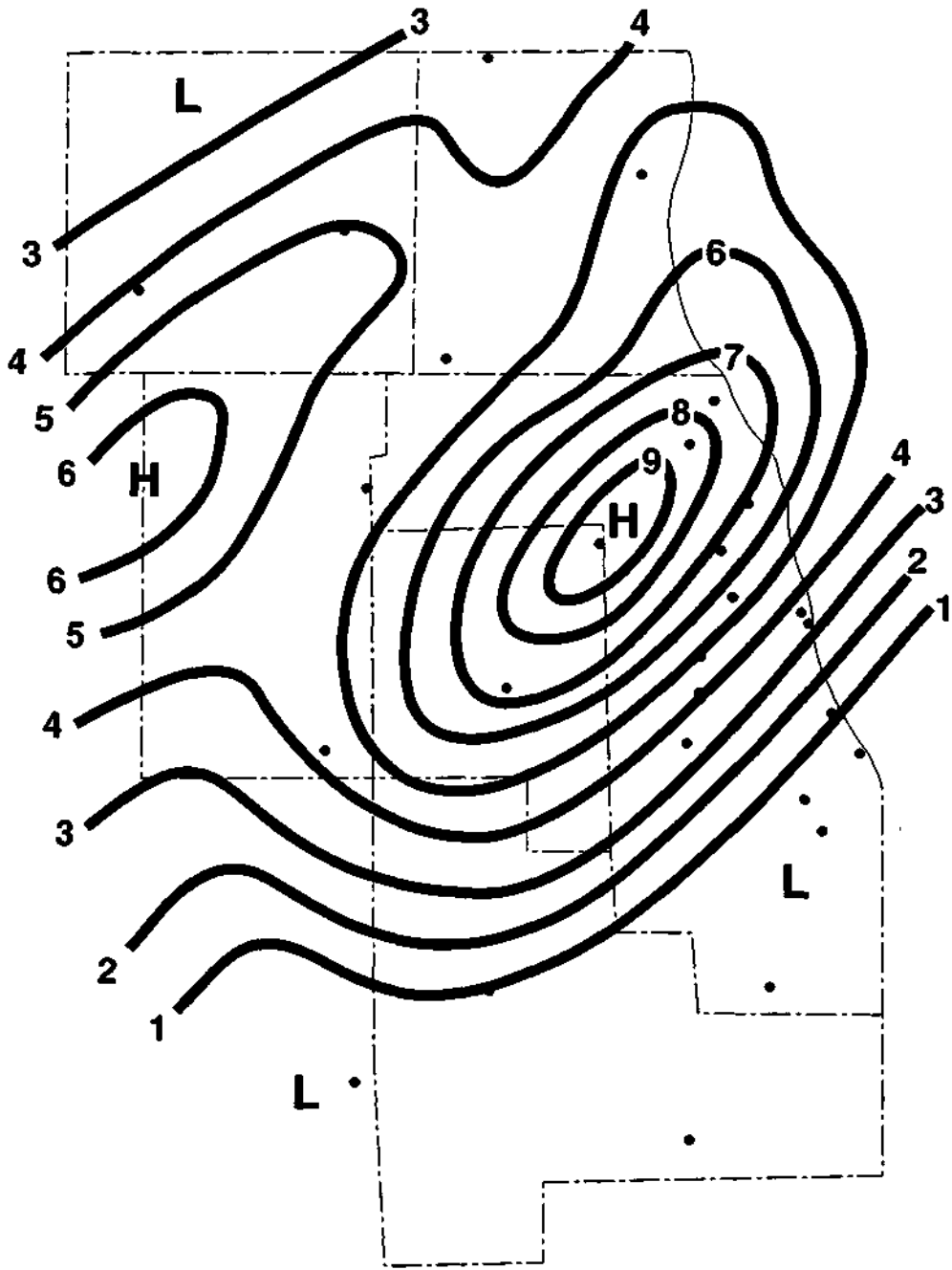


Figure 5-34. Maximum 24-hour rainfall (inches) in the storm in the Chicago metropolitan area, August 14-15, 1987.

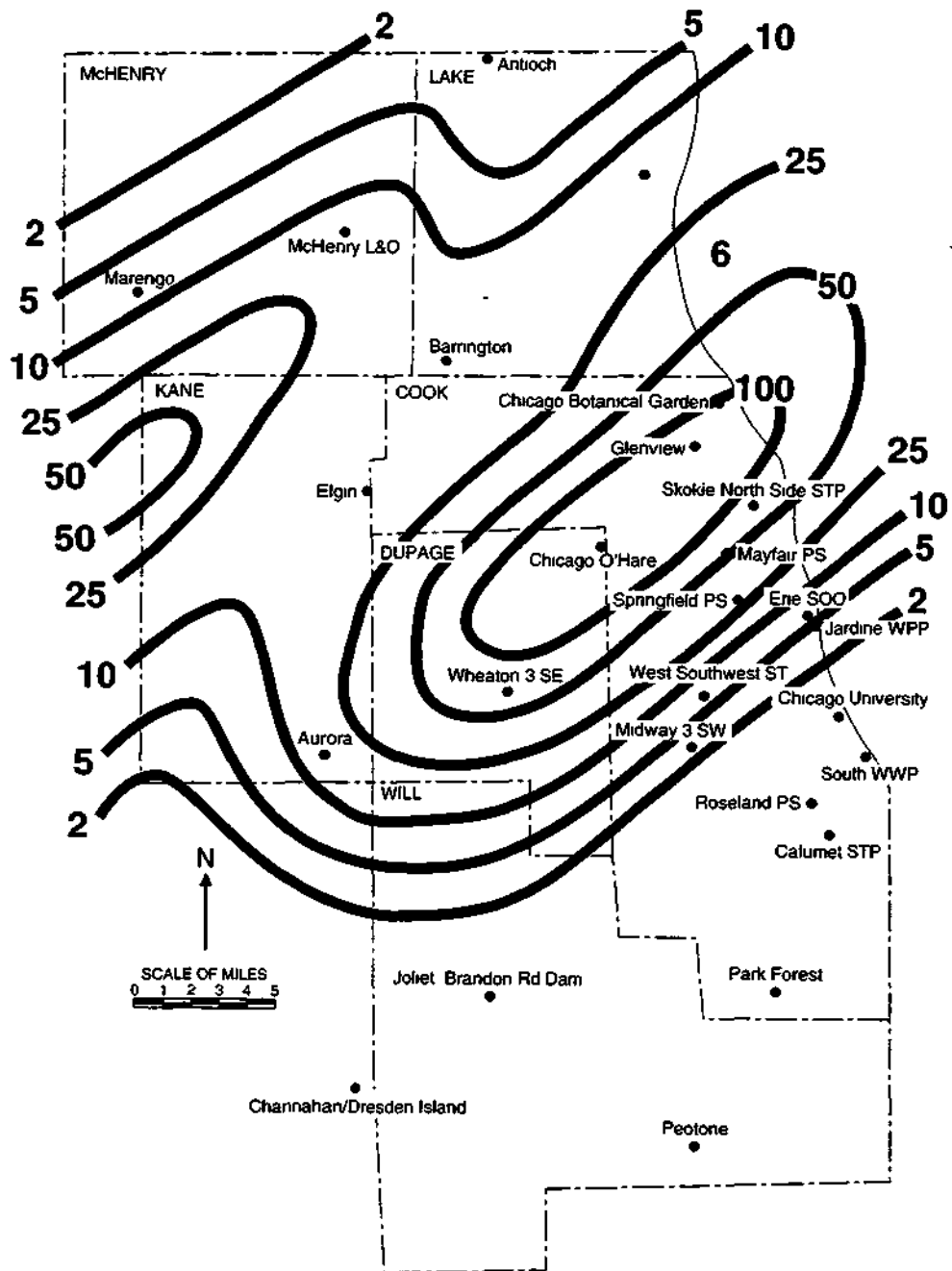


Figure 5-35. Average recurrence intervals of storm rainfall in the storm of August 14-15, 1987.

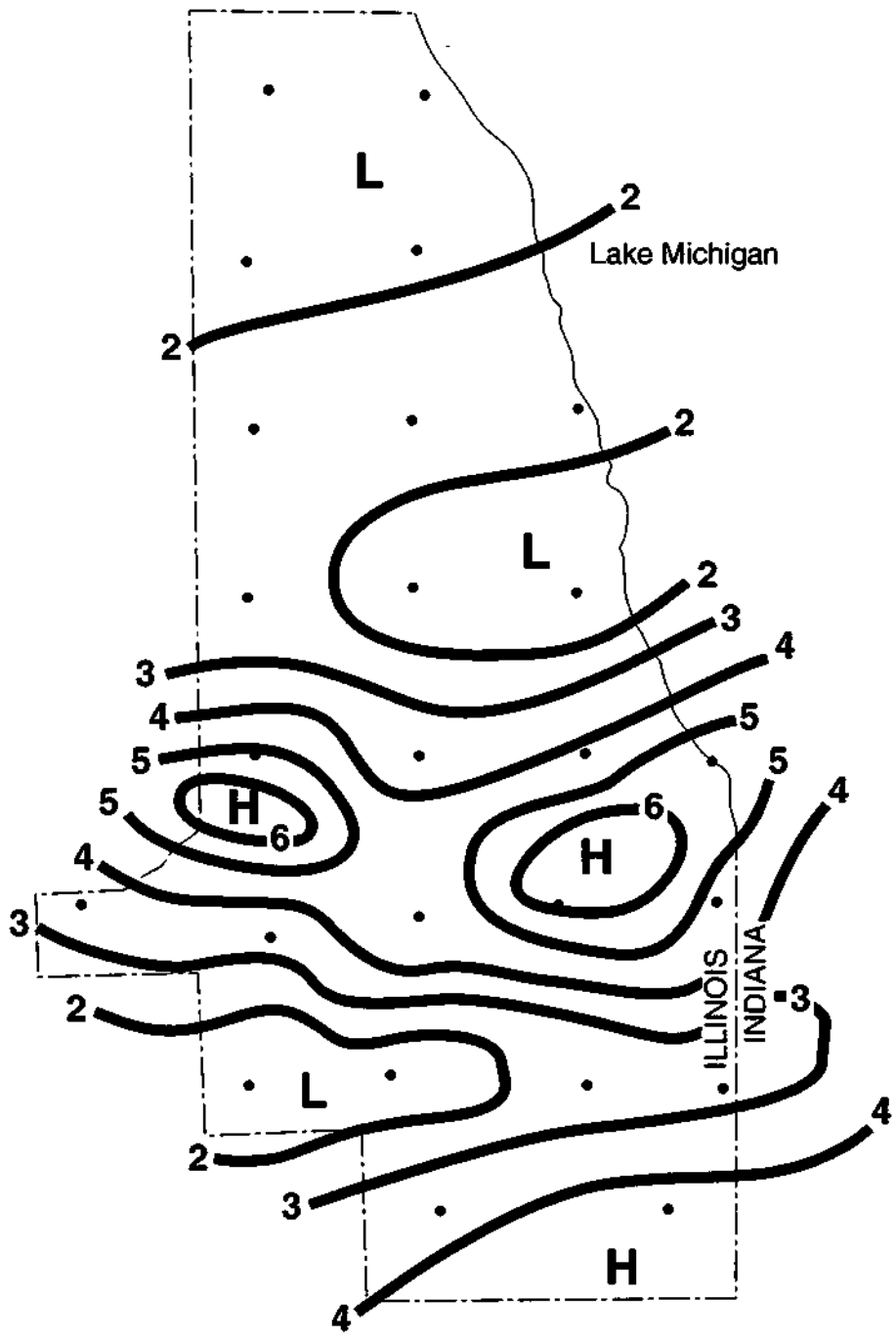


Figure 5-36. Maximum rainfall (inches) in the storm of June 7-9, 1993.

References

- Changnon, S.A., 1985: *Climate Fluctuations and Impacts: The Illinois Case*. Bulletin Amer. Meteor. Soc, 66, 142-151.
- Huff, F.A., 1979: *Hydrometeorological Characteristics of Severe Rainstorms in Illinois*. Report of Investigation 90, Illinois State Water Survey, Champaign, 18 pp.
- Huff, F.A., 1993: *100-Year Rainstorms in the Midwest: Design Characteristics*. Circular 176 (MCC Research Report 93-01), Illinois State Water Survey, Champaign, 20 pp.
- Huff, F.A., and J.R. Angel, 1989: *Frequency Distributions and Hydroclimatic Characteristics of Heavy Rainstorms in Illinois*. Bulletin 70, Illinois State Water Survey, Champaign, 177 pp.
- Huff, F.A., and J.R. Angel, 1992: *Rainfall Frequency Atlas of the Midwest*. Illinois State Water Survey Bulletin 71, Champaign, IL, 141 pp.
- Huff, F.A., H.W. Hiser, and G.E. Stout, 1955: *The October 1954 Storm in Northern Illinois*. Report of Investigation 27, Illinois State Water Survey, Urbana, 23 pp.
- Westcott, Nancy E., 1996: *Continued Operation of a Raingage Network for the Collection, Reduction, and Analysis of Precipitation Data for Lake Michigan Diversion Accounting: Water Year 1995*. Contract Report 601 (Prepared for U.S. Corps of Engineers, Chicago District and the U.S. Geological Survey), Illinois State Water Survey, Champaign.

Chapter 6. Impacts and Responses to the Storm

Stanley A. Changnon, Illinois State Water Survey

Part 1. Impacts

The record-setting rainfalls documented in Chapters 4 and 5 resulted in a wide variety of physical and socioeconomic impacts. The major direct physical impact was the excessive flooding along the Du Page, Des Plaines, Fox, and Kishwaukee Rivers, and their tributaries. The high rainfall rates and the flood waters also produced an enormous amount of erosion to existing physical structures like bridge abutments and roadways, and to soils. Excessive flooding was recorded in south Chicago, in numerous suburbs west and south of the city, and in several small rural communities.

Another damaging aspect associated with the rainstorm was the variety of severe storms. Four tornado funnels were sighted, excessive cloud-to-ground lightning occurred in the storms of July 17 and 18, and strong surface winds were reported throughout the heavy rain area. Lightning and the ensuing flooding caused eight deaths. The amount of emotional stress endured by the hundreds of thousands experiencing flood damage, delays in transportation, evacuation from residences, temporary residences, and efforts to rebuild lives was beyond measure but certainly excessive. Losses from the storms are estimated to be over \$500 million, making this the second worst weather disaster in the history of Illinois.

This chapter attempts to document as many of the impacts and responses to the flood as are known. However, it does not represent an exhaustive, in-depth analysis. It is based largely on available data, accounts in local newspapers, and on data and information provided by state and federal emergency management agencies.

Flooding and Erosion

Magnitude of River Flows

A record rainfall typically produces record, or near-record, streamflows on rivers and streams affected by the heaviest rains, and such was the case in the extreme storm event of July 17-18, 1996. All basins shown in Figure 6-1 had flows that were above flood stage. Fortunately, prior to the rainstorm, the level of flow in all basins shown in Figure 6-1 was relatively low. Just prior to the storm (on July 16), most streams were reporting their lowest flows of July 1996.

By 1600 LST on July 18, just two or three hours after the rains had ended, the peaks of record had already occurred on 14 U.S. Geological Survey streamgages. At 2200 LST on July 18, the flow in the Des Plaines River near Joliet was a record 26,000 cubic feet per second (cfs), with a mean velocity of 6.02 feet per second (fps). The next day, the flow of another seriously flooded river, the Fox River, had a velocity measured at Dayton (near the mouth) of 15 fps, nearly 10 mph.

Figure 6-2 shows the stage curves for three tributaries in the flooded region (in the Kishwaukee and Fox basins). These small basins show a rapid response to the rains on July 17-18, rising 10 feet or more in just a few hours.

Table 6-1 presents the peak stages achieved on several rivers, all of which exceeded their flood stages, and the dates of the peak value. The Fox and Kishwaukee Rivers (for which the basins are shown in Figure 6-1) exceeded their flood stages by 16 feet, setting new records. All streams in northeastern Illinois, ranging from the Pecatonica River in the far northwest to the Des Plaines and Kankakee Rivers in the east, had flows in excess of their flood stages. All these peaks occurred either one, two, three, or four days after the rainstorm ended, with the delay dependent upon basin size and the time to accumulate the flood waters. A smaller basin in the storm such as the Des Plaines River at Riverside (630 square miles) peaked on July 18, whereas the Kankakee River at Wilmington (5,150 square miles) peaked on July 22, four days after the rains ended. The accumulated flood flows of the Des Plaines, Du Page, Fox, and Kankakee Rivers created a flow that went above the flood peak on the Illinois River at Marseilles. Also, the heavy rains in northwestern Illinois, including the flood flows of the Rock River and its tributaries, brought the Mississippi River above flood stage at Keokuk by July 22.

The excessive runoff resulting from the July 17-18 rainstorm also brought the mean monthly river flows for July 1996 to levels much higher than normal for several rivers. Table 6-2 shows the July 1996 mean flows and the long-term averages at selected rivers. The July 1996 flows of the Rock, Fox, and Kankakee Rivers had chances of exceedance of 4 percent or less.

Residential Flooding. The excessive overland flows and the record flows on the area rivers created excessive residential flooding in 21 communities. Figure 6-3 shows the locations of those residential areas in the Chicago suburbs experiencing flooding: Aurora, Joliet, Chicago, Lockport, Frankfort, Lisle, Shorewood, Naperville, Lemont, Tinley Park, Orland Hills, Orland Park, Plainfield, DeKalb, Sycamore, Cortland, Kirkland, Sugar Grove, North Aurora, Channahon, and New Milford. Figure 6-3 shows the locations of those in the Chicago suburbs experiencing flooding.

Table 6-1. Selected Rivers that Exceeded Flood Stages after the July 17-18, 1996 Rainstorm

<i>River/Location</i>	<i>Peak stage, feet</i>	<i>Flood stage, feet</i>	<i>Date of peak</i>
Rock River at Rockton	11.4	10	July 20
Rock River at Joslin	17.4	12	July 22
Pecatonica at Rockford	14.5	13	July 19
Kishwaukee at Rockford	28.0	12	July 19
Des Plaines at Riverside	6.3	6	July 18
Du Page at Shorewood	14.6	6	July 18
Fox River at Dayton	28.0	12	July 21
Kankakee at Wilmington	5.7	5	July 22
Vermilion at Lenore	12.6	12	July 21
Illinois River at Marseilles	14.6	13	July 19
Mississippi at Keokuk	18.3	16	July 22

Table 6-2. Streamflows for July 1996 for Selected Rivers, July 1996

<i>River/location</i>	<i>Mean flow, cfs</i>	<i>Long-term average, cfs</i>	<i>Percent chance of exceedance of July 1996 value</i>
Rock River at Rockton	10,600	3,431	4
Rock River at Joslin	17,200	5,448	4
Pecatonica at Freeport	2,409	868	5
Kankakee at Momence	4,730	1,425	1
Fox at Dayton	2,600	1,187	3
Green River at Geneseo	962	546	15

Over the past 40 years, there has been an extensive development of suburban communities in the areas where the heaviest rainfall occurred on July 17-18 (Kane, Du Page, and Will Counties). Several of these suburban communities and their newer subdivisions became major targets for the damaging flooding of residences, including houses and trailer parks. Considerable suburban flooding occurred well beyond floodplains in areas where detention ponds were filled and excess water flow occurred overland, in gulleys, ditches, and streets, leading to water in basements and first floors of many residences.

The major residential flooding reported in the media (*Chicago Tribune, Joliet Herald News, Aurora Beacon News, Rockford Register-Star, DeKalb Midweek, and Daily Chronicle*) and government reports included the following:

- Approximately half of the homes in Aurora sustained flood damage.
- About 200 homes in the Mayfair subdivision in Joliet were severely damaged, and the city reported 8,000 other homes with flood damage.
- About 100 homes in Montgomery were badly damaged (at a cost of \$10 million), and 200 homes were flooded in the Parkview Estate Subdivision.
- Damage totalled \$40 million from severe flooding of 1,878 Shorewood homes, which affected 7,200 people.
- About 200 trailers in a Sycamore trailer camp were inundated, resulting in the loss of 152 trailers.
- A subdivision in Cortland was flooded by 8 feet of water and 78 homes were badly damaged.
- Chicago reported some 23,000 flooded basements.
- A Kirkland trailer park was flooded and 84 trailers were damaged or destroyed.
- Several subdivisions in and near lisle were flooded, with over 400 homes damaged.
- Between 60 and 80 homes in New Milford were flooded.

The Federal Emergency Management Agency (FEMA) estimated that more than 35,000 residences were flooded as a result of the July 17-18 rainstorm.

Business/Industry Flooding

Several businesses and industries built along the Fox River in Aurora and along the Des Plaines River in Joliet experienced damaging flooding. For example, a nursery in Aurora incurred losses of \$1.5 million after all of its plants and trees were swept away over an area of 200,000 square feet. A major shopping center in DeKalb was flooded, along with portions of Northern Illinois University, producing \$2.5 million in damages. Aurora reported that half of all its commercial establishments had flood damage. Many small businesses, typically without flood insurance, were damaged.

Businesses selling water pumps sold out of pumps at all area stores. Construction firms also were impacted: home building in the region had been delayed by a wet spring and then totally stopped for four to six weeks after the July rainstorm. However, carpenters and construction firms later achieved increased business from the extensive repairs to the many flooded homes.

Flooding of Highways and Streets

Numerous country roads, city streets, state and federal highways, and interstates were flooded, leaving many damaged. This brought two types of major problems: delays in human movement through the region, particularly in the three days during and after the rains (July 17-19), and damages to the streets and highways. For example, more than 200 vehicles were submerged by floodwaters in Naperville.

Some of the Illinois highways closed by flooding included Highways 23, 30, 38, and 72, and Interstates 55, 59, 80, and 88 were closed for more than one day. On July 19, I-80 and I-55 were still closed. Hooding along I-80 caused many vehicles to become trapped, forming what some called "Illinois' largest parking lot." Ten major highways in Kane County were closed for three days. Flooding of major highways closed off access to DeKalb and Naperville. Street and highway underpasses in many DuPage communities were under water, including Route 59 at Downers Grove.

Widespread damages to streets were reported because of the erosive powers of the flood waters, which also impacted stormwater and drainage systems. The force of the flood waters also damaged many bridges because the water frequently eroded the fill around the abutments causing their collapse. Kirkland lost two bridges. Four other rural road bridges were lost in DeKalb County. Damages to the bridges in DeKalb County were estimated \$0.5 million, and damage to bridges in Kane County represented a \$1 million loss.

Another major result of the flooding, particularly during the rainstorm, was a 280 percent increase in automobile accidents. Three persons were killed when their vehicles were inundated or swept away by flood waters.

Flooding of Railroads

Five major railroads experienced major flooding and damages, resulting in canceled or rerouted trains and delayed travel. The Burlington Northern-Santa Fe (formerly Atchison, Topeka & Santa Fe) line running alongside the Des Plaines River was subjected to severe flooding. The Southern Pacific line, which also runs along the Des Plaines River southwest of Chicago, also

experienced extensive damage. The Burlington Northern-Santa Fe (formerly Burlington Northern) mainlines running west from Chicago through Aurora, and then west of Aurora as two major separate lines, one running southwest to Galesburg and one west to Savanna, experienced flood damages. Burlington Northern's major Eola Yard was severely impacted by the flood.

The flooding and blockage of these main lines stopped Amtrak service, and METRA commuter service, extending southwest of Chicago to Joliet and west to Aurora. The Hill Yard in Aurora, where METRA equipment is stored, was covered by 5 feet of water by 8 a.m. (CDT) on July 18. METRA (commuter) service between Chicago and Aurora (87 trains normally operate each day) ceased on July 18 and 19, prohibiting 26,000 commuters each day from reaching their work places. METRA trains operating on the Southern Pacific Heritage Corridor line between Joliet and Chicago also could not operate until July 19. Amtrak stopped all its trains operating between Chicago and Galesburg, and between Chicago and St. Louis on July 18-19.

The damages to the railroads were of various forms, some due to erosion of raised tracks, some due to erosion and damage to bridges, and some due to mudslides. For example, mudslides near Aurora blocked the Burlington Northern-Santa Fe mainline, which also had numerous washouts of tracks west of Aurora over a 19-mile stretch. Several rail bridges were severely damaged. The Burlington Northern-Santa Fe experienced serious damage to two bridges in DeKalb County and four in Kane County.

The former Santa Fe mainline extending southwest from Chicago down the Des Plaines River valley was shut down by 6:00 a.m. CDT on July 18 because water had washed out both main tracks over a half-mile distance near Romeoville. The railroad responded by moving several special trains of ballast (rock) from Kansas, Oklahoma, and Texas to rebuild their Illinois lines. This mainline was re-opened late on July 19. There was also considerable water damage to the signals that control train movement. This caused train congestion at the huge Burlington Northern-Santa Fe Willow Springs railyards, leading to 30 trains stopped on the mainlines between Joliet and Willow Springs on July 18.

The Union Pacific Railroad also experienced problems on two mainlines: one extending west from Chicago through Geneva, and one extending from Chicago south through Dolton. Mudslides at Geneva and LaFox closed one track on the Union Pacific west line, limiting train movement and reducing train speeds. Water was over the Union Pacific tracks at DeKalb, and power lines fell over the tracks at Lombard, delaying METRA commuter trains. Commuter service on the Chicago to West Chicago line to Geneva was canceled on July 18. Downed trees due to the storm on the Union Pacific line south of Chicago stopped trains and caused signal outages for 12 hours.

The flood also affected the Canadian Pacific/Soo Line extending west from Chicago through Elgin. Portions of this line, including a branch from Davis Junction north to Rockford, were under water for two days. The railroad had to reroute 68 trains for a week at considerable expense. The Burlington Northern-Santa Fe was unable to move its many freight trains, and then detoured them on the Canadian Pacific lines to Minneapolis and points west. The train re-routing costs for the five flooded railroads exceeded \$12 million.

In summary, the floods caused four main problems for railroads and rail travelers in the suburban areas of Chicago. First, commuters on METRA and travelers on Amtrak were unable to travel or were severely delayed when trains were canceled; this included commuters located southwest and west of Chicago. Second, several major railroads including the Burlington Northern-

Sante Fe, Canadian Pacific/Soo, and the Southern Pacific had mainlines closed to freight train movement for 12 to 60 hours. Third, there was considerable damage to local rail lines, necessitating major repairs to tracks, to replace fills, and to rebuild bridges. Fourth, the closure of the lines led to two major shipping problems. First, 311 high-speed freight trains operating between Chicago and the West Coast had to undergo re-routings on nonflooded lines, causing great delays. Second, the delayed movement of over 300 freight trains brought crisis in the exchange of freight cars in the Chicago yards. The cost to the railroads in direct damages, delays, and the costs of rerouting were estimated at \$48 million.

Impacts on City Governments

As might be expected, with 21 communities experiencing severe flooding of residences and nine communities with extensive flooding of businesses, many city governments were severely impacted. This included the problems of damaged streets and bridges in communities, handling of flood-damaged materials, and the flooding of city-operated facilities, including sewage treatment plants and water treatment plants. The roads and bridges damaged in Kane County required an estimated \$1.8 million to repair. Damages to the streets and city structures in Sycamore were estimated at \$1 million. Most of the impacts to the communities in the flooded area were in the form of response activities, debris removal, and their related costs which are described elsewhere in of this chapter.

Agricultural Impacts

The heavy rainfall rates and rapidly moving flood waters produced two general impacts on regional agriculture. First, the high waters flooded crop lands, particularly those poorly drained or in and near river valleys, causing either serious yield reductions or total crop losses.

Corn and soybean crops were washed out along portions of the Kishwaukee and Fox Rivers, and crops were flooded in the low-lying areas throughout the storm region. Just after the flood, agricultural experts estimated a 5 to 7 percent loss of crops in DeKalb County. Numerous dairy farms in the rural areas west of the Chicago metropolitan area suffered flood damage to their facilities with losses of stored feed.

Second, the force of the high rain rates and swift moving flood waters caused a considerable amount of soil erosion on uplands and river lowlands. Research has shown that extensive erosion occurs with heavy rainfalls (Bhowmik et al., 1980), and the excessive rainfall rates on July 17-18, particularly during the nocturnal storm, undoubtedly created sizable amounts of soil erosion.

Yields of corn and soybeans in 1996 from the ten counties that experienced heavy rains during the storm, greater than 6 inches, were compared with those of eight adjacent counties. The comparison of corn yields rate the regional differences in 1996 against those in 1995. The ten-county area with heavy rains had an average yield change of +15 bushels per acre in corn from 1995 to 1996, whereas the eight adjacent counties experienced a 22 bushel per acre increase. Thus, the counties without the heavy July rains had an increase in yields that was nearly 50 percent (22 bushels versus 15 bushels) greater than in the flooded counties. This suggests that the heavy rains with direct losses due to flooding and ensuing ponding caused a loss of seven bushels per acre.

Soybean yields in the ten counties with heavy rains averaged 32.5 bushels per acre, whereas yields in the eight adjacent counties without heavy rains were 42 bushels per acre. The difference, a decrease of 9.5 bushels per acre, is sizable, 23 percent less yield than in the nonflooded counties from the heavy rains of July 17-18.

Societal Effects

Widespread concern quickly developed over the effect of the heavy rains and ensuing flooding on the health and welfare of the 3.4 million Illinois citizens living in the impacted area. Eight persons died as a result of the storm: five drowned (one in a flooded basement); two died from heart attacks while working during the flood; and one person was electrocuted by lightning. Health concerns led to free tetanus shots given by the Red Cross. There was also considerable concern over possible encephalitis outbreaks due to feared massive development of mosquitoes in the flood areas, but this did not occur.

One of the major societal impacts was stress, which was high among more than 35,000 flood-stricken families. Flood workers, including police and fire departments, worked overtime and were under great stress from the excessive hours.

There was the initial derived stress from flood damages and delays in transportation, but the flood forever altered the lives of many flood victims. Life savings were often used to pay for damages, and many mothers reportedly went back to work to help recoup family finances. With as many as 4,000 persons evacuated, there was the enormous stress due to loss of homes and personal possessions, as well as being displaced in various types of housing. Floodwaters brought snakes into several homes, giving rise to fears of snake bites. Social workers predicted that people made homeless by flood damages and who were barely scraping by would become "homeless."

Conflicts also resulted, producing further stress. For example, two engineers working for Orland Park were arrested for pumping water out of Orland Park into Tinley Park. Residents in certain communities such as Aurora and Joliet claimed their cities were giving greater help to those in affluent neighborhoods rather than to those in less affluent neighborhoods, producing conflict between residents and city managers. In addition, many who were flooded blamed upstream suburban developments for their plight.

Severe Storm Damages

The sequence of thunderstorms that produced the excessive rainfall on July 17-18 (Chapter 4) also produced other forms of damaging weather phenomena: high winds, hail, and frequent lightning. The lightning resulted in the death of one person and caused widespread power outages that affected 23,000 service units in the area. Two homes in Spring Grove and Harvard were burned due to lightning-set fires.

Winds in excess of 60 mph were observed in several locations, which caused extensive damage to trees and structures. Wind also caused trees to fall across railroad tracks and across certain highways in the Chicago area blocking traffic. Hail damaged crops in DeKalb and Gee Counties.

Water Quality Impacts

Excessive rains and flooding produced several problems affecting water quality. Faced with flooded basements and excessive water in the Chicago River system, the Metropolitan Water Reclamation District of Chicago had to release polluted water into Lake Michigan to ease the flood. The resulting polluted water led to beach closures lasting several days after the storm.

Sewage treatment plants in many communities were unable to handle the rush of flood waters through their sewage treatment systems. Thus, flood waters carried a considerable amount of raw sewage into local streams and rivers. At Sugar Grove, the flood damage caused the sewage treatment plant to be out of commission for eight weeks and repairs cost \$250,000. Sewage treatment plants in DeKalb and Plainfield were also seriously damaged, representing a repair cost of \$350,000 at Plainfield. Water treatment plants in some rural communities were also damaged and out of commission for a few days.

Beneficiaries

Every weather disaster provides a certain number of "winners" who benefit from the event, and the storm of July 1996 was no exception. Those involved in the selling of water pumps were overwhelmed with purchases and made record sales. Haulers of waste material were also major beneficiaries as materials from flooded homes had to be hauled away. For example, in Aurora, 75,000 tons of water-damaged material were hauled to landfills in three days with a total of more than 100,000 tons removed by July 24. Homebuilders and construction firms also reaped benefits in the aftermath of the flood due to the rebuilding of businesses and residences. The widespread rains of July 17-18 also affected the Chicago Board of Trade. Com futures fell 10 percent, from \$3.82 on July 12 to \$3.45 on July 19. Some investors won and some lost from this action.

Part 2. Responses

The July rainstorm and ensuing flooding produced responses ranging from the simple act of walking out the door of a flooded home to declaring most of northeastern Illinois a disaster area. Important in understanding the responses to disasters is to appreciate that there is considerable overlap between "impacts" and "responses." An impact is the physical damage and disruption, while a response is an action taken to ameliorate an impact.

There are several limitations in the compilation of the responses to a flood event of such recent occurrence. When the loss data and this document were assembled in the winter of 1996-1997, many responses were still occurring. Furthermore, costs of a sizable event like the July flood, due to both impacts and responses, cannot be measured with a high degree of accuracy. A thorough, highly detailed analysis of costs from an event of this magnitude would require intensive studies by several scientists over two or three years. Recognizing this, the reported values relating to losses, costs, and responses are best estimates based on reports from several individuals and institutions; thus, they are only approximations of the real costs.

Another concept used in this documentation of responses to the July 1996 rainstorm relates to the time of the response. "Immediate" responses are defined as those occurring during the storm

and within seven days thereafter. Responses more than seven days after the storm are considered "long term", and, as noted, many responses were still evolving at the time this report was prepared.

Immediate Responses

Responses to the myriad of flooding problems in the immediate aftermath of the storm could be classified into two general areas: actions of individuals and the actions of government agencies. Damaged private sector firms such as the local railroads also responded to make repairs to their facilities..

The principal response during the storm and three days after was the evacuation of individuals from flooded homes and communities. The number of persons who left their homes by boat, helicopter, or other means included 900 in Aurora, 800 in Orland Park, several hundred in Kirkland, 700 from a subdivision near Lisle, and 1,200 in Grundy County communities. In addition, several other towns reported evacuations ranging from 50 to 300 persons. Altogether, it is estimated that more than 4,000 people had to be evacuated from flooded residences and businesses.

Evacuations were handled by local police, fire departments, and state police. Governor Edgar sent three National Guard units to assist in evacuations, traffic direction, and other forms of assistance. During the first week after the storm, various groups including the Red Cross and Salvation Army established shelters for the evacuees, provided food, and in some cases clothing. Orland Park reported that many of the evacuees had been allowed to return to their homes by July 22, which was common in many other flooded communities.

The other major area of immediate responses concerned actions of government bodies. On July 18, Governor Edgar declared 15 counties in northeastern Illinois as State Disaster Areas. The Gubernatorial Proclamation is a requirement prior to requesting federal assistance. The initial State estimate was that \$24 million would be needed for low-interest loans. As a result of the Governor's letter requesting assistance for 11 of the 15 counties, President Clinton designated those 11 counties Major Disaster Areas on July 25. The following counties were designated major disaster areas: Cook, DeKalb, DuPage, Grundy, Kane, Kendall, LaSalle, Ogle, Stephenson, Will, and Winnebago (Figure 6-4). Federal programs that provide assistance to individuals, businesses, and jurisdictions (village, city, and county) or other public entities include personal and business (low-interest) loans, rental assistance, temporary housing, and up to 26 weeks of unemployment pay.

Working in concert with the Illinois Emergency Management Agency (JEMA) and the Small Business Administration, the Federal Emergency Management Agency (FEMA) formed 16 teams to perform preliminary damage assessments which determine whether Federal assistance is required. These groups began work on July 22, going from house-to-house to assess damages and check flood insurance coverage. Ironically, results showed that only one percent of those with flood damage had flood insurance, continuing a trend far worse than what had been found in another recent major Midwestern flood (Changnon, 1995).

A major activity of city governments in severely flooded locations involved the removal of damaged materials, such as ruined household goods and damaged house materials, from the flood zones. For example, in Aurora 5,000 tons of material, the equivalent of more than two months of garbage, was hauled to landfills during three days following the flood. In Naperville, 75 trucks were

used for several days to haul away flood-damaged materials, and the city of Chicago loaned 50 garbage trucks to Plainfield to help that city dispose of its flood debris.

The mayor of Aurora, the city with the greatest amount of flood damage, declared a city-wide emergency at 2 a.m. CDT on July 18, and directed fire trucks and the police to help evacuate people from flooded areas while the intense rains were still in progress. Many volunteer actions also occurred. For example, students at Northern Illinois University helped fill sandbags to protect their school from the flood in DeKalb. DuPage County's Trauma and Disaster Team went to work on July 19, providing information, giving tetanus shots, and counseling flood victims.

Longer Term Responses

Although the provision of shelter and food for individuals who were forced out of their homes was an immediate response, these activities continued for many weeks after the flood. The Salvation Army brought several mobile units to the flood areas to feed individuals impacted by the flood. Several communities used local schools, unoccupied in the summer, for temporary shelters. The Red Cross organized and set up emergency shelters and provided food in communities such as Rockford, DeKalb, and Frankfort. Furthermore, several food stores and food chains in the area provided free food to shelters established by various cities and volunteer groups.

Another activity that continued into the second and third weeks after the flood was the continual removal of flood-damaged materials. By July 24, debris removal in Aurora had amounted to more than 10,000 tons. Aurora added 100 trucks to haul waste, and it took 2½ weeks to get all the ruined materials to local landfills.

Along with the losses and misery, the flood produced a variety of interesting conflicts. Frequently, the victims of the flood and even the local municipal leaders became deeply concerned about the causes of the flooding. In many cases, upstream communities were thought to be at fault. Claims of inadequate water storage facilities, such as detention basins, in various communities were common. Recognition came that there was no central regional authority to deal with flood control and developments affecting flooding. The U. S. Army Corps of Engineers identified a need for flood planning in Chicago, and requested additional funds for such planning. Cities blamed other cities, regional authorities, and State agencies for many of their ills.

A fourth major area of response in the long-term category relates to government actions in two broad categories: 1) aid and assistance by federal, State and local agencies, and 2) the changing of rules, regulations, and laws, largely at the local scale, in response to the flooding.

Aid and Assistance by Government Agencies

In the beginning, the Illinois Emergency Management Agency estimated funding needs as follows: \$72.8 million in loans from the Small Business Administration; \$32.9 million for housing aid and individual grants; and \$28.1 million for public assistance to local governmental entities. The initial scoping of funding needed from the federal government amounted to \$133.8 million. The FEMA established a Disaster Field Office in the region, and an estimated 200 staff members were assigned there full-time from late July 1996 until it closed in late October.

The assistance, provided through FEMA, done as a result of the President's declaration for major disaster status in 11 counties, included three Federal programs:

- 1) *Individual Assistance Program* including Small Business Administration low-interest disaster loans and the Individual and Family Grant Program;
- 2) *Public Assistance Program* for State and local governments and certain private, nonprofit organizations to cover debris removal, protective measures, and repairs to facilities; and
- 3) *Hazard Mitigation Program* for State and local jurisdictions who sponsor a mitigation project that will eliminate or lessen the impact should the hazard/disaster reoccur.

All 11 counties were eligible for the Individual Assistance and Hazard Mitigation programs, and all counties except Winnebago were eligible for the Public Assistance Program, which provides 75 percent of the funds for eligible projects. The actions pursued under these three federal programs are now described.

1. *Individual Assistance Program (IA)*. For all types of assistance, individuals were directed to call the FEMA Tele-Registration 800 number. Table 6-3 lists the number of applications received from each of the 11 counties. Cook County led with more than 52,000 applications, which represents 70 percent of the 72,482 calls received. Other counties with a considerable number of applications included DeKalb, DuPage, Kane, and Will. Each of the remaining six counties had less than 1,000 applicants.

Table 6-4 shows the number of applications taken in three major Individual Assistance (IA)* Programs, the eventual eligible numbers, and the dollar amounts of the grants disbursed as of September 30, 1996. Please note that individuals who qualified for Small Business Administration (SBA) loans were ineligible for the Individual and Family Grant (IFG) Program; however, many individuals received temporary housing assistance in addition to SBA and IFG. Cook County led with more than 52,000 applications, 72 percent of the total. Other counties with a large number of applications included Kane, Will, DuPage, and DeKalb.

Table 6-3. Tele-Registration Applications for Federal Flood Assistance by Counties

<i>County</i>	<i>Number</i>	<i>County</i>	<i>Number</i>
Cook	52,482	LaSalle	269
DeKalb	1,499	Ogle	221
DuPage	2,929	Stephenson	137
Grundy	61	Will	5,891
Kane	7,499	Winnebago	688
Kendall	739	Total	72,482

**Table 6-4. Number of Applications for Aid
under Three Federal Programs, as of September 30, 1996**

<i>Individual assistance program name</i>	<i>Number of applicants</i>	<i>Number eligible</i>	<i>Grant funding disbursed</i>
Temporary Housing Program	68,147	58,471	\$128,080,236
Small Business Administration Loans	17,704	6,956	\$95,182,800
Individual and Family Grants	29,363	21,290	\$3,610,725*

Note:

*This figure was adjusted on April 17, 1997, at which time 14,020 applicants had been approved and a total of \$10,061,735 had been disbursed. The Individual and Family Grant Program is funded 75 percent by FEMA and 25 percent by the State of Dlinois.

The data in Table 6-4 reveal that the number of applicants, both applying and eligible, for the Temporary Housing Program led in the total funds disbursed at \$128 million, followed closely by \$95 million for SBA loans. The total funding dispersed as of September 30, 1996, was \$228,800,000.

In handling the thousands of requests for assistance, FEMA established ten recovery centers throughout the region by July 27. There, individuals could receive counseling and guidance about the various aid programs. More than 10,000 persons visited the centers during the first month after the flood, and more than 72,000 applications for funding assistance were received (Table 6-3).

2. *Public Assistance Program (PA)*. Government payments under the PA Program included grants to local and State government entities to cover 75 percent of the costs of debris removal, emergency measures taken during the flood, and for permanent repair of facilities such as roads, bridges, and public facilities. Since PA is a matching program, the IEMA administered the Federal reimbursement of the 75 percent, and the local entity was responsible for providing the other 25 percent in funds. Cook County received \$3.0 million, Will County, \$2.9 million, and Kane County, \$2.5 million, reflecting the suburban communities that were most severely impacted by the flood (Table 6-5).

In addition to receiving the 75 percent grant, the public entity received administrative costs on the total project. These costs are based on the following formula: 3 percent for the first \$100,000; 2 percent on the next \$900,000; 1 percent for the next \$4,000,000; and 1/2 percent for everything over \$5,000,000. As shown in Table 6-5, there were 267 applicants for PA funds. They received a total of \$13.8 million in federal funds and provided \$4.6 million themselves.

3. *Hazard Mitigation Grant Program (HMGP)*. The importance of hazard mitigation, taking action to reduce or permanently eliminate the long-term risk from natural hazards, was recognized after successful property acquisition programs following the Flood of 1993 (Changnon, 1996), as well as other major flood declarations in 1994, 1995, and in the spring of 1996. By acquiring homes, mobile homes, businesses, churches, and vacant lots from the floodplain, and turning private property into public ownership, the cycle of "damage-repair-and-damage-again" is broken.

Table 6-5. The Distribution of Federal Funds to Various Institutions and Counties as Part of the Public Assistance Program, as of April 8, 1997

<i>Public entity</i>	<i>Total expenses approved</i>	<i>75% federal FEMA</i>	<i>25% nonfederal local share</i>	<i>Number of applicants</i>
State Agencies	\$1,361,786	\$1,021,340	340,446	3
Northern Illinois University	441,750	331,313	110,437	1
Cook County	4,005,229	3,003,864	998,840	58
DeKalb County	1,095,298	821,484	273,814	35
DuPage County	2,028,652	1,521,497	507,155	32
Grundy County	34,607	25,955	8,652	1
Kane County	3,435,113	2,576,344	858,769	31
Kendall County	926,505	694,884	231,621	14
LaSalle County	275,294	206,473	68,821	13
Ogle County	800,758	600,571	200,187	22
Stephenson County	201,296	150,973	50,323	2
Will County	3,846,601	2,884,961	961,640	55
Winnebago-not declared for PA				
Totals	\$18,452,779	\$13,839,649	\$4,610,705	267

Since 1993, the State of Illinois through the Hazard Mitigation Grant Program (HMGP) has removed more than 1,700 structures from the floodplains of the Mississippi and Illinois Rivers and their tributaries. The HMGP is a voluntary program on the part of the property owner. It consists of 75 percent federal funding and 25 percent nonfederal funding. Jurisdictions must apply on behalf of their effected residents who have experienced repetitive flooding.

The HMGP was administered by Illinois for the July 1996 flood. As in previous flood disasters, property acquisition was the State's main priority. The other objectives being undertaken by the Federal-State mitigation effect are as follows:

- 1) To educate community officials and residents on mitigation techniques and alternatives.
- 2) To use wisely the resources and funding.
- 3) To support and encourage participation and compliance with the National Flood Insurance program.

All jurisdictions affected by the July 1996 flood received a letter dated September 3, 1996, from IEMA. It invited them to submit a pre-application for participation in the HMGP acquisition program. Five counties and 19 communities responded with potential HMGP projects totaling \$48,303,347; however \$14 million was for structural projects. All HMGP applications were reviewed by the Interagency Mitigation Advisory Group (IMAG), which is made up of representatives from Illinois and federal agencies. Since acquisition is the top objective, the structural projects were denied after the pre-application. Fourteen applicants were invited to submit formal applications for their proposed projects.

The State of Illinois' HMGP budget totals \$27,271,036; \$20,453,277 (75%) from FEMA and \$6,817,759 (25%), which will be matched by the local governments. Table 6-6 shows the projects and related expenditures that were recommended by the IMAG, as of April 22, 1997.

The recommended projects listed are submitted to FEMA for cost-effectiveness assessment, environmental consideration, and assurance of program eligibility. During the spring of 1997, the State of Illinois expects to receive approval from FEMA of the projects listed in Table 6-6. Then, jurisdictions will be advised.

All homeowners who voluntarily participate in their jurisdiction's buyout program will receive a pre-flood fair market value appraisal. Insurance monies received by the homeowners who were in the national Flood Insurance Program or who received Individual and Family Grants are deducted from the offer except in instances when receipts are presented, showing that these funds were spent on the home and that the owner did not have to seek temporary housing.

Several factors which either been set forth in FEMA guidance, or by policies developed by the IMAG, are:

- 1) Property acquired in the HMGP must remain in open space in perpetuity. No insurable structure can ever be built on the acquired floodplain land again.
- 2) The buyout is voluntary on the part of the property owner.

Table 6-6. Projects and Related Expenditures that IMAG Has Recommended, as of April 22, 1997, for the Hazard Mitigation Grant Program

<i>Jurisdiction</i>	<i>Number of structures</i>	<i>FEMA/IEMA share (75%)</i>	<i>Local share (25%)</i>	<i>Total cost</i>
DuPage County	47	\$5,766,453	\$1,922,151	\$7,688,604
LaSalle County	18	692,775	230,925	923,700
Montgomery	52	4,324,343	1,441,448	5,765,791
Ottawa	47	779,775	259,925	1,039,700
Shorewood	43	2,836,189	945,396	3,781,585
Illinois. Department of Natural Resources	15	328,688	109,562	438,250
Totals	222	\$14,728,223	\$4,909,407	\$19,637,630

- 3) The owner is offered a pre-flood fair market value based on an appraisal by an appraiser hired by the jurisdiction.
- 4) The appraisal is reviewed and certified by a State review appraiser.
- 5) The owner of the acquired property must relocate out of the floodplain.
- 6) The structure must be demolished with only the demolition contractor having salvageable rights due to potential contamination. An optional Salvage Program may be implemented by the jurisdiction; in this instance the homeowner must identify items to be removed prior to closing, and these items are totaled and deducted from the offer price.
- 7) Property containing underground storage tanks cannot be acquired until the tank is removed.

The IMAG will continue in the future to review the accepted HMGP potential projects resulting from the July 1996 flood. All jurisdictions that participate in the HMGP are responsible for completing a Hazard Mitigation Plan.

Changes in Rules, Regulations, and Laws

Certain communities in the severely flooded areas made interesting changes in rules and regulations. For example, Aurora, Naperville, and Montgomery chose to temporarily waive future permits and fees for the repair and rebuilding of flood-damaged homes. DuPage County also waived construction permits. Aurora decided on August 22 to limit future development of the city in certain areas, required that the Burlington Northern-Santa Fe Railroad improve its viaducts to minimize flooding, and also established requirements that new housing developments had to increase their stormwater retention capabilities to 25 percent. Naperville commissioned two firms to prepare new and improved maps of contours for future use in settling insurance claims related to flooding. Will and Kane Counties formed a joint committee to develop a regional approach to handle flooding.

Part 3. Summary

The July rainstorm caused eight deaths, and more than 35,000 homes were flooded. However, it is desirable, but difficult, to precisely assess the total costs of the July 17-18 rainstorm.

Two approaches were used to estimate the storm losses. One is based on a combination of government payouts (\$274 million), costs to the railroads, (\$48 million), losses in crops (\$67 million), costs to repair roads and bridges (\$220 million), and costs for housing and business losses not covered by government assistance (\$39 million). The total costs using this approach, based on data from a variety of sources, is \$648 million.

Another approach to estimate the storm costs uses the estimated losses reported by the counties. These values included Kane County (\$140 million), DuPage County (\$134 million), Will County (\$130 million), Cook County (\$160 million), DeKalb County (\$26 million), Kendall County (\$15 million), and those of all other counties combined totaled \$31 million. The sum of these estimates is \$635 million, slightly less than the sectoral approach. Accepting the fact that both approaches represent estimates from variety of sources, it appears reasonable to assume that the cost of the July 17-18 flood in Illinois was in the range of \$600 million to \$700 million. The Illinois Emergency Management Agency concluded that this was the second most damaging weather disaster in the state's history, with only the flood of 1993 producing higher loss for the state at \$1.4 billion (Changnon, 1996).

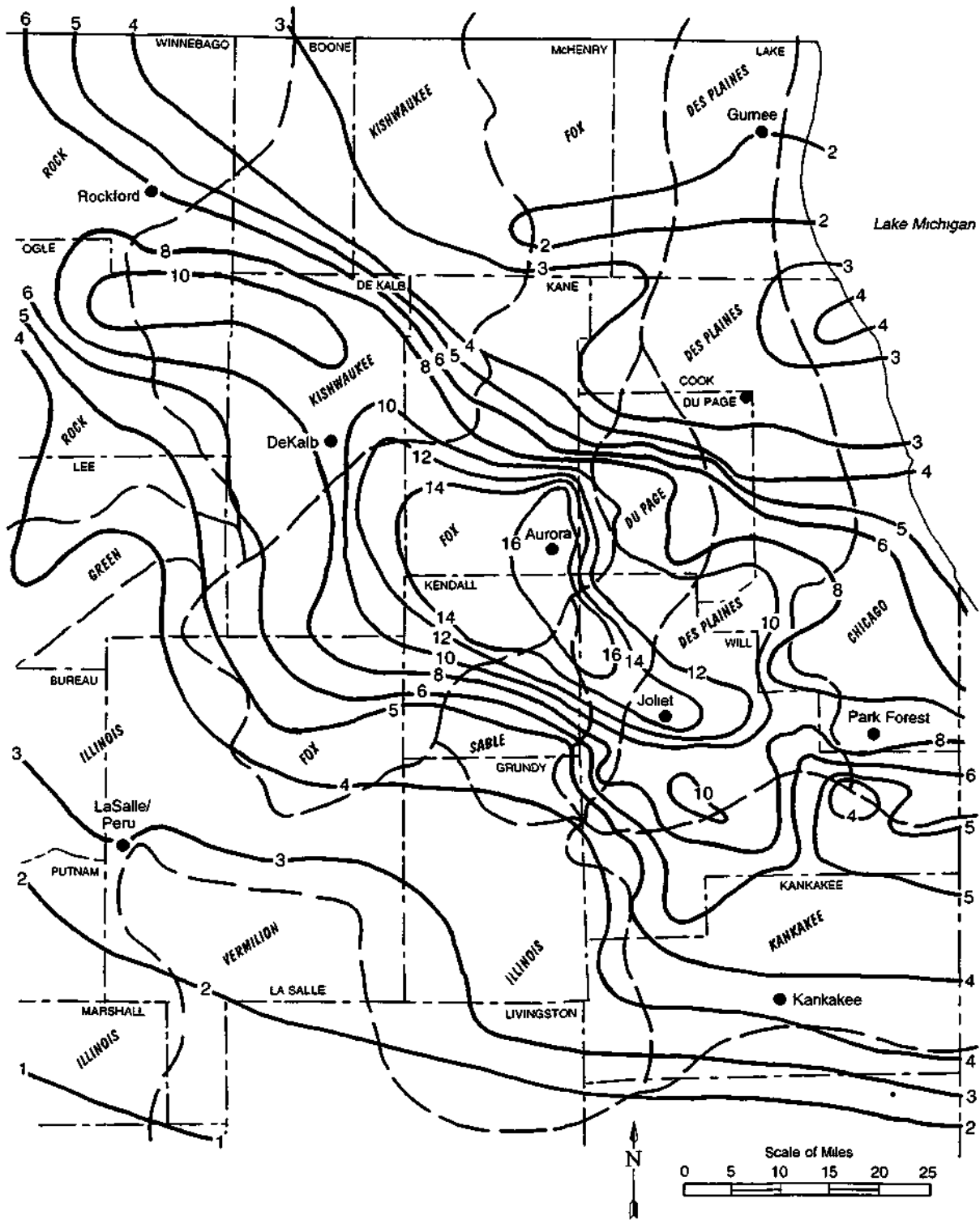


Figure 6-1. The total storm rainfall for July 17-18, 1996, and major river basins in the storm area. Many of the rivers and tributary streams in these basins experienced flooding as a result of the storm including the Kishwaukee, Fox, Sable, Des Plaines, DuPage, and Kankakee Rivers.

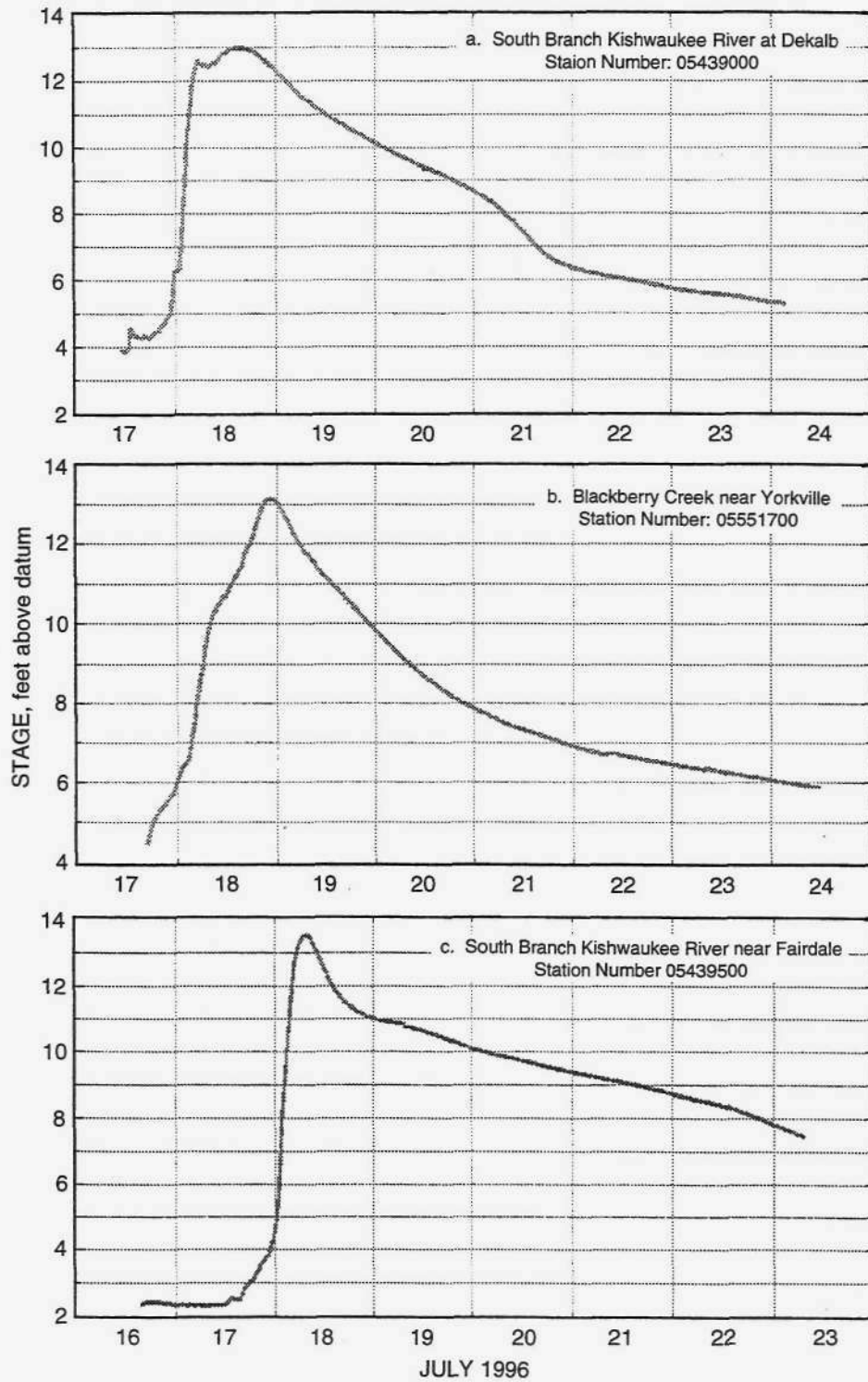


Figure 6-2. Stage curves for river flows on a) the South Branch of the Kishwaukee River at DeKalb, b) Blackberry Creek near Yorkville, and c) the South Branch of the Kishwaukee River near Fairdale. These show the sudden increases in flows during the storm and just after the heavy rains ended. Data provided by the U.S. Geological Survey.

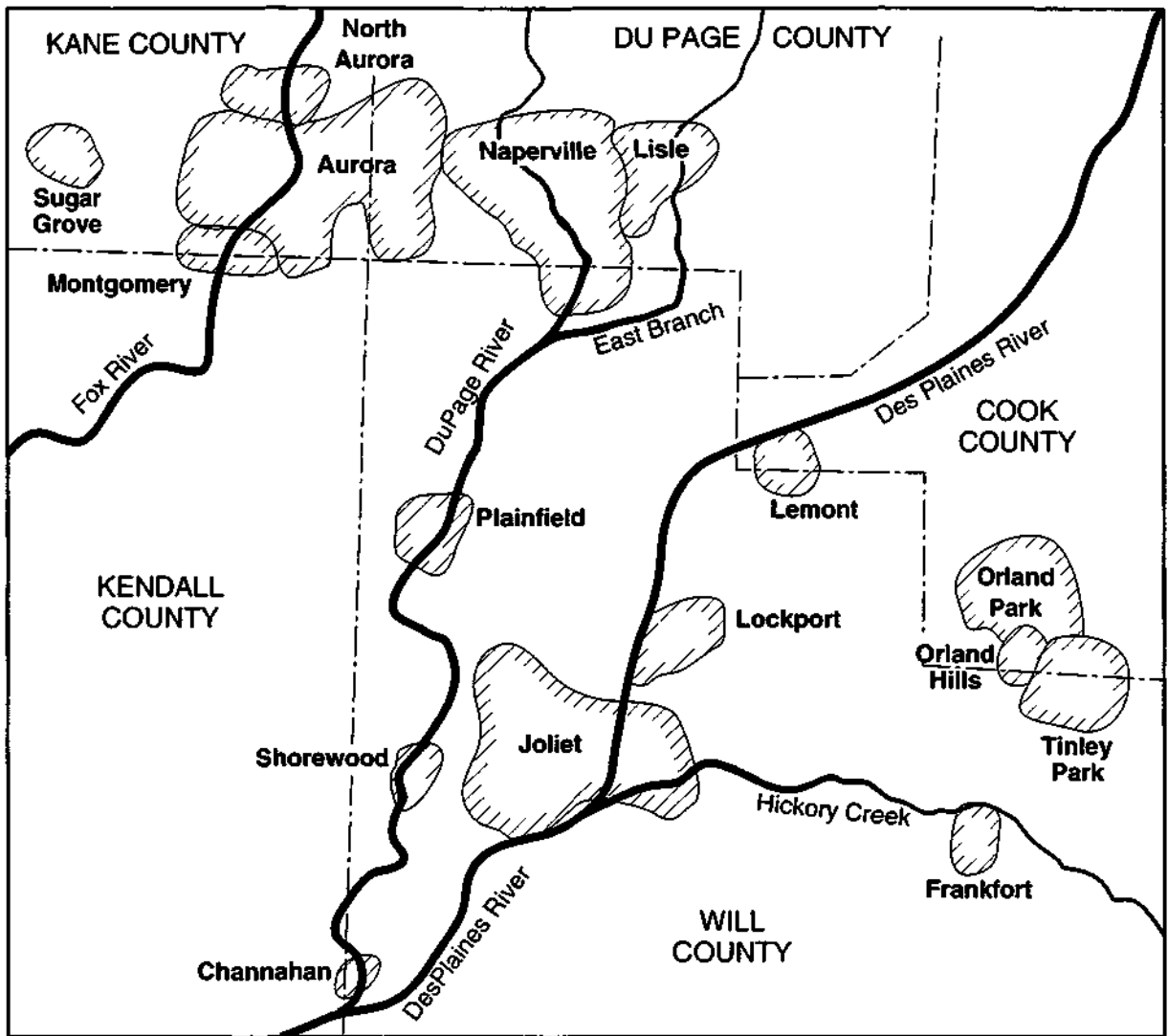


Figure 6-3. Suburban communities experiencing severe flooding as a result of the July 17-18 storm.

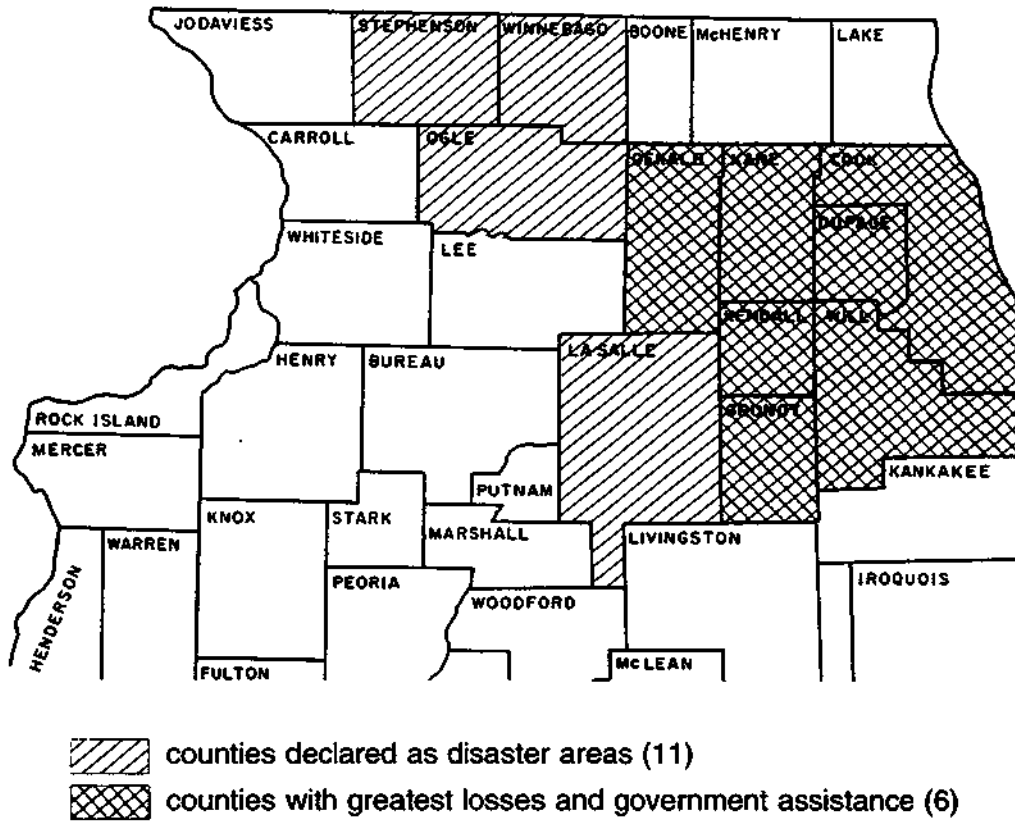


Figure 6-4. Counties declared Disaster Areas as a result of Illinois and federal government actions, and counties which experienced the greatest losses (>\$1 million) as a result of the July 17-18, 1996 storm.

References

- Changnon, S.A., 1996: Losers and Winners: A Summary of the Flood's Impacts. In *The Great Flood of 1993*, Westview Press, Boulder, CO, pp.276-299.
- Bhowmik, N.G., A.P. Bonini, W. Bogner, and R.Byrne, 1980: *Hydraulics of Flow and Sediment Transport in the Kankakee River in Illinois*. Report of Investigation 98, Illinois State Water Survey, Champaign, IL.

Chapter 7. Comparison of the Storm Rainfall as Measured by Radar and by Raingages

Nancy E. Westcott, Illinois State Water Survey

Since the early days of meteorological radar research in the 1950s, it has been recognized that radars have the potential to produce detailed spatial estimates of the rainfall in real time, patterns that were not possible using the normal number of raingages in an area. Various technical problems inherent to the older National Weather Service (NWS) radars have been alleviated with the development and deployment of the new Weather Surveillance Radar-1988 Doppler (WSR-88D) radars such that weather radar is now much closer to realizing its full potential in real-time rainfall estimation. These new radars take advantage of state-of-the-art radar engineering and software development that result in readily available hourly, 3-hour, and total storm rainfall amounts.

A new NWS WSR-88D 10-cm radar first became operational at Romeoville, Illinois, during the summer of 1995 and was operating during the July 1996 storm. Coincidentally, a number of raingage networks were being operated in the northern Illinois area by the Illinois State Water Survey (ISWS), the U.S. Army Corps of Engineers (COE), and the U.S. Geological Survey (USGS), as explained in Chapter 4. Juxtaposition of these radar and raingage facilities in northeastern Illinois (Figure 7-1) provided a good opportunity to compare radar-estimated and raingage observations of rainfall under unusually heavy rain conditions.

Data and Analysis Procedures

Radar Data

An extensive array of software has been developed for analyzing the WSR-88D radar data. The software is used to compute precipitation estimates for 1 degree (°) by 2 kilometer (km) bins out to a range of 230 km for each volume scan. Approximately 10 volume scans of three-dimensional radar reflectivity are collected every hour. These were used to compute hourly, 3-hour, and total storm rainfall accumulations at every volume scan. Rainfall was computed with a radar reflectivity - rainfall relationship of $Z = 300R^{1.4}$, and with a reflectivity cap of 53 dBZ (values >53 dBZ were set to 53 dBZ).

Raingage Data

Raingage data for the radar study were obtained from several sources. Data from 24 of the 25 Cook County Network (CCN) gages were available for the flood event, and four of the Illinois Climate Network (ICN) sites were located in the heavy rainfall area. Storm rainfall totals for the 24 weighing buckets gages in the CCN were calibrated using past storm measurements of the water in each bucket. Data also were obtained for six of the USGS/COE Chicago network of tipping bucket gages and from an NWS tipping bucket gage located three miles southwest of Midway Airport. Figure 7-1 shows the location of the 35 recording gages used in this study.

Analysis Software

The software package for the WSR-88D Algorithm Testing and Display System (WATADS) was obtained from the National Severe Storms Laboratory (NSSL), and it was used to compute radar estimated rainfall values at locations that correspond to the 35 recording raingage sites. This software computes a 3 x 3 array of radar-derived precipitation values centered on the (1 ° by 2 km) radar bin (area) closest to the raingage. The average, maximum, and minimum 1-hour accumulated precipitation values for these nine bins was derived for each raingage.

The analysis described here is based on the estimates of rain from the "best-fit" radar value, and from the "maximum" radar value. The best-fit radar value is defined as equal to the average radar amount when the nine radar values straddle the raingage value, and equal to the radar amount nearest the gage amount when all radar amounts were either more or less than the gage amount.

Within the July 17-18 storm period, radar rain estimates could be computed for 17 full hours of rain data. These 17 hours include most of the hours when heavy rain fell during the storm.

Results

Gage/radar (G/R) comparisons were made for the (17-hour) total storm rainfall and for individual 17 hourly rainfall accumulations. The hourly values are of great importance in flash-flood detection and heavy rain forecasting. Total storm amounts are particularly important to assess the storm's dimensions.

Total Storm Rainfall Comparison

The comparison of radar-estimated and gage rainfall totals was first made in terms of distance from the radar. The radar-estimated rainfall at the closest gage (COE gage 15, 11 km from the radar) was found to severely underestimate this gage's rainfall. The radar "best-fit" value was 2.9 inches, whereas the gage value was 7.5 inches (Figure 7-2). The maximum radar estimate (3.6 inches) also was well below the gage amount (Figure 7-3).

All radar-estimated values within 60 km of the radar were found to be less than the gage values, with G/R ratios of 1.2 to 2.8 (Figure 7-2). At ranges beyond 60 km, G/R ratios ranged from about 0.75 to 1.5. By omitting gage 15, the average ratio (G/ R) for the 24 gages within 60 km of the radar was 1.67 (with gage 15 added, it was 1.73). However, for the nine gages beyond 60 km, the average G/R ratio was 0.94, indicating the radar and gage values were very close.

This range dependence effect may result in part from the total gage amounts. Within 60 km of the radar, gage values ranged from 0.9 to 7.5 inches (with 71 percent 2.0 inches). Gage values beyond 60 km were from 0.8 to 4.8 inches, with only two of nine values exceeding 1.0 inch. Comparison of total storm gage rainfall amounts with the storm G/R ratios revealed that more of the smaller rainfall amounts were associated with low G/R ratios, whereas some of the larger total amounts were associated with large G/R ratios (Figures 7-4 and 7-5). However, for the majority of raingage sites, the scatter of G/R ratios is similar for rain amounts between 1 and 5 inches.

Hourly Rainfall Comparison

Within the 17-hour storm sample, there were 575 hourly gage-radar matched pairs. Figure 7-6 presents the "best-fit" hourly radar values and gage rainfall comparisons. There was considerable scatter among the pairs, but clearly, the radar underestimated the larger hourly rainfalls at the gages.

An hourly rainfall value of 0.25 inch was selected as the critical threshold for computation of precipitation statistics presented in Table 7-1. Comparison of the gage and the "best-fit" radar estimate yielded 135 pairs, or 23 percent of the total sample, where either the radar or gage exceeded 0.25 inch. The mean rainfall for the gage sample was about 60 percent larger than the radar sample.

Of these 135 pairs, the gage value was greater than the radar estimate by 0.25 inch for about 53 percent of the cases, was smaller than the radar estimate by 0.25 inches for only about 24 percent of the cases, and was nearly the same for about 23 percent of the cases (Table 7-2).

Comparisons of the gage value with the "maximum" radar estimate were made from 176 matched pairs (30 percent of the total sample). The gage value was larger by 0.25 inch in 40 percent

Table 7-1. Statistics Computed for the Hourly Rainfall Estimates (inches)

	<i>Gage</i>	<i>Best-fit radar</i>	<i>Gage</i>	<i>Maximum radar</i>
Sample	135	135	176	176
Mean	0.60	0.38	0.48	0.49
Median	0.41	0.32	0.33	0.42
Mode	0.06	0.00	0.00	0.00
Std.Dev.	0.47	0.31	0.47	0.38

Table 7-2. Frequency of Hourly Rainfall Accumulations, as Measured by Radar and Raingage

<i>Radar (inches)</i>	<i>0.0-0.24</i>	<i>0.25-</i>	<i>0.50-</i>	<i>0.75-</i>	<i>1.00-</i>	<i>1.25-</i>	<i>1.5-</i>	<i>1.75-</i>	<i>2.0-2.25</i>
1.25-1.5	0	0	0	0	0	0	0	0	0
1.00-	2	0	0	1	1	1	2	1	0
0.75-	2	2	1	4	0	0	0	0	0
0.50-	7	6	7	5	2	1	1	1	0
0.25-	14	16	2	1	0	1	2	0	1
0.0-0.24	0	24	10	8	4	4	1	0	0

Note: The radar value is the "best-fit" estimate.

Table 7-3. Frequency of Hourly Rainfall Accumulations as Measured by Radar and Raingage

<i>Radar (inches)</i>	0.0-0.24	0.25	0.50-	0.75	1.00-	1.25-	1.5-	1.75-	2.0-2.25
1.25-1.5	4	4	1	2	1	0	0	0	0
1.00-	3	2	0	2	0	1	2	1	0
0.75-	6	4	3	2	0	0	0	0	0
0.50-	17	6	4	4	2	1	1	1	0
0.25-	35	9	3	0	0	1	2	0	1
0.0-0.24	0	22	10	9	4	4	1	0	0

Note: The radar value is the "maximum" estimate.

of the pairs, smaller in 51 percent of the matched pairs (Table 7-3) and nearly equal in only about 9 percent of the cases. The mean hourly rainfall was nearly equal, as estimated by gage and by radar. The standard deviation of the radar values was greater for the sample of maximum values, but still less than that of the gage values.

Gage/Radar Comparisons from Previous Studies

A number of recent studies have compared radar and raingage rainfall amounts from convective precipitation, and results of certain of these studies are relevant to this study. Austin (1987), employing a 10-cm radar and applying a Reflectivity-Rainfall (Z-R) relationship ($Z=230R^{1.4}$) common for convective rains in New England, found that the radar overestimated convective rainfall. Using a Z-R relationship for intense convective storms, radar-estimated rain was found to be more in line with the gage values (Table 7-4). Best results were obtained when a rain rate maximum of approximately 4 inches/hour was applied to the data.

Table 7-4. Gage/Radar Rain Comparison for Four Intense Convective Storms (Austin, 1987)

<i>Max. storm gage rain (inches)</i>	<i>G/ R for $z = 230R^{1.4}$</i>	<i>G/ R for $z = 400R^{1.3}$</i>	<i>Number of R/G comparisons</i>	<i>Number of R/G comparisons with $max.Ze > 49$ dBZ</i>	<i>Date</i>
0.7	0.74	0.85	20	4	6/2/77
1.1	0.78	1.04	24	0	6/26/78
1.1	0.69	0.83	18	6	6/2/78
2.4	0.81	1.05	25	10	6/19/78

Note: Two Z-R relationships were used, and a maximum rain rate threshold of ~4 inches/hour was imposed. Thirty-three recording gages within 40-128 km of the radar located in New England were employed.

The disparity between the individual gage and radar point values in New England was attributed to the nonrepresentativeness of the gage catch, an effect especially pronounced when spatially sharp rainfall gradients exist. The nonrepresentative results from the small areal sampling in storms where the rainfall intensity can vary significantly over distances of less than a kilometer. Further, at any given time in a storm, the rainfall may change drastically over intervals of a few minutes. Alternately, rain rates observed by the radar at any given point may not be representative of intensities during the intervals between observations.

Klazura and Kelly (1995) found that for intense midlatitude convection and a tropical convective storm, the overall gage/radar ratio (G/ R) was 0.91, again indicating that the radar relative to the gages, overestimated the rainfall (Table 4-5). The radar overestimated the rain for most of the individual storms as well. This study used a Z-R relationship ($Z=300R^{1.4}$) that is very similar to one used in prior radar research in Illinois ($Z=300R^{1.35}$). A maximum reflectivity threshold of 53 dBZ has generally been employed in the NEXRAD raingage algorithm. This corresponds to a rain rate threshold of approximately 4 inches/hour. Of the 14 storms presented from the Austin study (1989) and from the Klazura and Kelly (1995) study, only the tropical convective storm (Table 7-5) had accumulated rainfall values comparable to those for the northern Illinois flood event. This event is notable in that the radar significantly underestimated the storm rainfall.

Klazura and Kelly (1995) compared 418 pairs of radar and raingage estimated rainfall accumulated values (storm total values), and found that the radar matched gage values in 63 percent of the cases, was greater in 26 percent of the cases, and was less in about 11 percent of the cases.

Klazura and Kelly (1995) also examined the gage/radar values according to the distance from the radar. A slight bias was found such that the radar overestimated rainfall at distant ranges and underestimated rainfall at close ranges, as shown below.

Table 7-5. Storms Employed in a Radar/Raingage Comparison

Max. storm gage rain (inches)	G/ R	Site	Precip. type	Number of gages	Duration (hours)	Avg. max. rain/hour	Month
0.55	0.69	OKC	IC	87	9	0.06	Jul
1.48	0.75	OKC	C	85	21	0.07	Oct
1.95	0.87	DEN	IC	92	2	0.98	Aug
1.64	0.87	LBB	IC	85	6	0.27	Aug
1.85	0.92	OKC	C	71	21	0.09	Aug
1.55	0.92	OKC	C	85	17	0.09	Jul
1.75	0.94	DEN	IC	47	2	0.88	Jun
0.78	1.01	OKC	IC	43	4	0.19	Jun
1.13	1.21	OKC	C	53	18	0.07	Sep
15.84	1.44	MLB	TropC	122	72	0.22	Nov

Note: C = convection, IC = intense convection, and Trop C = tropical convection. WSR-88D radar sites are located in Oklahoma City, Denver, Lubbock, and Melbourne (Klazura and Kelly, 1995).

<i>Distance</i>	<i>G/ R</i>
0- 50 km	1.16
50-100 km	0.99
100 - 150 km	0.97
150-230 km	0.86

These two studies (Austin, 1989; Klazura and Kelly, 1995) suggest a fairly close correspondence between gage and radar estimates of storm-total rainfall amounts for convective storms. Further, their results suggest that there is a tendency for the radar to overestimate rainfall.

As previously stated, earlier radar studies have suggested that for intense convective rainfall a good point-to-point match of individual hourly gage and radar values, both in time and space, is not always likely because of differences in the two measurement techniques.

Individual cumulative frequency distributions of hourly radar and gage values were compared to determine if explicit differences in the sample distributions could be observed. It can be seen that the "best-fit" radar-estimated rainfall (Figure 7-7a) is smaller than the gage rainfall for all rainfall categories, but the distributions diverge markedly at rates above about 0.3 inches per hour. This suggests that one reason the radar underestimated the rainfall may be related to the reflectivity cap of 53 dBZ that was imposed on the data. In other warm-season rainfall studies in Illinois, a cap of 56 dBZ has been imposed. This corresponds to a rain rate of approximately 7 inches per hour. Because the radar-rainfall measurements appeared to be most affected in the heavy rainfall region on July 17-18, allowing larger rainfall estimates may help alleviate the rainfall underestimation.

When the maximum radar estimates were used (Figure 7-7b), the distributions matched more closely at moderate rain rates. However, they overestimate lower rainfall values, and still underestimate rain at the higher values. This again suggests that the 53 dBZ cap may have been too low for the heavy rain rates associated with this July storm event.

Modified Precipitation Algorithm

The NEXRAD algorithm was modified in two ways: by increasing the maximum reflectivity threshold from 53 to 56 dBZ, and by increasing the maximum rain rate threshold from 4 to 7 inches/hour. In many cases the hourly rain value increased by about 0.03 inches, up to 0.3 inches in some instances.

An improvement was made in terms of the "best-fit" radar values within 60 km of the radar, although the radar bias was not eliminated (Figure 7-8). Within 60 km of the radar, the average ratio (G/ R) for the 25 gages within 60 km of the radar decreased from 1.67 to 1.40 (excluding the COE gage 15). However, for the nine gages outside of the 60 km, the G/R ratio decreased from 0.94 to 0.79, indicating that the radar overestimated rainfall by about 26 percent instead of 6 percent.

A comparison of gage and the "best-fit" radar estimate was made for 137 pairs or 23 percent of the total sample, where either the radar or gage estimate exceeded 0.25 inches (Table 7-6). The mean rainfall was about 40 percent larger for the gage sample, rather than about 67 percent larger.

**Table 7-6. Statistics Computed for Hourly Rainfall (inches),
for Raingages and Best-fit Radar Estimates,
Using Original and Modified NEXRAD Algorithm**

	<i>Gage</i>	<i>Best-fit</i>	<i>Gage</i>	<i>Modified</i>
Sample	135	135	137	137
Mean	0.60	0.38	0.59	0.42
Median	0.41	0.32	0.41	0.36
Mode	0.06	0.00	0.06	0.30
Std.Dev.	0.47	0.31	0.47	0.32
Correlation		0.09		0.13

**Table 7-7. Frequency of Hourly Rainfall Accumulations as
Measured by Radar and Raingage**

<i>Radar (inches)</i>	<i>Raingage rainfall (inches) categories</i>								
	<i>0.0-0.24</i>	<i>0.25-</i>	<i>0.50-</i>	<i>0.75-</i>	<i>1.00-</i>	<i>1.25-</i>	<i>1.5-</i>	<i>1.75-</i>	<i>2.0-2.25</i>
<i>1.25-1.5</i>	0	0	0	0	0	0	0	1	0
<i>1.00-</i>	2	0	1	0	1	1	2	0	0
<i>0.75-</i>	3	3	2	7	1	0	0	1	0
<i>0.50-</i>	8	7	7	3	1	1	2	0	0
<i>0.25-</i>	14	18	4	1	1	1	1	0	1
<i>0.0-0.24</i>	0	20	7	7	3	4	1	0	0

Note: The radar value is the "best-fit" estimate using the modified NEXRAD algorithm.

Of these 137 pairs, the gage value was greater than the radar estimate by 0.25 inches for about 46 percent of the cases and was smaller than the radar estimate by 0.25 inches for only about 29 percent of the cases. Using the modified algorithm (Table 7-7), the percent of cases that were nearly the same (24 percent) did not change. Thus, use of the modified algorithm did not improve the overall accuracy of the estimates, except in the most general of terms.

A comparison of the cumulative frequency curves (Figure 7-9) of the modified best-fit values with the raingage values indicates that as for the unmodified algorithm, the radar underestimates large rainfall amounts.

Time History of G/R Values

The average ratio (G/ R) was computed for all 35 gages on an hour by hour basis. This revealed that with time, the radar was found to both over- and underestimate rainfall (Table 7-8). The G/R ratio using the best-fit radar estimate was equal to or closer to 1.0 for three cases when the radar was observed to overestimate rain during hours when the total network rain from the 35 gages was between 0.5 and 6.0 inches (see shading in Table 7-8). The G/R ratio using the modified algorithm best-fit estimate was found to be substantially closer to 1.0 for three cases when the network rainfall

Table 7-8. Hourly Network Total Gage and Radar-Estimated Rainfall, and G/R Ratios

<i>Hour (CST)</i>	<i>Gage</i>	<i>Radar-best-fit*</i>	<i>(ΣG/ΣR)</i>	<i>Radar-modified*</i>	<i>(ΣG/ΣR)</i>
07-08	0.00	0.05	0.00	0.05	0.00
08-09	0.65	0.65	1.00	0.78	0.83
09-10	0.46	0.77	0.60	0.77	0.60
11-12	5.56	0.58	1.00	6.02	0.92
12-13	8.35	8.41	0.99	8.91	0.94
15-16	13.31	11.66	1.14	11.91	1.12
16-17	16.07	1.81	8.88	1.86	8.64
19-20	2.71	2.00	1.35	2.17	1.25
20-21	1.90	0.81	2.35	0.86	2.21
21-22	1.97	3.15	0.63	3.23	0.61
22-23	3.82	4.29	0.89	4.93	0.77
23-00	2.21	2.57	0.86	2.74	0.81
00-01	3.46	4.64	0.75	4.79	0.72
01-02	10.69	9.71	1.10	11.63	0.92
03-04	15.83	7.05	2.25	10.61	1.49
04-05	9.11	2.69	3.39	5.08	1.79
05-06	6.93	1.60	4.33	4.13	1.68

Note: *Values in inches.

Table 7-9. Statistics Computed for Hourly Rainfall (inches), for Raingages and Best-fit Radar Estimates, Using Modified NEXRAD Algorithm for all 17-Hours and for the 16-Hour Period

	<i>Gage</i>	<i>Modified</i>	<i>Gage</i>	<i>Modified</i>
Sample	137	137	119	119
Mean	0.59	0.42	0.55	0.48
Median	0.41	0.36	0.38	0.41
Mode	0.06	0.30	0.06	0.30
Std.Dev.	0.47	0.32	0.46	0.31
Correlation		0.13		0.29

totaled between 6.5 and 16.0 inches (see shading in Table 7-8). During most hours, the average (G/ R) ratio using the modified algorithm fell between 0.60 and 2.21, with a median value of 0.92.

For one of the 17-hour periods (16:00-17:00 LST), the G/R ratio exceeds 8.0 for both methods. At this point in time, it is unclear what might have caused the huge discrepancy in rainfall values for this period. Deleting this hour of data from the analysis substantially improves the overall average ratio (G/ R) from 1.40 to 1.15 for 119 pairs of values (Table 7-9). Examination of the cumulative frequency curve (Figure 7-10) for this data showed a striking improvement for hourly values of 0.5 inches or less. However, there still remains a large discrepancy for values over 0.5.

Figure 4-4 presents the total storm rainfall map based on the measurements of the weather radar data for the Chicago (Romeoville) NWS data. Comparison of this pattern with that of Figure 4-3, which is based on 657 raingage measurements, shows a good relationship. Both maps show that

the heavy rain core of the storm at the Wisconsin-Illinois border is in the same location, extends southeastward, and then assumes a more easterly orientation from Chicago eastward into northwestern Indiana. Also shown are the somewhat heavier rains that extended westward from the main high towards Iowa and a secondary rainfall high northeast of O'Hare Airport. Thus, at least qualitatively, the storm totals from the radar were reasonably accurate.

Conclusions

From this study, it appears that the radar performs relatively well on average for hourly rainfall accumulations of less than 0.5 inches. For larger rainfall accumulations, however, the radar substantially underestimates rainfall. Modification of the NEXRAD algorithm somewhat improved the radar rainfall estimates of heavy rainfall, but did not fully compensate for the radar underestimation of gage rainfall. For the network as a whole, the total storm rainfall pattern, was well represented by the radar.

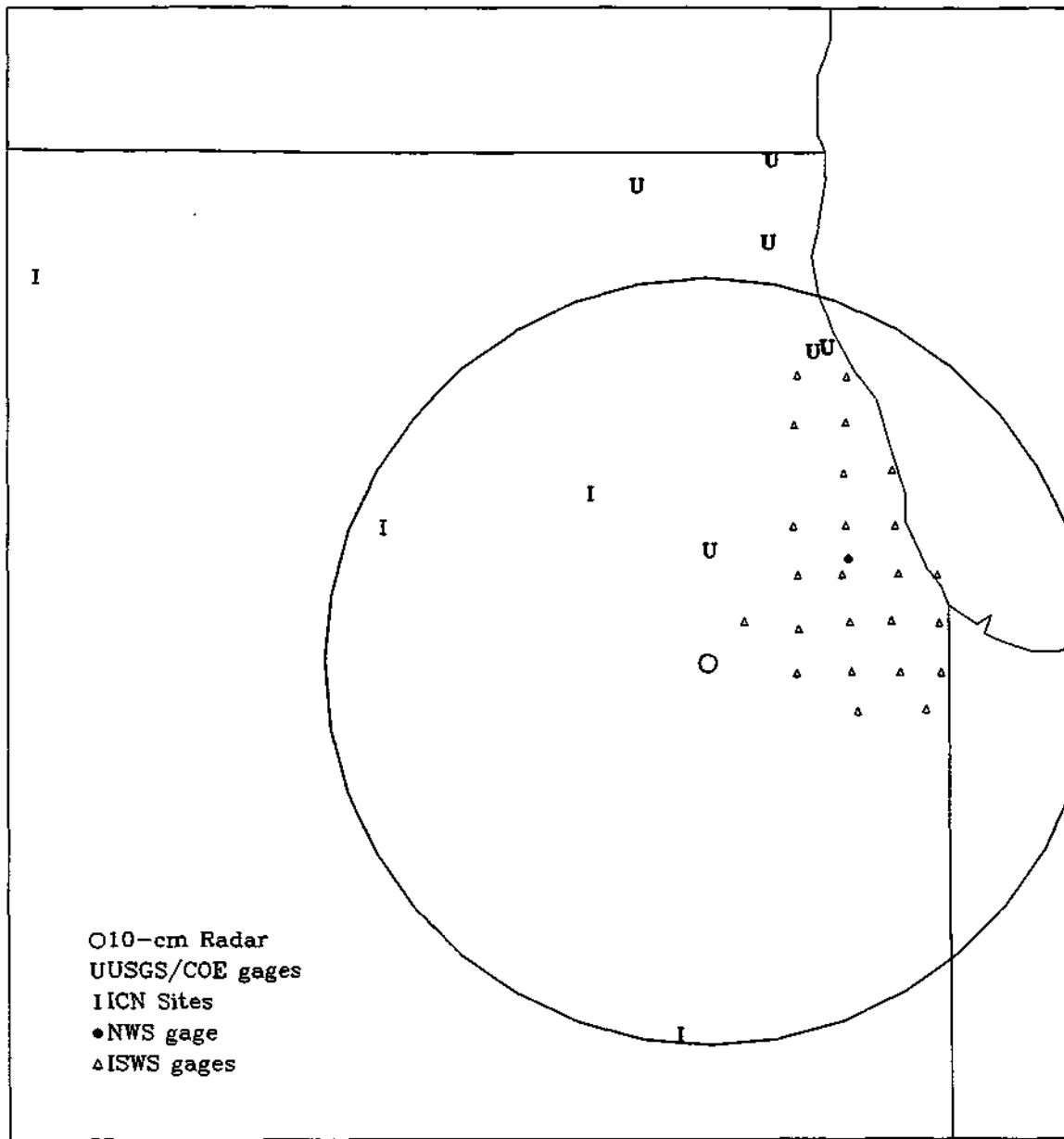


Figure 7-1. Location of the WSR-88D 10-cm Doppler radar in Romeoville, Illinois, and site locations for gages employed in this study. The 75 km range ring is shown.

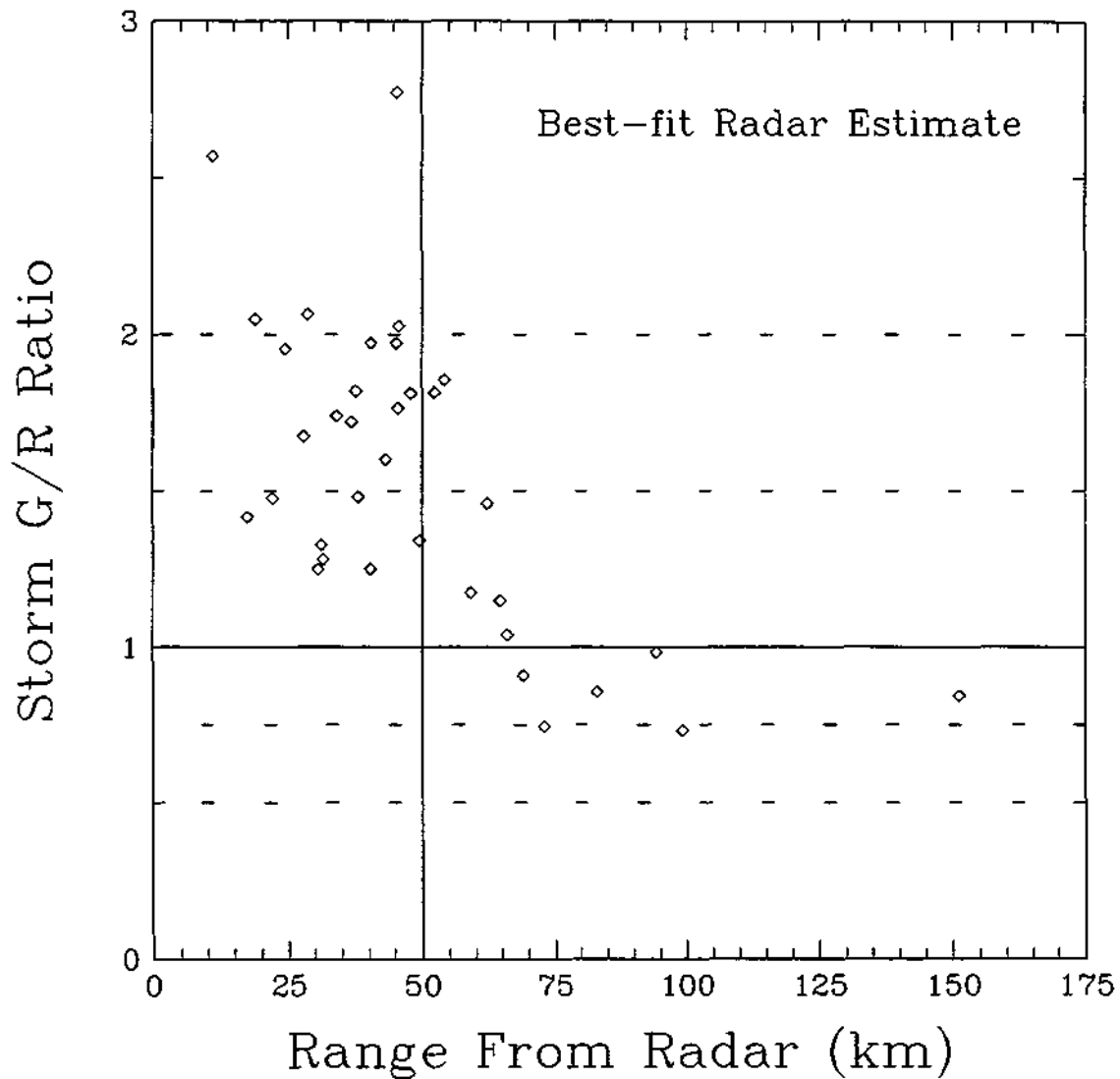


Figure 7-2. Gage/radar ratio (G/ R) using the "best-fit" radar estimate vs. distance of each gage site from radar for total storm. Gage data were summed over the same 17 hours as the radar data where full radar coverage was available.

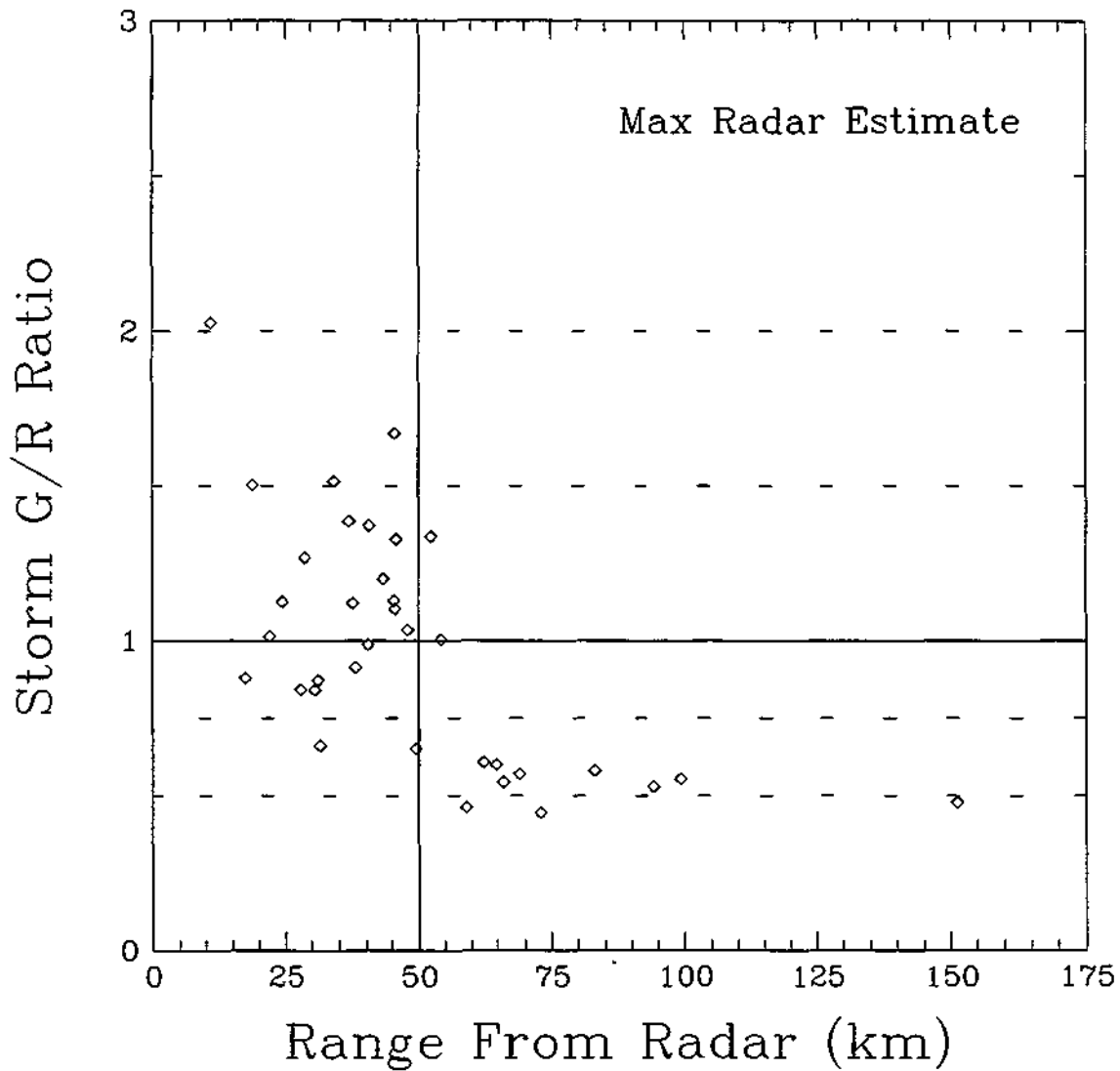


Figure 7-3. Gage/radar ratio (G/ R) using "maximum" radar estimate vs. distance of each gage site from the radar for total storm. Gage data at each site were summed over the same 17 hours as the radar data where full coverage was available.

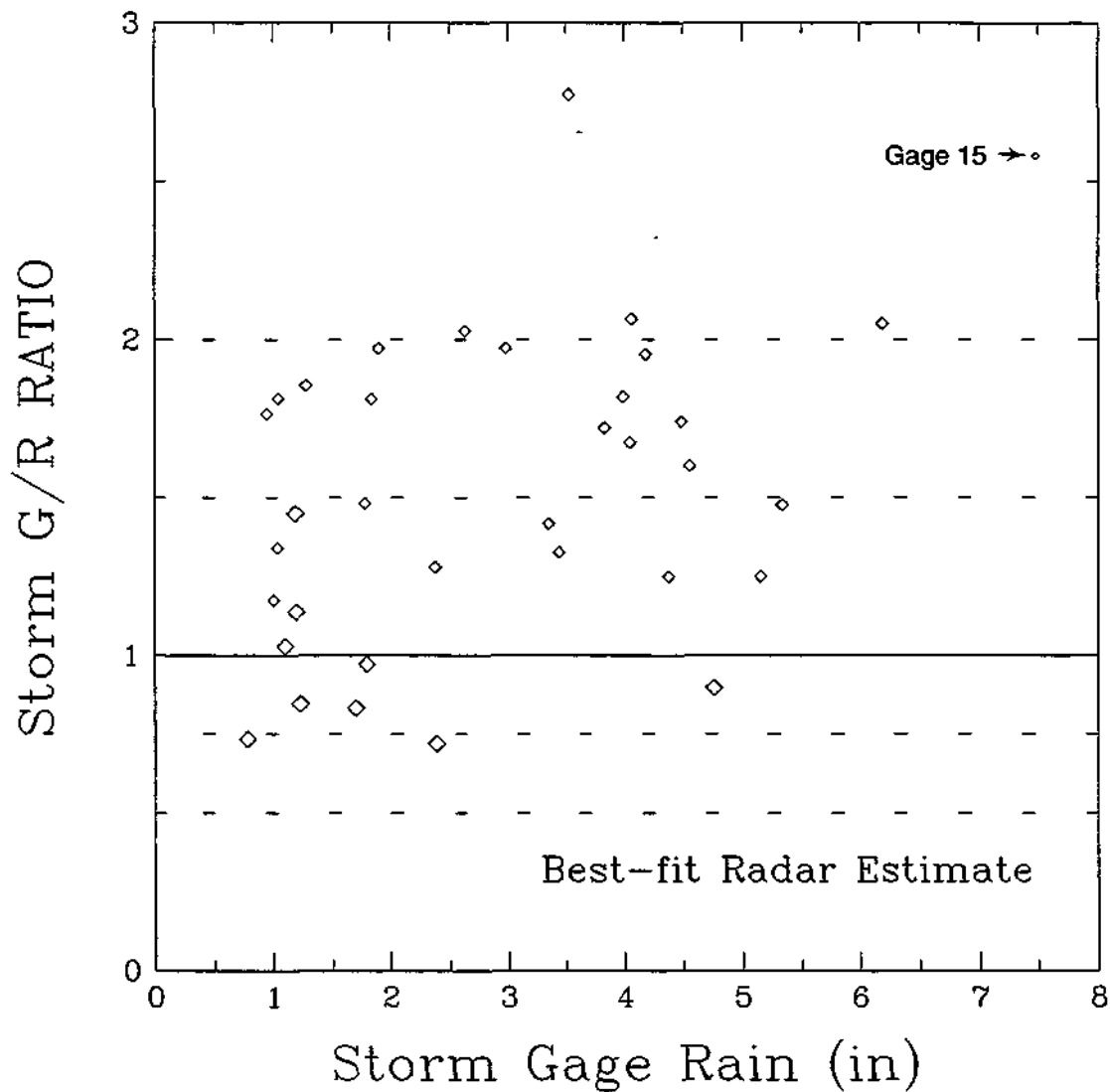


Figure 7-4. Gage/radar ratio (G/ R) using "best-fit" radar estimate vs. magnitude of rain at each gage site. Gage data at each site were summed over the same 17 hours as radar data where full radar coverage was available. Larger diamond markers indicate values at ranges beyond 60 km.

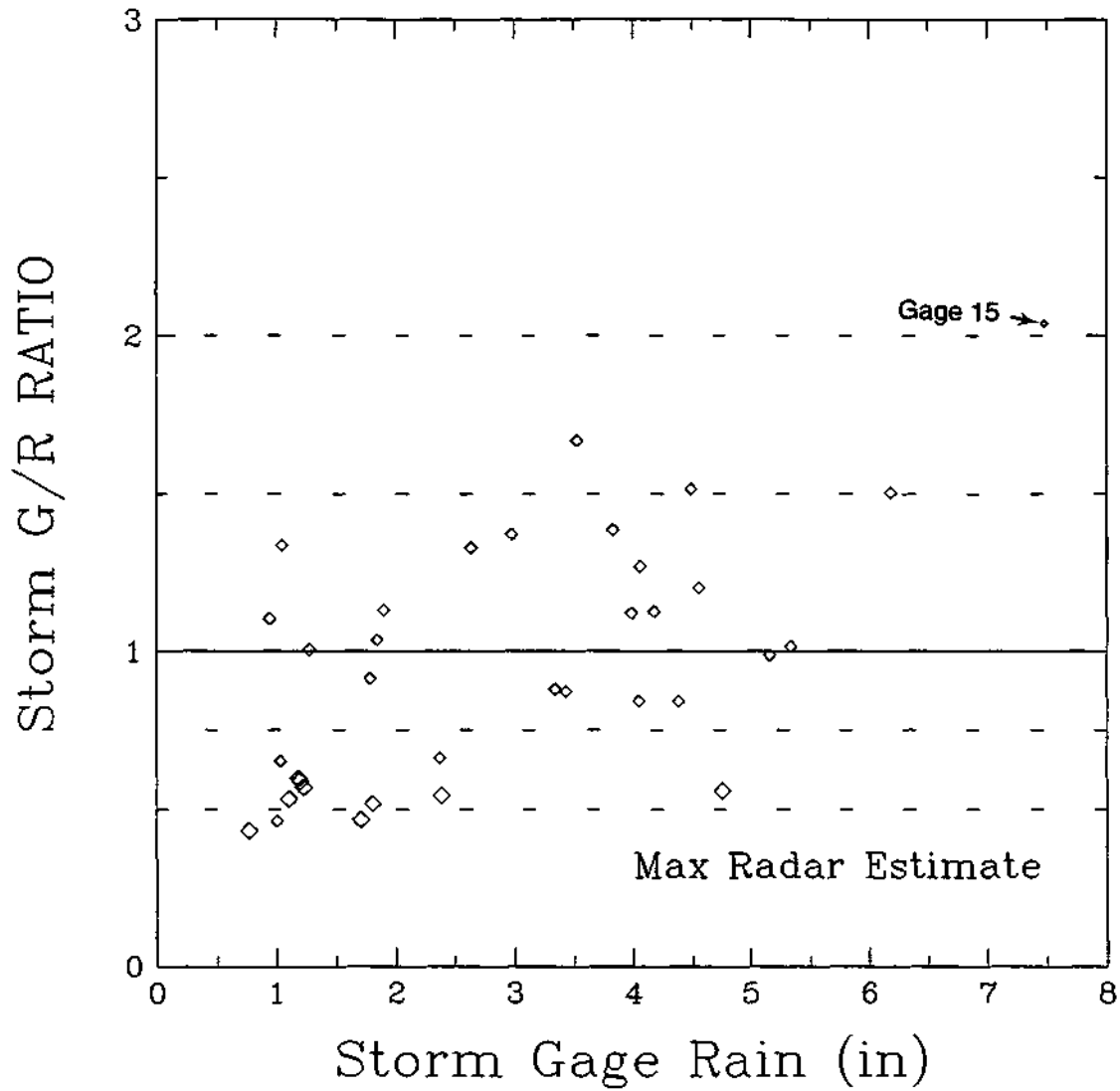


Figure 7-5. Gage/radar ratio (G/ R) using maximum radar estimate versus magnitude of rain at each gage site. Gage data were summed over the same 17 hours when complete data was available.

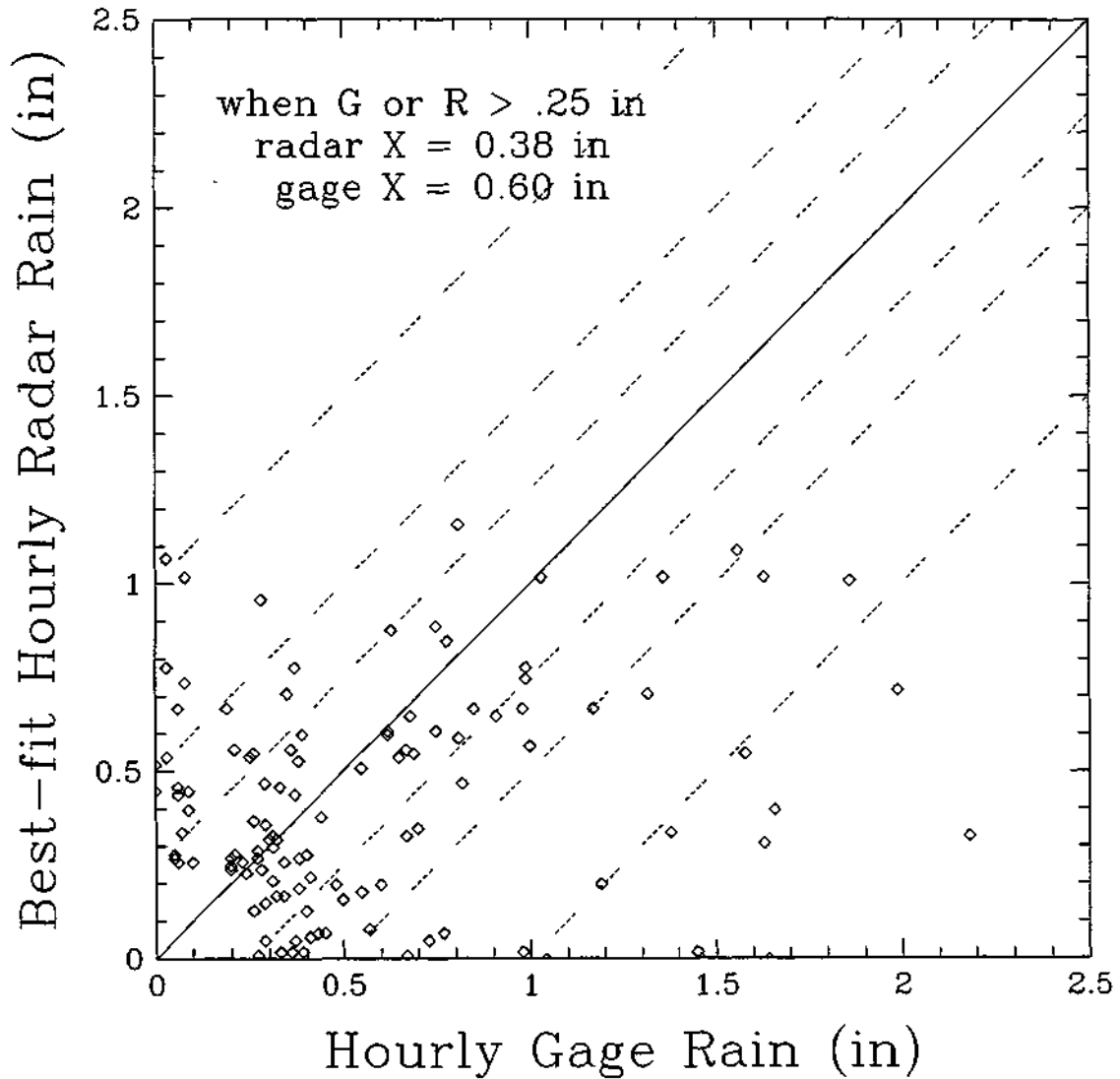


Figure 7-6. Comparison of hourly "best-fit" radar-estimated rainfall at 35 gages with the corresponding gage value. Only pairs where either the gage or the radar estimate were greater than 0.25 inches were included. Sample means are indicated.

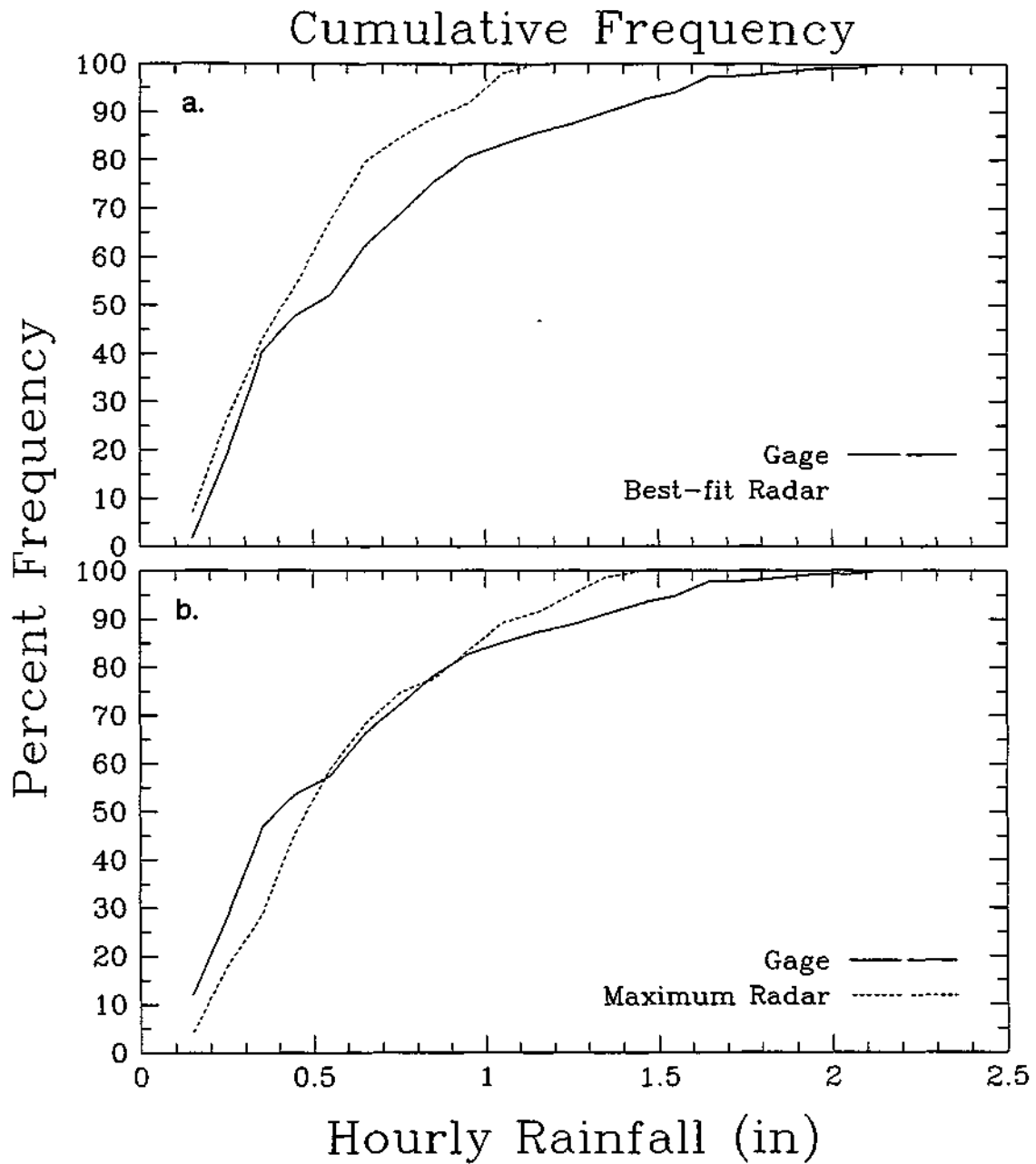


Figure 7-7. Cumulative frequency for curves of hourly gage values and the hourly radar estimates of rainfall using the original NEXRAD parameters for a) the best-fit radar estimates, and b) the maximum radar estimate. Only gage and radar estimates greater than 0.25 inches were included.

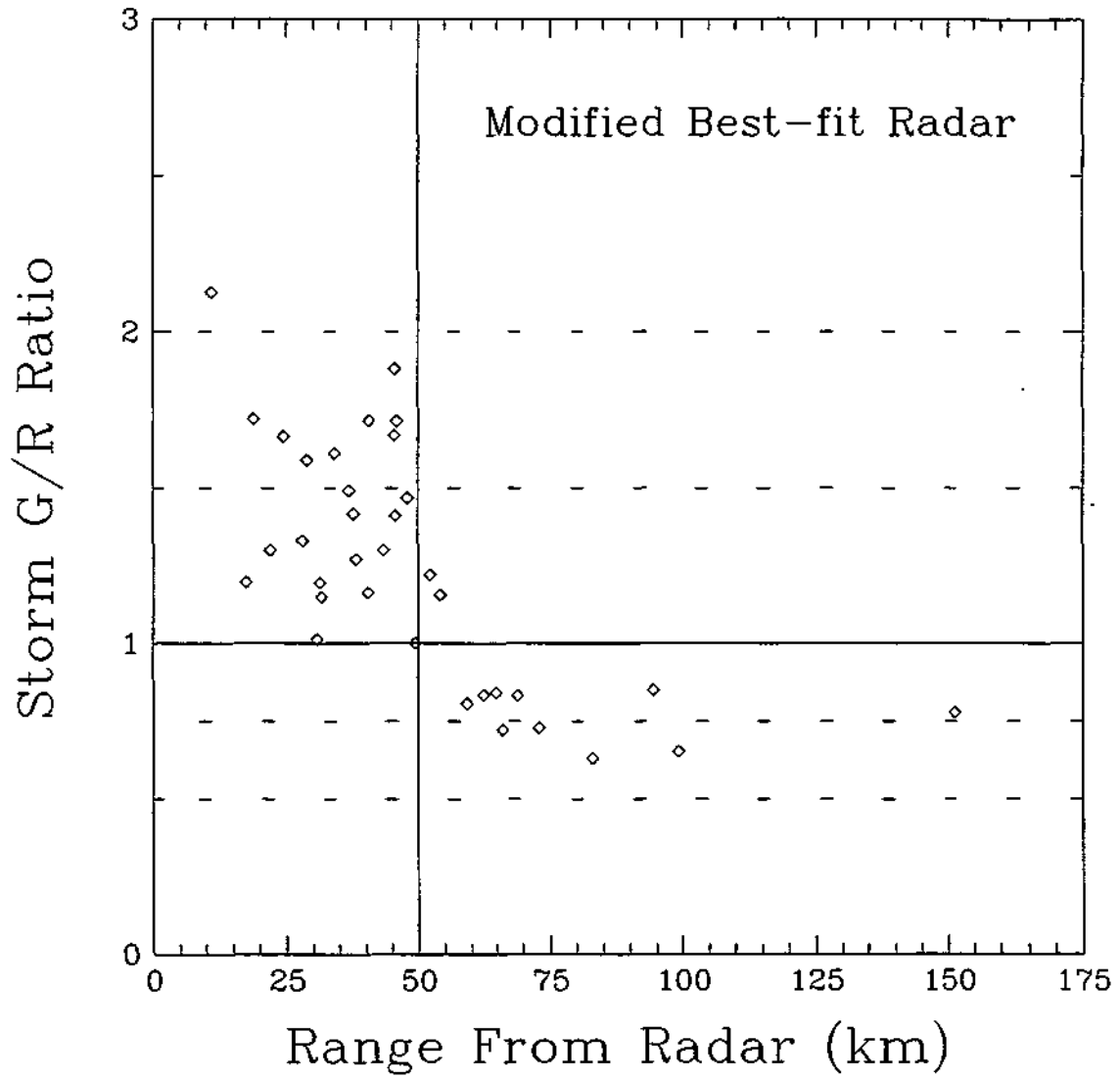


Figure 7-8. Gage/radar ratio (G/ R) using modified "best-fit" radar estimate vs. gage site distance from the radar. Gage and radar data were summed over the 17 hours when there were common data.

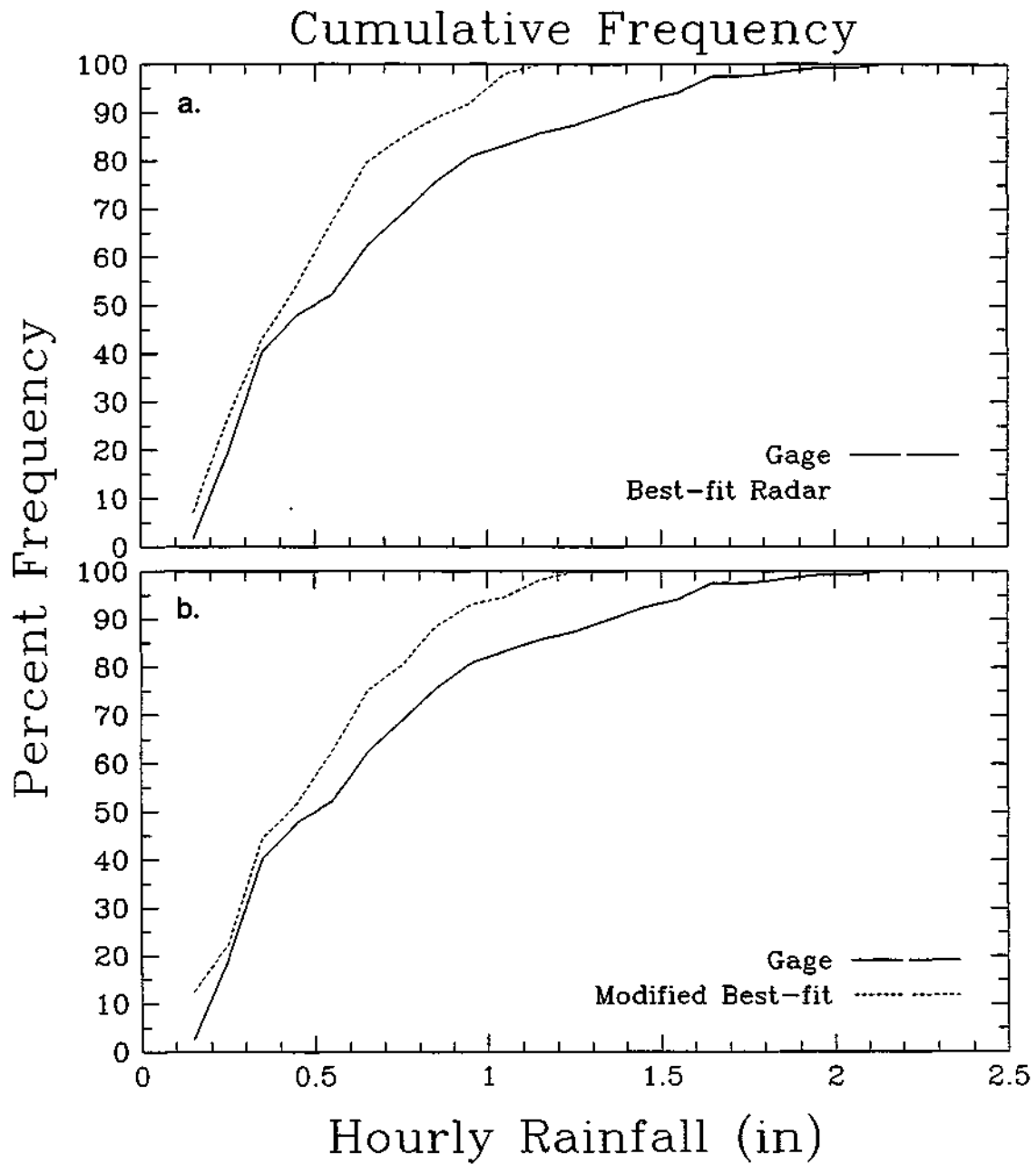


Figure 7-9. Cumulative frequency curves of hourly gage values and hourly radar estimates for a) best-fit using the original NEXRAD parameters and b) best-fit estimate using modified radar-rainfall algorithm. Only gage and radar estimates greater than 0.25 inches were included.

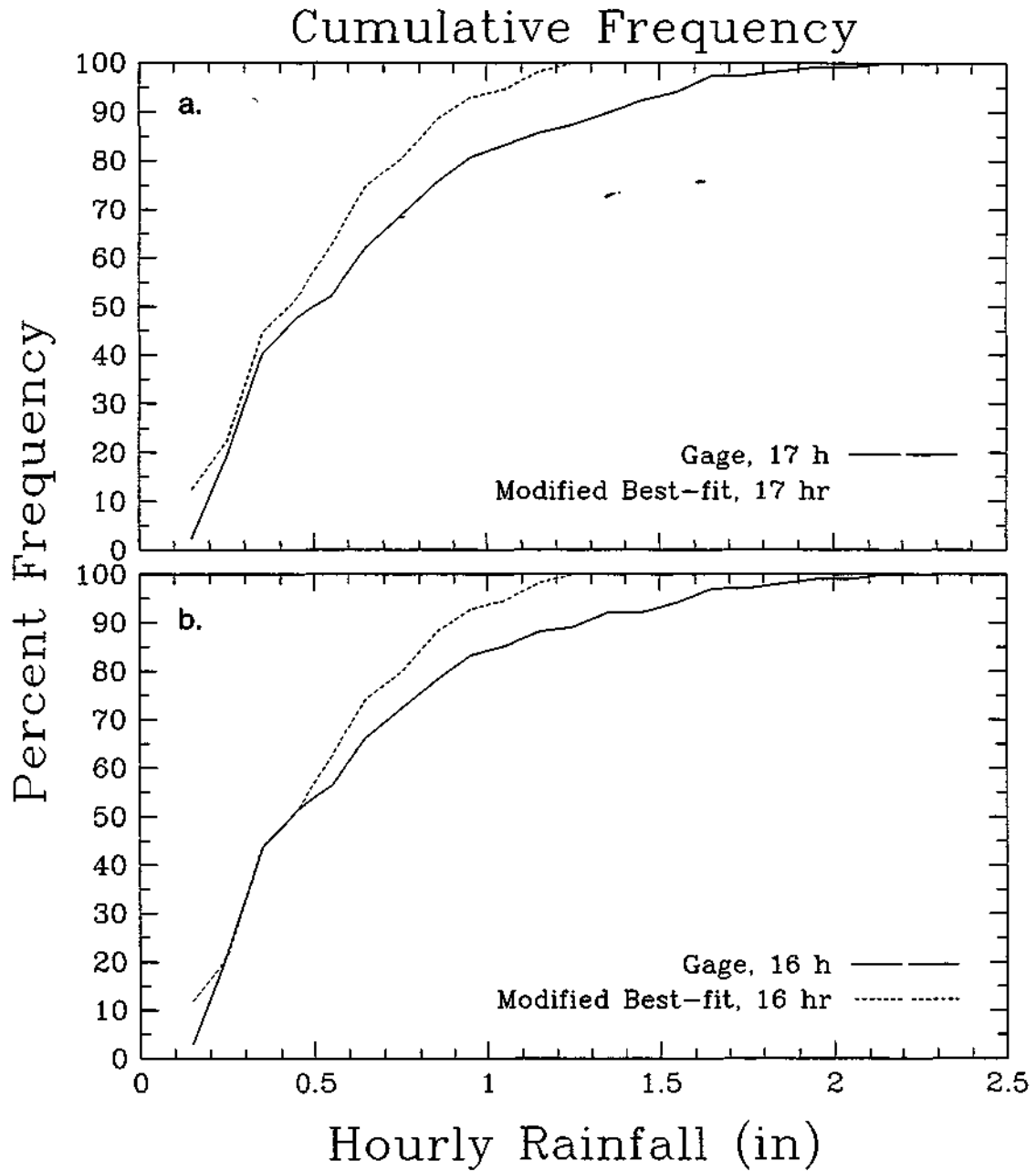


Figure 7-10. Cumulative frequency curves of the hourly gage values and the hourly radar estimates using the modified radar-rainfall algorithm for a) the 17-hour sample and b) the 16-hour sample. Only gage and radar estimates greater than 0.25 inches were included.

References

- Austin, P.M., 1987: Relation between measured radar reflectivity and surface rainfall. *Mon. Wea. Rev.*, **115**, 1053-1070.
- Klazura, G.E., and D.S. Kelly, 1995: A comparison of high resolution rainfall accumulation estimates from the WSR-88D precipitation algorithm with rain gage data. *Preprints, 27th Con. on Radar Meteorology*, Vail, CO, October 9-13, 1995, Amer. Meteor. Soc, Boston, 31-34.

